

PROCEEDINGS BOOK OF THE 8th
**ADVANCED
ENGINEERING DAYS**

8 December 2023 / MERSIN, TURKIYE

International Engineering Symposium



Congress Chairman

PROF. DR. MURAT YAKAR

<http://aed.mersin.edu.tr/>



ISBN: 978-605-72800-7-7



8th Advanced Engineering Symposium

I would like to thank all of the contributing authors and reviewers to the 8th Advanced Engineering Days (AED) Symposium, on 8 December 2023. In this international symposium there are 34 papers. 16 of them are from Türkiye and the rest are from 9 different countries. We would like to see you in the 9th AED.

Best regards

Prof. Dr. Murat YAKAR

**The proceedings of the
8th Advanced Engineering Days**



Editor-in-Chief

Prof. Dr. Murat YAKAR

Editors

Prof. Dr. Fatmir BASHOLLI

Res. Asst. Aydın ALPTEKİN

ISBN: 978-605-72800-7-7

Mersin, 2023

HONOR BOARD

Ali Hamza PEHLİVAN – Governor of Mersin Province
Prof. Dr. Erol YAŞAR – Rector of Mersin University
Prof. Dr. Orhan AYDIN – Rector of Tarsus University
Prof. Dr. Ömer ARIÖZ – Rector of Toros University

SCIENCE BOARD

Prof. Dr. Murat YAKAR (Mersin University)
Prof. Dr. İlker Fatih KARA (Mersin University)
Prof. Dr. Mehmet Cihan AYDIN (Bitlis Eren University)
Prof. Dr. Ali Rıza SÖĞÜT (Konya Technical University)
Prof. Dr. Şükrü DURSUN (Konya Technical University)
Prof. Dr. Fatmir BASHOLLI (Albanian University, Albania)
Prof. Dr. Donato ABRUZZESE (Roma “Tor Vergata” University, Italy)
Prof. Dr. Edmönd Höxha (Albania University, Titana Albania)
Prof. Dr. Hysen Mankolli (University of Maryland College Park, USA)
Prof. Dr. Erdem KOCADAĞISTAN (Erzurum Atatürk University)
Prof. Dr. Sailesh Iyer (Rai University, India)
Prof. Dr. Khalil Valizadeh KAMRAN (University of Tabriz, IRAN)
Prof. Dr. Spase Shumka (Albania Agriculture University, Albania)
Prof. Dr. Mehmet Cihan AYDIN (Bitlis Eren University)
Assoc. Prof. Dr. Arif Oğuz ALTUNEL (Kastamonu University)
Assoc. Prof. Dr. Furkan AYAZ (Mersin University)
Assoc. Prof. Dr. Erdiñç AVAROĞLU (Mersin University)
Assoc. Prof. Dr. Nida NAYCI (Mersin University)
Assoc. Prof. Dr. Musa ÇIBUK (Bitlis Eren University)
Assoc. Prof. Dr. Ümit BUDAK (Bitlis Eren University)
Assoc. Prof. Dr. Beyhan KOCADAĞISTAN (Erzurum Atatürk University)
Assoc. Prof. Dr. Barış BULDUM (Mersin University)
Assoc. Prof. Dr. İskender ÖZKUL (Mersin University)
Assoc. Prof. Dr. Şenay GÜNGÖR (Nevşehir Hacı Bektaş Veli University)
Assoc. Prof. Dr. Lyudmyla Symochko (Uzhhorod National University, Ukraine)
Assoc. Prof. Dr. Davron Aslonqulovich Juraev (University of Economy and Pedagogy) Uzbekistan
Asst. Prof. Dr. Mehmet Rida Tur (Batman University)
Dr. Hakan DOĞAN (Turkish State Meteorological Service)
Dr. Fatih ADIGÜZEL (Nevşehir Hacı Bektaş Veli University)
Dr. Cihan YALÇIN (Ministry of Industry and Technology)

ORGANIZING BOARD

Prof. Dr. Murat YAKAR (Mersin University)
Prof. Dr. Cengiz ALYILMAZ (Uludağ University)
Prof. Dr. Semra ALYILMAZ (Uludağ University)
Prof. Dr. Şükrü DURSUN (Konya Technical University)
Prof. Dr. Mehmet Cihan AYDIN (Bitlis Eren University)
Prof. Dr. Erdem KOCADAĞISTAN (Erzurum Atatürk University)
Assoc. Prof. Dr. Furkan AYAZ (Mersin University)
Assoc. Prof. Dr. Beyhan KOCADAĞISTAN (Erzurum Atatürk University)
Asst. Prof. Dr. Vahdettin DEMİR (KTO Karatay University)
Asst. Prof. Dr. Esra URAY (KTO Karatay University)
Asst. Prof. Dr. Ali ULVÍ (Mersin University)
Dr. Hakan DOĞAN (Turkish State Meteorological Service)
Lect. Atilla KARABACAK (Mersin University)
Lect. Şafak FİDAN (Mersin University)
Res. Asst. Aydın ALPTEKİN (Mersin University)
Res. Asst. Ramazan AKKURT (Mersin University)
Res. Asst. Abdurahman Yasin YİĞİT (Mersin University)
Res. Asst. İrem YAKAR (Istanbul Technical University)
Eng. Engin KANUN (Mersin University)
Eng. Mücahit Emre ORUÇ (Mersin University)
Eng. Seda Nur Gamze HAMAL (Mersin University)

Technical Program of AED-8

8 December 2023

Time	Session 1
10.00-10.10	Development of plastic scintillator with thermal polymerization Tonguç Özdemir, Isıl Yıldırım
10.10-10.20	Mathematical correlations of machine learning, which is a component of artificial intelligence Hüseyin Fırat Kayıran, Ulviye Demirbilek, Mesut Türk
10.20-10.30	Determination of long-term water surface level change in lakes by integration of UAV and satellite data and future estimation with ARIMA Yunus Kaya, Fusun Balik Sanli, Saygin Abdikan
10.30-10.40	Analysis of bus accidents by use of geographic information systems Mehtap Sagir Kayim, Ugur Alganci, Dursun Zafer Seker
10.40-10.50	GIS-based analysis approach for metro and bus integration in public transportation Muhammed Semih Solak, Ugur Alganci, Dursun Zafer Seker

Time	Session 2
11.00-11.10	Analysis of security challenges in SCADA systems, a technical review on automated real-time systems Fatmir Basholli, Besjana Mema, Dolantina Hyka, Albina Basholli, Adisa Daberдини
11.10-11.20	ChatGPT in Albanian higher education: Transformation of learning and virtual interaction Besjana Mema, Fatmir Basholli, Dolantina Hyka
11.20-11.30	Applications of the Helmholtz equation Davron Aslonqulovich Juraev, Praveen Agarwal, Ebrahim E. Elsayed, Nauryz Targyn
11.30-11.40	Electrochemical analysis of corrosion inhibitor synthesized using chlorine organomixture and ammonia <i>Khalilov Jamshid Akmal ugli, Nurkulov Fayzulla Nurmuminovich, Djalilov Abdulahat Turapovich</i>
11.40-11.50	Protection of buildings on a university campus from lightning strikes Fatmir Basholli, Joana Minga, Alketa Grepcka

Time	Session 3
12.00-12.10	A comparative study on the lateral displacement response of short monopiles with different plug materials Özgür Lütfi Ertuğrul, Fatma Dülger Canoğulları
12.10-12.20	Lymph nodes and their role in immunity Ceren Canatar, Furkan Ayaz
12.20-12.30	Exploration of the Pb-Zn deposit using IP/Resistivity methods: A case study in Sudöşegi (Simav-Kütahya) Cihan Yalçın, Hürşit Canlı
12.30-12.40	Examination of buildings with different number of floors using non-linear time history analysis according to TBEC-2018 and EC 8 seismic codes Mehmet Yılmaz, Hüsnü Can
12.40-12.50	Investigation of stone deterioration in Gaziantep Historical Gümrük Inn İlhami Ay, Murat Dal, Şefika Ergin
12.50-13.00	Investigation of stone deterioration in Gaziantep Kumandan Fountain İlhami Ay, Murat Dal, Şefika Ergin

Time	Session 4
13.00-13.10	The impact of alternative fuels to diesel in reducing pollution from vehicles Asllan Hajderi, Ledia Bozo, Fatmir Basholli
13.10-13.20	Estimation of surface urban heat island (SUHI) effect over four populated cities of Andhra Pradesh state of India Jagadish Kumar MOGARAJU
13.20-13.30	Investigation of headway distribution of traffic dominated by motorcycles Hassan Shuaibu Abdulrahman, Stephen Sunday Kolo, Mahmud Abubakar, Mohammed Shehu
13.30-13.40	A techno-economic analysis of a single-axis tracked bifacial photovoltaic plant connected in Albanian distribution system Andi Hida, Rajmonda Bualoti, Pavlina Qosja
13.40-13.50	Obtaining and testing results of PF-1 brand corrosion inhibitor obtained based on the processing of chlorinated organic waste used in the oil and gas industry Khalilov Jamshid Akmal ugli, Nurkulov Fayzulla Nurmuminovich, Djalilov Abdulahat Turapovich

Time	Session 5
14.00-14.10	Evaluating the performance of object-based machine learning and deep learning models in classifying different maize genotypes with multispectral UAV imagery Osman Yavuz Altuntas, Ismail Colkesen, Umut Gunes Sefercik, Taskin Kavzoglu, Mustafacan Saygi, Muhammed Yusuf Ozturk, Mertcan Nazar, Ilyas Aydin, Hasan Tonbul
14.10-14.20	3D modelling of cultural heritage with point cloud generation by integrating UAV and terrestrial photogrammetry techniques Emine Kurt, İbrahim Halilullah Çetin, Füsün Balık Şanlı, Burak Akpınar
14.20-14.30	LULC mapping accuracy enhancement through multispectral UAV imagery with nDSM integration Ilyas Aydin, Umut Gunes Sefercik
14.30-14.40	UAV-based rockfall hazard detection via roughness analysis in Karaköprü, Şanlıurfa using photogrammetric point clouds Nizar Polat, Yunus Kaya
14.40-14.50	Pixel based classification of Lavandula sp. using high resolution UAV orthophotos Seyma Akca, Nizar Polat


Time	Session 6
15.00-15.10	Influence of wheel diameter difference on their stability against derailment Angela Shvets
15.10-15.20	The application of SVD method in image compression and digital watermarking Ornela Gordani, Aurora Simoni
15.20-15.30	Algorithm for determining restrictions on train control Kostiantyn Zheliezynov, Artem Akulov, Oleksandr Zabolotnyi, Eugene Chabaniuk, Angela Shvets
15.30-15.40	Correlation of core strategic business factors in development of Albanian wood industry Alketa Grepcka, Leonidha Peri, Fatmir Basholli
15.40-15.50	Circular economy toward a sustainable concept in the wood processing sector in Albania Ina Vejsiu, Erald Kola
15.50-16.00	Algebra and its applications in technical and engineering problems Davron Aslonqulovich Juraev, Murot Nashvandovich Bozorov
16.00-16.10	Quality of irrigation water in the region of In Salah, South Algeria Ballah Abderrahmane
16.10-16.20	Increasing the efficiency of worn-out urban fabric areas with an emphasis on the segmentation of buildings in the 4th district of Tabriz in Iran Shiva Sattarzadeh Salehi, Firouz Jafari

Content	Page
Development of plastic scintillator with thermal polymerization Tonguç Özdemir, Isil Yıldırım	1-3
Mathematical correlations of machine learning, which is a component of artificial intelligence Hüseyin Fırat Kayıran, Ulviye Demirbilek, Mesut Türk	4-7
Determination of long-term water surface level change in lakes by integration of UAV and satellite data and future estimation with ARIMA Yunus Kaya, Fusun Balik Sanli, Saygin Abdikan	8-11
Analysis of bus accidents by use of geographic information systems Mehtap Sagir Kayim, Ugur Alganci, Dursun Zafer Şeker	12-14
GIS-based analysis approach for metro and bus integration in public transportation Muhammed Semih Solak, Ugur Alganci, Dursun Zafer Şeker	15-17
Analysis of security challenges in SCADA systems, a technical review on automated real-time systems Fatmir Basholli, Besjana Mema, Dolantina Hyka, Albina Basholli, Adisa Daberdini	18-22
ChatGPT in Albanian higher education: Transformation of learning and virtual interaction Besjana Mema, Fatmir Basholli, Dolantina Hyka	23-27
Applications of the Helmholtz equation Davron Aslonqulovich Juraev, Praveen Agarwal, Ebrahim Eldesoky Elsayed, Nauryz Targyn	28-30
Electrochemical analysis of corrosion inhibitor synthesized using chlorine organomixture and ammonia <i>Khalilov Jamshid Akmal Ugli, Nurkulov Fayzulla Nurmuminovich, Djalilov Abdulahat Turapovich</i>	31-34
Protection of buildings on a university campus from lightning strikes Fatmir Basholli, Joana Minga, Alketa Grepcka	35-38
A comparative study on the lateral displacement response of short monopiles with different plug materials Özgür Lütfi Ertuğrul, Fatma Dülger Canoğulları	39-42
Lymph nodes and their role in immunity Ceren Canatar, Furkan Ayaz	43-44
Exploration of the Pb-Zn deposit using IP/Resistivity methods: A case study in Sudöşeği (Simav-Kütahya) Cihan Yalçın, Hürşit Canlı	45-48
Examination of buildings with different number of floors using non-linear time history analysis according to TBEC-2018 and EC 8 seismic codes Mehmet Yılmaz, Hüsnu Can	49-51
Investigation of stone deterioration in Gaziantep Historical Gümrük Inn İlhami Ay, Murat Dal, Şefika Ergin	52-55
Investigation of stone deterioration in Gaziantep Kumandan Fountain İlhami Ay, Murat Dal, Şefika Ergin	56-59
The impact of alternative fuels to diesel in reducing pollution from vehicles Asllan Hajderi, Ledia Bozo, Fatmir Basholli	60-63
Estimation of surface urban heat island (SUHI) effect over four populated cities of Andhra Pradesh state of India Jagadish Kumar Mogaraju	64-67
Investigation of headway distribution of traffic dominated by motorcycles Hassan Shuaibu Abdulrahman, Stephen Sunday Kolo, Mahmud Abubakar, Mohammed Shehu	68-70

A techno-economic analysis of a single-axis tracked bifacial photovoltaic plant connected in Albanian distribution system Andi Hida, Rajmonda Bualoti, Pavlina Qosja	71-74
Obtaining and testing results of PF-1 brand corrosion inhibitor obtained based on the processing of chlorinated organic waste used in the oil and gas industry Khalilov Jamshid Akmal Ugli, Nurkulov Fayzulla Nurmuminovich, Djalilov Abdulahat Turapovich	75-78
Evaluating the performance of object-based machine learning and deep learning models in classifying different maize genotypes with multispectral UAV imagery Osman Yavuz Altuntas, Ismail Colkesen, Umut Gunes Sefercik, Taskin Kavzoglu, Mustafacan Saygi, Muhammed Yusuf Ozturk, Mertcan Nazar, Ilyas Aydin, Hasan Tonbul	79-82
3D modelling of cultural heritage with point cloud generation by integrating UAV and terrestrial photogrammetry techniques Emine Kurt, İbrahim Halilullah Çetin, Füsün Balık Şanlı, Burak Akpınar	83-85
LULC mapping accuracy enhancement through multispectral UAV imagery with nDSM integration Ilyas Aydin, Umut Gunes Sefercik	86-88
UAV-based rockfall hazard detection via roughness analysis in Karaköprü, Şanlıurfa using photogrammetric point clouds Nizar Polat, Yunus Kaya	89-92
Pixel based classification of Lavandula sp. using high resolution UAV orthophotos Seyma Akca, Nizar Polat	93-96
Influence of wheel diameter difference on their stability against derailment Angela Shvets	97-99
The application of SVD method in image compression and digital watermarking Ornela Gordani, Aurora Simoni	100-102
Algorithm for determining restrictions on train control Kostiantyn Zheliezynov, Artem Akulov, Oleksandr Zabolotnyi, Eugene Chabaniuk, Angela Shvets	103-108
Correlation of core strategic business factors in development of Albanian wood industry Alketa Grepcka, Leonidha Peri, Fatmir Basholli	109-111
Circular economy toward a sustainable concept in the wood processing sector in Albania Ina Vejsiu, Erald Kola	112-113
Algebra and its applications in technical and engineering problems Davron Aslonqulovich Juraev, Murot Nashvandovich Bozorov	114-116
Quality of irrigation water in the region of In Salah, South Algeria Abderrahmane Ballah	117-120
Increasing the efficiency of worn-out urban fabric areas with an emphasis on the segmentation of buildings in the 4th district of Tabriz in Iran Shiva Sattarzadeh Salehi, Firouz Jafari	121-124



Development of plastic scintillator with thermal polymerization

Tonguç Özdemir ^{*1}, Isıl Yıldırım ¹

¹Mersin University, Chemical Engineering Department, Mersin, Türkiye, tonguc.ozdemir@gmail.com, isilyldrm181@gmail.com

Cite this study: Özdemir, T., & Yıldırım, I. (2023). Development of plastic scintillator with thermal polymerization. *Advanced Engineering Days*, 8, 1-3

Keywords

Plastic Scintillator
Polystyrene
Thermal polymerization

Abstract

In this study, development of a plastic scintillator based on polystyrene and doped with 1,4-bis[2-(phenyloxazole)]-benzene (POP) and 2,5-diphenyloxazole (PPO) was produced using the thermal polymerization process is studied. Plastic scintillators are used for the detection of radiation and they are vital for the radiation safety and protection. Thermal polymerization was used and the monomer were used after removal of retarder via alumina. The scintillation was confirmed with the radiation detector.

Introduction

Plastic scintillators are homogeneous and amorphous materials containing scintillating substances (mostly organic fluorescent compounds) dissolved in a polymer matrix consisting of aromatic [1]. They convert the energy of the incoming ionizing radiation into visible or UV light [2].

The emission spectrum of the polymer matrix in the ultraviolet region (300-350 nm) does not fit the spectral sensitivity region of photodetectors (425 nm) and cannot be used as a scintillator due to low scintillation efficiency [3-4]. Therefore, scintillator additives are added into the polymer matrix.

Scintillator substances are generally divided into two groups primary and secondary scintillators. Primary scintillators are enabled to carry out two main functions that are (1) converting captured energy to light emission and (2) wavelength shifters. Since the light emission does not comply with the sensitivity of the photomultiplier tube (PMT), that is, the emission wavelength cannot reach the desired level (425 nm), the secondary scintillator (wavelength shifter) is inevitably added.

The studies conducted by Zaitseva et. al. that the maximum light output is obtained at relatively lower dye concentrations of about 1 wt% of 2,5-diphenyloxazole (PPO). The increasing of dye concentration above the optimum value can decrease the light output and also the fluorescence intensity due to the effect of concentration quenching [5].

Material and Method

Plastic scintillators were produced by thermal polymerization method in a mold. The plastic scintillator was prepared by using styrene as the polymer base matrix, 2,5-diphenyloxazole (PPO) as the primary scintillator and 1,4-bis[2-(phenyloxazolyl)]-benzene (POPOP) as the wavelength shifter or secondary scintillator.

The inhibitory substance contained in the styrene monomer was absorbed by activated alumina granules for the production of plastic scintillators. PPO content was up to 3% by weight and that of POPOP was 0.15% by weight were added to the purified styrene monomer. The resulting mixture was mixed continuously in a magnetic mixer for 6 hours and at a constant temperature of 40°C (Figure 1). The rotation speed was adjusted regularly depending on the viscosity of the mixture. When a homogeneous solution was obtained, it was placed in vacuum.

First, the air bubbles that were dissolved were removed. After that, the temperature of the oven was gradually increased to 120°C and kept constant for the polymerization reaction to occur. After the polymerization reaction was completed, the temperature was gradually cooled to prevent the formation of air bubbles that may occur inside the polystyrene material. Figure 2 shows the temperature profile during the polymerization process.

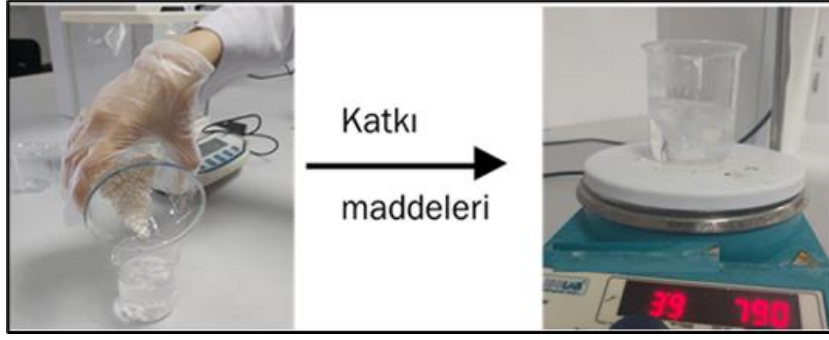


Figure 1. Dissolving additives.

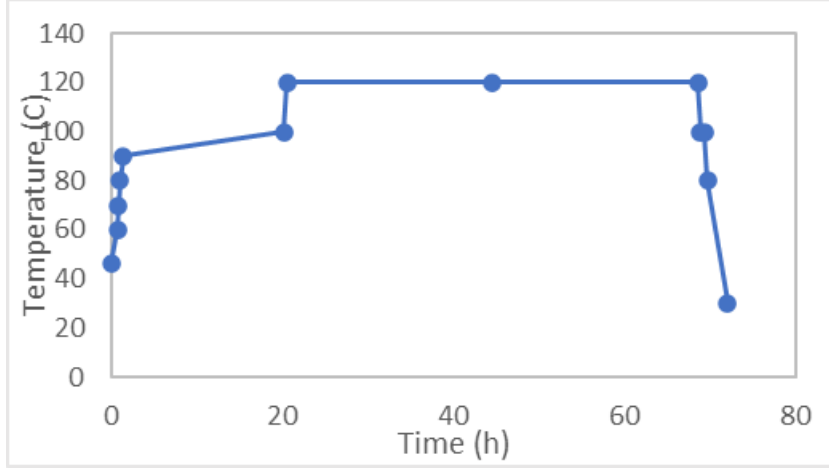


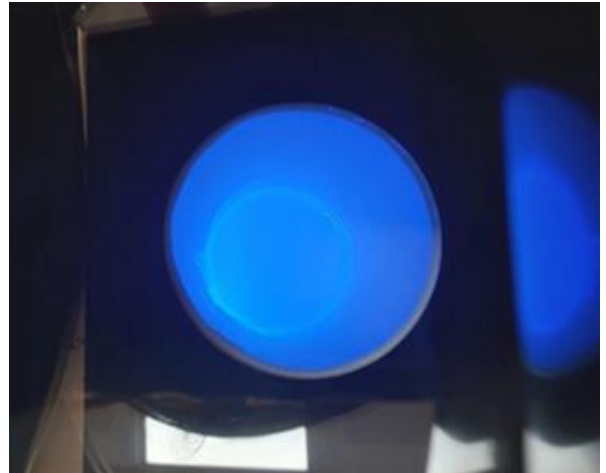
Figure 2. Temperature profile of the polymerization process.

Results and Discussion

Photographs of the produced polystyrene-based plastic scintillator taken under white and UV light are shown in **Figure 1**Figure 3(a) and 3(b). When these plastic scintillators are excited with UV, the blue color could be seen. In the secondary scintillator, it absorbs the light emitted by the primary scintillator and consequently produces photons in the visible range. As a result of the production process, scintillation under UV is performed using plastic scintillators.



(a)



(b)

Figure 3. Polystyrene based plastic scintillator under white (a) and UV illumination (b) (color online).

Conclusion




Plastic scintillator with thermal polymerization with a unique thermal history has been developed. The scintillation of the materials was observed via the UV. The scintillator could be used for the detection of radioactivity.

References

1. Yakar, M., Oktar, O., Arı, G., Gündüz, Ö., Demirel, H., & Demirbaş, A. (2011). Ticari polistiren kullanılarak düşük maliyetli plastik sintilatör üretimi. Türkiye Atom Enerjisi Kurumu.
2. Köllö, Z. (2022). Studies on a plastic scintillator detector for activity measurement of tritiated water. Nuclear Science and Techniques, 20-22.
3. Alex, L., Paulraj, R., Sonu, & Tyagi, M. (2023). Green emitting plastic scintillator with neutron/gamma pulse shape discrimination for fast neutron detection. *Journal of Materials Science: Materials in Electronics*, 34(7), 576. <https://doi.org/10.1007/s10854-023-10018-4>
4. Aytan, Ö. (2019). Real time environmental radiation dose monitoring system design. İstanbul Üniversitesi, 9-21.
5. Alex, L., Paulraj, R., & Tyagi, M. (2022). Effect of PPO and POPOP activators on the scintillation performance of polystyrene-based scintillator. *Journal of Optoelectronics and Advanced Materials*, 24(July-August 2022), 365-371.



Mathematical correlations of machine learning, which is a component of artificial intelligence

Hüseyin Fırat Kayıran^{*1}, Ulviye Demirbilek², Mesut Türk³

¹ARDSI, Mersin Provincial Coordination Unit, Mersin, Türkiye, huseyinfirat kayiran@tkdk.gov.tr

²Mersin University, Department of Mathematics, Türkiye, ulviyedemirbilek@mersin.edu.tr

³Malazgirt Secondary School, Şahinbey, Gaziantep, Türkiye, mesut252@gmail.com

Cite this study: Kayıran, H. F., Demirbilek, U., & Türk, M. (2023). Mathematical correlations of machine learning, which is a component of artificial intelligence. *Advanced Engineering Days*, 8, 4-7

Keywords

Artificial intelligence
Mathematics
Machine learning

Abstract

Artificial intelligence can be explained as a mathematical phenomenon. Artificial intelligence comes together from systems that imitate human intelligence. Driverless cars, robots, vacuum cleaners, games are used in automated trading, corporate resource management. In general; robots and unmanned aircraft can be produced with artificial intelligence. The main basis that creates artificial intelligence is mathematics. Machine Learning has also become an indispensable part of our lives today as a sub-branch of artificial intelligence. In this study, the literature review was conducted and the studies about Machine Learning were mentioned. The findings obtained by establishing mathematical correlations are explained.

Introduction

Machine learning (Machine Learning) is replacing artificial intelligence as a branch that uses statistics and computer science and has recently become very popular. Artificial intelligence can be called the process of creating models based on existing data and defining complex relationships. Since past studies have shown the necessity of machines to learn data, research has focused on this issue [1]. The purpose of machine learning is to create systems that make predictions by making inferences from mathematical and statistical operations and data. Today, many different machine learning models have been born for the inference process [2] The manufacturing industry needs support to take advantage of data-intensive availability to meet its needs, such as quality improvement initiatives, production cost estimation, process optimization, and a better understanding of customer requirements [3].

Artificial Intelligence (AI)

We can define artificial intelligence in many ways. For example, it is the ability of a computer system to imitate human cognitive functions such as learning and problem solving. Through artificial intelligence, a computer system uses mathematical functions and logic to mimic thought processes that allow people to learn from new information and make decisions [4]. The concept of machine learning was invented by American researcher Arthur Samuel, who worked at IBM. In 1959, he created the first checkers program that could play by itself and learn by itself [5]. Artificial intelligence machines use various algorithms to successfully complete their tasks or achieve their goals. These algorithms have been developed using various approaches such as case-based reasoning, artificial neural network, statistical approaches, rule-based approaches and many more techniques [6]. Although artificial intelligence usually refers to the intelligence displayed by machines, it is an innovative technology that takes place in many areas of our lives, from semi-autonomous cars on the road to robotic vacuum cleaners in our homes [7]. The purpose of machine learning is to ensure that machine hardware has the intelligence and ability of humans by artificial methods. As scientists continue to have doubts about intelligence, there is no definitive definition of artificial intelligence in the scientific community [8]. The taxonomy and subfields of artificial intelligence, which are quoted from a sample study, are given in Figure 1 [9].

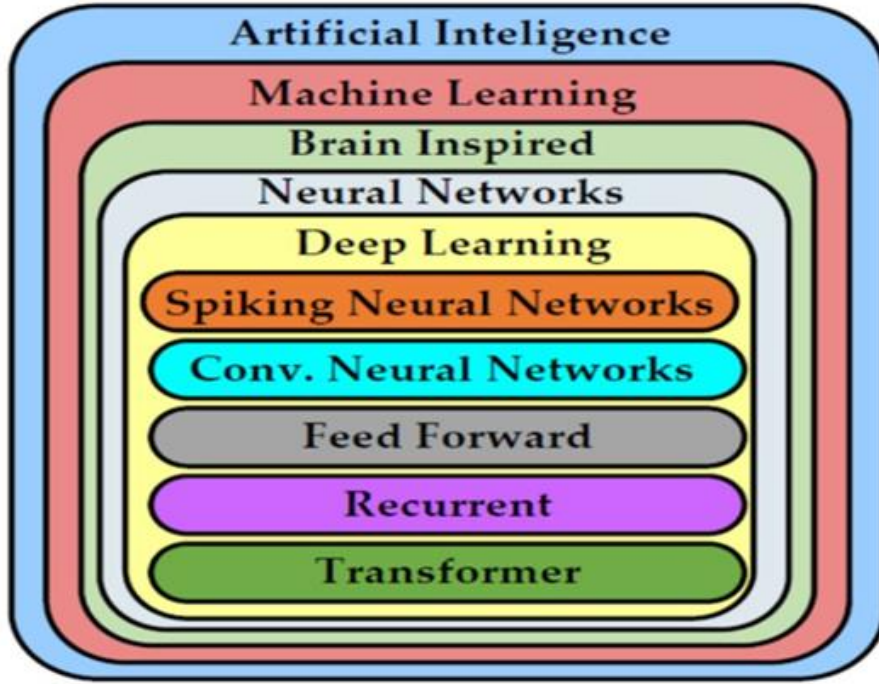


Figure 1. The taxonomy of artificial intelligence.

Machine Learning

Some information about machine learning is given above. Again, to give information about this topic; It is a set of algorithms that parse data sets and then learn to apply what has been learned to make informed decisions. It imitates human intelligence. It consists of the training and testing phase. At the learning stage, a new model is created by using the examples in the data set and learning the algorithms and features into the system. As a result, the desired results can be achieved by estimating the trial data with the Learning model application engine [10-11-12]. It imitates human intelligence. It consists of the training and testing phase. At the learning stage, a new model is created by using the examples in the data set and learning the algorithms and features into the system. As a result, estimates are made for the trial data with the Learning model application engine. The results obtained are successful [10-11-12]. The single most important concept from calculus in the context of machine learning is the gradient. Gradients generalize derivatives to scalar functions of several variables. The gradient of $f: \mathbb{R}^d \rightarrow \mathbb{R}$, denoted ∇f , is given by [13]. An example theorem used for machine learning is given in Equation 1.

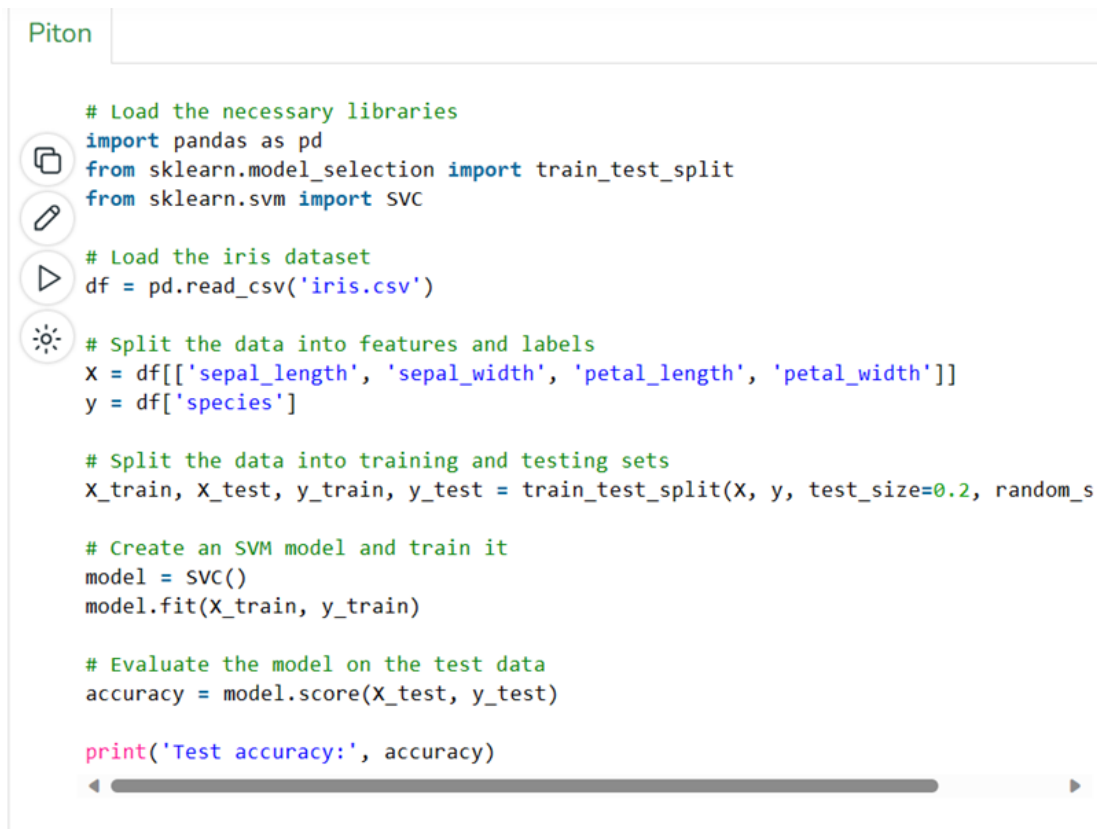
$$\nabla f = \begin{bmatrix} \frac{\partial f}{\partial x_1} \\ \vdots \\ \frac{\partial f}{\partial x_n} \end{bmatrix} \quad \text{i.e.} \quad [\nabla f]_i = \frac{\partial f}{\partial x_i} \quad (1)$$

Literature review of studies conducted through mathematical codes used within the scope of machine learning

In this section, a literature search was conducted for scientific studies that make human life easier by using machine learning and mathematical functions. The bibliographies of the findings obtained are indicated. Machine learning is the ability of computers to make decisions and create solutions about similar events that will occur in the future by learning information and experiences related to an event in another language [15]. For example; Hegg's rule If cell A is close enough to stimulate cell B and is constantly involved in activating cell B, changes can be made to one or both cells so that the effectiveness of cell A is increased [14]. Again, to briefly mention a mathematical algorithm; the self-learning algorithm updates a memory matrix $W = |w(a,s)|$ So that it can execute the following machine learning procedure at each iteration: Perform the action A in case S, get the result state s' , Calculate the Feeling of Being in the Result State $V(s')$

Update the crossbar memory $w'(a,s) = w(a,s) + v(s')$ [16]

The following is an example excerpt from a website; a simple example of machine learning in Python that shows how to train a model to predict the types of iris flowers based on dish leaf and petal measurements is given below [17]:



```

Piton

# Load the necessary libraries
import pandas as pd
from sklearn.model_selection import train_test_split
from sklearn.svm import SVC

# Load the iris dataset
df = pd.read_csv('iris.csv')

# Split the data into features and labels
X = df[['sepal_length', 'sepal_width', 'petal_length', 'petal_width']]
y = df['species']

# Split the data into training and testing sets
X_train, X_test, y_train, y_test = train_test_split(X, y, test_size=0.2, random_s

# Create an SVM model and train it
model = SVC()
model.fit(X_train, y_train)

# Evaluate the model on the test data
accuracy = model.score(X_test, y_test)

print('Test accuracy:', accuracy)

```

Figure 2. Estimation of iris flower species in Python based on dish leaf and petal measurements [17]:

As can be understood from Figure 2, the reference number given above, a mathematical software is being developed by coding. In a different study, dentists used artificial intelligence. Analysis has been performed in orthodontics using artificial intelligence and machine learning. The results obtained have been positively shared with the literature [18]. In a different study, they tried to diagnose Breast Cancer on the Kent Ridge 2 data set with the help of machine learning techniques, mathematical codes were used in the results obtained. It is understood that the results offer positive contributions to the literature [19]. In a dark study conducted by; they used the traditional classification method and SVM algorithm from machine learning algorithms for the detection of diabetes disease. As a result, they detected the disease with a success rate of 0.924 [20]:

Conclusion

In this study, literature studies on the applicability of machine learning, which is a sub-branch of artificial intelligence, through mathematical correlations were examined. In the study, the definition of machine learning was made and the applications of mathematical function were investigated. In the results of the study, it is thought that machine learning can be used to make inferences with mathematical techniques along with software and data prepared in a desired study.

References

1. <https://www.oracle.com/tr/artificial-intelligence/machine-learning/what-is-machine-learning/>
2. https://erdincuzun.com/makine_ogrenmesi/makine learning-methods/
3. Davis, J., Edgar, T., Graybill, R., Korambath, P., Schott, B., Swink, D., ... & Wetzel, J. (2015). Smart manufacturing. Annual Review of Chemical and Biomolecular Engineering, 6, 141-160. <https://doi.org/10.1146/annurev-chembioeng-061114-123255>
4. <https://cig-rdlab.gitbook.io/ml/lectures/zanyatie-1>
5. <https://practicum.yandex.ru/blog/chto-takoe-mashinnoe-obuchenie/>
6. Vaishya, R., Javaid, M., Khan, I. H., & Haleem, A. (2020). Artificial Intelligence (AI) applications for COVID-19 pandemic. Diabetes & Metabolic Syndrome: Clinical Research & Reviews, 14(4), 337-339. <https://doi.org/10.1016/j.dsx.2020.04.012>

7. Li, J. H. (2018). Cyber security meets artificial intelligence: a survey. *Frontiers of Information Technology & Electronic Engineering*, 19(12), 1462-1474. <https://doi.org/10.1631/FITEE.1800573>
8. Wang, H., Feng, Y., Xing, B., Zhang, X., Wang, Z., Wu, J., & Huang, X. (2021). A Blockchain-based Protocol for Power Data Preservation in Ping Dingshan vs. Wang Case. In 2021 IEEE 4th International Conference on Electronics and Communication Engineering (ICECE), 43-48. <https://doi.org/10.1109/ICECE54449.2021.9674419>
9. Khan, F. H., Pasha, M. A., & Masud, S. (2021). Advancements in microprocessor architecture for ubiquitous AI— An overview on history, evolution, and upcoming challenges in AI implementation. *Micromachines*, 12(6), 665. <https://doi.org/10.3390/mi12060665>
10. <https://www.ibm.com/topics/machine-learning>
11. Sandhya, N., & Charanjeet, K. R. (2016). A review on machine learning techniques. *International Journal on Recent and Innovation Trends in Computing and Communication*, 4(3), 451-458.
12. <https://www.oracle.com/tr/artificial-intelligence/machine-learning/what-is-machine-learning/>
13. Thomas, G. (2018). *Mathematics for Machine Learning*. PHD Thesis, University of California, Berkeley, 47.
14. Hebb, D. O. (2005). *The organization of behavior: A neuropsychological theory*. Psychology press.
15. https://en.wikipedia.org/wiki/Machine_learning
16. Öztemel, E. (2006). *Yapay sinir ağları*. Papatya Yayınevi.
17. <https://www.geeksforgeeks.org/getting-started-machine-learning/>
18. Büyük, S. K., & Hatal, S. (2019). Artificial intelligence and machine learning in orthodontics. *Ortadoğu Tıp Dergisi*, 11(4), 517-523. <https://doi.org/10.21601/ortadogutipdergisi.547782>
19. Bektaş, B., & Babur, S. (2016). Performance Evaluation of Breast Cancer Diagnosis Using Machine Learning Techniques, *TipTekno"16 Medical Technologies Congress*, October 27-29, Antalya.
20. Jain, D., & Singh, V. (2018). Feature selection and classification systems for chronic disease prediction: A review. *Egyptian Informatics Journal*, 19(3), 179-189. <https://doi.org/10.1016/j.eij.2018.03.002>



Determination of long-term water surface level change in lakes by integration of UAV and satellite data and future estimation with ARIMA

Yunus Kaya*¹, Fusun Balik Sanli ², Saygin Abdikan ³

¹Harran University, Department of Geomatics Engineering, Türkiye, yunuskaya@harran.edu.tr

²Yildiz Technical University, Department of Geomatics Engineering, Türkiye, fbalik@yildiz.edu.tr

³Hacettepe University, Department of Geomatics Engineering, Türkiye, sayginabdikan@hacettepe.edu.tr

Cite this study: Kaya, Y., Şanlı, F. B., & Abdikan, S. (2023). Determination of long-term water surface level change in lakes by integration of UAV and satellite data and future estimation with ARIMA. *Advanced Engineering Days*, 8, 8-11

Keywords

ARIMA
Future estimation
Water surface level
Unmanned Aerial Vehicle
Remote sensing

Abstract

Lakes are the largest element of freshwater bodies on the Earth's surface and play an important role in the Earth's water cycle. Inland water bodies, such as natural lakes and human-made reservoirs, are vital for supplying drinking water. Some saltwater lakes, such as Lake Burdur, are not used for drinking water but are home to endangered animal and plant species. Accurate and regular monitoring of inland water bodies and estimation of future water levels are crucial for ecological conservation and management of water resources. In this study, the water surface level (WSL) changes in Lake Burdur, a Ramsar site, between 1984 and 2022 were investigated by integrating the Digital Elevation Model (DEM) obtained by Unmanned Aerial Vehicle (UAV) and shoreline information obtained from Landsat mission. In addition, annual water level elevation changes between 2022 and 2040 were estimated with the AutoRegressive Integrated Moving Average (ARIMA) time series analysis model. As a result of the study, correlation between water level and reference data was determined with $r=0.999$ and an average error margin of 31 cm. In the future forecast obtained with the ARIMA model, it is seen that the water level height decreases to 830,61 m.

Introduction

Water bodies play a critical role in socio-economic development, the establishment of healthy ecosystems, energy, and food production [1]. Inland water resources such as lakes and dams are vital for people, animals, and plants that depend on wetlands. Lakes are important components of water ecosystems in regulating regional climates, providing water resources, and maintaining ecological balance [2]. Lakes such as Lake Burdur, which are home to some plants and animals despite being salty water, also play an important role in the protection and maintenance of living ecosystems. However, lakes are among the most sensitive and fragile aquatic ecosystems. Natural factors and anthropogenic activities can cause rapid short-term changes in lakes [3].

Remote sensing data has become important for earth observation since the launch of the first satellite. Landsat satellite data have been among the most widely used, especially since the United States Geological Survey (USGS) announced in 2008 that the images would be freely available [4]. Although optical images can successfully identify spatial changes in lakes, they do not provide information about water surface level (WSL). Unmanned Aerial Vehicles (UAVs), which have been used in many areas in the last decade, allow the collection of earth information more precisely than most satellite remote sensing data due to their high resolution. However, since UAVs do not have a predetermined flight plan like satellite systems, these studies focus only on current WSLs, making it difficult to assess long-term changes in WSL. In the literature review, no study was found to determine the changes in WSLs from past to present using DEMs on the lakeshore.

It is important to make estimates for the future as well as precise determinations of WSLs in terms of water resources management and action planning. The AutoRegressive Integrated Moving Average (ARIMA) model is used to estimate future WSL [5]. In this study, the WSL of Lake Burdur, a Ramsar site, was determined by UAV and Landsat integration. The obtained water level heights were then used to predict future WSLs.

Material and Method

UAV Based DEM

UAV flights were performed from 6 different locations homogeneously distributed around Burdur Lake, which was selected as the study area and is the largest Ramsar site in Turkey. Ground control points (GCPs) were used for each UAV flight to increase horizontal and vertical accuracy. Orthophotos and Digital Elevation Models (DEMs) were produced by evaluating the photographs obtained from UAV flights with the Structure from Motion (SfM) algorithm together with GCPs.

Determination of Shoreline with Landsat Data

In order to determine the shoreline of the lake, Landsat images from June of each year were used. Suitable (cloud-free) images covering the study area were processed by Google Earth Engine (GEE), a cloud-based geographic analysis platform, to determine the shoreline. Water and non-water areas were determined using the Modified Normalized Difference Water Index (MNDWI), Automatic Water Extraction Index (AWEI) and Normalized Difference Vegetation Index (NDVI) (Table 1). After the indices were calculated, the pixels were filtered using Eq. (4) to obtain the lake area.

Table 1. Water and vegetation indices used in the study.

$MNDWI = \frac{(Green - SWIR)}{(Green + SWIR)}$	(1)
$AWEI = 4 * (Green - SWIR2) - (0.25 * NIR + 2.75 * SWIR1)$	(2)
$NDVI = \frac{(NIR - Red)}{(NIR + Red)}$	(3)

$$\text{Lake} = NDVI < 0 \text{ and } MNDWI > 0 \text{ and } AWEI > 0 \quad (4)$$

Points were generated at 2 meters intervals on the shorelines. Then, UAV based DEMs were integrated with the points. The heights of the point were determined from the DEM data closest to the point. Outliers in the generated points were eliminated with the Interquartile range (IQR) method [6]. Since the ellipsoidal height obtained from UAV data does not represent the water level height, the ellipsoidal heights were converted to orthometric heights using Eq. (5).

$$H = h - N \quad (5)$$

Where;

H represents the orthometric height,

h represents the ellipsoidal height,

N represents the geoid height.

Average WSLs were obtained by averaging all points converted to orthometric heights.

Future WSL Estimation with ARIMA Model

ARIMA is a data analysis model used to determine the dynamics of time series and includes AutoRegressive (AR), Integrated (I), and Moving Average (MA) components [7]. AR behaves like a multiple regression model. However, it uses past values of the same series instead of external factors. The AR process is commonly used in time series where the current value is directly influenced by previous values. The MA model is a time series analysis that investigates the link between the current value of a time series and previous error components or residual values. It is a statistical model that recognizes that the current value of a series is driven by a linear combination of error terms at past time points. 'I' eliminates any trends or seasonality in the data by measuring the difference between consecutive data.

Results

Water surface level and accuracy analysis

The shorelines of the lake were determined from cloud-free Landsat data in June from 1984 to 2022. Points were created at 2-meter intervals along the shorelines, to which elevation information was added from a high-

resolution UAV-based DEM. Outliers between points were removed using the IQR method. Orthometric heights were then obtained by subtracting the geoid height in the flight area from the ellipsoidal heights. After removing the outliers, the measurement accuracy was significantly improved in some years. The difference between the non-filtered and filtered dataset and the reference value was 30 cm and 21 cm, respectively (Figure 2). This indicates that removing outliers improved the overall accuracy by 9 cm. Across all 39 years of dates, the maximum WSL was 854,466 m in 1984 and the minimum WSL was 838,226 m in 2022. Over 38 years, the WSL increased only between 2002 and 2004, with a downward trend in all other years (Figure 1). There is a 99.9% correlation between the calculated WSL and the reference data.

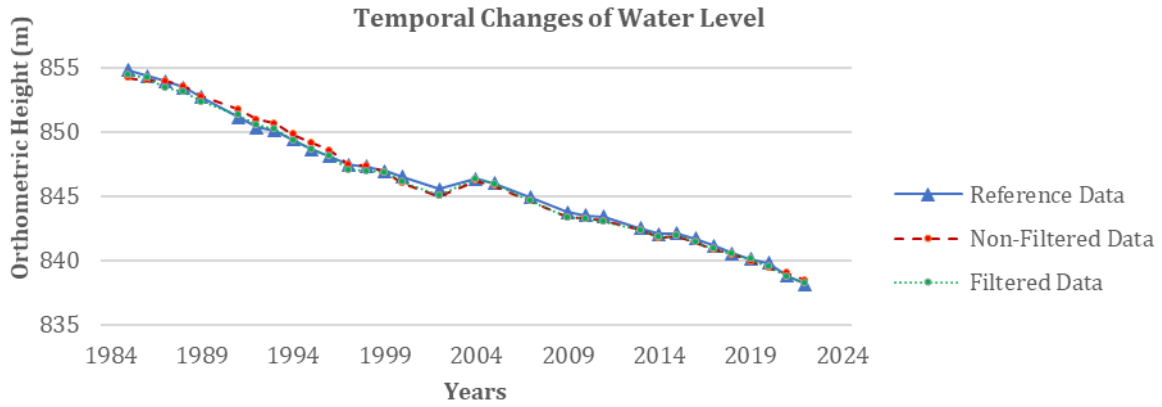


Figure 1. Temporal changes of water level with filtered, non-filtered and reference data [Adopted from [8]]

Future Estimation with ARIMA Model

In order to determine future WSLs with the ARIMA model, 70% of the 39 years of elevation data produced between 1984 and 2022, i.e. 27 of them (1984-2010) were used as the train set and 30% (2011-2022) was used as the validation set. In the study, the p parameter of the AR model and the d parameter of the I model are taken as 1 [7]. For the q parameter, a combination between 0-3 values was made. The accuracy of the validation set was investigated using different parameters (Table 2).

Table 2. Different ARIMA parameters and accuracy.

Parameters	RMSE (m)	Correlation
1, 1, 0	0.45	0.99
1, 1, 1	0.46	0.99
1, 1, 2	0.45	0.99
1, 1, 3	0.43	0.99

The most appropriate parameter was ARIMA (1, 1, 3), which has the least Root Mean Square Error (RMSE). Then, future estimation was performed with ARIMA (1, 1, 3) parameters for the years 2023-2040 (Figure 2).

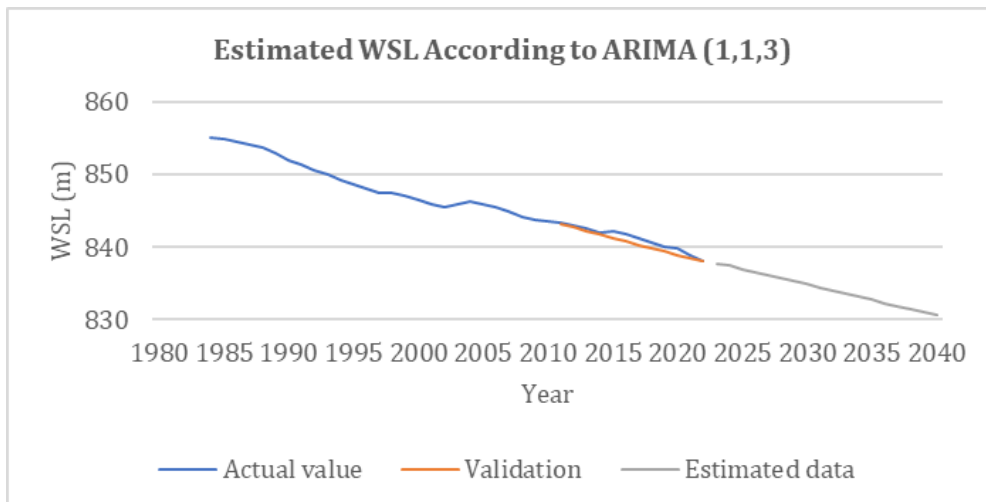


Figure 2. Estimation of WSLs between 2023 and 2040 with ARIMA model.

Conclusion

It is important to determine lake WSL changes and to plan water management using future WSL estimation. In this study, we investigated the long-term changes of WSLs using UAV-Landsat integration. We found a high correlation of $r=0.999$ between the calculated WSL and reference elevations, and the average ΔH elevation error was 21 cm. The ARIMA model was also used to estimate the WSL for the next 18 years.

Our proposed method for WSL determination in inland waters has the advantage of long-term change detection and high accuracy and correlation compared to other methods. In addition, future WSL estimation can be used as data for environmental planning on the lake.

Acknowledgments

The authors would like to acknowledge that this conference paper is submitted in partial fulfillment of the requirements for the PhD degree at Yildiz Technical University. We would like to thank the General Directorate of Mapping for providing local geoid height data and the General Directorate of State Hydraulic Works for the ground truth data.

References

1. Tottrup, C., Druce, D., Meyer, R. P., Christensen, M., Riffler, M., Dulleck, B., ... & Paganini, M. (2022). Surface water dynamics from space: a round robin intercomparison of using optical and sar high-resolution satellite observations for regional surface water detection. *Remote Sensing*, 14(10), 2410. <https://doi.org/10.3390/rs14102410>
2. Yang, K., Smith, L. C., Andrews, L. C., Fettweis, X., & Li, M. (2022). Supraglacial drainage efficiency of the Greenland Ice Sheet estimated from remote sensing and climate models. *Journal of Geophysical Research: Earth Surface*, 127(2), e2021JF006269. <https://doi.org/10.1029/2021JF006269>
3. Bridgewater, P., & Kim, R. E. (2021). The Ramsar convention on wetlands at 50. *Nature Ecology & Evolution*, 5(3), 268-270. <https://doi.org/10.1038/s41559-021-01392-5>
4. Pardo-Pascual, J. E., Sánchez-García, E., Almonacid-Caballer, J., Palomar-Vázquez, J. M., Priego De Los Santos, E., Fernández-Sarría, A., & Balaguer-Beser, Á. (2018). Assessing the accuracy of automatically extracted shorelines on microtidal beaches from Landsat 7, Landsat 8 and Sentinel-2 imagery. *Remote Sensing*, 10(2), 326. <https://doi.org/10.3390/rs10020326>
5. Khatibi, R., Ghorbani, M. A., Naghipour, L., Jothiprakash, V., Fathima, T. A., & Fazelifard, M. H. (2014). Inter-comparison of time series models of lake levels predicted by several modeling strategies. *Journal of Hydrology*, 511, 530-545. <https://doi.org/10.1016/j.jhydrol.2014.01.009>
6. Yuan, M., Yin, W., Tao, Z., Tan, W., & Hu, Y. (2020). Association of radiologic findings with mortality of patients infected with 2019 novel coronavirus in Wuhan, China. *PloS one*, 15(3), e0230548. <https://doi.org/10.1371/journal.pone.0230548>
7. Hossain, M. M., & Abdulla, F. (2015). Forecasting the sugarcane production in Bangladesh by ARIMA model. *Journal of Statistics Applications & Probability*, 4(2), 297-303.
8. Kaya, Y., Sanli, F. B., & Abdikan, S. (2023). Determination of long-term volume change in lakes by integration of UAV and satellite data: the case of Lake Burdur in Türkiye. *Environmental Science and Pollution Research*, 1-19. <https://doi.org/10.1007/s11356-023-30369-z>



Analysis of bus accidents by use of geographic information systems

Mehtap Sagir Kayim^{*1}, Ugur Alganci², Dursun Zafer Şeker²

¹Istanbul Technical University, Graduate School, Geographical Information Technologies Program, Türkiye, sagirme@itu.edu.tr

²Istanbul Technical University, Department of Geomatics Engineering, Türkiye, alganci@itu.edu.tr, seker@itu.edu.tr

Cite this study: Kayım, M. S., Algancı, U., & Şeker, D. Z. (2023). Analysis of bus accidents by use of geographic information systems. *Advanced Engineering Days*, 8, 12-14

Keywords

Bus accidents
GIS
Traffic congestion
Heatmap

Abstract

In today's modern world, Geographic Information Systems (GIS) play an important role in effectively processing intricate location data. This multi-purpose technology is successful in collecting, storing, processing and managing location-related data in various fields such as City Information Systems, Traffic Information Systems, Vehicle Tracking Information Systems and Map Information Systems. Its applications contain multiple sectors, greatly improving our lives and providing solutions to numerous challenges. Notably, GIS holds promise in metropolises where high population density and excessive vehicle use cause traffic congestion and accidents. The process begins with the compilation of historical accident data, creating datasets for meaningful analysis. This analysis reveals accident-prone locations, paving the way for targeted improvements and accident reduction. Considering Istanbul, a metropolis where daily public transportation served 8,095,092 passengers in 2023, faced an average of 45 bus accidents per day. In this study, it is examined how GIS can be combined with public transportation analysis and what kind of improvements can be made to prevent these accidents.

Introduction

Road transport systems form the basis of public transport and provide economical and efficient mobility for millions of people. In big cities like Istanbul, public buses are an integral part of daily life. The use of public buses in public transportation is quite common. Unfortunately, accidents are unavoidable. In our country, it is reported that a traffic accident occurs every 45 minutes, resulting in the loss of 10-15 lives each day and an annual economic loss of up to 5 quadrillion. Traffic accidents are a significant cause of death worldwide, with approximately 50% of all accidents resulting in fatalities. In one year, an average of 45,000 people lose their lives in traffic accidents in the United States, 8,000 in Italy, 8,500 in France, 2,000 in Greece, 1,300 in the Netherlands, and 6,000 in our country [1,2]. These statistics highlight the importance of traffic safety and the need for measures to reduce accidents.

Identifying the common causes of accidents is an important step in reducing accidents. Main causes can be listed below:

- **Driver Error:** One of the most common causes of accidents is driver errors. This includes errors such as distraction (texting, talking on the phone), tiredness, driving under the influence of alcohol or drugs, misjudging road conditions, poor driver training, experience and driving ability.
- **Excessive Speed:** Driving at speeds higher than recommended or inappropriate for current road conditions can increase stopping distances and cause collisions.
- **Mechanical Failures:** Mechanical failures of the bus (from brake or steering failure to tire blowout) can lead to accidents.
- **Road and Weather Conditions:** Poor road conditions such as potholes and bumps or adverse weather conditions such as fog, snow, heavy rain can make driving dangerous.
- **Traffic Congestion:** The unpredictability of other road users in heavy traffic can be a challenging process for bus drivers to manage.

- Blind Spots: The large design of buses can result in blind spots, increasing the risk of accidents [3].

Traffic accidents are a natural and unavoidable event. However, measures need to be taken by the relevant authorities to reduce deaths and injuries. GIS tools are used to determine what measures should be taken in specific road segments or intersections. With the help of available data, expected accidents can be predicted in the relevant road segment. This is an important tool in making strategic decisions to enhance traffic safety [4]. The resources allocated to efforts to reduce traffic accidents are insufficient. Identifying areas with high accident rates is a critical step for conducting cost-benefit analyses. This information is necessary to ensure the most effective use of resources and thus minimize accidents in the riskiest areas [5].

This study aims to examine the causes of bus accidents that have occurred in the last five years in detail, identify the geographical points where these accidents occur, and provide recommendations for these areas.

Material and Method

Creating and querying the database is one of the most critical stages of the study. In this process, the use of Geographic Information Systems (GIS) technology plays an important role in querying data and processing the results with statistical and geographical analysis. GIS is more advantageous than other information systems because it can store geographical data and process them on the map. These features allow users to more easily query and visually perceive their data, and this has been successfully used for accident analysis of buses used in public transportation in the city of Istanbul [6]. Heat map is a two-dimensional visualization technique created by coloring the map. The clustering of the data can be clearly seen from the tone change in the colors. It provides a great advantage to the user in the analysis of complex data [7].

This study aims to create a heat map showing the geographical distribution of accidents using accident data collected between 2018 and 2023. This map will clearly show areas with high accident rates across the city and will be used to improve traffic safety and identify accident prevention strategies. The accident data for the period 2018-2023 is parameterized as Route Code, Bus Number, Latitude/Longitude Points, and Time (Table 1). The use of these parameters will help in better understanding the causes of accidents and, particularly, in identifying trends in accidents concerning geographical location and time.

Table 1 – An example of data transformation for accident data.

DateTime	Latitude	Longitude	RouteCode	BusNumber
23/09/30 20:19:26	40,991577	28,8447037	146	A-1709
23/09/30 17:31:58	41,014015	29,1896172	131T	C-971
23/09/30 16:55:45	41,041008	29,0858173	11Y	M2281
23/09/30 16:40:11	40,979775	29,0831318	19F	C-1516
23/09/30 16:10:59	41,092545	28,8640785	36V	O2285
23/09/30 15:34:59	41,154152	28,6197681	336H	K1578
23/09/30 14:11:04	41,032085	28,8340900	97GE	A-1836
23/09/30 12:19:13	41,011590	28,7921352	98	M2528
23/09/30 12:07:24	41,066284	28,7306600	78Ş	T1008
23/09/30 09:44:28	41,037990	29,0668583	15ÇK	C-1779
23/09/30 08:06:34	41,028233	29,0744343	15ÇK	C-1779
23/09/30 07:00:56	41,091705	28,9883823	DT1	B-259

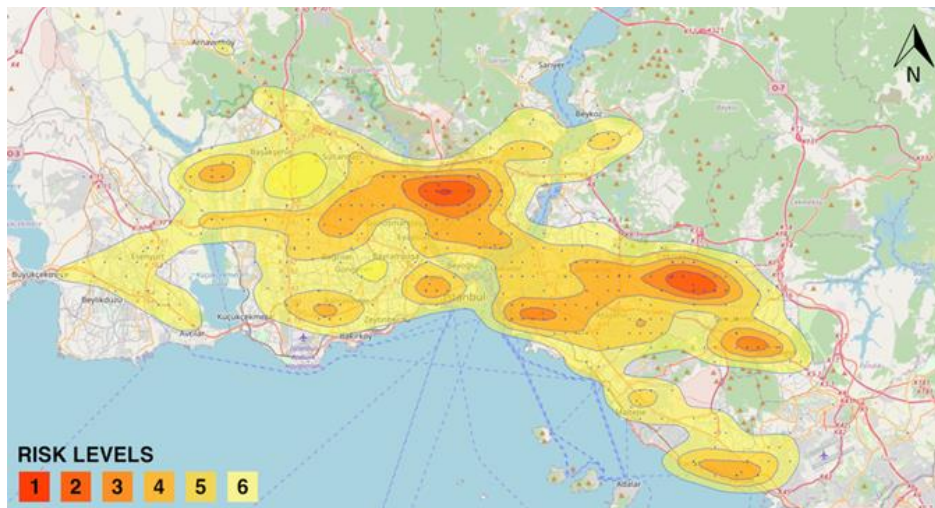


Figure 1. Heat Map of Bus Accidents in Istanbul Province's Public Transportation.

After preparing the accident data table, a heat map representing the geographical distribution of accidents that occurred in Istanbul is created using this data. This heat map is designed to prominently display areas with high accident rates across the city (Figure 1). Such a map is a critical tool, especially for identifying points with high accident frequency and planning measures that can be taken to prevent accidents in relevant areas, and can be used to increase traffic safety and determine accident prevention strategies.

Results

The heat map in Figure 1 provides a color-coded image showing accident densities in Istanbul. Red areas represent highly dense accident points, orange areas represent dense accident points, and light orange areas represent less dense accident points.

According to the analysis results, there are areas where accidents are concentrated on both the Anatolian side and the European side. While the area where accidents are concentrated on the European side includes Şişli, Kağıthane and Alibeyköy districts; On the Anatolian side, the areas where accidents are most common are Dudullu, Sarıgazi and Kirazlıdere districts. There are intercity bus terminals in Alibeyköy district on the European side and Dudullu district on the Anatolian side. There are public transport bus garages in Kağıthane district on the European side and Sarıgazi district on the Anatolian side. Şişli district, also located on the European side, is the busiest stop of the Metrobus system, with a daily passenger count of 1,000,000. As can be understood from here; these centers are very busy main stops. To reduce these accidents that occur in the main centers where public transport buses, intercity buses and transfer points are very dense, the bus terminals and garages in these centers should be moved out of the city or the roads should be widened.

Discussion

One of the most important pieces of information needed in accident analysis is the geographical location where accidents occur. Geographic location provides a lot of information to solve the problem. The cause of the accident that occurred in the same place for similar reasons may also be the same. Therefore, analyzing the geographical locations of accidents with GIS is correct in terms of ensuring traffic safety [8]. Categorizing accident areas in this manner assists in determining what improvements need to be made in relevant locations. This information can be utilized in prioritizing traffic regulations and safety measures. This study provides a road map aimed at preventing bus accidents using geographic information technologies, and such analyzes are an important step to increase traffic safety.

Conclusion

In this study, the causes of bus accidents are summarized and their spatial distribution is analyzed with the use of GIS tools. This analysis helped to understand some of the reasons behind accidents and results provided that main bus accident locations are corresponding to main bus stations where the number of busses and general traffic density is high. This study was designed to guide the process of developing preventive measures using strategic planning and data.

References

1. Erdoğan, S., & Güllü, M. (2004). Coğrafi bilgi sistemleri ile trafik kazalarının analizi: Afyon Örneği. *Jeodezi ve Jeoinformasyon Dergisi*, (91), 29-33.
2. SIS (State Statistics Institute): (2003). Highway Traffic Accident Statistics, Ankara
3. Rolison, J. J., Regev, S., Moutari, S., & Feeney, A. (2018). What are the factors that contribute to road accidents? An assessment of law enforcement views, ordinary drivers' opinions, and road accident records. *Accident Analysis & Prevention*, 115, 11-24. <https://doi.org/10.1016/j.aap.2018.02.025>
4. Dereli, M.A., Erdoğan, S., Soysal, Ö., Çabuk, A., Tiryakioğlu, İ., Akbulut, H., Dündar, S., Yalçın, M., Gülal, A.E., Kantar, M., & Arslan, Y. (2015). Coğrafi bilgi sistemleri destekli trafik kaza kara nokta belirleme: ampirik Bayes uygulaması. *Harita Teknolojileri Elektronik Dergisi*, 7(2), 36-42. <https://doi.org/10.15659/hartek.15.06.69>
5. Yılmaz, İ., Erdogan, S., Baybura, T., Güllü, M., & Uysal, M. (2007). Coğrafi Bilgi Sistemi Yardımıyla Trafik Kazalarının Analizi. *Afyon Kocatepe Üniversitesi Fen Ve Mühendislik Bilimleri Dergisi*, 7(2), 135-150.
6. Tuncuk, M., & Karaşahin, M., (2004). Detection of traffic accident black spots using geographic information systems: The Example of Isparta. 3rd Geographic Information Systems Informatics Days, Fatih University, Istanbul.
7. <https://gislayer.com/tr/docs/editor/66-yogunluk-haritasi/>
8. Akın, D., & Eryılmaz, Y. (2001). Geographic information system supported traffic accident analysis. *Geographic Information Systems Informatics Days*, 13-14 November, Fatih University, Istanbul,



Advanced Engineering Days

aed.mersin.edu.tr



GIS-based analysis approach for metro and bus integration in public transportation

Muhammed Semih Solak¹, Ugur Alganci², Dursun Zafer Şeker²

¹Istanbul Technical University, Graduate School, Geographical Information Technologies Program, Türkiye, solakmuh@itu.edu.tr

²Istanbul Technical University, Geomatics Engineering Department, Türkiye, alganci@itu.edu.tr, seker@itu.edu.tr

Cite this study: Solak, M. S., Alganci, U., & Şeker, D. Z. (2023). GIS-based analysis approach for metro and bus integration in public transportation. *Advanced Engineering Days*, 8, 15-17

Keywords

Bus
Integration
GIS
Metro
Public Transport

Abstract

In metropolitan cities, public transportation is always a sign of civilization. Geographic information Systems (GIS) aided map-based applications play an important role in studies on public transportation. Within the scope of this study, Istanbul Transportation payment system data, all trip data and public transportation routes are evaluated together. Integration and optimization studies have been carried out between buses and metros with the use of these data sets. Study; the route started by importing the stops, routes and timetables for all modes into the Visum simulation model. All fare systems applied in Istanbul were integrated into the model separately. District-based analyses were made for the randomly selected day of May 22, 2023, and passenger movements were analyzed in hourly breakdowns. The movements of 7,693,856 daily trips made by a total of 4,414,292 passengers were examined. Analyzes of the current model and actual trip values were performed. Hourly-based travel analyses were realized. It has shown that GIS can be used efficiently in integrated transportation for Istanbul.

Introduction

In our changing and developing world; the population of cities that are symbolic in historical, social, economic and touristic terms is increasing day by day. The increasing population also brings with it infrastructure and superstructure investments in many areas. In addition, increment in attraction centers along with population growth and the expansion of the city also cause many problems in terms of transportation. In a time when the analytical world and big data are so developed, it is inevitable to direct investments correctly by making future modeling and simulation studies using all possible data. Integration is a set of practices that will improve the reliability and accessibility of the public transportation system and make it more attractive than the use of private vehicles [1]. Istanbul is a city where 10 metro lines are under construction at the same time. Bus integration is inevitable for subways under construction. Determining integration points and using simulation models and location-based services to reorganize at these points is an efficient method for future planning. Considering the available bus lines in Istanbul, it was planned to have direct lines from the neighborhoods to as many centers as possible.

As a result of lines coming to the center from as many neighborhoods as possible, corridors were formed where 40-50 lines pass from the same point. Since these corridors are on main arteries (Anatolian Side: E-5, European Side: Unkapanı, Millet Caddesi, Şişli), bus lines are exposed to private vehicle traffic. This situation reduces the efficiency of bus lines as a result of extending travel and waiting times at the stop. The main line feeder line model is a model that has been successfully implemented in many countries. Considering the metros as main lines and feeding the metros with bus lines, allows reducing parallel routes and using resources efficiently. This study aims to represent new metro networks in the model and to develop a model that will accurately predict integration points.

Material and Method

The hourly Origin-destination (OD) matrices were created in line with Istanbul Transportation payment system data obtained from trips in the field. It gives the passengers' journeys during the day with determined

algorithms. All roads in Istanbul are divided into 99 types according to the number of lanes and free flow speed. The work was done in ArcGIS base and was imported into Visum with shape format. All stops and lines have been integrated into the Visum network. The stops are divided into zones. Daily OD stop-zone matches have been provided. All lines in the public transportation system are defined in the model with their departure times. Assignments are made based on timetable, not headway. The Visum model can be run with 4 different assignment models. The parameter we chose for Istanbul is the Kirchoff principle [2]. Time-effect impedances that determine the travel time have been created.

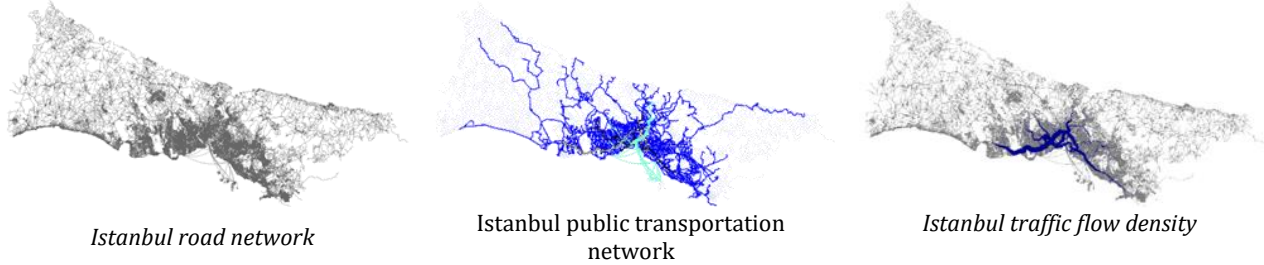


Figure 1. Current Istanbul flow chart (Visum Simulation).

In Figure 1, the flow chart created based on the road network, public transportation network and OD matrices integrated into the Visum simulation model is visualized.

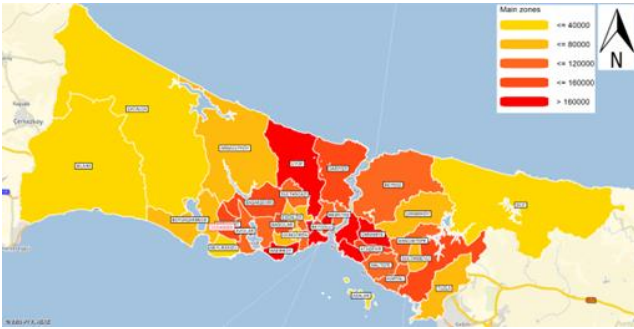


Figure 2. District-based travel density

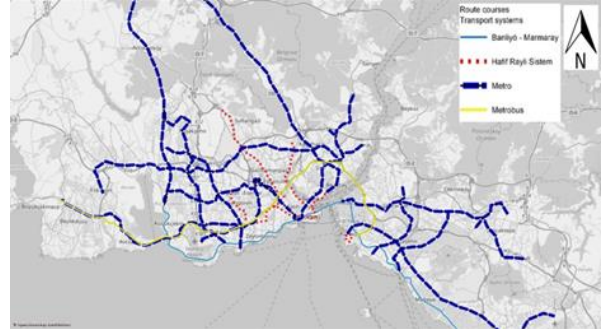


Figure 3. Existing and under-construction metro lines

In Figure 2, the distribution of transportation payment system data according to Istanbul districts is shown, and in Figure 3, the current rail system map of Istanbul and the subways under construction are shown in the Visum model. These maps are an important point in determining the integration points of metros. Integration points were determined by evaluating maps and trip data.

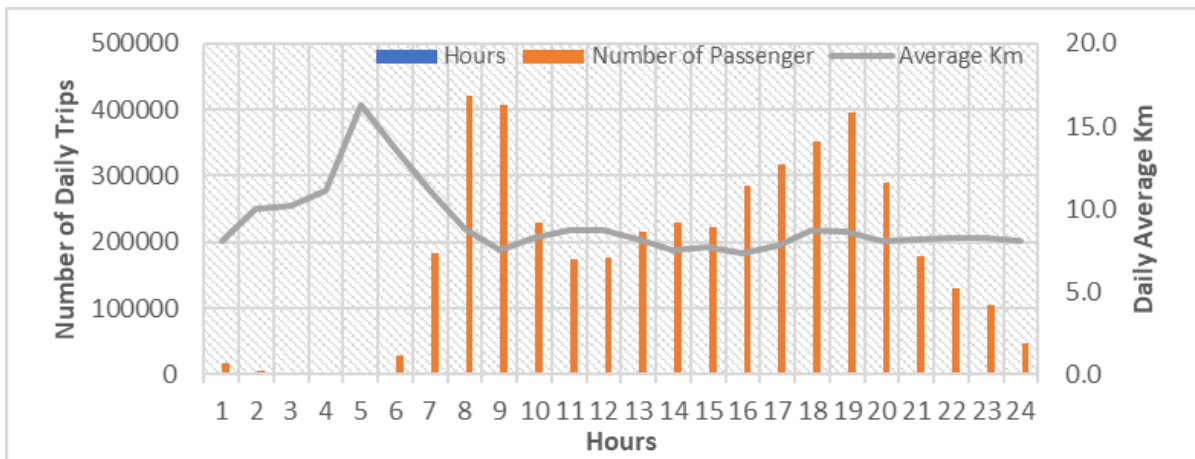


Figure 4 – Average trip and average distance per hour for May 22, 2023.

It was analyzed that there was a total of 4,414,292 trips in the OD matrix created based on transportation payment system data on May 22, 2023. The regions where these passengers are most concentrated are given in Figure 2. The number of trips made by these passengers during the day is 7,693,856 [3]. Average travel distance data was calculated with the OD we created. On average, passengers travel 9.13 km. The hourly average mileage chart of passengers is analyzed in Figure 4.

Results

In the visuals presented, it was determined in which areas the metro lines had dense travel. A representative map was created, with intensity increasing from yellow to red. The routes of the subways and the routes of the new subways to be opened were drawn in the model. Maps and analytics help identify integration points. Prioritization of integration points can also be done with stop-based analysis.

This study could be evaluated as a decisive step in establishing the integration between the metro and bus transportation.

Discussion

Integrating buses into the metro at integration points determined by identifying lines running parallel to the metro can be an efficient method. This reorganization of bus lines provides vehicle savings, unit/km savings, and reduction in CO₂ emissions, traffic congestion and waiting times. With the implementation of the project, short-term travel, high integration, comfortable transportation, sustainable transportation and reduced traffic density will be achieved. Geographic information systems and simulation applications such as Visum play an important role in realizing these projects [4].

By correctly importing the existing model and data into the model, integrated transportation plans can be made in line with planning on a macro scale. Metro and BRT routes can be identified [5].

There are many ways to create an origin-destination matrix. Some studies have used the Gravity model with O-D matrix estimation, generation, attraction, and constraint [6]. In a study conducted in Norrköping, an O-D matrix was created based on traffic counts [7]. In this study, a matrix was created with Istanbul transportation payment system data in order not to miss the daily movements of passengers. The number of passengers to be estimated for origin and destination has been reduced to a minimum.

Conclusion

In this study, the integration of Istanbul with the developing metro networks and all other public transportation modes was examined and the main line feeder line model was proposed. The main lines are determined as the regions where metros pass and the bus lines in regions where there are no metros. As the number of subways increases day by day, passengers will start to use the subways, but buses will come into play in areas where there is no rail system. As a result of the modeling, the integration points of the subways were determined with the origin destination matrix formed by transportation payment system data. It is emphasized that the subways are considered as main lines and that the bus lines operate in a structure that feeds the subways. In the model, analyzes are made using the route, stops for all modes, departure times and routes, and the focus is on identifying the right regions. An integrated transportation model is aimed with the reorganizations made in this area. In Istanbul, it has been determined that traffic density is very high during peak hours and operating speeds of bus lines fall below 15km/h. Ensuring metro and bus integration is very important for efficient use of resources.

References

1. Deveci, M., Canitez, F. & Çetin, D., N. (2015). Toplu Ulaşımında Entegrasyon Basamakları: Kavramsal Bir İnceleme, 22.
2. Uspalyte-Vitkuniene, R., & Burinskiene, M. (2008, May). Integration of public transport and urban planning. In Proc. of the 7th International Conference Environmental Engineering: Selected Papers, 3, 22-23.
3. İETT Genel Müdürlüğü, Ulaşım Planlama Dairesi Başkanlığı, İstanbul, 2023.
4. Borrego, C., Tchepel, O., Salmim, L., Amorim, J. H., Costa, A. M., & Janko, J. (2004). Integrated modeling of road traffic emissions: application to Lisbon air quality management. *Cybernetics and Systems: An International Journal*, 35(5-6), 535-548. <https://doi.org/10.1080/0196972049051904>
5. Madhavi, G., & Supriya, J. (2017). Development of BRT Network For Visakhapatnam Using Bead Tool and Visum, 237.
6. Ramli, M. I., Runtulalo, D., Yatmar, H., & Mangessi, A. (2020, June). An estimation of origin-destination matrices for a public transport network in Makassar using macrosimulation VISUM. In IOP Conference Series: Materials Science and Engineering, 875(1), 012027. <https://doi.org/10.1088/1757-899X/875/1/012027>
7. Lindström, A., & Persson, F. (2018). Estimation of hourly origin destination trip matrices for a model of Norrköping.



Analysis of security challenges in SCADA systems, a technical review on automated real-time systems

Fatmir Basholli¹, Besjana Mema², Dolantina Hyka², Albina Basholli³, Adisa Daberdini⁴

¹Albanian University, Department of Engineering, Tirana, Albania, fatmir.basholli@albanianuniversity.edu.al

²Mediterranean University of Albania, Department of Information Technology, Albania, dolantina.hyka@umsh.edu.al; besjana.mema@umsh.edu.al

³Polytechnic University of Tirana, Faculty of Mathematics Engineering and Physics Engineering, Tirana, Albania, e-mail: a.basholli@fimif.edu.al

⁴Aleksander Xhuvani University, Informatics Department, Elbasan, adisa.daberdini@uniel.edu.al

Cite this study: Basholli, F., Mema, B., Hyka, D., Basholli, A., & Daberdini, A. (2023). Analysis of security challenges in SCADA systems, a technical review on automated real-time systems. *Advanced Engineering Days*, 8, 18-22

Keywords

Cloud security
Critical infrastructure
Honeynet
Industrial control systems
SCADA

Abstract

Cybersecurity is a rapidly growing concern in many technological areas of the industrial economy. Supervisory Control and Data Acquisition (SCADA) systems are particularly vulnerable to cyber-attacks and must be equipped with the appropriate tools and techniques to detect attacks, accurately distinguish them from normal traffic, overcome cyberattacks when they are present and to prevent them from disrupting these systems. The three main goals of IT cybersecurity are confidentiality, integrity, and availability (CIA), but these three goals have different levels of importance in the technology industry operational (OT), where availability comes before confidentiality and integrity. Cloud cyberattacks are increasing rapidly, posing a major challenge to such systems. One of the layers of security in both IT and OT are honeypots. Honeypots are used as a security layer to mitigate attacks, known attacker techniques, and network and system vulnerabilities that attackers can exploit. In this paper, we recommend the use of SCADA honeypots for the early detection of possible malicious intrusions within a network of SCADA devices, where an analysis of SCADA honeypots gives us the opportunity to know which protocols are attacked most often, as well as the behaviors, locations and attackers' intentions. We use an ICS/SCADA honeypot called Conpot, which simulates real ICS/SCADA systems with several ICS protocols and ICS/SCADA PLCs.

Introduction

Hydroelectric plants, thermal plants, and water treatment plants are examples of traditional industrial systems that are designed to operate in highly controlled and segregated environments. However, the recent exposure of industrial control systems (ICS) to the Internet has made access and technological adaptation easier, which has led to the exploitation of security holes by attackers to launch attacks against ICS. These attacks can significantly affect the economy and national security of countries [1-3]. SCADA systems are considered a type of industrial control systems that allow users to monitor and control industrial processes locally or remotely through sensors and actuators. SCADA systems allow industrial organizations to operate critical infrastructure by controlling and monitoring real-time data and processes of various sectors, such as power generation systems, oil, gas, and manufacturing plants. SCADA systems have evolved from independent platform and infrastructure with proprietary communication mechanisms and protocols to Internet-based SCADA, with full integration into corporate information technology (IT) networks and the adoption of various Internet protocols such as Broadcast Control Protocol/Internet Protocol (TCP/IP) [4-6]. As complex industrial operations require efficient advanced environments, the idea of moving SCADA systems to the cloud has been proposed.

The paper highlights the potential impact of OT cyberattacks on national security and the economy and provides valuable insights into the various components of OT networks, including PLCs, RTUs, and HMIs.

Additionally, the study explores the use of honeypot technology as a security layer, and highlights the importance of investing in new security technologies. The paper concludes by discussing some of the most notable OT incidents and highlights the need for organizations to prioritize OT cybersecurity and take steps to prevent these attacks [7-10].

Material and Method

The common misconception of SCADA systems is that they are considered isolated and 'secure', with a lower chance of cyber-attack. Risk analysis and management methodologies are disproportionately focused on outdated SCADA systems, in which basic protocols are developed without regard to modern security requirements. SCADA systems are directly or indirectly connected to the Internet with corporate networks, user terminals and infrastructure as a result of its driving forces for integration with effective organizational platforms, work scheduling and intelligent power configurations [11-12].



SCADA systems are becoming more vulnerable to network vulnerabilities and Internet security threats as a result of rapid technical advances, changing operating frameworks and evolving business cultures. These changes and perspectives require an appropriate risk management strategy that includes Industrial Control Mechanisms, IT, Communications, access control, distribution networks and operations, as well as SCADA systems connected to the enterprise, network operators and Internet channels. Organizations should promote a safety culture for the SCADA system, procedures and regulations [13-15].

A SCADA network typically includes a central control server, a communications module, and one or more remote locations with field devices. Location-based SCADA sensor nodes continuously monitor various aspects of the electromagnetic apparatus, sending data to field monitoring systems such as Programmable Logic Controllers (PLCs) and Remote Terminal Units (RTUs). Field control systems will provide digital information to a command post, where software will evaluate essential data and set allowable variable limits. This information is then sent to equipment in the field, where actions are taken to reduce various risks or improve system performance. The information is stored in the data history and displayed on the Human Machine Interface (HMI), which centrally monitors the data [16-20].

Ethernet/IP, Modbus, DNP3, Profinet, and other SCADA protocols are commonly used over large geographic areas. More than a wide area network (WAN), protocols communicate over satellites, wireless or electromagnetic systems, wireless carriers, traditional telecommunications, and/or outsourced telecommunications mediums. Due to the expansion of network connectivity and online access of assets in the SCADA system, there is a risk of multiple vulnerabilities and cyber attacks. To increase the security of SCADA networks, it is vital to implement appropriate security measures [21-23].

This study addresses and examines the following aspects of automated SCADA systems:

- What is the SCADA system, what is it for and the benefits of using this system.;
- A review of relevant technologies based on the latest research and studies by designing a risk assessment framework without disturbing the environment in their future works.;
- Potential risk areas of SCADA systems and risk assessments for reducing or eliminating specific risks in the system.;
- Threat analysis and various cybersecurity challenges of cloud-based SCADA systems.

Results and Discussion

The application of the SCADA system and its impact on the management of Ujesjelles Kanalizime companies

What is SCADA?, Real-time process control system used for central monitoring and remote control of pumping station and urban wastewater treatment plant. SCADA is not just a hardware, nor a software. It is a concept, it is a system as a proper combination of hardware, software and protocol.

Why is SCADA needed?, The possibility to remotely collect different data in different places; The possibility to control the process remotely; The ability to create reports on the current and past state of the system; The ability to send the necessary information to engineers and operators in real time. Benefits of SCADA – s:

- *Allows an operator at the main facility to monitor and control the process that is distributed across different locations.*
- *Eliminates the need for service personnel to go to each location for inspection.*
- *Data collection.*

- Real-time monitoring, system modification, problems, increasing equipment life, automatic report generation.
- Reduction of operating cost.
- Provides instant system performance information.
- Improves system efficiency and performance.
- Reduces the number of worker hours (labor cost) needed for defects or services.
- Compliance of facilities with regulatory agencies through automatic report generation.

Practical implementation of SCADA at a Pump Station

The Station Control System, the local SCADA is composed of two identical workstations (ws01 & ws02) with additional software that allows the completion of the operating station. The architecture of the SCADA System is client / server. The server is responsible for managing and maintaining the underlying data where the process data is kept. Customer access process data through service calls. SCADA at the ADM building has workstation ws03 which exchanges data with TPS_PLC through level 2 Ethernet LAN, the protocol it connects to is TCP / IP.

Telecontrol

The telecontrol system is composed of appropriate software and electronic equipment in order to ensure the safe and reliable transfer of data for commands, measurements, statuses and alarm signals between the control center and individual units.

SCADA - Wastewater Treatment Plant (application project)

PLC1 is located in the Operations Building and is responsible for:
Cooling and Heating System; UPS.

PLC2 is located at the Inlet Pump Station and is responsible for:
Inlet Pumps 1, 2; Fine Shutters 1,2; Spiral Pump; MCC fan

PLC3 is located in the Operations Building and is responsible for:

The first phase of aeration of the Baths; the second phase of aeration of the Baths; Water Service System; Flow Circulation Measurement. The Control System with automation at the highest level ensures that plant operators receive all the relevant information and have a reflection of the current state of all plant processes in the control room.

Grills. The cleaning of the grills takes place in 2 ways, where the first way is the control through the minimum and maximum level of water that starts the cleaning cycle of the grills; while the second mode is the automatic mode where time control is a priority since the cleaning cycle starts automatically. Aeration of the treatment tanks, the Operator will have the possibility to choose a pre-set aeration program for different cases of the current load of dirty water (50%, 75% and 100%) by means of the SCADA system [24-26].



Figure 5. Position of instruments for control and monitoring

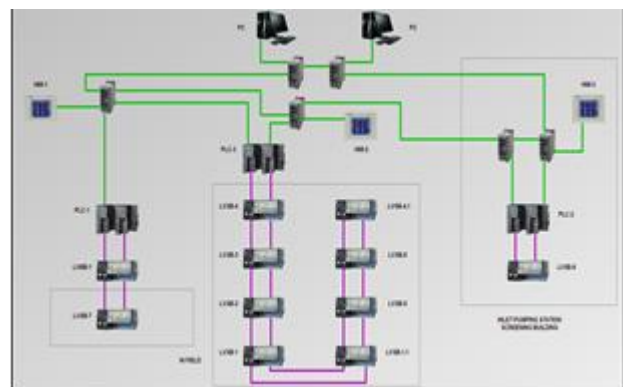


Figure 6. Computer network of SCADA - s

Conclusion

SCADA is a computer-based system for industrial process control, which collects real-time data from remote locations. Connecting SCADA equipment to the Internet presents security vulnerabilities where various cyber attacks target the system's network. This research proposed a study and an analysis of vulnerabilities and cyber attacks affecting the security of SCADA systems, moving the traditional system to the cloud environment, because

SCADA systems depend on real-time industrial operations. Organizations can use honeypots, which are decoy systems designed to lure attackers away from real assets, to gather information about the types of attacks being launched against their systems.

References

1. Cai, N., Wang, J., & Yu, X. (2008, July). SCADA system security: Complexity, history and new developments. In 2008 6th IEEE International Conference on Industrial Informatics, 569-574. <https://doi.org/10.1109/INDIN.2008.4618165>
2. Mema, B., & Basholli, F. (2023). Internet of things in the development of future businesses in Albania. *Advanced Engineering Science*, 3, 196-205.
3. Kelly, C., Pitropakis, N., Mylonas, A., McKeown, S., & Buchanan, W. J. (2021). A comparative analysis of honeypots on different cloud platforms. *Sensors*, 21(7), 2433. <https://doi.org/10.3390/s21072433>
4. Basholli, F., Daberdini, A., & Basholli, A. (2023). Detection and prevention of intrusions into computer systems. *Advanced Engineering Days (AED)*, 6, 138-141.
5. Zeng, P., & Zhou, P. (2018). Intrusion detection in SCADA system: A survey. In *Intelligent Computing and Internet of Things: First International Conference on Intelligent Manufacturing and Internet of Things and 5th International Conference on Computing for Sustainable Energy and Environment, IMIoT and ICSEE 2018, Chongqing, China, September 21-23, 2018, Proceedings, Part II 5* (pp. 342-351). Springer Singapore.
6. Basholli, F., Mezini, R., & Basholli, A. (2023). Security in the components of information systems. *Advanced Engineering Days (AED)*, 7, 185-187.
7. Nazir, S., Patel, S., & Patel, D. (2020). Cloud-based autonomic computing framework for securing SCADA systems. In *Innovations, algorithms, and applications in cognitive informatics and natural intelligence*, 276-297. <https://doi.org/10.4018/978-1-7998-3038-2.ch013>
8. Demertzis, K., & Iliadis, L. (2018). A computational intelligence system identifying cyber-attacks on smart energy grids. *Modern discrete mathematics and analysis: with applications in cryptography, information systems and modeling*, 97-116. https://doi.org/10.1007/978-3-319-74325-7_5
9. Tariq, N., Asim, M., & Khan, F. A. (2019). Securing SCADA-based critical infrastructures: Challenges and open issues. *Procedia computer science*, 155, 612-617. <https://doi.org/10.1016/j.procs.2019.08.086>
10. Rubio, J. E., Alcaraz, C., Roman, R., & Lopez, J. (2019). Current cyber-defense trends in industrial control systems. *Computers & Security*, 87, 101561. <https://doi.org/10.1016/j.cose.2019.06.015>
11. Mema, B., Basholli, F., Xhafaj, D., Basholli, A., & Hyka, D. (2023). Internet of things in the development of future businesses in Albania. *Advanced Engineering Days*, 7, 139-141
12. Molle, M., Raithel, U., Kraemer, D., Graß, N., Söllner, M., & Aßmuth, A. (2019). Security of cloud services with low-performance devices in critical infrastructures. *CLOUD COMPUTING 2019*, 98.
13. Zhang, S., Luo, X., & Litvinov, E. (2021). Serverless computing for cloud-based power grid emergency generation dispatch. *International Journal of Electrical Power & Energy Systems*, 124, 106366. <https://doi.org/10.1016/j.ijepes.2020.106366>
14. Shen, J., Xu, J., Cai, K., & Ji, Y. (2021). Retracted: Access Point Authentication Scheme of SCADA System Based on Cloud Computing Technology. In *Journal of Physics: Conference Series*, 1748(2), 022010. <https://doi.org/10.1088/1742-6596/1748/2/022010>
15. Basholli, F., Hyka, D., Basholli, A., Daberdini, A., & Mema, B. (2023). Analysis of cyber-attacks through simulation. *Advanced Engineering Days (AED)*, 7, 120-122.
16. Yang, X., Yuan, J., Yang, H., Kong, Y., Zhang, H., & Zhao, J. (2023). A Highly Interactive Honeypot-Based Approach to Network Threat Management. *Future Internet*, 15(4), 127. <https://doi.org/10.3390/fi15040127>
17. Hyka, D., & Basholli, F. (2023). Health care cyber security: Albania case study. *Advanced Engineering Days (AED)*, 6, 121-123.
18. Mellado, J., & Núñez, F. (2022). Design of an IoT-PLC: A containerized programmable logical controller for the industry 4.0. *Journal of Industrial Information Integration*, 25, 100250. <https://doi.org/10.1016/j.jii.2021.100250>
19. Yang, Y. S., Lee, S. H., Chen, W. C., Yang, C. S., Huang, Y. M., & Hou, T. W. (2022). Securing SCADA Energy Management System under DDos attacks using token verification approach. *Applied Sciences*, 12(1), 530. <https://doi.org/10.3390/app12010530>
20. Harizaj, M., Bisha, I., & Basholli, F. (2023). IOT integration of electric vehicle charging infrastructure. *Advanced Engineering Days (AED)*, 6, 152-155.
21. Kumar, A., Bhushan, B., Malik, A., & Kumar, R. (2022). Protocols, solutions, and testbeds for cyber-attack prevention in industrial SCADA systems. *Internet of Things and Analytics for Agriculture, Volume 3*, 355-380. https://doi.org/10.1007/978-981-16-6210-2_17
22. Daberdini, A., Basholli, F., Metaj, N., & Skenderaj, E. (2022). Cyber security in mail with Fortiweb and Fortinet for companies and institutions. *Advanced Engineering Days (AED)*, 5, 81-83.

23. Polat, H., Türkoğlu, M., Polat, O., & Şengür, A. (2022). A novel approach for accurate detection of the DDoS attacks in SDN-based SCADA systems based on deep recurrent neural networks. *Expert Systems with Applications*, 197, 116748. <https://doi.org/10.1016/j.eswa.2022.116748>
24. Hyka, D., Hyra, A., Basholli, F., Mema, B., & Basholli, A. (2023). Data security in public and private administration: Challenges, trends, and effective protection in the era of digitalization. *Advanced Engineering Days (AED)*, 7, 125-127.
25. Franco, J., Aris, A., Canberk, B., & Uluagac, A. S. (2021). A survey of honeypots and honeynets for internet of things, industrial internet of things, and cyber-physical systems. *IEEE Communications Surveys & Tutorials*, 23(4), 2351-2383. <https://doi.org/10.1109/COMST.2021.3106669>
26. Basholli, A., Mema, B., Basholli, F., Hyka, D., & Salillari, D. (2023). The role of education in cyber hygiene. *Advanced Engineering Days (AED)*, 7, 178-181.



ChatGPT in Albanian higher education: Transformation of learning and virtual interaction

Besjana Mema ¹, Fatmir Basholli ² Dolantina Hyka ¹

¹Mediterranean University of Albania, Department of Information Tecnology , Albania, besjana.mema@umsh.edu.al
dolantina.hyka@umsh.edu.al

²Albanian University, Department of Engineering, Tirana, Albania, fatmir.basholli@albanianuniversity.edu.al

Cite this study: Mema, B., Basholli, F., & Hyka, D. (2023). ChatGPT in Albanian higher education: Transformation of learning and virtual interaction. *Advanced Engineering Days*, 8, 23-27

Keywords

ChatGPT
Higher education
AI

Abstract

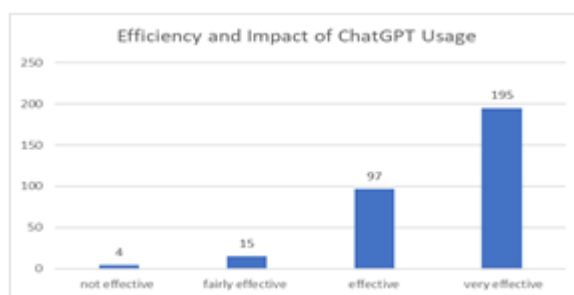
The integration of artificial intelligence (AI) in education has brought about significant improvements in the efficiency of the educational process, global learning promotion, personalized learning experiences, intelligent content creation, and the optimization of educational management. AI, as a technology, holds great potential in education, particularly in fostering personalized learning tailored to the individual needs and interests of each student. However, the implementation of AI in education presents challenges and ethical considerations, such as data privacy, equitable access to education, and the evolving role of educators. Striking a balance between technology and the essential role of educators is crucial to ensure a focus on holistic student development and preparation for a changing world. Despite the recent introduction of ChatGPT, there is a lack of systematic reviews on its impact on education. Therefore, the main objective of this paper is to analyze existing situation on the use of ChatGPT in higher education in Albania, addressing questions about the state of scientific research, benefits and challenges of implementation, and future trends in the field. An *online* questionnaire will be proposed and distributed to obtain this information. The collected data will be elaborated on and analyzed.

Introduction

Machine learning, inspired by the human brain's knowledge acquisition, generates new ideas and makes decisions. Neural networks, particularly in NLP, play a crucial role, categorized into supervised, unsupervised, semi-supervised, or reinforced learning. Chatbots, like ChatGPT, simulate human conversation and are widely used in education, especially language learning. ChatGPT, developed by OpenAI, is an advanced language model employing deep learning and NLP, building upon the success of earlier versions like GPT-3. With the ability to handle complex tasks requiring human intelligence, ChatGPT is recognized as an innovative learning tool, attracting researchers' interest. It supports multiple languages, offers natural conversational experiences, and adapts content based on user instructions, making it promising for language learning and teaching. In the era of profound digitization, we are moving through, the use of artificial intelligence technology has deeply influenced various fields, including higher education. This article sheds light on the extraordinary role that technology, with a particular emphasis on the ChatGPT model, has taken in transforming the learning paradigm. In this analysis, we will explore the advantages and challenges of using artificial intelligence in the educational process, examining the integration of ChatGPT with traditional teaching methodologies and the possibilities for improving the quality of learning [1-3].

Additionally, we have dedicated special attention to the use of ChatGPT in creating educational materials, evaluating the quality compared to that prepared by traditional educators. On another dimension, we investigate advancements in the use of ChatGPT to create virtual assistants, declaring a thorough analysis of students' experiences with these assistants and their role in individual learning. Furthermore, we examine the ethical challenges and considerations that arise with the integration of artificial intelligence technologies in the academic

environment and provide concrete proposals for addressing them. Ultimately, we open a window into the future, discussing the prospects of using ChatGPT in higher education and interacting with the expected trends in the fields of artificial intelligence and automatic learning technology. This article aims to contribute a clear and well-argued perspective to the debate on the use of artificial intelligence technology in higher education, offering in-depth analysis and a framework for understanding the impact of these developments on current and future education. In this research, we construct an analytical journey aiming to understand how artificial intelligence technology, particularly the ChatGPT model, has the potential to transform the learning experience in higher education [4-5]. For this purpose, we will explore fundamental issues related to the integration of this technology into teaching, focusing on the changes it brings to how learning materials are prepared, delivered, and perceived. At the core of this analysis is the question of how the use of ChatGPT can empower educational enterprises and provide a more personalized and enriched learning experience. Special emphasis will be placed on assessing the quality of materials created through this technology and their impact on the level of qualifications and knowledge of students [6]. We also focus on changes in the roles of the teacher and student, analyzing how technology influences the dynamics of the classroom and the relationship between students and virtual assistants based on ChatGPT. This analysis will help us assess whether the use of artificial intelligence technologies in education has the capacity to improve student inclusion and outcomes. Through a detailed examination of the ethical challenges arising from this transformation, our efforts are directed towards defining boundaries and suggesting necessary guidelines for the ethical and sustainable use of artificial intelligence technology in higher education. At the end of this analytical journey, we aim to provide an overarching vision for the future use of ChatGPT in education, displaying a comprehensive overview of the current impact and hoping to assist in articulating the necessary guidelines for the advanced and sustainable use of this technology in the higher education environment [7-8].



Material and Method

The study aims to analyse the impact of using the ChatGPT tool in higher education in Albania through a developed online questionnaire. The data, obtained from the responses of 311 randomly selected students, have been collected and analysed. Using a quantitative methodology, the study shows that ChatGPT has a positive impact on the teaching-learning process. While ChatGPT has the potential to enhance the educational experience, successful implementation depends on teachers' familiarity with its operation. These findings serve as a strong foundation for future research and decision-making regarding the integration of ChatGPT in the educational context. The questionnaire aims to identify the advantages and challenges of using ChatGPT, comparing it with traditional teaching methodologies. To examine the possibilities of using ChatGPT in creating teaching materials, experiments and simulations have been conducted, including the creation of lectures, exercises, and other teaching materials. To assess the progress in using ChatGPT to create virtual assistants, a study focused on students' experiences with these assistants has been developed. The discussion on future perspectives is conducted through an assessment of recent trends in the field of artificial intelligence and automatic learning technology. Regarding the methodology used during analysis and research, it is primarily based on quantitative methods with practical, numerical, comparative data, and information obtained from an online questionnaire sent to a random group of students. A total of 311 students participated in the survey. From the collected and analysed data, the alpha coefficient, also known as the internal consistency coefficient, is found to be 0.83. This indicates a high consistency among the questions. The students included in the responses are students from both bachelor's and master's programs. Specifically, 32.7% of the students are in the master's program, while 67.3% are in the bachelor's program. The questionnaire includes students from all Albanian universities, both public and private [9-11].

Results and Discussion

1. Have you had experience with the use of ChatGPT technology in the learning environment?

Analyzing the responses to the question (Figure 1), we observe that the majority of users have had significant experience with the use of ChatGPT technology in the learning environment. The responses often and very often are higher figures, indicating a frequent or intensive experience.

2. How would you rate the efficiency of ChatGPT in assisting your learning?

This presentation indicates that the majority of users have assessed the use of ChatGPT as effective or very effective in assisting learning. Highlighting each value in this way can provide a more detailed and written overview of users' perceptions and experiences regarding the efficiency of ChatGPT in learning assistance (Figure 2). The numerical average of the responses shows about 3.50, indicating an average rating of the efficiency of ChatGPT technology in learning assistance according to responses given by users. This result indicates that users have rated the use of ChatGPT as effective in learning assistance.

3. What are the major challenges you have encountered in using ChatGPT in your learning?

Here are some potential challenges that may have arisen in the use of ChatGPT in education:

-Lack of Personalized Responses: In general, technologies like ChatGPT may face challenges in providing personalized and individually tailored responses to the needs of each student.

-Risk of Misinformation: Content generated by ChatGPT may include inaccurate, unverified, or inappropriate information, especially if there is a lack of quality control processes.

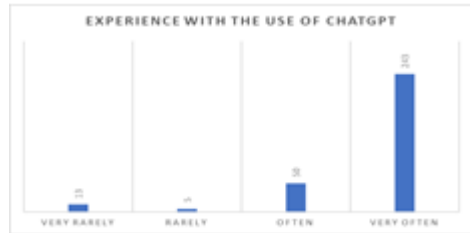


Figure 1. Experience with the Use of ChatGPT



Figure 2. Efficiency and Impact of ChatGPT Usage

Technical, Ethical, and Security Challenges. The use of artificial intelligence technologies may pose technical challenges and concerns regarding data security and privacy, especially in an academic environment.

The use of artificial intelligence technologies raises ethical challenges, including issues of information justice and its impact on the autonomy and self-determination of students.

-Mismatch with Traditional Methodologies. In some cases, the use of ChatGPT may not align with traditional learning methodologies, creating a mismatch between technology and established teaching practices.

4. How often do you use ChatGPT technology in general at your university?

Based on the given responses, we can interpret that the use of ChatGPT technology at your university is often or very often. These numbers indicate that the majority of users have determined that ChatGPT technology is used regularly or very often at your university. This assessment suggests a widespread and significant use of this technology in the university setting, perhaps for educational purposes, content creation, or assistance for students.

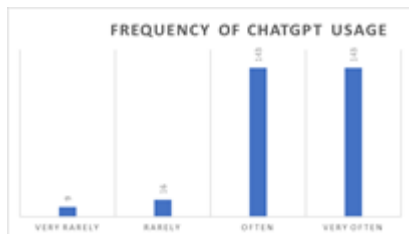


Figure 3. Frequency of ChatGPT Usage

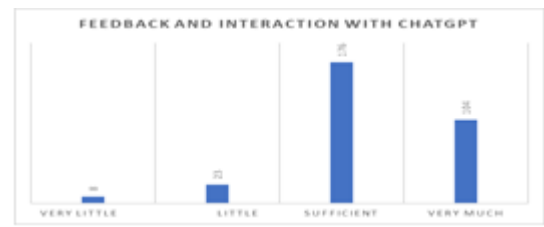


Figure 4. Frequency of using ChatGPT in effectiveness of learning

5. Do you think that the frequency of using ChatGPT can enhance the effectiveness of learning in your classroom?

Based on the given responses, (Figure 4), we can interpret that the majority of users believe that the frequent use of ChatGPT can increase the effectiveness of learning in their class. These numbers show that a significant portion of users appreciates that the repeated use of ChatGPT can bring about an improvement in the efficiency of learning in their class. This can be interpreted as a positive perspective regarding the potential of ChatGPT technology to enhance the learning experience and outcomes in the classroom. The calculation of the average value (mean) can be done by using the sum of the product of the numbers for each response and dividing it by the number of collected responses: Thus, the average of the responses indicates an average rating of 3, which can be interpreted as a positive consensus among users that the frequent use of ChatGPT can enhance the effectiveness of learning in the classroom.

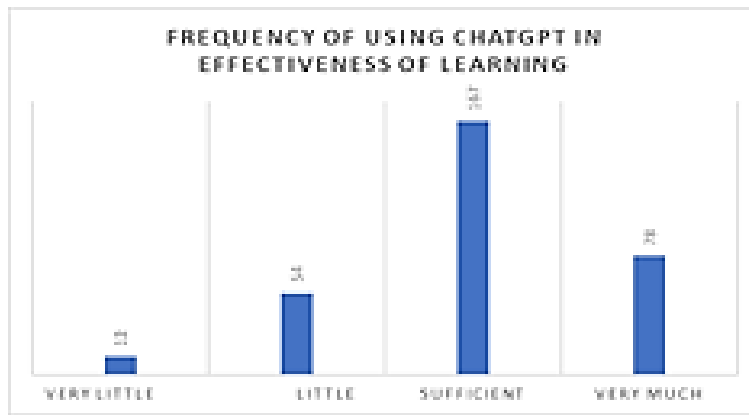


Figure 5. Feedback and Interaction with ChatGPT

Table 1. Descriptive Statistics

	N	Minimum	Maximum	Mean	Std. Deviation
chatGPT	311	1.00	6.00	2.1254	1.6432
Valid (listwise)	311				

6. Have you ever received feedback from ChatGPT in your scientific work or exercises?

Based on the given responses, we can interpret that the majority of users have received feedback from ChatGPT in their scientific work or exercises. These numbers show a dominance of positive evaluations, indicating that users have benefited from the feedback provided by ChatGPT in their scientific work or exercises. This result suggests that this AI tool has had a positive impact on the process of creating scientific papers and exercises for users.

7. How has this feedback influenced your work and knowledge development?

Based on the given responses, we can interpret that the majority of users have affirmed that feedback from ChatGPT has had a positive impact on their work and knowledge development.

"Descriptive statistics" present the collected information in a suitable, usable, and understandable form. After gathering the data, descriptive statistics allow us to calculate their frequency, measures of central tendency (such as mean, median, mode), etc., and to identify characteristics in the distribution of results. Table 1 below describes the standard deviation from the average of the responses extracted from the questionnaire for specific variables. For the variable of using ChatGPT in higher education in Albania, the deviation from the mean is 1.164, with an average of 2.12.

Conclusion

Let's summarize the results of the main questions:

1. Efficiency of ChatGPT Usage in Learning: The majority of users evaluate the use of ChatGPT as effective or very effective in learning.
2. Impact on Creating Educational Materials: Users see potential in using ChatGPT for creating lectures and educational materials.
3. Virtual Assistance and Support for Students: Users perceive progress in using ChatGPT for creating virtual assistants and providing support in individual learning.
4. Challenges and Ethical Considerations: Users acknowledge the ethical challenges associated with the use of artificial intelligence technologies in education and suggest proposals for addressing them.
5. Future Perspectives and Recommendations: Discussion of future possibilities for ChatGPT usage in higher education and interaction with expected trends in artificial intelligence and machine learning technologies.
6. Usage and Distribution of Technology: The majority of users confirm frequent use of ChatGPT at their university.
7. Potential for Enhancing Learning Efficiency: Users see potential to increase learning efficiency by utilizing ChatGPT more frequently.
8. Receiving Feedback from ChatGPT: The majority of users have benefited from feedback provided by ChatGPT in their scientific work or exercises.
9. Impact of Feedback on Work and Knowledge Development: Users have assessed that feedback from ChatGPT has had a positive impact on their work and knowledge development [12-15].

References

1. Montenegro-Rueda, M., Fernández-Cerero, J., Fernández-Batanero, J. M., & López-Meneses, E. (2023). Impact of the implementation of ChatGPT in education: A systematic review. *Computers*, 12(8), 153. <https://doi.org/10.3390/computers12080153>
2. Dempere, J., Modugu, K. P., Hesham, A., & Ramasamy, L. (2023). The impact of ChatGPT on higher education. Dempere J, Modugu K, Hesham A and Ramasamy LK (2023) The impact of ChatGPT on higher education. *Front. Educ*, 8, 1206936. <https://doi.org/10.3389/educ.2023.1206936>
3. Pajaziti, A., Basholli, F., & Zhaveli, Y. (2023). Identification and classification of fruits through robotic system by using artificial intelligence. *Engineering Applications*, 2(2), 154-163.
4. Li, L., Ma, Z., Fan, L., Lee, S., Yu, H., & Hemphill, L. (2023). ChatGPT in education: A discourse analysis of worries and concerns on social media. *Computers and Society*. <https://doi.org/10.48550/arXiv.2305.02201>
5. Frieder, S., Pinchetti, L., Griffiths, R. R., Salvatori, T., Lukaszewicz, T., Petersen, P. C., ... & Berner, J. (2023). Mathematical capabilities of chatgpt. *Machine Learning*. <https://doi.org/10.48550/arXiv.2301.13867>
6. Baskara, R. (2023). Exploring the implications of ChatGPT for language learning in higher education. *Indonesian Journal of English Language Teaching and Applied Linguistics*, 7(2), 343-358.
7. Rexha, G., Anxhaku, A., & Tosuni, B. (2019). Education about standardization in engineering studies: Albanian University case. 15th International Conference "Standardization, prototypes and quality: a means of Balkan countries collaboration", 24 - 25 October 2019, Edirne (Turkey).
8. Tosuni, B., & Mbroci, P. (2020). Një vështrim i përgjithshëm mbi përdorimin e e-commerce në Shqipëri. *Optime*, 12(1-2), 185-193.
9. Basholli, F., Daberdin, A., & Basholli, A. (2023). Detection and prevention of intrusions into computer systems. *Advanced Engineering Days (AED)*, 6, 138-141.
10. Mema, B., Rexha, G. & Gjonaj, M. (2022). Impact of Covid19 on Business Digitalization in Albania. Proceedings of the International Conference "International conference on intelligence-based transformations of technology and business shaping the future: digital economy and recent technology trends October 13-14, 2022 Tirana, Albania, ISBN:978-9928-4615-9-9
11. Fauzi, F., Tuhuteru, L., Sampe, F., Ausat, A. M. A., & Hatta, H. R. (2023). Analysing the role of ChatGPT in improving student productivity in higher education. *Journal on Education*, 5(4), 14886-14891. <https://doi.org/10.31004/joe.v5i4.2563>.
12. Iskender, A. (2023). Holy or unholy? Interview with open AI's ChatGPT. *European Journal of Tourism Research*, 34, 3414-3414. <https://doi.org/10.54055/ejtr.v34i.3169>
13. Basholli, F. (2022). Cyber warfare, a new aspect of modern warfare. CONFSEC 2022, VI International Scientific Conference, 05-08. December 2022, Borovets, Bulgaria.
14. Mema, B., Basholli, F., Xhafaj, D., Basholli, A., & Hyka, D. (2023). Internet of things in the development of future businesses in Albania. *Advanced Engineering Days*, 7, 139-141.
15. Hyka, D., & Basholli, F. (2023). How secure is our medical data? Is Albania ready for the digitalization of the health care system?. *Engineering Applications*, 2(3), 235-242.



Applications of the Helmholtz equation

Davron Aslonqulovich Juraev ^{*1,2} , Praveen Agarwal ² , Ebrahim Eldesoky Elsayed ³ ,
Nauryz Targyn ⁴ 

¹University of Economics and Pedagogy, Department of Scientific Research, Innovation and Training of Scientific and Pedagogical Staff, Uzbekistan, juraevdavron12@gmail.com

²Anand International College of Engineering, Department of Mathematics, Jaipur, India, goyal.praveen2011@gmail.com

³Mansoura University, Faculty of Engineering, Department of Electronics and Communications Engineering, Mansoura, Egypt, engebrahem16@gmail.com

⁴Kazakh-British Technical University, International School of Economic; Institute of Mathematics and Mathematical Modeling, Department of Mathematical Modeling and Mathematical Physics, Almaty, Kazakhstan, targyn.nauryz@gmail.com

Cite this study: Juraev, D. A., Agarwal, P., Elsayed, E. E., & Targyn, N. (2023). Applications of the Helmholtz equation. *Advanced Engineering Days*, 8, 28-30

Keywords

Wave equation
Helmholtz equations
Fundamental solution
Physical properties
Laplacian

Abstract

In this paper, we are talking about the Helmholtz equation and its physical meaning. Helmholtz equation is used to solve problems in physics such as seismology, electromagnetic radiation, and acoustics. It applies to a wide variety of situations that arise in electromagnetics and acoustics. It is also equivalent to the wave equation assuming a single frequency. In water waves, it arises when we Remove The Depth Dependence. Often there is then a cross over from the study of water waves to the study of scattering problems more generally. Also, if we perform a Cylindrical Eigenfunction Expansion we find that the modes all decay rapidly as distance goes to infinity except for the solutions which satisfy Helmholtz's equation. This means that many asymptotic results in linear water waves can be derived from results in acoustic or electromagnetic scattering.

Introduction

First, we will briefly talk about the Helmholtz equation. The Helmholtz equation, named after Hermann von Helmholtz, is a linear partial differential equation. Associated with the equation are the Laplacian, amplitude, and wavenumber. The Helmholtz equation is also an eigenvalue equation. The Helmholtz differential equation can be solved by separating the variables of everything in polar coordinate systems. The Helmholtz equation often arises in the study of physical problems involving partial differential equations (PDEs) in both space and time. The Helmholtz equation, which represents a time-independent form of the wave equation, results from applying the technique of separation of variables to reduce the complexity of the analysis.

The Helmholtz equation, named after Hermann von Helmholtz, is used in physics and mathematics. This is a partial differential equation, and its mathematical formula is:

$$\nabla^2 W + k^2 W = 0. \quad (1)$$

Here ∇^2 – Lapsasian, k – wavenumber, W – amplitude. The unknown function W is defined by \mathbf{R}^n (in practice, the Helmholtz equation is applied for $n = 1, 2, 3$).

The Helmholtz equation finds application in such concepts of solving physical problems as seismology, acoustics and electromagnetic radiation.

Seismology: The scientific study of earthquakes and their propagating elastic waves is known as seismology. Other study areas are tsunamis (due to environmental effects) and volcanic eruptions (due to seismic sources). There are three types of seismic waves: body waves which have P-waves (primary waves) and S-waves (secondary or shear waves), surface waves and normal waves.

To understand P waves, we have to first look into the basics of seismology and seismic waves. The waves of energy that travel through the earth and cause earthquakes and related phenomena are seismic waves. There are two types of seismic waves:

- 1) body waves;
- 2) surface waves.

Body waves are the waves that can travel through the layers of the earth. They are the fastest waves and as a result, the first waves that seismographs can record. Body waves can move through all states of matter including rocks and molten lava. Surface waves can only travel on the surface of the earth. The Helmholtz function is defined as the thermodynamic function of a system which is equal to the difference between the internal energy and the product of the system's temperature and entropy.

The Helmholtz equation was solved by many and the equation was used for solving different shapes. Simeon Denis Poisson used the equation for solving rectangular membrane. Equilateral triangle was solved by Gabriel Lamé and Alfred Clebsch used the equation for solving circular membrane. The Helmholtz free energy is defined as the work done which is extracted from the system such that the temperature and volume are constant. Whereas Gibbs free energy is defined as the maximum reversible work which is extracted from the system such that the temperature and pressure are constant.

Fundamental Solutions to the Helmholtz Equation

The Helmholtz equation naturally appears from general conservation laws of physics and can be interpreted as a wave equation for monochromatic waves (wave equation in the frequency domain). The Helmholtz equation can also be derived from the heat conduction equation, Schrodinger equation, telegraph and other wave-type, or evolutionary, equations. The Helmholtz equation is used in the study of stationary oscillating processes. If $k = 0$, then equation (1) becomes the Laplace equation.

It is known that the Helmholtz equation in different spaces has different fundamental solutions describing a certain physical process. The Equation (1) has the following fundamental solutions for $n = 1, 2, 3$. [1-3].

$$\text{For } n = 1, \quad W = \frac{ie^{ik|\xi-\eta|}}{2k}$$

$$\text{For } n = 2, \quad W = -\frac{i}{4} H_0^{(1)}(k|\xi-\eta|)$$

$$\text{For } n = 3, \quad W = \frac{e^{ik|\xi-\eta|}}{4\pi|\xi-\eta|}$$

$$\text{Finally, for general } n, \quad W = c_d k^p \frac{H_0^{(1)}(k|\xi-\eta|)}{2k}$$

$$\text{where } p = \frac{n-2}{2} \text{ and } c_d = \frac{1}{2i(2\pi)^p}.$$

These fundamental solutions for different factorizations of the Helmholtz equation are also the same. Using the fundamental solutions of the Helmholtz equation, for various factorizations of the Helmholtz operator, approximate solutions of the Cauchy problem were constructed, in which the solution is presented in explicit form. More precisely, the Carleman matrix is constructed, which allows finding a regularized solution [4-27].

Conclusion

Helmholtz equation is important for various applications. Some of them are as follows:

- It is used in seismology which is the scientific study of earthquakes and elastic waves.
- Explaining and analyzing natural disaster like Tsunamis.
- This equation also plays an important role in Medical imaging.
- Through this equation Volcanic eruptions can be explained and predicted.
- This equation is also important for the calculation of Electromagnetism

References

1. Abramowitz, M. & Stegun, I. (1964). Handbook of Mathematical functions with Formulas, Graphs and Mathematical Tables. New York: Dover Publications. ISBN: 978-0-486-61272-0.
2. Riley, K. F.; Hobson, M. P. & Bence, S. J. (2002). Mathematical methods for physics and engineering. "Chapter 19". New York: Cambridge University Press. ISBN: 978-0-521-89067-0.
3. Riley, K. F. (2002). Mathematical Methods for Scientists and Engineers. "Chapter 19". Sausalito, California: University Science Books. ISBN: 978-1-891389-24-5.
4. Juraev, D. A. (2012). The construction of the fundamental solution of the Helmholtz equation. Reports of the Academy of Sciences of the Republic of Uzbekistan, (4), 14-17.
5. Juraev, D. A. (2016). Regularization of the Cauchy problem for systems of elliptic type equations of first order. Uzbek Mathematical Journal, (2), 61-71.
6. Juraev, D. A. (2017). The Cauchy problem for matrix factorizations of the Helmholtz equation in an unbounded domain. Siberian Electronic Mathematical Reports, 14, 752-764
7. Juraev, D. A. (2017). Cauchy problem for matrix factorizations of the Helmholtz equation. Ukrainian Mathematical Journal, 69(10), 1364-1371.
8. Juraev, D. A. (2018). On the Cauchy problem for matrix factorizations of the Helmholtz equation in a bounded domain. Siberian Electronic Mathematical Reports, 15, 11-20.
9. Juraev, D. A. (2018). The Cauchy problem for matrix factorizations of the Helmholtz equation in R^3 . Journal of Universal Mathematics, 1(3), 312-319.
10. Zhuraev, D. A. (2018). Cauchy problem for matrix factorizations of the Helmholtz equation. Ukrainian Mathematical Journal, 69(10), 1583-1592.
11. Juraev, D. A. (2018). On the Cauchy problem for matrix factorizations of the Helmholtz equation in a bounded domain R^2 . Siberian Electronic Mathematical Reports, 15, 1865-1877.
12. Juraev, D. A. (2019). The Cauchy problem for matrix factorizations of the Helmholtz equation in R^3 . Advanced Mathematical Models & Applications, 1(4), 86-96.
13. Juraev, D. A. (2019). On the Cauchy problem for matrix factorizations of the Helmholtz equation. Journal of Universal Mathematics, 2(2), 113-126.
14. Juraev, D. A. (2020). The solution of the ill-posed Cauchy problem for matrix factorizations of the Helmholtz equation. Advanced Mathematical Models & Applications, 5(2), 205-221.
15. Juraev, D. A., & Noeiaghdam, S. (2021). Regularization of the ill-posed Cauchy problem for matrix factorizations of the Helmholtz equation on the plane. Axioms, 10(2), 1-14.
16. Juraev D. A. (2021). Solution of the ill-posed Cauchy problem for matrix factorizations of the Helmholtz equation on the plane. Global and Stochastic Analysis, 8(3), 1-17.
17. Juraev D. A., & Gasimov Y. S. (2022). On the regularization Cauchy problem for matrix factorizations of the Helmholtz equation in a multidimensional bounded domain. Azerbaijan Journal of Mathematics, 12(1), 142-161.
18. Juraev D. A. (2022). On the solution of the Cauchy problem for matrix factorizations of the Helmholtz equation in a multidimensional spatial domain. Global and Stochastic Analysis, 9(2), 1-17.
19. Juraev, D. A., & Noeiaghdam, S. (2022). Modern problems of mathematical physics and their applications. Axioms, 11(2), 1-6.
20. Juraev, D. A., & Noeiaghdam, S. (2022). Modern problems of mathematical physics and their applications. Axioms, MDPI. Switzerland, 1-352.
21. Juraev, D. A., Shokri, A. & Marian, D. (2022). Solution of the ill-posed Cauchy problem for systems of elliptic type of the first order. Fractal and Fractional, 6(7), 1-11.
22. Juraev, D. A., Shokri, A. & Marian, D. (2022). On an approximate solution of the Cauchy problem for systems of equations of elliptic type of the first order. Entropy, 24(7), 1-18.
23. Juraev, D. A., Shokri, A. & Marian, D. (2022). On the approximate solution of the Cauchy problem in a multidimensional unbounded domain. Fractal and Fractional, 6(7), 1-14.
24. Juraev, D. A., Shokri, A. & Marian, D. (2022). Regularized solution of the Cauchy problem in an unbounded domain. Symmetry, 14(8), 1-16.
25. Juraev, D. A. & Cavalcanti, M. M. (2023). Cauchy problem for matrix factorizations of the Helmholtz equation in the space R^m , Boletim da Sociedade Paranaense de Matematica, 41(3s.), 1-12.
26. Juraev, D. A. (2023). The Cauchy problem for matrix factorization of the Helmholtz equation in a multidimensional unbounded domain, Boletim da Sociedade Paranaense de Matematica, 41(3s), 1-18.
27. Juraev, D. A., Ibrahimov, V. & Agarwal, P. (2023) Regularization of the Cauchy problem for matrix factorizations of the Helmholtz equation on a two-dimensional bounded domain, Palestine Journal of Mathematics, 12(1), 381-403.



Electrochemical analysis of corrosion inhibitor synthesized using chlorine organomixture and ammonia

Khalilov Jamshid Akmal Ugli ^{*1}, Nurkulov Fayzulla Nurmuminovich ¹, Djalilov Abdulahat Turapovich ¹

¹Tashkent Research Institute of Chemical Technology, Department of Technology, Uzbekistan, jamshidkhalilov885@gmail.com, fnurkulov82@gmail.com

Cite this study: Ugli, K. J. A., Nurmuminovich, N. F., & Turapovich, D. A. (2023). Electrochemical analysis of corrosion inhibitor synthesized using chlorine organomixture and ammonia. *Advanced Engineering Days*, 8, 31-34

Keywords

Corrosion inhibitors
Nitrogen
Organic Compounds
Fatty acids
Gas-condensate well

Abstract

The article discusses the physicochemical properties of phosphorus-nitrogen-containing corrosion inhibitors for the oil and gas industry. As a result of the synthesis, corrosion inhibitors of metals were obtained and their level of protection was checked. CEM results were studied.

Introduction

Corrosion is the second leading cause of many industrial deaths. The causes of equipment failure in the oil and gas industry were evaluated from a 1993 survey (Ratnayake, 2012). Corrosion accounted for 60% of all maintenance costs for production platforms in North Sea oil and gas equipment (Steinsmo and Heggelung, 1993). One of the world's leading oil and gas companies announced in a 2003 survey that annual corrosion costs were \$900 million (Thams and Al Zahrani, 2006). Another survey conducted in 2006 found that corrosion in the oil and gas industry in the United States cost up to \$1.372 billion annually (Simmons, 2008). These data show that the economic consequences of corrosion in the oil and gas industry over the years are enormous. The global cost of corrosion in the oil and gas industry will increase further in the near future due to very high energy demand (Finsgar and Jackson, 2004) [1].

This review, based on our scientific and industrial experience, identified a clear gap in a comprehensive approach to consider wellbore corrosion processes throughout the life of oil and gas well tubing. In addition, with a new and comprehensive approach, we focused on the chemical effects of steel casing and tubing in a variety of environments, including completion fluid, acid and stimulation fluid, and production flow.

Phosphorus-nitrogen containing oil-soluble corrosion inhibitors are hydrophobic surfactants that fill the pores, increase inhibitor absorption by liquid hydrocarbons, and increase corrosion resistance [2].

Among the organic inhibitors, oil-soluble corrosion inhibitors of the acceptor type, which are amino acids and their derivatives, are widely used. These can be aliphatic, aromatic amines, amino acids, anilines, imidazolines, as well as five-membered, six-membered heterocycles containing nitrogen.

Corrosion of metals is one of the urgent technical and economic problems. The loss of metal equipment, products and structures due to corrosion is about 2-4% of the gross national product. In addition, in the petrochemical and chemical industry, as a result of the corrosion of equipment, toxic chemical products are released, and as a result, they pollute the atmosphere, water sources, and soil [3].

Material and Method

The physico-chemical properties and analysis results of our PF-1 brand corrosion inhibitor with this synthesized new composition were studied.

Physico-chemical characteristics of PF-1 brand corrosion inhibitor obtained on the basis of chlorinated organic waste processing:

Table 1. Properties

Properties	PF-1
1. Appearance	Transparent
2. Color	Pale yellow
3. Density at 20 0C, g/cm ³	1...1,3
4. Nitrogen content, % by weight	7,0...9, 5
5. Ph environment at 20 0C	6,5-7
6. Corrosion protection level at a concentration of 150 mg/l	98,5
7. Solubility:	
- In gasoline	Complete
- In the condensate	Complete
- In the water	30% of weight gain
-In the case of I-20	Complete
8. Fluidity cCt at 20 0C	15

In order to study the inhibition efficiency of corrosion inhibitors, practical experiments were carried out in hermetically sealed containers with a capacity of 1000 ml. An electrochemical method was used to determine the inhibition efficiency, and the practical experiments were carried out for 2 hours.

The inhibition mechanism and effectiveness of corrosion inhibitors were also studied by measuring the polarization curve outputs in the CS-350 potentiostat. In this case, it is possible to determine the inhibition efficiency of the surface of the steel electrode from the difference between the potentials of the steel in the solution with and without the inhibitor. Current supplied to this process is also called corrosion current. We can see that the amount of corrosion current is significantly reduced as a result of the inhibition of the surface of the steel electrode in solutions containing a corrosion inhibitor.

According to it, the product formed by the interaction of chlorinated organic waste with ammonia was placed in a three-necked flask equipped with a reflux condenser, a thermometer and a stirrer, vegetable oil was added and a homogeneous mass was formed.

Results and Discussion

Electrochemical experiments were carried out on steel plate geometrical samples. A solution of Ag/AgCl was used as the standard electrode. In this the value of the corrosion current of the solution containing the corrosion inhibitor obtained on the basis of the treatment of organochlorine waste, which we investigated, was different depending on the type of inhibitor and the environment. This value decreased with increasing concentration of corrosion inhibitor.

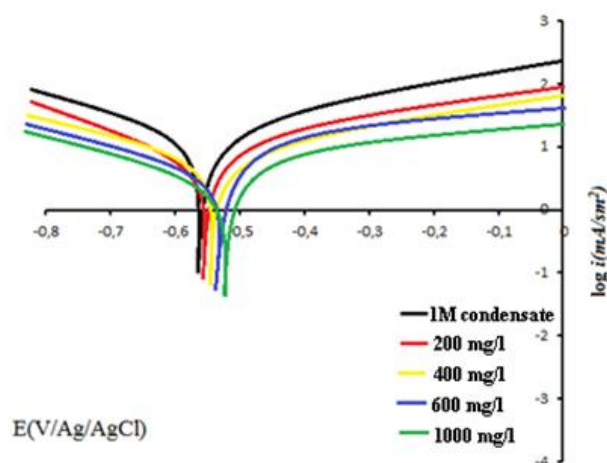


Figure 1. Polarization curves of PF-1 corrosion inhibitor at different concentrations in 1 M condensate medium for 2 hours at 298 ± 1 K for St3 grade steel.

As can be seen from Figure 2, the curves shifted towards the lower current density in the presence of inhibitors, which indicates that the inhibition efficiency of the corrosion inhibitor is higher in the condensate environment.

As the concentration of the inhibitor increases, the current density decreases on both the anode and cathode sides of the curves. However, the Tafel slopes and corrosion potential remained almost unchanged. Obviously, the PF-1 inhibitor works as a mixed type inhibitor, simultaneously reducing the dissolution of metal at the anode and

the release of hydrogen at the cathode to the corrosion process. From this result, it can be seen that the inhibition efficiency is shown by blocking the metal surface of the adsorbed inhibitors.

As the concentration of PF-1 brand corrosion inhibitor in the solution increases, the electrical resistance of the solution also increases, as a result, the potential of the corrosion current value also decreases and the corrosion current value decreases to 0.095 ± 0.01 i, (mA/cm²). When the concentration of PF-1 corrosion inhibitor was 1000 mg/l, its efficiency was 91.23% in a 1M condensate environment.

The electrochemical analysis of this PF-1 brand corrosion inhibitor in gasoline environment was studied and the potential curves were analyzed.

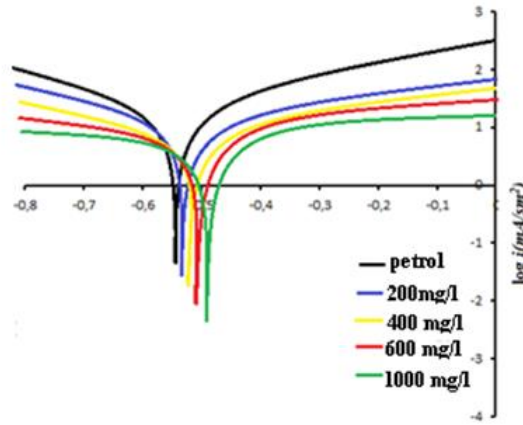


Figure 2. Polarization curves for steel grade St3 recorded for 2 hours at 298 ± 1 K at different concentrations of corrosion inhibitor PF-1.

In Figure 3, the corrosion current value of the solution with and without PF-1 corrosion inhibitor decreased from 0.98 ± 0.11 i, (mA/cm²) to 0.08 ± 0.001 i, (mA/cm²). PF-1 brand corrosion inhibitor showed 95.47% efficiency in gasoline environment.

This was investigated using SEM of the ST3 steel grade we used in the test.

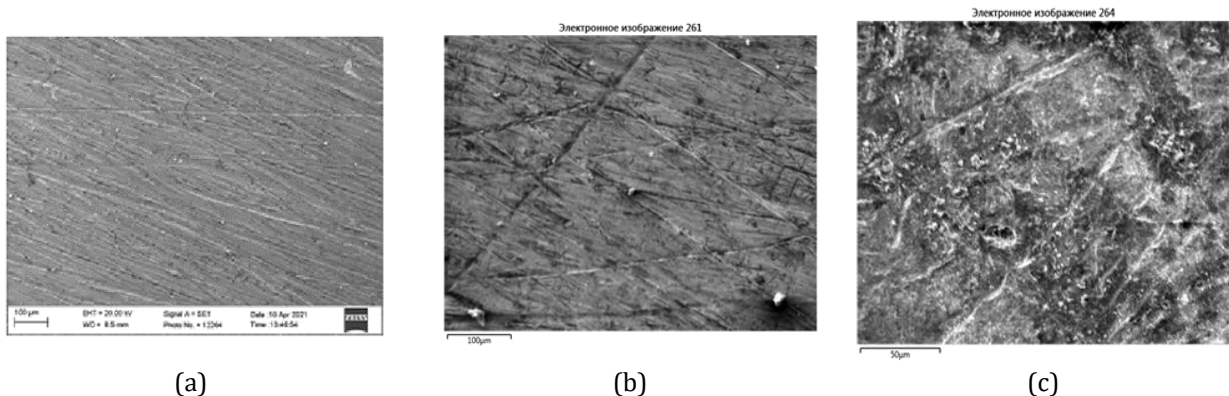


Figure-3. SEM view of ST3 steel sample a) pure metal, b) inhibitory environment, c) non-inhibitory condensate environment.

In our research results obtained by scanning electron microscope, we can see that the PF-1 brand corrosion inhibitor we researched protects the metal surface from corrosion.

Conclusion

According to the electrochemical test results of this method, a series of tests from the low-concentration test program were conducted. The level of protection in the condensate environment at a concentration of 1000 mg/l was 91.23%, and the level of protection in the gasoline environment was 95.47%.

PF-1 brand corrosion inhibitors can be used in oil, gas, gas condensate wells, well drilling, oil and fatty acid production.

References

1. Obot, I. B., Onyeachu, I. B., Umoren, S. A., Quraishi, M. A., Sorour, A. A., Chen, T., ... & Wang, Q. (2020). High temperature sweet corrosion and inhibition in the oil and gas industry: Progress, challenges and future perspectives. *Journal of Petroleum Science and Engineering*, 185, 106469. <https://doi.org/10.1016/j.petrol.2019.106469>
2. Askari, M., Aliofkhaezrai, M., Jafari, R., Hamghalam, P., & Hajizadeh, A. (2021). Downhole corrosion inhibitors for oil and gas production—a review. *Applied Surface Science Advances*, 6, 100128. <https://doi.org/10.1016/j.apsadv.2021.100128>
3. "Защитные свойства консервационных масел и ингибиторов коррозии" А.Ф.Хужакулов, А.А.Алимов, М.Ж.Махмудов. Молодой ученый-2013.
4. "Ингибиторы коррозии металлов" Л.П.Даниловская; Р.С.Крымская; Санкт-Петербург 2017.
5. "Ингибиторы коррозии металлов" Л.П.Даниловская; Р.С.Крымская; Санкт-Петербург 2017.
6. Korroziyadan himoya qilish "O'quv qo'llanma, H.V.Do'stov". Toshkent-2019.
7. "Ингибиторы коррозии металлов" Л.П.Даниловская; Р.С.Крымская; Санкт-Петербург 2017.
8. Korroziyadan himoya qilish "O'quv qo'llanma, H.V.Do'stov". Toshkent-2019.



Protection of buildings on a university campus from lightning strikes

Fatmir Basholli¹, Joana Minga¹, Alketa Grepcka²

¹Albanian University, Department of Engineering, Tirana, Albania, fatmir.basholli@albanianuniversity.edu.al;
j.minga@au.edu.al

²Agricultural University of Tiranaolytechnic, Mathematics Department, Tirana, Albania, agrepcka@ubt.edu.al

Cite this study: Basholli, F., Minga, J., & Grepcka, A. (2023). Protection of buildings on a university campus from lightning strikes. *Advanced Engineering Days*, 8, 35-38

Keywords

Lightning strike
Hazardous area analysis
Overvoltage
Overcurrent
Simulation

Abstract

This study aims to analyze and propose effective methodologies for lightning protection on university campuses. Lightning strikes can be a potential hazard and can lead to serious consequences for the safety and well-being of members of the university community and the many laboratory and information technology equipment that support the academic process. To meet this challenge, we propose an integral approach that includes advanced meteorological monitoring, advanced warning system, and appropriate building infrastructure to reduce the impact of lightning strikes, through a transient electromagnetic wave propagation analysis model. of lightning in the protective net placed on the terraces of the buildings. By means of this simulated study with the help of the ATPDraw software package, we calculate the values of voltages and discharge currents and do their analysis. Based on the results of this study, it is intended to draw up guidelines and standards for the protection of the university campus from lightning strikes, thus ensuring a safe and stable environment for all participants of this community.

Introduction

Lightning strikes pose a significant risk to university campuses. Such an incident can cause significant human and material damage and can negatively affect the daily life and operation of a higher education institution. Lightning can be defined as a temporary high discharge to the ground that occurs when certain regions of the atmosphere reach a sufficiently large electrical charge relative to the ground. From this phenomenon arises a large current that affects sensitive electrical and electronic systems and causes their malfunction or destruction. From a lightning strike, the discharge current is the single most important quantity. Electrical problems of lightning protection can be treated and are solvable by knowing the waveform and amplitude of the current. The efficiency of protection against unwanted lightning events is closely related to the proper design of the protection systems. The main goal of any protection system against a direct lightning strike is to discharge the current generated by the lightning to the ground in the shortest possible time. During this time, objects and people, as well as electrical and electronic systems, can be damaged. Much research has been done on grounding systems, both theoretically and experimentally. The theoretical treatment in this work is based on analytical, empirical and mostly numerical methods [1-2]. Protection from direct lightning strikes according to the IEC-62305 standard, represents an important problem, is based on this standard and is simulated by means of the ATP (Alternative Transient Program) software package. Clark's model was used for the simulation, where the segments were replaced by lossy lines, with distributed parameters. The placement of lightning rods is controlled by the method of protective angles and rotating spheres. In this framework, we will examine some of the main aspects involved in the protection and minimization of risks from this natural phenomenon, where the treatment of this issue is important to guarantee that university campuses are prepared and safe in the face of possible natural challenges [3-4].

Material and Method

1. Calculation of R, L, C parameters of direct impact protection systems.

Any protection system, from direct lightning strikes, consists of conductors that have a certain placement in space. In the special case, it consists of conductors with vertical and horizontal placement [5-7]. In function of the position, the capacity is calculated and further in function of it, the inductance of the conductor is calculated (Figure 1,2)

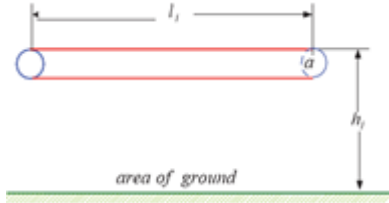


Figure 1. A horizontal circular conductor

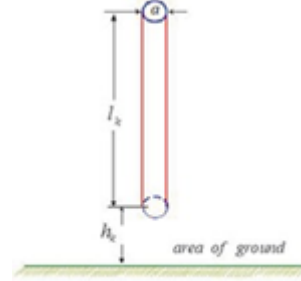


Figure 2. A vertical circular conductor

In Figure 1, we l_j mark the length, the h_j height from the ground and the a radius.

In Figure 2, we mark the length l_k , height from the ground h_k , a and radius.

For the conductor with horizontal placement as in (Figure 1), its capacity is calculated according to formula (1), while for the conductor with vertical placement, as in (Figure 2), its capacity is calculated according to formula (2).

$$C_j = \frac{2 \cdot \pi \cdot \varepsilon_0 \cdot l_j}{\ln\left(\frac{2h_j}{a}\right) - D_1} \quad [F] \quad (1)$$

$$C_j = \frac{2 \cdot \pi \cdot \varepsilon_0 \cdot l_k}{\ln\left(\frac{l_k}{a}\right) - D_2} \quad [F] \quad (2)$$

2. Separation of the conductors of the protection system, into separate segments with lengths that are part of the length of the electromagnetic wave that propagates in the surrounding environment and calculation of the maximum frequency of the lightning current source.

Any function related to time can be transformed into the frequency domain by means of the integral Fourier transform. Considering the frequency spectrum as finite, i.e. ignoring very high frequencies, the maximum frequency, for practical purposes, is calculated starting from the time of the wave front τ_f using formula (3); In function of the maximum frequency, it is possible to determine the minimum length of the electromagnetic wave. Thus, in function of the length of the electromagnetic wave λ_{\min} , the length of the segment ΔL that will be represented by the equivalent electric circuit is calculated. Formula (4) serves as a criterion for calculating the length of the segment; In external environments, that is, for external protection systems against direct lightning strikes, the dielectric and magnetic constants of the void are according to formulas (5-7).

$$f_{\max} \approx \frac{1}{\tau_f} \quad (3) \quad \Delta L < \frac{\lambda_{\min}}{10} \quad (4) \quad \begin{matrix} \varepsilon = \varepsilon_0, \\ \mu = \mu_0 \end{matrix} \quad (5) \quad \lambda_{\min} = \frac{c}{f_{\max}} \quad (6) \quad \lambda_{\min} = \frac{300}{f_{\max} [MHz]} \quad (m) \quad (7)$$

The double integration is done along the axis of the segment (prime gamma curve, in figure 3) and according to the curve on the surface of the segment that is parallel to its axis. The second integral is applied, when the segment (conductor) is inclined, which is calculated from (Figure 4).

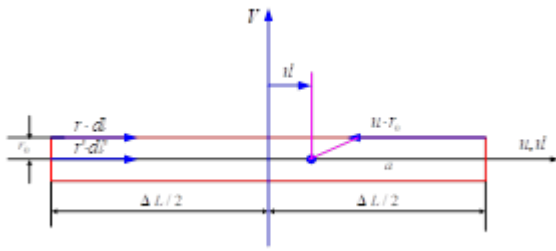


Figure 3. Ways of integration by axis

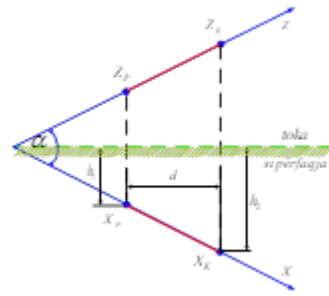


Figure 4. Oblique segment, coordinates

Calculate the length of the conductor:

$$\Delta L = \sqrt{d^2 + (h_2 - h_1)^2} \quad (8)$$

Results and Discussion

Protection of the main campus building from direct lightning strikes

Figure 5 shows the protection with lightning rods with a height of 5 m of the main building.

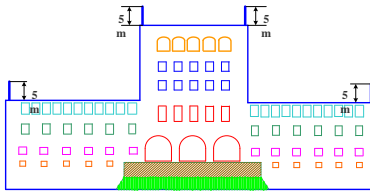


Figure 5. Protection with lightning rods with a height of 5 m

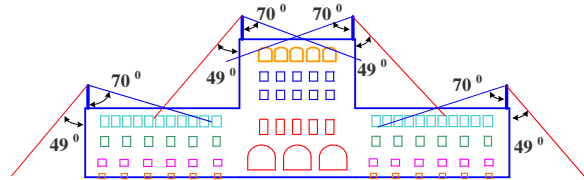


Figure 6. Determination of protective angles

Based on the international standard: IEC-62305, the protection angles have been found, referring to different plans, shown in Figure 6, while Figure 7 shows the areas of coverage from lightning strikes after the placement of additional lightning rods.

Figure 7 shows the coverage areas from lightning strikes. after installing additional lightning rods.

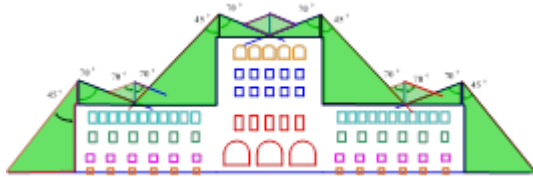


Figure 7. Lightning strike coverage areas

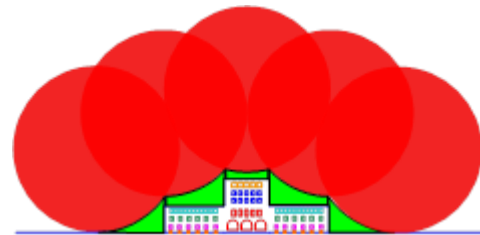


Figure 8. View of full lightning strike coverage

Figure 8 shows the view from above of the terraces of the main building of the university campus, after we have added three additional lightning rods. As it is clearly seen from Figure 8, the protection against direct lightning strike of all the terraces of the campus building is perfectly covered [8-12].

Conclusion

From the analysis it turned out that by adding three more lightning rods, we meet the requirements of protection from direct lightning strikes. As a result of the shock of the standard lightning wave: 1.2/50 [μs], with a peak of 10 [kA], large overvoltages and overcurrents occur, which by installing earthings with small earthing resistances up to 2 [Ω], it is possible to reduce of overvoltages at different points of the protective network. For the analysis of the protection of objects above ground from direct lightning strikes, the European standards IEC 62 350-1, up to the IEC-62 530-4 series should be used. As the value of the grounding resistance increases, the voltage at the connection point of the down conductors with the grounders increases. This leads to an increase in the voltage of the step, of the touch, bringing great danger to the electric shock of the living organisms.

References

1. Iosseli, U. V., Kothanov, A. S., & Stlyrski, M. G. (1990). Capacitance Calculation, Energy Press
2. Sarajcev, P., & Goic, R. (2011). A review of current issues in state-of-art of wind farm overvoltage protection. *Energies*, 4(4), 644-668.
3. Basholli, F., & Daberdini, A. (2023). Monitoring and assessment of the quality of electricity in a building. *Engineering Applications*, 2(1), 32-48.
4. Gao, C., Li, L., Li, B., & Zhao, Z. (2006, February). Computation of power line tower lightning surge impedance using the electromagnetic field method. In 2006 17th International Zurich Symposium on Electromagnetic Compatibility, 124-127. <https://doi.org/10.1109/EMCZUR.2006.214885>
5. Basholli, F., & Daberdini, A. (2022). Influence of terrain and atmospheric conditions on the propagation of radio waves. 1st International Scientific Conference in Mathematics and Physics, and their Applications, 151-160
6. Moreno, P., Naredo, J. L., Bermúdez, J. L., Paolone, M., Nucci, C. A., & Rachidi, F. (2004). Nonuniform transmission tower model for lightning transient studies. *IEEE transactions on power delivery*, 19(2), 490-496. <https://doi.org/10.1109/TPWRD.2003.823210>
7. Basholli, F., Merkuri, L., & Daberdini, A. (2022). Magnetic and electric fields in high - voltage power transmission lines, impact on the environment". *Optime*, XIV Year of Publication, 2, 232-249
8. De Conti, A., Visacro, S., Soares, A., & Schroeder, M. A. O. (2006). Revision, extension, and validation of Jordan's formula to calculate the surge impedance of vertical conductors. *IEEE transactions on electromagnetic compatibility*, 48(3), 530-536. <https://doi.org/10.1109/TEMC.2006.879345>
9. Basholli, F., & Daberdini, A. (2022). Monitoring and evaluation of the quality of electricity in a building. *Advanced Engineering Days (AED)*, 5, 77-80.
10. Kaouche, S., Nekhoul, B., Kerroum, K., & Drissi, K. E. K. (2007). Induced disturbance in power network by lightning. *Journal of Communications Software and Systems*, 3(1), 52-58. <https://doi.org/10.24138/jcomss.v3i1.269>
11. Basholli, F., & Kola, J. (2022). Adaptation of computer power supply to laboratory equipment. *OPTIME*, XIV Year of Publication, 2, 250-258
12. Visacro, S., Soares Jr, A., Schroeder, M. A. O., Cherchiglia, L. C., & de Sousa, V. J. (2004). Statistical analysis of lightning current parameters: Measurements at Morro do Cachimbo Station. *Journal of Geophysical Research: Atmospheres*, 109(D1). <https://doi.org/10.1029/2003JD003662>



A comparative study on the lateral displacement response of short monopiles with different plug materials

Özgür Lütfi Ertuğrul ¹, Fatma Dülger Canoğulları ²

¹Mersin University, Engineering Faculty, Department of Civil Engineering, Mersin, Türkiye, ertugrul@mersin.edu.tr

²Toros University, Engineering Faculty, Department of Civil Engineering, Mersin, Türkiye, fatma.dulger@toros.edu.tr

Cite this study: Ertuğrul, Ö. L., & Canoğulları, F. D. (2023). A comparative study on the lateral displacement response of short monopiles with different plug materials. *Advanced Engineering Days*, 8, 39-42

Keywords

Monopile
Finite element method
Lateral displacement

Abstract

Today wind energy is regarded as a major source in the energy market and power generation. An offshore wind turbine is supported by a stable platform located above the ocean surface, together with a combination of rotor-nacelle-tower structure and the foundation. In the most often used system, the tower is fixed onto the monopile foundation by a transition piece. Monopiles are large-scale steel pipes that are often driven into the seabed by impact; their typical dimensions range from 8 m to 10 m in diameter, 30 m to 40 m in length, and weigh as much as 1000 tons. In this study, a small-scale monopile foundation with different plug materials is modeled using the Plaxis 3D finite element software.

Introduction

Wind is considered among the most significant and reliable sources of kinetic energy. With the utilization of wind turbines, the kinetic energy produced by constant winds can be utilized as a continuous and renewable source of electricity. The substructure and base support an offshore wind turbine and its rotor-nacelle-tower combination, which is situated on a stable platform. The tower is placed on a monopile foundation via a passage in the most widely used technique.

A typical monopile consists of a steel pipe, with the bottom part open and the top part closed. The diameter and length of the monopile vary depending on the project requirements, water depth, soil conditions, and the size of the turbine. Monopiles can be large-scale structures that can reach dozens of meters in diameter and extend deep into the seabed.

In the installation process, monopile hydraulic hammer or vibration equipment is used to crash into the seabed to the desired depth. The soil resistance and friction between the monopile and the surrounding seabed provides the stability necessary for the wind turbine. By transferring the weight and loads from the wind turbine's tower and wings to the ocean floor, the monopile serves as the primary structure supporting the whole system.

Material and Method

Monopiles are the most common type of foundation used to support offshore wind turbines [1]. They may be installed and designed to accommodate a wide range of subsurface conditions. A monopile is a long and hollow steel tube that is driven up to 80 m into the sea floor. Some of the monopile protrudes above the sea floor to attach to the transition piece, connecting the monopile to the tower. The tower supports the nacelle and the rotor of the turbine. Monopiles must withstand the forces from wind, waves, ice, currents, and boats over the life of the turbine, which can be up to 50 years [2]. Figure 1 depicts a monopile with a diameter of 7.5 meters, which is located at the Gode Wind Offshore Wind Farm.

In literature, many methods are utilized in monopile design projects, however finite element approach stands out as the most versatile tool with powerful modeling capabilities. In this study, the short monopile model (H=8m) was produced using the Plaxis 3D [4] software and modeled as an empty hollow cylinder pile, a soil-filled steel pile, and a concrete-filled steel pile. It is known that monopiles are typically longer however, to minimize the

complexity associated with the pile flexural deflections, a short model was considered to compare the effect of different inner plug materials including concrete.

The monopile geometry modeled with Plaxis 3D is shown in Figure 2.



Figure 1. A 7.5 m diameter monopile for Gode Wind Offshore Wind Farm [3]

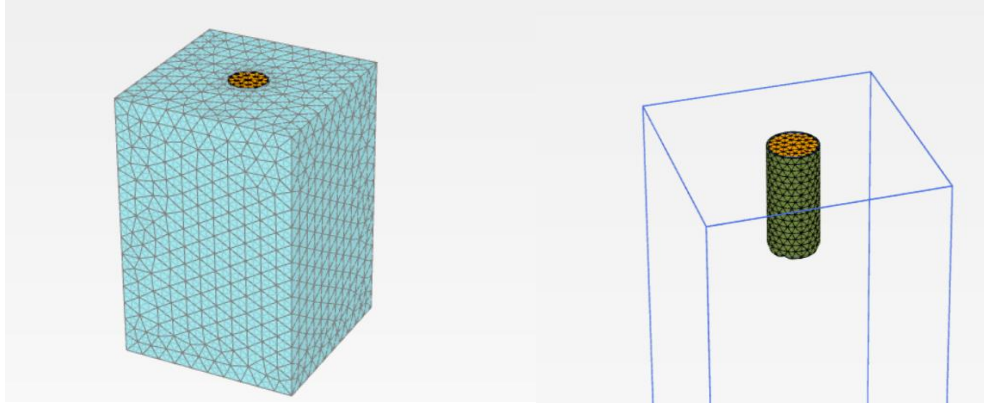


Figure 2. Perspective view of the monopile geometry

Table 1 provides the properties of the soil, monopile and concrete used in 3D modeling. Furthermore, the pile has been chosen to have a diameter of 1 m, a length of 8 m, and a steel thickness of 0.05 m. The modeling results of the short pile, simulated in three different setups, were compared.

In the modeling study, static analyses were carried out by applying a force in horizontal direction, without considering of dynamic and time varying nature of wind and wave loads. The applied horizontal load in all three analyses is 1000 kN.

Table 1. Properties of the soil, monopile and concrete

	Unit weight (kN/m ³)	Modulus of elasticity (kN/m ²)	Poisson ratio	Angle of internal friction (°)
Soil	19	50x10 ³	0,3	30
Monopile	78	210x10 ⁹	0,2	-
Concrete	24	25x10 ⁶	0,2	-

Results and Discussion

According to the results of static analysis, the total horizontal displacement obtained for the hollow cylindrical pile model is 4.56 mm, for the soil-filled pile model is 4.26 mm and for the concrete-filled pile model is 3.82 mm. Horizontal displacement contours obtained through finite element analyses are shown in Figure 3. It is observed that a concrete inner plug within the monopile significantly decreases the lateral displacements and the reduction in displacements is 6.5% for the ordinary soil plug and 16.2% for the concrete infill. The decrease in the displacements is very promising, since the wind turbines requires very strict tilting requirements in order to run properly during service lifespan.

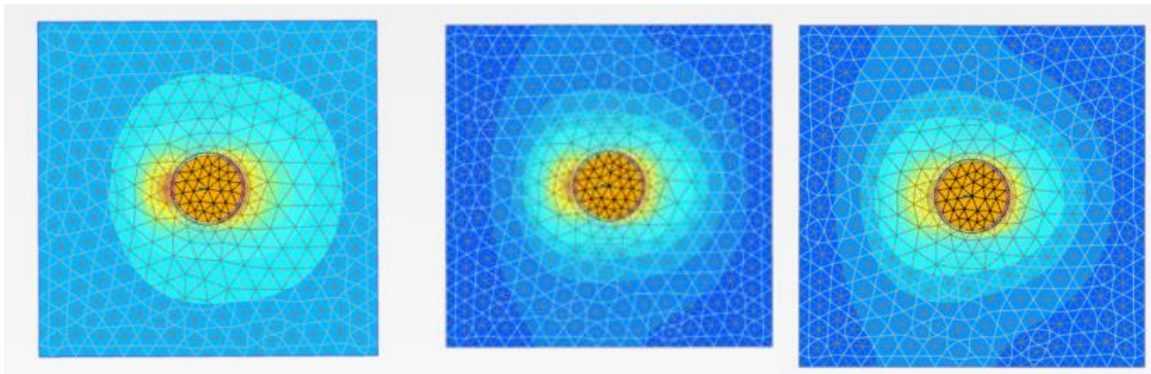


Figure 3. Horizontal displacement contours a) hollow cylindrical pile model b) soil-filled pile model c) concrete-filled pile model

An examination of the horizontal displacement values of the pile in contour view also supports the previous finding about the horizontal displacements of the monopile. The reduced displacements in the soil also decrease the extent of the yield zone around the pile body, which decreases the amount of soil softening thus contributing to the lateral resistance. The graph showing the horizontal displacement as a function of pile depth for three different models is presented in Figure 4. An investigation of the Fig.4 also shows that there is a well observed rotation point at -6.25-meter elevation along the pile body, which is approximately 20 percent of height above the pile bottom.

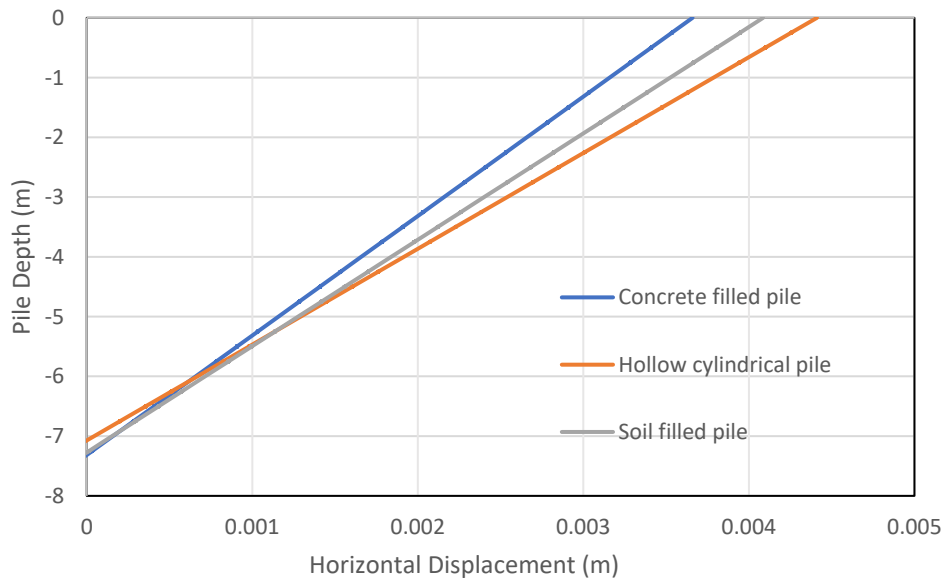


Figure 4. Pile depth - horizontal displacement curves for three model

Conclusion


For the preliminary design of monopiles, different loads are taken into consideration. These loads are the self-weight of the whole structure, lateral wind and wave loads and turbine blade loadings. Most significant load for the monopiles supporting the wind turbines are the lateral loads. In this study, short monopile models with different inner plug materials were analyzed under a constant lateral load and the lateral displacement of the monopile body is compared. Main motivation of this analyses is to investigate the effect of inner plug characteristics on the lateral displacement of the monopile. Analyses results indicated that stiffer inner plug materials are reducing the lateral displacements of the pile body. The reduction in the displacements of the monopile top may reach up to 16% which is considered a very important decrease since the lateral displacement reduction on top of the tower will be higher. It is well known that wind turbines are running under strict tilting requirements hence stiff infill plugs within the monopile body may provide significant cost reductions in the overall cost of the wind turbine structures resting on monopiles.

References

1. Lesny, K., & Hinz, P. (2009). Design of monopile foundations for offshore wind energy converters. *Contemporary Topics in Deep Foundations*, 512-519. [https://doi.org/10.1061/41021\(335\)64](https://doi.org/10.1061/41021(335)64)
2. Ebin, D. M. A. (2012). The response of monopile wind turbine foundations in sand to cyclic loading. Master Thesis, Tufts University.
3. Kallehave, D., Byrne, B. W., LeBlanc Thilsted, C., & Mikkelsen, K. K. (2015). Optimization of monopiles for offshore wind turbines. *Philosophical Transactions of the Royal Society A: Mathematical, Physical and Engineering Sciences*, 373(2035), 20140100. <https://doi.org/10.1098/rsta.2014.0100>
4. Plaxis 3D, User Manual (2020). Bentley Systems.



Lymph nodes and their role in immunity

Ceren Canatar*¹, Furkan Ayaz^{1,2} 

¹Mersin University, Biotechnology Department, Türkiye, cerencanatar07@gmail.com

²Mersin University, Biotechnology Research and Application Center, Türkiye, furkanayaz@mersin.edu.tr

Cite this study: Canatar, C., & Ayaz, F. (2023). Lymph nodes and their role in immunity. *Advanced Engineering Days*, 8, 43-44

Keywords

Lymph nodes
Lymphoid organs
Lymphadenopathy
Immune system

Abstract

Lymph nodes play crucial role in the immune system cell development and response. The spleen, mucosa-associated lymphoid tissue and lymph nodes are the secondary (peripheral) lymphoid organs, but they constitute the immune system. It is known that lymph nodes in the class of secondary (peripheral) lymphoid organs with different functions have different shapes (round, oval or bean-shaped). Lymph nodes connected to each other by lymphatic vessels are located in different regions (thorax, axilla, abdomen, inguinal region and neck region). Lymph nodes are important to generate immune response against foreign molecules in our body. In this proceeding study, we will be reviewing the lymph nodes and their functions in the immunity.

Introduction

The environment necessary for the defense against a pathogen invasion is provided by the immune system, and the organs that make up this system are categorized as primary (central) lymphoid organs and secondary (peripheral) lymphoid organs. The thymus and bone marrow are considered as the primary (central) lymphoid organs, while the spleen, mucosa-associated lymphoid tissue and lymph nodes are considered as the secondary (peripheral) lymphoid organs. T lymphocytes are produced in the bone marrow and complete their development in the thymus, while B lymphocytes are produced and developed in the bone marrow. T lymphocytes developing in the thymus and B lymphocytes developing in the bone marrow migrate into the secondary (peripheral) lymphoid organs with different functions after this development [1-4].

The development of secondary lymphoid organs can occur during embryogenesis as well as in the early postnatal period, and most of the interactions in this development, both molecular and cellular, are well understood. However, not all of these interactions are fully understood [5].

The lymph nodes, which are connected to each other by lymphatic vessels, that is, located along these vessels and located between the secondary (peripheral) lymphoid organs, can have a round or oval shape or be in the form of beans [5, 6]. There may be approximately 300-500 lymph nodes in the body [6, 7]. It is stated that lymph nodes are abundant in the thorax, axilla, abdomen, inguinal and neck region [8].

Results

With the entry of foreign substances into the body, the lymph nodes have a role in the necessary defense against these substances. They are involved in both the adaptive and innate immune response to eventually create the effectiveness of the vaccines [3, 7]. In addition to their immune functions, lymph nodes also have roles as filters for both tissue fluids and tissues [9].

Lymph nodes allow the encountering of the dendritic cells and T cells. This event takes place in order to initiate the immune response. The immune response is directed to an antigenic stimulus [10].

In some cases, the enlargement of the lymph nodes may occur. This event may be caused by an antigenic stimulus. Changes that occur in the shape, size and number of lymph nodes are described as lymphadenopathy. In the case of lymphadenopathy, lymph nodes that are found to have grown to sizes that would be considered abnormal can be seen. Various reasons may play a role in the occurrence of lymphadenopathy, which is very common in childhood. Some fungal infections, some viral infections including measles and rubella, toxoplasma infection which is a parasitic infection, some bacterial infections including syphilis and tuberculosis, some autoimmune diseases, some drug reactions are among the causes of diffuse lymphadenopathy. In addition, some reasons play a role in the emergence of regional lymphadenopathy. Some infections are known to be a common cause of regional lymphadenopathy [3, 11].

Conclusion

The aging state, which has many effects on both tissues and organs, can also affect the immune system at a level that can be considered as critical for the overall health. Effect of the aging include decreased response to vaccines and increased incidence of both cancer and certain autoimmune disorders. Depending on this situation, irregularity may occur in the structures of the lymph nodes [7]. Lymph nodes are critical for the development of a proper immune response against the pathogens. The size as well as function of the lymph nodes decline by age [7].

In summary, more research and studies are needed in order to have more detailed information about the aging of the lymph nodes and to clearly understand and illuminate the mechanisms involved in the aging and loss of function in the lymph nodes [7]. In this way the development of late age chronic disorders, cancer and autoimmune diseases might be prevented.

References

1. Salman, T., & Dinçkal, Ç. (2022). Kanser ve immünoterapi. Sağlık Biyoteknolojisi, 1, 78-84.
2. Bilal, T., & Altınar, A. (2019). Beslenmeye bağlı stres faktörlerinin bağışıklık üzerine etkisi. Hayvanlarda Beslenme ve Bağışıklık İlişkisi, 1, 68-80.
3. Aydoğdu, S., Göksu Yılmaz, T., & Tuğcu, D. (2015). Lenfadenopatiye Yaklaşım: Vaka Sunumu ve Literatürün Gözden Geçirilmesi. Çocuk Dergisi, 15(3-4), 118-123.
4. Ruddle, N. H., & Akirav, E. M. (2009). Secondary lymphoid organs: responding to genetic and environmental cues in ontogeny and the immune response. The Journal of Immunology, 183(4), 2205-2212.
5. Randall, T. D., Carragher, D. M., & Rangel-Moreno, J. (2008). Development of secondary lymphoid organs. Annual Review of Immunology, 26, 627-650.
6. Ramadas, A. A., Jose, R., Varma, B., & Chandy, M. L. (2017). Cervical lymphadenopathy: Unwinding the hidden truth. Dental Research Journal, 14(1), 73.
7. Cakala-Jakimowicz, M., Kolodziej-Wojnar, P., & Puzianowska-Kuznicka, M. (2021). Aging-related cellular, structural and functional changes in the lymph nodes: A significant component of immunosenescence? An overview. Cells, 10(11), 3148.
8. Songu, M., & Katılmış, H. (2012). Enfeksiyondan korunma ve immün sistem. Journal of Medical Updates, 2(1), 31-42.
9. Elmore, S. A. (2006). Histopathology of the lymph nodes. Toxicologic pathology, 34(5), 425-454.
10. Saxena, V., Li, L., Paluskievicz, C., Kasinath, V., Bean, A., Abdi, R., ... & Bromberg, J. S. (2019). Role of lymph node stroma and microenvironment in T cell tolerance. Immunological reviews, 292(1), 9-23.
11. Ayata, A. (2004). Çocukluk çağında lenfadenopatiler. SDÜ Tıp Fakültesi Dergisi, 11(2), 26-29



Advanced Engineering Days

aed.mersin.edu.tr



Exploration of the Pb-Zn deposit using IP/Resistivity methods: A case study in Sudöşeği (Simav-Kütahya)

Cihan Yalçın*¹, Hürşit Canlı²

¹Ministry of Industry and Technology, World bank PIU, Ankara, cihan.yalcin@sanayi.gov.tr

²Haliç Mineral Exploration and Drilling, Department, İstanbul, hursitcanli@gmail.com

Cite this study: Yalçın, C., & Canlı, H. (Year). Exploration of the Pb-Zn deposit using IP/Resistivity methods: A case study in Sudöşeği (Simav-Kütahya). *Advanced Engineering Days*, 8, 45-48

Keywords

Pb-Zn
IP/Resistivity
Geological Structure
Chargeability
Profile

Abstract

The investigation of Pb-Zn deposits holds significant importance in fulfilling the worldwide need for lead and zinc, crucial elements utilized in a wide range of industries, including battery manufacturing and construction. Preliminary geological investigations conducted in the Sudöşeği region of Simav-Kütahya have revealed the existence of favorable conditions conducive to the occurrence of Pb-Zn mineralization. The Sudöşeği region located in Simav-Kütahya has been recognized as a highly prospective area for the occurrence of lead-zinc (Pb-Zn) mineral deposits. This study utilizes the induced polarization (IP) and resistivity methods to effectively characterize subsurface geological structures and evaluate the potential for a Pb-Zn deposit. Geophysical techniques provide valuable insights into the variations in conductivity and chargeability of the subsurface, thereby assisting in the identification of mineralized zones. The results of our study demonstrate noteworthy associations between atypical IP and resistivity patterns and established geological characteristics, thereby confirming the efficacy of this integrated methodology in the field of mineral exploration. Chargeability values were observed in profile L 100, which is one of the profiles where geophysical methods were employed. These values were identified as potential indicators of mineralization. This case study exemplifies the significant role played by IP and resistivity methods in the identification of Pb-Zn deposits, highlighting their effectiveness in improving resource assessment and extraction strategies.

Introduction

The geological community has been diligently pursuing effective techniques for the identification and evaluation of mineral deposits over an extended period of time. Traditional methods of exploration, such as geological mapping and drilling, possess certain limitations in terms of their extent of coverage, financial implications, and potential environmental consequences. As a result, geophysical methods have garnered considerable interest as valuable tools in the field of mineral exploration. Induced polarization (IP) and resistivity techniques have demonstrated their efficacy in the identification and characterization of subsurface mineral deposits. The investigation of Pb-Zn ore systems is of considerable importance owing to their substantial economic value and extensive geographical distribution. Copper, lead, and zinc are essential elements that play a critical role in a wide range of industries, including electronics, construction, and transportation. Hence, it is imperative to develop effective methodologies for the identification and assessment of these deposits in order to satisfy worldwide demand and enhance the efficient utilization of resources.

Electrical resistivity tomography (ERT) is a commonly employed geophysical technique utilized for the purpose of characterizing subsurface structures and gaining insights into geological formations [1-2]. The data obtained from this study offers significant insights into the spatial variation of electrical resistivity within the subsurface. Consequently, it facilitates the identification and characterization of diverse geological formations as well as potential areas of mineralization.

The utilization of induced polarization (IP) represents an additional geophysical methodology that offers significant contributions in the understanding of subsurface conditions. This technology possesses the capacity to identify minute conductive rocks that may not be easily detectable using alternative methodologies. The utilization of IP measurements enables the detection of sulfur in minerals, mineral deposits, and soils, while also providing insights into the polarizability of subsurface materials [3].

The integration of these methods yields a potent approach, as it enables the acquisition of data pertaining to both the electrical conductivity and polarizability characteristics of the materials present beneath the surface. This data can be utilized to ascertain regions where sulfide minerals are prone to occur, given that these minerals generally exhibit low resistivity and high chargeability.

Geological formations in which sulfide minerals are present commonly display characteristics of low resistivity and high chargeability [4-5]. The geophysical signatures observed in this study may serve as indicators of the existence of sulfide mineralization, specifically lead-zinc (Pb-Zn) deposits. Resistivity and induced polarization (IP) methods have been effectively employed in numerous studies pertaining to mineral exploration, specifically in the context of lead-zinc (Pb-Zn) exploration [6-7].

The mining of lead-zinc (Pb-Zn) in Türkiye has a rich historical background that can be traced back to the Roman era [8]. Initial geological investigations conducted in the Sudöşeği area of Simav-Kütahya have revealed the existence of conducive circumstances for the occurrence of lead-zinc mineralization [9]. These conditions encompass the occurrence of rocks containing lead and zinc, such as the Eğrigöz Plutonic Complex. Hydrothermal fluids capable of transporting lead and zinc ions are observed. The occurrence of structural traps, such as faults and fractures, can facilitate the entrapment of hydrothermal fluids, thereby contributing to the genesis of mineral deposits [9].

Based on the existing body of evidence, it is probable that the Sudöşeği region possesses the capacity to accommodate substantial lead-zinc mineralization. However, additional investigation and assessment are required in order to verify the existence of a mineral deposit and determine its economic viability. This study employs the induced polarization (IP) and resistivity methods in order to enhance our comprehension and demarcate potential ore deposits.

Material and Method

By employing the principle of induced polarization, the IP/Resistivity method is capable of delineating the spatial distribution of subsurface resistivity and chargeability. The true chargeability, denoted by the symbol (M''), refers to the ratio between the voltage obtained after the current supply is ceased and the voltage measured during the current supply. Typically, the range of values for this parameter lies within the interval of 0 to 1000 mV/V, and its unit of measurement is expressed as millivolts per volt (mV/V).

The resistivity method involves the utilization of a stainless steel electrode that is inserted into the ground to facilitate the injection of an electric current. Subsequently, two electrodes are strategically positioned at multiple locations to quantify the voltage differential present in the soil. The voltage that is measured is typically recorded in volts, often in millivolts. Similarly, the current that is applied is typically measured in amperes, commonly in milliamperes. The aforementioned numerical values, in conjunction with the geometric factor K of the electrode array, are employed to calculate the apparent resistivity (measured in ohm-meters) at the specific location of measurement. The assigned value is located beneath the middle of the electrode array system.

In the research field, a resistivity and IP measurement device with 84 electrodes, specifically an AGI brand, 8-channel system, was employed. The Pole-Dipole Gradient method was utilized to generate a total of 6 profiles, employing electrode spacing within the range of 25 meters. The line was generated utilizing a Magellan handheld GPS device, which possesses a positioning accuracy of 3 meters. The data that was gathered was subjected to analysis using the EarthImager 2D evaluation software. This study presents data from 2 profiles.

Geotomo's RES2DINV and RES3DINV programs were utilized to perform reverse resolution operations on the resistivity and chargeability data, aiming to achieve a geological representation that is more accurate and in line with reality. The effects of topography were corrected using GPS elevation data obtained from the profiles in the process of reverse resolution. The report appendix contains graphs illustrating the charging and self-resistance profiles for the reverse solutions. The charts employed warm red-purple hues to depict elevated charging and self-resistance values, while cooler colors like green and blue were utilized to represent lower values. This study focuses on areas with high chargeability, which is considered to be important targets for metallic refinement.

Results

The L 100 profile was initially conducted in a highly controlled manner, during which corrosion phenomena were observed (Figure 1). Upon analyzing the charging interval that arises from the transformation of land data into geophysical sections, it is evident that two closure forms extend from scale 125 of the profile to scale 175. This extension is observed at the depth of the initial closure, specifically between 1060 and 1015. An observation was made of a unit exhibiting a high electrical permeability and a low self-resistance, positioned in a location where the resistance was favorable.

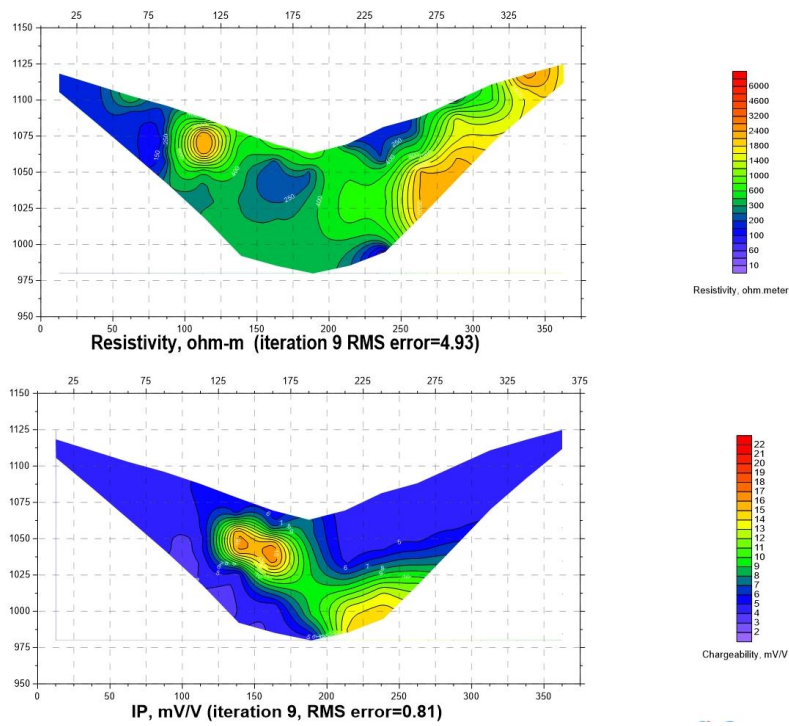


Figure 1. The inverted resistivity and IP sections with topography of the L100 profile.

The L 200 profile represents (Figure 2) a comprehensive examination of the region in which the fault is situated, conducted in a perpendicular manner. Upon examining the charging interval that arises from the conversion of land data into geophysical sections, it becomes evident that a charging anomaly is present. This anomaly is characterized by varying values observed between the measurement points 150-200. An anomaly has been detected within the measurement range of 150-200 points, specifically indicating a low charging value ranging from 1050 to 1000 cylinders. Furthermore, there has been an observation of a transmissible unit of resistance.

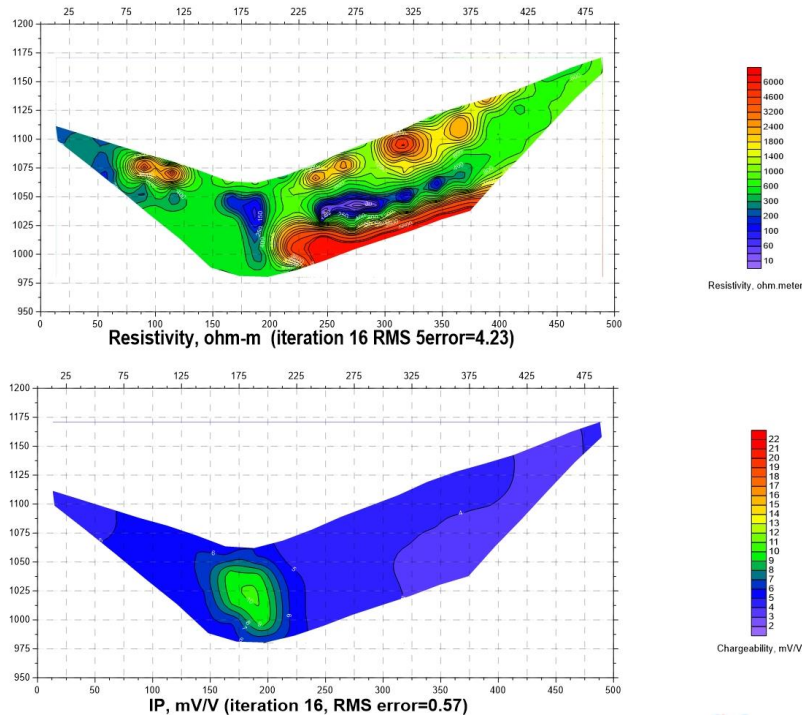


Figure 2. The inverted resistivity and IP sections with topography of the L200 profile.

Discussion

The induced polarization (IP) method provides valuable insights into the electrical chargeability of subsurface materials, enabling the identification of mineralized zones and alteration fronts that are commonly associated with lead-zinc (Pb-Zn) deposits. Through the analysis of the gradual decline in induced polarization, it

is possible to deduce the existence of sulfide minerals that serve as indicators of mineralization. In contrast, the resistivity method offers insights into the distribution of electrical resistivity, enabling the delineation of geological structures and the identification of regions that may contain ore-bearing formations.

In the studies carried out, the profiles were determined to be poorly upright in the NW- SE direction, and the L 100 profile presented in this study observed the charging values and these values were also determined that there is a possibility of reversal.

The study conducted by Yalçın et al. [10] in the Kavşut region of Göksun-Kahramanmaraş is a significant example of utilizing the IP and resistivity methods to identify polymetallic enrichments. This research has valuable implications for the improvement of mineral exploration methodologies and the sustainable utilization of resources in the Kavşut area and beyond [10]. In a separate investigation, Yalçın and Canlı [11] likely sought to enhance comprehension of Pb-Zn mineralization in the Yahyalı region of Kayseri, Türkiye by employing geophysical techniques such as IP/RESISTIVITY. Their objective would have been to aid in resource assessment and promote sustainable mining practices.

Conclusion

This study provides a persuasive argument for the utilization of IP and resistivity techniques in the investigation of Pb-Zn deposits, specifically in the Sudöşeği area of Simav-Kütahya. The strong correlation observed between abnormal geophysical indicators and established geological characteristics highlights the effectiveness of this integrated methodology. Through the integration of IP and resistivity techniques, we have effectively delineated prospective mineralized zones, providing significant insights for the assessment of resources and the planning of extraction activities. The increasing global demand for lead and zinc necessitates the use of advanced geophysical methods, which play a vital role in the sustainable and responsible exploitation of mineral resources.

References

1. Loke, M.H., & Barker, R.D. (1996). Rapid least-squares inversion of apparent resistivity pseudo sections using a quasi-Newton method. *Geophysical Prospecting*, 44, 131-152. <https://doi.org/10.1111/j.1365-2478.1996.tb00142.x>
2. Dusabemariya, C., Qian, W., Bagaragaza, R., Faruwa, A., & Ali, M. (2020). Some experiences of resistivity and induced polarization methods on the exploration of sulfide: A Review. *Journal of Geosciences and Environment Protection*, 8, 68-92. <https://doi.org/10.4236/gep.2020.811004>
3. Olowofela, J.A., Ajani, O.O., & Oladunjoye, M.A. (2008). Application of induced polarization method to delineate sulphide ore deposit in Osina Area of Benue State, Nigeria. *Ife Journal of Science*, 10(1), 137-150.
4. Langore, L., Alikaj, P., & Gjovreku, D. (1989). Achievements in copper sulphide Exploration in Albania with IP and EM Methods. *Geophysical Prospecting*, 37, 975-991. <https://doi.org/10.1111/j.1365-2478.1989.tb02243.x>
5. Yoshioka, K., & Zhdanov, M.S. (2005). Three-dimensional nonlinear regularized inversion of the induced polarization data based on the cole-cole model. *Physics of the Earth and Planetary Interiors*, 150(1-3), 29-43. <https://doi.org/10.1016/j.pepi.2004.08.034>
6. Sono, P., Nthaba, B., Shemang, E.M., Kgosidintsi, B., & Seane, T. (2021). An integrated use of induced polarization and electrical resistivity imaging methods to delineate zones of potential gold mineralization in the Phitshane Molopo area, Southeast Botswana. *Journal of African Earth Sciences*, 174, 104060. <https://doi.org/10.1016/j.jafrearsci.2020.104060>
7. Moreira C.A., Lopes S.M., Schweig C., & Seixas A.R. (2012). Geoelectrical prospection of disseminated sulfide mineral occurrences in Camaquã Sedimentary Basin, Rio Grande do Sul State, Brazil. *Revista Brasileira de Geofísica*, 30, 169-179.
8. Haniçlı, N., Öztürk, H., & Kasapçı, C. (2019). Carbonate-hosted Pb-Zn deposits of Turkey. Chapter 10 In: Pirajno, F., Dönmez, C., Şahin, M.B. (Eds.), *Mineral Resources of Turkey, Modern Approaches in Solid Earth Sciences*. Springer Nature, Switzerland, 497–533. https://doi.org/10.1007/978-3-030-02950-0_10
9. Oyman, T. (2019). Epithermal Deposits of Turkey. Chapter 4 In: Pirajno, F., Dönmez, C., Şahin, M.B. (Eds.), *Mineral Resources of Turkey, Modern Approaches in Solid Earth Sciences*. Springer Nature, Switzerland, 159–223.
10. Yalçın, C., Canlı, H., Haznedaroğlu, K., & Akbulut, F. (2023). Investigating the Kavşut (Göksun-Kahramanmaraş) Cu-Pb-Zn deposit by using IP/Resistivity Methods. *Advanced Engineering Days*, 7, 73-76.
11. Yalçın, C., & Canlı, H. (2023). Investigating the Yahyalı (Kayseri, Türkiye) Pb-Zn deposit by using IP/Resistivity Methods. *Advanced Engineering Days*, 7, 69-72.



Examination of buildings with different number of floors using non-linear time history analysis according to TBEC-2018 and EC 8 seismic codes

Mehmet Yılmaz ^{*1}, Hüsnü Can ²

¹KTO Karatay University, Department of Civil Engineering, Türkiye, 32mf20@gmail.com

²Gazi University, Department of Civil Engineering, Türkiye, husnucan@gazi.edu.tr

Cite this study: Yılmaz, M., & Can, H. (2023). Examination of buildings with different number of floors using non-linear time history analysis according to TBEC-2018 and EC 8 seismic codes. *Advanced Engineering Days*, 8, 49-51

Keywords

SAP 2000
TBEC-2018
Eurocode 8
Nonlinear time history analysis
Seismic performance

Abstract

As a result of the earthquakes that have occurred on the earth from the past to the present, the issue of earthquake performance of structures has come to the fore in structural and earthquake engineering. In Turkey, with the Turkish Seismic Code (TSC-2007) conditions were defined for the first time in the regulation for the evaluation and reinforcement of existing structures. Within the scope of this research, the carrier system; Consisting of a unhollow reinforced concrete shear wall frame system with high ductility, located in the 1st degree seismic zone, having the same floor formwork plan; The seismic performance evaluation of 10, 15 and 20 storey existing reinforced concrete buildings was made by using nonlinear time history analysis according to Turkish Building Earthquake Code 2018 (TBEC-2018) and Eurocode 8 (EC 8) earthquake codes. Within the scope of the study, SAP200 (v25) computer software was used for modeling of the structures and performance analysis. In scope of the data obtained, it has been determined that TBEC-2018 is on the safer side compared to Eurocode 8.

Introduction

Earthquakes are among the natural disasters that occur on earth and cause loss of life and property. Our country is in the Alpine-Himalayan seismic zone, which is one of the important and active seismic zones in terms of earthquake risk, starting from the Azores Islands and extending to Southeast Asia [1].

As a result of the earthquakes that have occurred since the existence of the universe until today, the subject of seismic performance of structures has gained significant importance in the fields of structural engineering and earthquake engineering [2]. With the opportunities offered by today's construction technology, earthquake-resistant high-rise constructions have become widespread in our lives. The collapse of many buildings and the loss of lives because of the recent severe earthquakes which are Izmir, Elazığ, Van, Kahramanmaraş and Hatay show that sufficient precautions have not been taken regarding the safety of existing constructions [3]. To minimize the damage caused by earthquakes on structures and the loss of life, buildings must be designed to be earthquake resistant.

Material and Method

In this study there are 3 constructions which are 10, 15 and 20 stories with have 7 spacings for X direction and 5 spacings for Y direction. These constructions have been considered as existing buildings in the 1st degree seismic zone in Bayraklı district of Izmir province, at 38.4633126 north latitude and 27.18229563 east longitude. The carrier system of constructions is a unhollow reinforced concrete shear wall frame system with high ductility (Figure 1). These constructions have the same floor plans, and each floor is 3m height. The purpose of use of the

buildings is residential. Using the PEER database, ground motion records were selected according to TBEC-2018 [4] part 2, part 5, EN 1998-1:2004 [5] (Eurocode 8 part 1) part 3 and part 4.

Ground motion records were selected by choosing the fault type, magnitude, Joyner-Boore-distance (R_{jb}) and shear wave speed (V_{s30}) parameters appropriately. Ground motion records selected according to both seismic codes were scaled on the PEER [6] database. The obtained scaling coefficients were tested with the SeismoMatch [7] program. SAP2000 [8], a computer software, was preferred for analysis and calculations. Effective section stiffnesses were assigned for the modeled structures according to both seismic codes, and plastic hinges were defined. Then, the following steps were followed:

For nonlinear time history analysis, the response spectrum is defined according to both seismic codes.

According to TBEC-2018, AFAD [9] interactive web application was used for response spectrum.

Response spectrum data defined according to Eurocode were taken from the EN 1998-1 (2004)[5] regulation.

11 ground motion records were selected for TBEC-2018 and 4 ground motion records were selected for Eurocode 8.

Ground motion records were identified with the time history function, then they were matched with the response spectrum.

After the matching process was completed, nonlinear time history (direct integration) function was defined as a load case and analyzes were performed.

Tablo 10. Yapı hakkında genel bilgiler

Kat Adedi	10	15	20
Kullanım Amacı	Konut	Konut	Konut
Deprem Bölgesi	1	1	1
Zemin Sınıfı	ZD	ZD	ZD
Kat Yüksekliği (m)	3	3	3
Toplam Bina Yüksekliği (m)	30	45	60
Beton Sınıfı	C35	C35	C35
Donatı Çeliği	S420	S420	S420
Kolon Kesiti (cmxcm)	65x60	85x75	95x90
Kiriş Kesiti (cmxcm)	25x50	25x50	30x55
Döşeme Kalınlığı (cm)	15	15	15
P. Duvar Kalınlığı (cm)	25	25	30

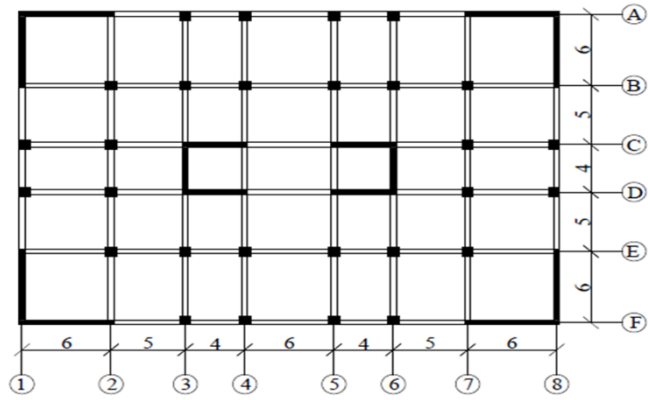


Figure 1. General information about constructions and floor plans.

Results

Data regarding the top floor displacements, and damage levels of structural elements for the most unfavorable of the analysis performed as an example are included in Tables 1, 2, 3 and 4.

Table 1. Damage performances for beams (20-storey)

Beams	TBEC-2018	EC 8	% (TBEC-2018)	% (EC 8)
SH (DL)	884	775	65	56.98
KH (SD)	473	574	34.78	42.21
GÖ (NC)	3	11	0.22	0.81

Table 2. Damage performances for columns (20-storey)

Columns	TBEC-2018	EC 8	% (TBEC-2018)	% (EC 8)
KK	275	244	49.11	43.57
SH (DL)	260	279	46.43	49.82
KH (SD)	25	37	4.46	6.61

Table 3. Damage performances for shear walls (20-storey)

Columns	TBEC-2018	EC 8	% (TBEC-2018)	% (EC 8)
KK	114	113	95	94.17
SH (DL)	4	5	3.33	4.17
KH (SD)	2	2	1.67	1.67

Table 4. Max top floor displacement for all time history analysis

	Ux (cm)	Uy (cm)
10 kat		
TBEC-2018	10.58	10.54
EC 8	16.28	16.53
15 kat		
TBEC-2018	18.46	19.25
EC 8	28.73	29.41
20 kat		
TBEC-2018	29.63	28.59
EC 8	42.37	42.26

Discussion

Although there are studies on determining the seismic performance of existing reinforced concrete buildings according to TBEC-2018 or EC 8, the studies carried out with both regulations are very few. While most of the identified studies are related to the TSC-2007 and Eurocode 8, very few studies are related to TBEC-2018 and Eurocode 8. Due to the lack of sufficient studies and the lack of common and clear findings among the studies conducted, in this study, the nonlinear time history analysis to be carried out according to Eurocode 8 was investigated more comprehensively. The nonlinear time history analysis in Eurocode 8 chapter 3 and chapter 4 was supplied the conditions, analyzes have been made.

Conclusion

As a result of the modal analysis, the building vibration periods obtained according to TBEC-2018 are greater than the values obtained according to Eurocode 8. The reason for this is due to effective section stiffness. As a result of the most unfavorable time history analysis; The maximum displacement values of buildings obtained according to TBEC-2018 were lower than EC 8. According to the data obtained from the analyses, the seismic performance of the structures was determined as controlled damage (significant damage) according to both seismic codes. When we look at the overall numerical data, especially the data of the most unfavorable analysis, it seems that TBEC-2018 is on the safer side compared to Eurocode 8.

References

1. Özmen, B., & Nurlu, M. (1999). Deprem bölgeleri haritası ile ilgili bazı bilgiler. TMMOB Jeoloji Mühendisleri Odası Haber Bülteni, 99(2-3), 32-35.
2. Dılmaç, H., Ulutaş, H., Tekeli, H., & Demir, F. (2018). An evaluation on seismic performance of existing reinforced concrete buildings in Turkey. Mehmet Akif Ersoy Üniversitesi Fen Bilimleri Enstitüsü Dergisi, 9(Ek (Suppl.) 1), 224-237. <https://doi.org/10.29048/makufebed.443126>
3. Çeltik, B. (2023). Mevcut Betonarme Bir Yapının Performans Değerlendirmesi İle Güçlendirme Sonrası Analiz Sonuçlarının Doğrusal Ve Doğrusal Olmayan Hesap Yöntemleriyle Karşılaştırılması. MS Thesis, KTO Karatay Üniversitesi.
4. T.C. İçişleri Bakanlığı, & Başkanlığı, (2018). Türkiye Bina Deprem Yönetmeliği. Resmi Gazete. <https://www.mevzuat.gov.tr/mevzuat?MevzuatNo=24468&MevzuatTur=7&MevzuatTertip=5>
5. European Commission. (2004). EN 1998-1:2004 Eurocode 8: Design of structures for earthquake resistance - Part 1: General rules, seismic actions and rules for buildings. Joint Research Center. <https://eurocodes.jrc.ec.europa.eu/EN-Eurocodes/eurocode-8-design-structures-earthquake-resistance>
6. <https://ngawest2.berkeley.edu>
7. Seismosoft. (n.d.). SeismoMatch (v2023). <https://seismosoft.com/>
8. SAP2000. (2000). Structural Analysis and Design (v25.1.0). Computers and Structures, Inc. <https://www.csiamerica.com/products/sap2000>
9. AFAD, T., İ. İ. B. A., & A. D. Y. B. (2019). Türkiye deprem tehlike haritası. <https://www.afad.gov.tr/turkiye-deprem-tehlike-haritasi>



Advanced Engineering Days

aed.mersin.edu.tr



Investigation of stone deterioration in Gaziantep Historical Gümrük Inn

İlhami Ay ¹, Murat Dal ², Şefika Ergin ³

¹Hakkari University, Çölemerik Vocational School, Hakkari, Türkiye, ilhamiay@hakkari.edu.tr

²Munzur University, Faculty of Fine Arts, Design and Architecture, Tunceli, Türkiye muratdal1122@gmail.com

³Dicle University, Institute of Science and Technology, Diyarbakır, Türkiye, sefika@dicle.edu.tr

Cite this study: Ay, İ., Dal, M. & Ergin, Ş. (2023). Investigation of stone deterioration in Gaziantep Historical Gümrük Inn. *Advanced Engineering Days*, 8, 52-55

Keywords

Stone Deterioration
Gaziantep
Historical Gümrük Inn
Type of Deterioration

Abstract

In traditional stone structures, the strength value and durability of the stone are important in terms of transferring the structure to future generations. It is important for the structures to determine the deterioration and causes of the deterioration on the surface of the stone as a result of climatic and external factors and to offer solutions. In this study, the deterioration of the Historical Gümrük Inn in Gaziantep is discussed. In this context, the deterioration was visually examined, classified and analyzed as physical, chemical, biological and anthropogenic. It is aimed that the data obtained from the study will be the basis for the conservation projects to be carried out in the coming years.

Introduction

Stone material has been used in different areas and purposes throughout human history. Stone material is preferred more than other main construction materials because it has features such as chiseling, drilling and processing. It is also frequently used due to its low cost compared to other construction materials [1].

The durability and strength properties of stone materials are important for traditional stone structures to survive longer and to be passed on to future generations. Stone materials are used in different areas of human life. Apart from main construction products such as load-bearing walls, columns, slabs and facade elements, they are also preferred in different areas [2, 3].

The stone material used in traditional stone buildings deteriorates on the stone surface as a result of internal and external factors [4-6]. It is important for the structures to detect the stone deterioration, to investigate the causes and to take measures against deterioration [7, 8]. It is aimed that the data obtained from the studies will lead the academic studies and conservation projects to be carried out on this building in the coming years.

Material and Method

In this study, stone deterioration in the Historical Customs Inn located in Şekeroğlu Neighborhood of Gaziantep was investigated. The deterioration was visually analyzed and recorded by photographs. The two-story and single courtyard inn serves as a museum today. The building, which does not have a proper position due to the location of the building, was built of black and white cut stone. In this study, the deterioration of the inner courtyard and facade walls of the building were examined, identified and classified [9]. According to the classification, deterioration is analyzed in four groups: physical, chemical, biological and anthropogenic [10].

Results

When the stones used in traditional stone structures are exposed to climatic factors, natural factors and human influences, degradation occurs on the stone surfaces. These degradations change the petrographic

properties of the stone. In some cases, the deterioration of stone surfaces also causes other deterioration [11, 12]. Detection of deterioration in natural stones is important in terms of taking precautions and transferring them to future generations [13, 14]. In this context, in this study, stone deterioration occurring in Gaziantep Gümrük Han was identified, classified and analyzed. The deterioration is categorized as physical, chemical, biological and anthropogenic deterioration.

Surface losses that occur on stone surfaces as a result of changes in the petrographic properties of the stone as a result of internal and external factors are called physical deterioration. Capillary cracks, fragment breaks, surface abrasions, cuts and joint losses can be given as examples of physical deterioration [15]. The physical deterioration observed in the Historical Gümrük Inn structure is shown in Figure 1.



Figure 1. Physical deteriorations in Historical Gümrük Inn

The deterioration of stone surfaces as a result of climatic and atmospheric factors such as temperature and humidity is called chemical deterioration. Crystallization, salinization, discoloration and foliation are the types of chemical deterioration [16]. The chemical deterioration of the Historical Gümrük Inn is shown in Figure 2.



Figure 2. Chemical deteriorations in Historical Gümrük Inn

The degradation of the stone surface as a result of the reaction of biological substances with the stone surface is called biological degradation. Algae growth, plant growth, plant accumulation are types of biological degradation [17-18]. Biological degradation in the historical Gümrük Han structure is shown in Figure 3.



Figure 3. Biological deteriorations in Historical Gümrük Inn

Anthropogenic deterioration is the deterioration that occurs as a result of the damage caused to traditional stone structures consciously or unconsciously by humans [19]. Incorrect restoration practices, misuse, neglect and wear and tear are the types of anthropogenic deterioration. The types of anthropogenic deterioration in the Historical Gümrük Inn structure are shown in Figure 4.



Figure 4. Anthropogenic deteriorations in Historical Gümrük Inn

Conclusion

This study focuses on the deterioration observed in Gaziantep Historical Customs Inn. The deterioration was identified by visual analysis and categorized and analyzed. Physical, chemical, biological and anthropogenic deterioration were observed.

The data obtained in the study is intended to form a basis for both academic studies and future restoration projects. In addition, this study is important in terms of taking the necessary measures to ensure the survival of traditional stone buildings for a longer period of time.

References

1. Hasbay, U., & Hattap, S. (2017). Doğal Taşlardaki Bozunma (Ayrışma) Türleri ve Nedenleri. *Bilim ve Gençlik Dergisi*, 5(1), 23–45.
2. Fitzner, B., & Heinrichs, K. (2001). *Damage Diagnosis on Stone Monuments – Weathering Forms, Damage Categories and Damage Indices*. 1–49.
3. Adin, H. (2007). Mardin ve Midyat'ta Kullanılan Bina Yapı Taşlarının Bazı Fiziksel Özellikleri. *Mühendis ve Makina*, 48(570), 13–17.
4. Biçen Çelik, A., Ergin, Ş., Dal, M., & Ay, İ. (2023). Analysis of Stone Deterioration on the Facades of Hatuniye Madrasah. *Journal of Architectural Sciences and Applications*, 8(1), Article 1. <https://doi.org/10.30785/mbud.1302007>
5. Dal, M., & Öcal, A. D. (2013). Investigations on Stone Weathering of Ottoman Architecture: A Kırklareli Hızırbey Kulliyeh Case Study. *Paripex- Indian Journal of Research*, 2(13), 1–6
6. Dal, M., & Öcal, A. D. (2013). Limestone In Islamic Religious Architecture: İstanbul And Turkish Thrace. *METU Journal Of The Faculty Of Architecture*, 30(01). <https://doi.org/10.4305/METU.JFA.2013.1.2>
7. Ay, İ., Ergin, Ş., & Dal, M. (2023). Geleneksel Taş Yapılarda Meydana Gelen Taş Alterasyonları: Gaziantep Hamam Müzesi Örneği. *UMTEB - XIII International Scientific Research Congress*, 515–523.
8. Ay, İ., Ergin, Ş., & Dal, M. (2023). Geleneksel Taş Yapılarda Meydana Gelen taş Alterasyonları: Gaziantep Millet Hanı Örneği. *UMTEB - XIII International Scientific Research Congress*, 507–514.
9. Dal, M. (2021). The Deterioration Problems Observed in the Natural Building Blocks of Saint George Church in Diyarbakır Province. *Online Journal of Art and Design*, 9(1), 254–262.
10. Öcal, A. D., & Dal, M. (2012). Doğal Taşlardaki Bozunmalar (Müka Matbaası). *Mimarlık Vakfı İktisadi İşletmesi*.
11. Ergin, Ş., Gökdemir, B., Yardımlı, S., & Dal, M. (2022). Deterioration On The Stone Surfaces Of The Diyarbakır Nebi Mosque. *International Refereed Journal of Design And Architecture*, 0(27), 1–32. <https://doi.org/10.17365/TMD.2022.TURKEY.27.01>
12. Ergin, Ş., Dal, M., & Çelik, A. (2020). Şeyh Çabuk Camii Cephelerinde Görülen Taş Bozunma Sorunlarının İrdelenmesi ve Kimyasal Analizlerinin Karşılaştırılması. In *Mimarlık Üzerine-1* (pp. 103–124). IKSAD Yayınevi.
13. Dal, M., & Yardımlı, S. (2021). Taş Duvarlarda Yüzey Bozunmaları. *Kent Akademisi*, 14(2), 428–451. <https://doi.org/10.35674/kent.922313>
14. Dal, M., Ergin, Ş., Çelik, A. B., & Ay, İ. (2023). Stone alterations in Hatuniye Madrasah. *Advanced Engineering Days (AED)*, 7, 77–80.

15. Ay, İ., Dal, M., Ergin, Ş., & Çelik, A. B. (2023). Stone alterations in Kasımiye Madrasah. *Advanced Engineering Days (AED)*, 7, 81–84.
16. Çelik, A. B., Ay, İ., Dal, M., & Ergin, Ş. (2023). Stone alterations in Zinciriye Madrasah. *Advanced Engineering Days (AED)*, 7, 89–91.
17. Tokmak, M., & Dal, M. (2020). Classification of Physical, Chemical and Biological Deteriorations Observed in Ankara Stone Monuments. *International Journal of Pure and Applied Sciences*, 6(1), 8–16. <https://doi.org/10.29132/ijpas.718466>
18. Dal, M., Zülfiyar, H. C., & Dolar, A. (2020). Mimari Taş Yapılarda Görülen Biyolojik Bozunmalar. In *Geleneksel ve Çağdaş Mimari Yapılar Üzerine Akademik Çalışmalar* (pp. 29–62). İksad Yayınevi.
19. Ergin, Ş., Çelik, A. B., Ay, İ., & Dal, M. (2023). Stone alterations in Şehidiye Madrasah. *Advanced Engineering Days (AED)*, 7, 85–88.



Advanced Engineering Days

aed.mersin.edu.tr



Investigation of stone deterioration in Gaziantep Kumandan Fountain

İlhami Ay ¹, Murat Dal ², Şefika Ergin ³

¹Hakkari University, Çölemerik Vocational School, Hakkari, Türkiye, ilhamiay@hakkari.edu.tr

²Munzur University, Faculty of Fine Arts, Design and Architecture, Tunceli, Türkiye, muratdal1122@gmail.com

³Dicle University, Institute of Science and Technology, Diyarbakır, Türkiye, sefika@dicle.edu.tr

Cite this study: Ay, İ., Dal, M. & Ergin, Ş. (2023). Investigation of stone deterioration in Gaziantep Kumandan Fountain. *Advanced Engineering Days*, 8, 56-59

Keywords

Stone Deterioration
Gaziantep
Commander Fountain
Type of Deterioration

Abstract

In traditional stone structures, the strength value and durability of the stone are important in terms of transferring the structure to future generations. It is important for the structures to determine the deterioration and causes of the deterioration on the surface of the stone as a result of climatic and external factors and to offer solutions. In this study, the deterioration of the Commander Fountain in Gaziantep is discussed. In this context, the deterioration was visually examined, classified and analyzed as physical, chemical, biological and anthropogenic. It is aimed that the data obtained from the study will be the basis for the conservation projects to be carried out in the coming years.

Introduction

Throughout human life, stone material has been used in different areas of people's lives. The high durability and strength of the stone material is important in terms of the permanence of the structures made of stone and their transfer to future generations. People have used stone material in different areas in traditional buildings. The main ones are; bearing walls, columns, flooring and facade elements. Apart from these, it is also used in construction, coating, sculpture, tombstone making, gravel, porcelain and glass industry, optical industry and ornaments [1, 2].

Stone material has been preferred more than other construction materials. The fact that stone material can be processed such as machining, drilling, chiseling is effective in this. In addition, the lower cost of stone material has made it the main construction material of many buildings [3].

Natural stones deteriorate on stone surfaces due to internal and external factors such as adverse climatic conditions, traffic density and user errors [4-6]. In order to prevent deterioration in buildings, it is important to investigate and identify the causes and to transfer them to future years [7, 8]. It is aimed that this study will form the basis for the studies in the following years and lead the repair projects in terms of addressing the existing problems.

Material and Method

In this study, the stone deterioration of the Commander Fountain adjacent to the northern façade of Gaziantep Historic Kır Kahvesi was visually analyzed. The deterioration was photographed and recorded. The Commander Fountain was built with black and white cut stones and does not have any ornamentation other than these stones. The fountain has a hexagonal form. The upper part of the fountain has twelve sides and is covered with a bulbous dome and there is a baba at the end. In addition, no water flows from the fountain today. The deterioration on the walls of the Commander's Façade structure was analyzed, identified and classified [9].

According to the classification, deterioration was analyzed in four groups: physical, chemical, biological and anthropogenic [10].

Results

When natural stones are exposed to external factors such as climatic factors, natural factors or human effects, deterioration occurs on the stone surface. These deteriorations reduce the strength of the stone. In some cases, deteriorations prepare the ground for the formation of other deteriorations or accelerate the process [11, 12]. It is necessary to identify the deterioration of the stone and take measures to transfer it to future generations [13], [14]. In this context, the deterioration of the structure was analyzed as physical, chemical, biological and anthropogenic deterioration.

Surface losses on stone surfaces as a result of internal and external factors are called physical deterioration. Capillary cracks, fragment breaks, surface abrasions, cuts and joint losses are examples of physical deterioration [15]. The physical deterioration observed in the structure of the Kumandan Fountain is shown in Figure 1.



Figure 1. Physical deteriorations in Kumandan Fountain

The deterioration that occurs on the stone surface as a result of atmospheric events and climatic factors is called chemical deterioration. Color change, crystallization, salinization, crusting and foliation are the types of chemical deterioration [16]. Chemical deterioration occurring in the structure is shown in Figure 2.



Figure 2. Chemical deteriorations in Kumandan Fountain

The deterioration of organic substances on the stone surface is called biological deterioration. Algae growth, plant growth, bioaccumulation are the types of biological deterioration [17, 18]. Biological deterioration in the structure is shown in Figure 3.

Anthropogenic deterioration is the deterioration of traditional historic stone buildings caused by the conscious or unconscious damage caused by humans [19]. Destructions such as misapplication, misuse and periodic wear and tear are types of anthropogenic deterioration. Anthropogenic deteriorations in the structure are given in Figure 4.



Figure 3. Biological deteriorations in Kumandan Fountain



Figure 4. Anthropogenic deteriorations in Kumandan Fountain

Conclusion

This study focuses on the deterioration observed at the Gaziantep Commander Fountain. The deterioration was determined by visual analysis and categorized and analyzed. Physical, chemical, biological and anthropogenic deterioration were observed.

It is aimed that the data obtained in the study will form a basis for future conservation projects. In addition, this study is important in terms of taking the necessary measures to ensure that traditional stone buildings survive for a longer period of time.

References

1. Hasbay, U., & Hattap, S. (2017). Doğal Taşlardaki Bozunma (Ayrışma) Türleri ve Nedenleri. *Bilim ve Gençlik Dergisi*, 5(1), 23-45.
2. Fitzner, B., & Heinrichs, K. (2001). *Damage Diagnosis on Stone Monuments – Weathering Forms, Damage Categories and Damage Indices*. 1-49.
3. Adin, H. (2007). Mardin ve Midyat'ta Kullanılan Bina Yapı Taşlarının Bazı Fiziksel Özellikleri. *Mühendis ve Makina*, 48(570), 13-17.
4. Biçen Çelik, A., Ergin, Ş., Dal, M., & Ay, İ. (2023). Analysis of Stone Deterioration on the Facades of Hatuniye Madrasah. *Journal of Architectural Sciences and Applications*, 8(1), Article 1. <https://doi.org/10.30785/mbud.1302007>
5. Dal, M., & Öcal, A. D. (2013). Investigations on Stone Weathering of Ottoman Architecture: A Kırklareli Hizirbey Kulliyeh Case Study. *Paripex- Indian Journal Of Research*, 2(13), 1-6
6. Dal, M., & Öcal, A. D. (2013). Limestone In Islamic Religious Architecture: İstanbul And Turkish Thrace. *METU Journal Of The Faculty Of Architecture*, 30(01). <https://doi.org/10.4305/METU.JFA.2013.1.2>
7. Ay, İ., Ergin, Ş., & Dal, M. (2023). Geleneksel Taş Yapılarda Meydana Gelen Taş Alterasyonları: Gaziantep Hamam Müzesi Örneği. *UMTEB - XIII International Scientific Research Congress*, 515-523.
8. Ay, İ., Ergin, Ş., & Dal, M. (2023). Geleneksel Taş Yapılarda Meydana Gelen taş Alterasyonları: Gaziantep Millet Hanı Örneği. *UMTEB - XIII International Scientific Research Congress*, 507-514.
9. Dal, M. (2021). The Deterioration Problems Observed in the Natural Building Blocks of Saint George Church in Diyarbakır Province. *Online Journal of Art and Design*, 9(1), 254-262.
10. Öcal, A. D., & Dal, M. (2012). Doğal Taşlardaki Bozunmalar (Müka Matbaası). *Mimarlık Vakfı İktisadi İşletmesi*.
11. Ergin, Ş., Gökdemir, B., Yardımlı, S., & Dal, M. (2022). Deterioration On The Stone Surfaces Of The Diyarbakır Nebi Mosque. *INTERNATIONAL REFEREED JOURNAL OF DESIGN AND ARCHITECTURE*, 0(27), 1-32. <https://doi.org/10.17365/TMD.2022.TURKEY.27.01>
12. Ergin, Ş., Dal, M., & Çelik, A. (2020). Şeyh Çabuk Camii Cephelerinde Görülen Taş Bozunma Sorunlarının İrdelenmesi ve Kimyasal Analizlerinin Karşılaştırılması. In *Mimarlık Üzerine-1* (pp. 103-124). IKSAD Yayınevi.
13. Dal, M., & Yardimli, S. (2021). Taş Duvarlarda Yüzey Bozunmaları. *Kent Akademisi*, 14(2), 428-451. <https://doi.org/10.35674/kent.922313>
14. Dal, M., Ergin, Ş., Çelik, A. B., & Ay, İ. (2023). Stone Alterations in Hatuniye Madrasah. *Advanced Engineering Days (AED)*, 7, 77-80.

15. Ay, İ., Dal, M., Ergin, Ş., & Çelik, A. B. (2023). Stone Alterations in Kasımiye Madrasah. *Advanced Engineering Days (AED)*, 7, 81–84.
16. Çelik, A. B., Ay, İ., Dal, M., & Ergin, Ş. (2023). Stone Alterations in Zinciriye Madrasah. *Advanced Engineering Days (AED)*, 7, 89–91.
17. Tokmak, M., & Dal, M. (2020). Classification of Physical, Chemical and Biological Deteriorations Observed in Ankara Stone Monuments. *International Journal of Pure and Applied Sciences*, 6(1), 8–16. <https://doi.org/10.29132/ijpas.718466>
18. Dal, M., Zülfiyar, H. C., & Dolar, A. (2020). Mimari Taş Yapılarda Görülen Biyolojik Bozunmalar. In *Geleneksel ve Çağdaş Mimari Yapılar Üzerine Akademik Çalışmalar* (pp. 29–62). İksad Yayınevi.
19. Ergin, Ş., Çelik, A. B., Ay, İ., & Dal, M. (2023). Stone Alterations in Şehidiye Madrasah. *Advanced Engineering Days (AED)*, 7, 85–88.



The impact of alternative fuels to diesel in reducing pollution from vehicles

Asllan Hajderi ^{*1}, Ledia Bozo ² Fatmir Basholli ¹

¹ Albanian University, Department of Engineering, Tirana, Albania; ashajderi@yahoo.com; fatmir.basholli@albanianuniversity.edu.al

² University of Tirana, Faculty of Natural Sciences, Department of Informatics, Tirana, Albania; lediabozo@gmail.com

Cite this study: Hajderi, A., Bozo, L., & Basholli, F. (2023). The impact of alternative fuels to diesel in reducing pollution from vehicles. *Advanced Engineering Days*, 8, 60-63

Keywords

Diesel engines
Reducing environmental pollution
Alternative fuels
Reduction of carbon dioxide

Abstract

The main source of energy for vehicles is currently internal combustion engines. These engines emit the main pollutants carbon oxide, carbon dioxide, hydrocarbons, nitrogen oxides, and particles matters into the atmosphere. The biggest polluter of nitrogen oxides and particles are diesel engines. For this purpose, the addition of alternative fuels ethanol, methanol, biodiesel, and Fischer-tropsch fuel to conventional diesel fuel in the amount of 5-15% has been studied, to see their impact on the reduction of carbon dioxide and pollution. For this, the analytical method of carbon dioxide calculation, experimental data from the literature and experimental measurements of the opacity coefficient were used. From the obtained results, it results that in reduction of CO₂ affect more the fuels B15 up to 11.5%, M-15 up to 9%, FT 15 up to 7.5% and E-15 up to 6%. Also, M 15 has the greatest impact on the reduction of particles and nitrogen oxides with a reduction of 45% and 30% respectively, followed by E 15 with 30% and 20% and B15 and FT15 with 30% and 25%. Experimental measurements of the opacity coefficient confirm that the use of M15 and E15 fuels reduces pollution by 35% and 25%.

Introduction

In recent years, it has been determined that the acceptable limit of the level of CO₂ without causing serious consequences for the environment is 450 ppm [1], while if the limit value of 750 ppm is exceeded, we will have an irreparable environmental crisis, which is thought to be reached around the year 2100, if this rate of CO₂ production continues.

Several studies have determined that to meet the energy needs of an ever-growing population, energy needs in 2040 will double, in 2070 they will triple and in 2100 they will quadruple. The result of this forecast indicates an increase of more than 300% of CO₂ gas in the atmosphere [2]. At the world level in 2014, more than 30 billion tons of CO₂ were produced, which comes from the production of electricity in 45% and from transport in 18% [3].

Conventional fuels consisting of hydrocarbons extracted from fossil oil are mainly used in transport vehicles. From the use of these fuels in vehicle, mainly carbon dioxide and other polluting gases such as CO, CH, NO_x and carbon particles are released into the atmosphere. Carbon dioxide before it was considered harmless to humans, but in the last years after 2010 it is considered dangerous, because it affects the global warming of the atmosphere. Diesel engines have a higher degree of pollution than engines with gasoline, because they release high amounts into the atmosphere of nitrogen oxides, and carbon particles. Nitrogen oxides affect the greenhouse effect of the atmosphere, while PM particles affect human lung damage and cancer.

Under these conditions, the International Energy Agency (IEA) predicts the forced use of biofuels in vehicles, up to 5% in 2030 [4]. This attention for biofuels is related to the fact that the use of biodiesel reduces emissions net of CO₂ with 78.45%, particles with 32%, CO with 35% and NO_x with 8%, in compared with diesel [5,6].

Based on the needs to reduce the amount of CO₂ produced by vehicles and pollution caused by vehicles, we have undertaken this study for diesel fuels mixed with alternative fuels, in order to reduce the pollution.

Material and Method

To carry out the study, the analytical method of calculating the carbon dioxide released by alternative fuels during combustion in the engine and experimental measurements performed for 3 cars with diesel engines.

Diesel fuels used in vehicles

The fuel that is commonly used in diesel engines is called diesel and is a mixture of heavy hydrocarbons, which have a large molecular mass, with carbon atoms 12-22, with boiling points from 149-399° C. According to the molecular mass, 2 categories of diesel are used [9]:

Light diesel with chemical formula $C_{12.3}H_{22.2}$ with a molecular weight of about 170, which has a low viscosity and is easily injected, but is more expensive and is used in engines with high pressures.

Heavy diesel with chemical formula $C_{14.6}H_{24.8}$ with a molecular weight of about 200, which has a higher viscosity and is injected with some difficulty but is less expensive and widely used in vehicles. The density of diesel varies in 0.83-0.86 kg/dm³ and the calorific power, in 9500-10500 kcal/kg.

Compound fuels with additives of alternative fuels in fossil diesel

We have formed several fuels of mixing of diesel with alternative fuels ethanol, methanol, biodiesel and Fischer-Tropsch, in a percentage of 5%, 10% and 15%, which we named with the brands: E-5, E-10, E-15; M-5, M-10, M-15; B-5, B-10, B-15 and FT-5, FT-10, FT-15. In additions of alternative fuels, we have stopped up to 15%, so that their use in diesel engines does not damage the engine's work and does not require.

The alternative fuels used in the study have the following characteristics [9]:

a) Ethanol is known as ethyl alcohol or wheat alcohol, is a chemical compound with the formula C_2H_5-OH . Ethanol has a calorific value of 6400 kcal/kg, lower than diesel.

b) Methanol, known as methyl alcohol, or wood alcohol, is a chemical compound with the formula CH_3-OH . Methanol has a low calorific value of 4200 kcal/kg.

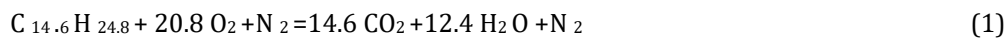
c) Biodiesel fuel is a renewable fuel that can be produced from vegetable oils, animal fats, or recycled restaurant fats. Its characteristics are in accordance with the specifications of the standards for use in diesel engines. Biodiesel is a clean fuel, which does not release polluting emissions during combustion. The creation of carbon is almost 4 times less than conventional diesel [5].

d) Fischer-Tropsch synthetic fuels are produced from fossil products or biomass using CO and H₂ extracted in a process similar to hydrogenation, producing gasoline and diesel. They have the same characteristics and performance as diesel and burn cleanly, reducing the level of greenhouse gases to 80%, CO₂ to 50% and carbon particles to 20-50% [9].

Estimation of the amount of carbon dioxide released by the burning of fuels

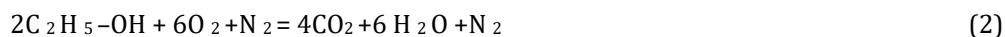
To determine the amount of carbon dioxide, we will use the equation of the chemical reaction of fuel combustion, [12] that we will use for mixtures that are:

a) Diesel. In the study we are taking the second most used category. The combustion process is expressed by:



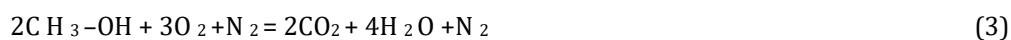
So during the burning of 1 kg diesel, will be released : $14.6 \times 44 / 200 = 3.21$ kg CO₂.

b) Ethanol. The combustion equation of pure ethanol is expressed as:



So, during the burning of 1 kg ethanol, are released: $4 \times 44 / 2 \times 46 = 1.91$ kg CO₂.

c) Methanol. The combustion equation of pure methanol is expressed as:



So, during the burning of 1 kg methanol, are released: $2 \times 44 / 2 \times 32 = 1.37$ CO₂

d) Biodiesel fuels. Pure biodiesel (B100) during combustion releases 4 times less CO₂ [5], so 0.8 kg CO₂

e) Fischer-Tropsch synthetic fuels. Clean fuel (FT100) during combustion releases 50% of the CO₂ of diesel [10], thus releasing 1.6 kg CO₂.

The amount of CO₂ released by burning 1 kg of composite fuel will be calculated:

$$G_{CO_2} = G_K \times P_i + G_D \times P_i' \quad (5)$$

Where:

G_K – Amount of CO₂ produced by the alternative fuel (100%), obtained from estimates b,c,d,e

G_D – The amount of CO₂ produced by the second type of diesel, obtained from the estimate a .

P_i – The percentage that the alternative fuel occupies in the composite fuel, which are: 0.05, 0.1 and 0.15

P_i' – The percentage of diesel in the composite fuel, which are respectively 0.95, 0.9 and 0.85

The results of the calculations performed for the composite fuels are shown in Figure 1.

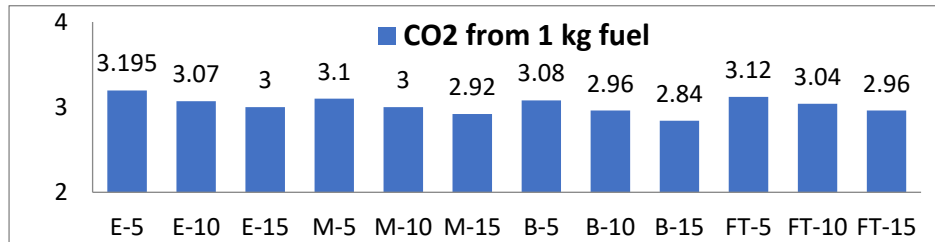


Figure 1. Amount of CO₂ for brands of formed fuels.

Experimental determination of the degree of vehicles pollution

For vehicles with diesel engines, the evaluation of the degree of pollution is done by the opacity coefficient, which indicates the degree of turbidity caused by the combustion gases escaping into the atmosphere.

Thus, for fuels composed with ethanol and methanol, experimental measurements of the opacity coefficient were performed at the vehicle technical control center for 3 vehicles with diesel engines equipped with the 3 types of fuel systems currently used in diesel engines.

For the above three vehicles, the measurements were carried out according to the relevant methodology [10] for fossil fuel and for mixed fuel brands E-5 E-10 E-15 M-5 M-10 M-15.

The results of the measurements performed for the 3 mixtures ethanol and methanol are shown in Figure 2.

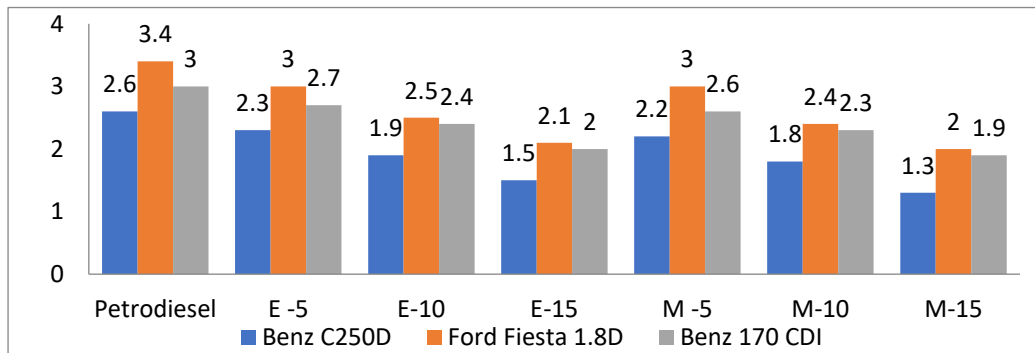


Figure 2. Opacity coefficient for the 5 fuels formed with alternative fuels

Results

The results of the calculations show that ethanol produces 1.5 times less carbon dioxide than diesel, methanol 2.2 times less, biodiesel 4 times less and Fischer-Tropsch fuel 2 times less than diesel. While the results for the amount of carbon dioxide produced by the fuel blends, biodiesel, Fischer-Tropsch, methanol and ethanol, up to 15%, reduce carbon dioxide by 11.3%, 7.5%, 8.7% and 6% respectively. And the results of experimental measurements from fig. 3, show that fuel M 15 and E15 affect the reduction of the opacity coefficient by 35% and 25%, respectively.

Based on the above results, we propose mixed fuels with 10 to 15% Biodiesel, Fischer-Tropsch, methanol and ethanol, because this provides us a total reduction of greenhouse gases (CO₂) up to 11.5%, but also a significant reduction of environmental pollution from particles around 30-45%.

Conclusion

The use of Fischer-Tropsch diesel fuel in vehicle achieves a reduction of carbon dioxide up to 2 times and pollution from nitrogen oxides and carbon particles by 80% and 50%, respectively, compared to conventional diesel.

The use of M15 and E 15 fuels achieves a reduction of carbon dioxide by 8.7% and 6% respectively, and the degree of pollution by NOx and carbon particles up to 35% and 25% compared to conventional diesel.

The use of M15 and E 15 fuels reduces the opacity coefficient by 35% and 25%, respectively compared to conventional diesel.

References

1. Glasby, G. P. (2006). Drastic reductions in utilizable fossil fuel reserves: an environmental imperative. *Environment, development and sustainability*, 8, 197-215. <https://doi.org/10.1007/s10668-005-5753-4>
2. Holdren, J. P. (2006). The energy innovation imperative: Addressing oil dependence, climate change, and other 21st century energy challenges. *Innovations: Technology, governance, globalization*, 1(2), 3-23. <https://doi.org/10.1162/itgg.2006.1.2.3>
3. WRI (World Resources Institute) (2011). "Climate Analysis Indicators Tool" Version 8.0 ultimo accesso aprile 2011 www.cait.wri.org
4. IEA (International Energy Agency) (2010). Sustainable production of second -generation biofuels (OECD)
5. Agarwal, A. K. (2007). Biofuels (alcohols and biodiesel) applications as fuels for internal combustion engines. *Progress in energy and combustion science*, 33(3), 233-271. <https://doi.org/10.1016/j.pecc.2006.08.003>
6. Rakopoulos, C. D., Rakopoulos, D. C., Hountalas, D. T., Giakoumis, E. G., & Andritsakis, E. C. (2008). Performance and emissions of bus engine using blends of diesel fuel with bio-diesel of sunflower or cottonseed oils derived from Greek feedstock. *Fuel*, 87(2), 147-157. <https://doi.org/10.1016/j.fuel.2007.04.011>
7. Carraretto, C., Macor, A., Mirandola, A., Stoppato, A., & Tonon, S. (2004). Biodiesel as alternative fuel: Experimental analysis and energetic evaluations. *Energy*, 29(12-15), 2195-2211. <https://doi.org/10.1016/j.energy.2004.03.042>
8. Mahate V., & Bisen A. (2019). Impacts and Challenges of Biodiesel Use in Transport sector – An overview *IJRSET*, 8(1), 444-450
9. Halderman D. J. (2012). Automotive technology principles, diagnosis and service, 918-945
10. Hajderi A., & Sefa, S. (2015). The impact of alternative fuels in vehicles to reduce the global warming. *Interdisciplinary Journal of Research and Development (IJRD)*, 2(2), 35-42



Estimation of surface urban heat island (SUHI) effect over four populated cities of Andhra Pradesh state of India

Jagadish Kumar Mogaraju *¹ 

¹International Union for Conservation of Nature Commission on Ecosystem Management, Agro-ecosystems, India, jagadishmogaraju@gmail.com

Cite this study: Mogaraju, J. M. (2023). Estimation of surface urban heat island (SUHI) effect over four populated cities of Andhra Pradesh state of India. *Advanced Engineering Days*, 8, 64-67

Keywords

SUHI
Urban Heat Island
Climate
Temperature
Population

Abstract

This work reports the probable effect of population ingress in generating urban heat islands over four cities of Andhra Pradesh state of India. We identified twenty-six UHIs and chose four UHIs based on the population data. The period from 1961 to 1990 was selected as the reference period, and 2003 to 2020 was selected as the study period to determine the deviations in mean temperatures. We framed a methodology to filter and select the UHIs to know the effect of SUHI using online resources for data and plots that are free of cost and user-friendly. One out of four UHIs exhibited a stronger deviation in night-time temperatures than in day-time temperatures. We observed that the rise in population equally contributes to the temperature deviations over the long term in the selected areas. We conclude that the population ingress may influence land surface temperatures and induce the SUHI effect.

Introduction

Population growth and other variables can change the thermal characteristics of land, thereby generating surface urban heat islands (SUHI) [1]. Normalized Difference Vegetation Index (NDVI) and seasonal variations have influenced the SUHI effect over some of the regions in India [2]. Index-based built-up Index (IBI) and NDVI values were used to determine the land surface temperature (LST) variations that aided in explaining urban microclimate (SUHI effects) [3]. Urban agglomeration (reduction of natural resources) has a definite effect on varying LST, leading to urban heat islands that may lead to climate anomalies [4]. Increasing LST and urban population can induce a domino effect of irreversible environmental damage that may have long-term effects on the quality of life (QOL) [5, 6]. Evidently, the population ingress into urban areas in various unsustainable approaches led to reduced green cover (vegetation), leaving the inhabited terrain and UHIs [7]. Landsat 8 and Sentinel 2,3 data were used in various studies to explain the extent and effects of UHIs (SUHI effects) [8–10]. The surface urban heat islands can be characterized using simplified urban-extent algorithms (using Google Earth engine) with vegetation as a controlling factor [11]. The datasets and plots needed to investigate urban heat islands and the SUHI effect can be easily obtained online with no charges and limited effort and are user-friendly [12,13]. The present study is aligned with contemporary research [14–17] and aimed at filling the gaps in terms of filtering and selecting UHIs based on population and demonstrating the SUHI effect with reference period (1961 to 1990) and study period (2003 to 2020).

Material and Method

The datasets needed for this study were obtained from NASA (AQUA Land Surface Temperature (LST) and MODIS TERRA) and <https://open-meteo.com/en/docs/historical-weather-api>. The population data (2001/2011) was obtained from the Census of India website (<https://censusindia.gov.in>). The SUHI temperature deviations were obtained from a previous study on urban heat islands by Chakraborty and Lee, 2019. The plots for this study were prepared from the Python-based application provided by Jan Kühn, 2023 (https://github.com/yotkadata/meteo_hist). The population data collected was used to filter the areas with a high population. There are approximately 26 urban heat islands spread across the study area. We filtered out the urban heat islands with high populations and selected four out of 26 UHIs. The SUHI deviations were studied, the years

in which there is high deviation were selected, and the annual temperature deviation for the selected years was studied and plotted for reporting. The reference period considered in this study is from 1961 to 1990, as recommended by the World Meteorological Organization (WMO), and the study period is from 2003 to 2020. The study areas are given in Figure 1, and detailed methodology is given in Figure 2.



Figure 1. Harmonized Landsat and sentinel images of four Urban Heat Islands

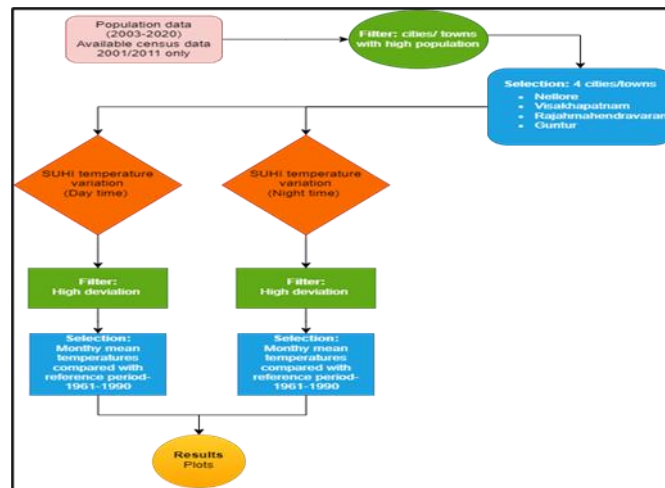


Figure 2. Method

Results

The results are given from Figure 3 to figure 6. We obtained 4 UHIs out of 26 UHIs based on the population data. They are Nellore, Visakhapatnam, Rajamahendravaram, and Guntur. The change in population from 2001 to 2011 for these cities is 28% (Nellore), 22% (Visakhapatnam), 14% (Rajamahendravaram), and 24% (Guntur). We observed an increase of 2.8 °C in Sep-Oct/2011 and a 2.6 °C increase in May/2020 compared to the reference period for Nellore UHI (Figure 4 a-c). We observed an increase of 2.2 °C in Dec/2016 and about 3.4 °C increase in May/2020 compared to the reference period for Visakhapatnam UHI (Figure 4 a-c). We observed an increase of 4.8 °C in Jun/2014, and about 2.8 °C in Nov/2020 compared to the reference period for Rajamahendravaram UHI (Figure 5 a-c). We observed an increase of 4.6 °C in May/2013 and about 3.9 °C in April/2016 compared to the reference period for Guntur UHI (Figure 6 a-c).

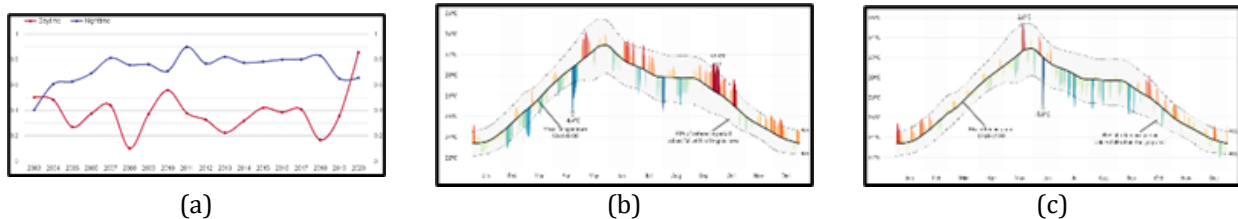


Figure 3. Nellore (UHI) (a) Annual change (°C), (b) Mean temperature variation in 2011, (c) 2020

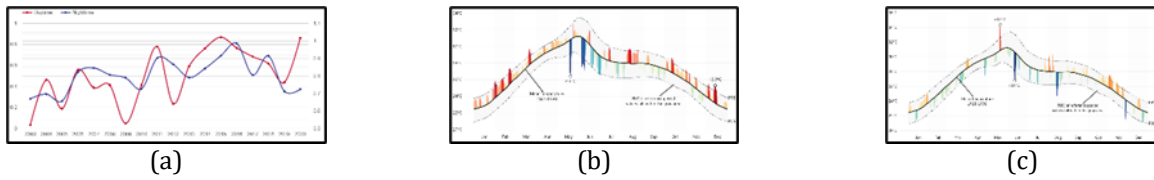


Figure 4. Visakhapatnam (UHI) (a) Annual change (°C), (b) Mean temperature variation in 2016, (c) 2020

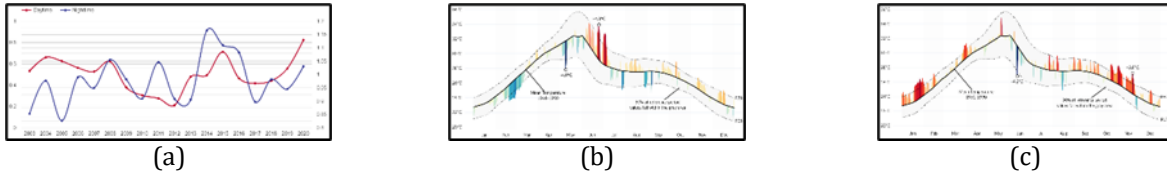


Figure 5. Rajamahendravaram (UHI) (a) Annual change (°C), (b) Mean temperature variation in 2014, (c) 2020

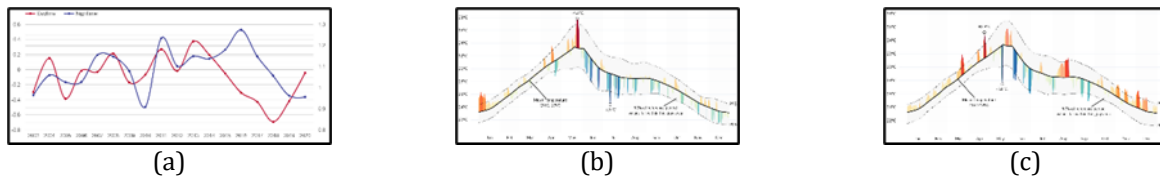


Figure 6. Guntur (UHI) (a) Annual change (°C), (b) Mean temperature variation in 2013, (c) 2016

Discussion

This work was initiated on the premise that there will be a clear indication of population growth and the SUHI effect. Keeping in view our research premise, we observed the following that may be worth discussing. Nellore UHI: The population increase of 28% from 2001 to 2011 has affected the SUHI temperature deviations (discrete), supporting our view. The night-time temperatures were relatively less affected than day-time temperatures. Visakhapatnam UHI: The population increase of 22% from 2001 to 2011 has affected the SUHI temperature deviations (discrete), supporting our view. The night-time temperatures and day-time temperatures were affected. Rajamahendravaram UHI: The population increase of 14% from 2001 to 2011 has affected the SUHI temperature deviations (discrete), supporting our view. The night-time temperatures were more deviated than day-time temperatures. Guntur UHI: The population increase of 24% from 2001 to 2011 has affected the SUHI temperature deviations (discrete), supporting our view. The night-time temperatures and day-time temperatures were affected.

Conclusion

We conclude that population growth may have a role in inducing the SUHI effect over the highly populated urban heat islands. We also opine that sustainable population ingress methods can improve the quality of life in the future. Some of the vegetation renewal practices can improve the livability in the urban zones.

References

1. Sannigrahi, S., Rahmat, S., Chakraborti, S., Bhatt, S., & Jha, S. (2017). Changing dynamics of urban biophysical composition and its impact on urban heat island intensity and thermal characteristics: the case of Hyderabad City, India. *Modeling Earth Systems and Environment*, 3(2), 647–667. <https://doi.org/10.1007/s40808-017-0324-x>
2. Bhanage, V., Kulkarni, S., Sharma, R., Lee, H. S., & Gedam, S. (2023). Enumerating and Modelling the Seasonal alterations of Surface Urban Heat and Cool Island: A Case Study over Indian Cities. *Urban Science*, 7(2), 38. <https://doi.org/10.3390/urbansci7020038>
3. Sharma, R., Pradhan, L., Kumari, M., & Bhattacharya, P. (2021). Assessing urban heat islands and thermal comfort in Noida City using geospatial technology. *Urban Climate*, 35, 100751. <https://doi.org/10.1016/j.uclim.2020.100751>
4. Vani, M., & Prasad, P. R. C. (2020). Assessment of spatio-temporal changes in land use and land cover, urban sprawl, and land surface temperature in and around Vijayawada city, India. *Environment, Development and Sustainability*, 22(4), 3079–3095. <https://doi.org/10.1007/s10668-019-00335-2>

5. Jafari-Sirizi, R., Oshnooei-Nooshabadi, A., Khabbazi-Kenari, Z., & Sadeghi, A. (2022). Determination of the Quality of Life using Hybrid BWM-TOPSIS Analysis: Case study of Tabriz (District 1,2,3 and 8), Iran. *Türkiye Uzaktan Algılama Dergisi*, 4(1), 7–17. <https://doi.org/10.51489/tuzal.1066578>
6. Khamesi-Maybodi, M. H. (2022). GIS-Based Assessment of Land Surface Temperature Changes Over Khorramabad City (Lorestan, Iran). *Türkiye Uzaktan Algılama Dergisi*, 4(2), 87–95. <https://doi.org/10.51489/tuzal.1116553>
7. Yamak, B., Yağci, Z., Bilgilioğlu, B. B., & Çömert, R. (2021). Investigation of the effect of urbanization on land surface temperature example of Bursa. *International Journal of Engineering and Geosciences*, 6(1), 1–8. <https://doi.org/10.26833/ijeg.658377>
8. Mushore, T., Odindi, J., & Mutanga, O. (2022). “Cool” Roofs as a Heat-Mitigation Measure in Urban Heat Islands: A Comparative Analysis Using Sentinel 2 and Landsat Data. *Remote Sensing*, 14(17), 4247. <https://doi.org/10.3390/rs14174247>
9. Hidalgo García, D., & Arco Díaz, J. (2021). Modeling of the Urban Heat Island on local climatic zones of a city using Sentinel 3 images: Urban determining factors. *Urban Climate*, 37, 100840. <https://doi.org/10.1016/j.uclim.2021.100840>
10. Bagyaraj, M., Senapathi, V., Karthikeyan, S., Chung, S. Y., Khatibi, R., Nadiri, A. A., & Asgari Lajayer, B. (2023). A study of urban heat island effects using remote sensing and GIS techniques in Kancheepuram, Tamil Nadu, India. *Urban Climate*, 51, 101597. <https://doi.org/10.1016/j.uclim.2023.101597>
11. Chakraborty, T., & Lee, X. (2019). A simplified urban-extent algorithm to characterize surface urban heat islands on a global scale and examine vegetation control on their spatiotemporal variability. *International Journal of Applied Earth Observation and Geoinformation*, 74, 269–280. <https://doi.org/10.1016/j.jag.2018.09.015>
12. Historical Weather API | Open-Meteo.com. (n.d.). Retrieved November 30, 2023, from <https://open-meteo.com/en/docs/historical-weather-api>
13. Historical Meteo Graphs | Jan Kühn. (n.d.). Retrieved November 30, 2023, from <https://yotka.org/projects/meteo-hist>
14. Neog, R., Acharjee, S., & Hazarika, J. (2019). Evaluation of spatio-temporal pattern of surface urban heat island phenomena at Jorhat, India. *Arabian Journal of Geosciences*, 12(10), 316. <https://doi.org/10.1007/s12517-019-4484-z>
15. He, B.-J., Wang, J., Zhu, J., & Qi, J. (2022). Beating the urban heat: Situation, background, impacts and the way forward in China. *Renewable and Sustainable Energy Reviews*, 161, 112350. <https://doi.org/10.1016/j.rser.2022.112350>
16. Muthiah, K., Mathivanan, M., & Duraisekaran, E. (2022). Dynamics of urban sprawl on the peri-urban landscape and its relationship with urban heat island in Chennai Metropolitan Area, India. *Arabian Journal of Geosciences*, 15(23), 1694. <https://doi.org/10.1007/s12517-022-10959-w>
17. Nikkala, S., Peddada, J. R., & Neredimelli, R. (2022). Correlation analysis of land surface temperature on landsat-8 data of Visakhapatnam Urban Area, Andhra Pradesh, India. *Earth Science Informatics*, 15(3), 1963–1975. <https://doi.org/10.1007/s12145-022-00850-3>



Investigation of headway distribution of traffic dominated by motorcycles

Hassan Shuaibu Abdulrahman*¹, Stephen Sunday Kolo ¹, Mahmud Abubakar ¹,
Mohammed Shehu ¹

¹Federal University of Technology, Civil Engineering Department, Nigeria, abdul.hassan@futminna.edu.ng;
s.kolo@futminna.edu.ng; mahmud1879@futminna.edu.ng; moh.shehu@futminna.edu.ng

Cite this study: Abdulrahman, H. S., Kolo, S. S., Abubakar, M., & Shehu, M. (2023). Investigation of headway distribution of traffic dominated by motorcycles. *Advanced Engineering Days*, 8, 68-70

Keywords

Motorcycles
Headway distribution
Kernel distribution
Goodness-of-fit
P-value

Abstract

The use of lower class vehicles such as two or three wheelers have become the preferred urban transport in some developing countries. However, most of the traffic theories adopted are from developed countries where cars are prevalent. The headway probability distribution models can be used to describe vehicle-to-vehicle interactions. Most of these distributions are parametric and makes an underlining assumption about the data. A case study was conducted to investigate the performance of the different probability distributions that best describes the vehicle to vehicle interaction of motorcycle dominated road in Bida, Niger state Nigeria. The different parametric distributions and non-parametric distribution (Kernel) of the data were tested for the goodness-of-fit. The test results indicate that the kernel distribution fits best with improved P-values which in turn gives a better description for the headways than other distribution models considered. This study can serve as a foundation for developing generalized headway models in developing countries.

Introduction

Headway studies can be used to depict the individual vehicle-to-vehicle interaction in order to ascertain the safe operations of highways. The importance of carrying out such traffic analysis includes; analysis of road safety issues, estimation of road capacity and level of service, and the ease of data collection, etc. [1]. The probability distribution models can be used to describe headway data. These models are location dependent and sensitive to local conditions such as class of vehicles, driver behaviors etc. In some cities in Nigeria, the use of lower class vehicles such as two or three wheelers as personal and public transport is fast becoming the main stay in urban mobility. In 2016 alone, motorcycles form about 50% of all newly registered vehicles in Nigeria [2]. Previous studies on motorcycles in Nigeria concentrated on issues such as; their emergence as a public transportation mode, characteristics, education and road safety concerns [3,4,5]. Motorcycle traffic does not behave like conventional vehicles because they tend to be more aggressive, drive parallel to other vehicles, creating a near zero headways which might cause the risk of accidents [6]. Most important works pertaining to headway modelling are related to other vehicle interaction other than motor cycles [7]. While those relating to motorcycles have varied distributions representing this phenomenon especially for heterogeneous traffic where vehicles arrivals tend to be random in nature. This suggests a non-normal distribution which agrees with the probability distribution of homogeneous traffic [8- 9]. Furthermore, these distributions are parametric i.e.it is assumed that the observed data agrees with a particular distribution. These presumptions may affect the efficacy of the model especially under different circumstances of time, location and other human- induced factors [10]. Despite the persistent accidents recorded due to the proliferation of motorcycle use in some parts of Nigeria, only a few reports can be found in the literature on motorcycle headway models especially in Nigeria. This study is presents application of non-parametric distribution method in defining the headway data of motorcycle dominated traffic in Nigeria.

Material and Method

Due to high proportion of motorcycle in traffic flow, Landzhu road in Bida LGA Niger state was selected based on pre-feasibility studies that was carried out on some selected roads. The selected road has more than 70% of motor cycle traffic, 28% of car traffic and very about 2% heavy vehicles. Landzhu road is 2 lanes 2-way. The road width of is 7.5m. The data was collected using a digital video recorder for morning, afternoon and evening peak hours 8.00-9.00 am, 1.00-2.00 pm and 5.00-6.00pm respectively. Only headway data involving motorcycles were collected. The data was analysed using the following process; Histogram (check for skewness of data), descriptive statistics, and determine best fit distribution (common parametric vs non-parametric).

Results

The results of descriptive statistics, hypothesis testing, and best distribution are thus presented.

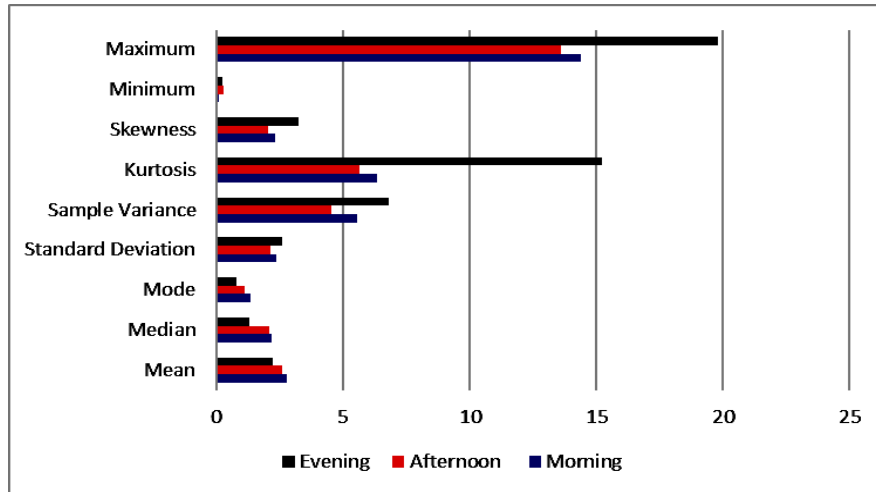


Figure 1. Quantitative description of the data set.

Discussion

Figure 1 Shows the descriptive statistics for the headway data sets. The headway data for all times is right skewed which implies that the higher headway values are fewer and more vehicles drive at shorter headways. This represents a non-normal distribution. Similarly, the kurtosis values are non-zero strengthening the earlier argument. The degree to which these descriptive statistics values vary can be attributed to the different times the data was collected. In all statistics, the modal headway during the evening peak is lower than for other peaks. This implies a dangerous attitude of the motor cycles riders riding at shorter headways where there is poor visibility and a potential for accidents. Even though its standard deviation is higher which shows the presence of outliers. This may not be unconnected with the fact little or no enforcement exists during the evenings.

Table 1. Hypothesis Testing and Best Fit based on P-value.

SN	Distributions	Morning		Afternoon		Evening	
		P values	Chi ²	P values	Chi ²	P values	Chi ²
1	Weibull	0.0003	1	0.0054	0	0.1029	1
2	Inverse Gaussian	0.0516	0	0.0724	0	0.5194	0
3	Gamma	0.0125	1	0.0014	0	0.2763	1
4	Lognormal	0.2388	0	0.0316	0	0.6162	1
5	Log-logistic	0.5506	0	0.028	0	0.6832	1
6	Burr	0.3099	0	0.0663	0	0.4557	0
7	Generalized Extreme Value	0.2693	0	0.0517	0	0.4717	0
8	Kernel	0.6809	0	0.9589	0	0.8532	0

One of the simpler methods of modelling data with a smooth function is the parametric polynomial trend line equations. It fits a polynomial function of a certain degree to the data the degree of the polynomials determines number bends. The trend line equations were fitted to probability density functions and the following equations

ensued for morning, afternoon, and evening data respectively with high R^2 . The high variations in headway data resulted high degree of the polynomial equations which may not necessarily capture the true relationships especially for complex. However, it may be necessary to confirm the nature of the distribution by using Chi-square distribution to test a more powerful non-parametric method. Table 1 shows the result of hypothesis test as regards

$$y = -0.00006x^6 + 0.0025x^5 - 0.0408x^4 + 0.3269x^3 - 1.346x^2 + 2.5594x - 1.4592 \quad R^2 = 0.99 \quad (1)$$

$$y = -0.00004x^6 + 0.0018x^5 - 0.0283x^4 + 0.226x^3 - 0.93x^2 + 1.77x - 0.95 \quad R^2 = 0.99 \quad (2)$$

$$y = -0.00006x^6 + 0.0023x^5 - 0.0435x^4 + 0.2692x^3 - 1.06x^2 + 1.88x - 976 \quad R^2 = 0.96 \quad (3)$$

whether the distribution belongs to a known distribution. “0” and “1” represents acceptance or rejection of hypothesis. The null hypothesis is that the data comes from same distribution and the alternative is that it does not. From the Table 1 it can be seen that the headway data agrees with the null hypothesis with only a few. Considering the P-value in Table 1, it can be seen the kernel distribution has the highest P-values for all cases. Although some parametric models performed well at different time periods, the kernel distribution still outperforms them. This is because the kernel distribution tends to conform with the given data and this may lead to the problem of overfitting. Another point because the non-parametric distribution fits best can be attributed to randomness of the headway distribution associated with motorcycles. This makes it difficult to have realistic assumptions about the underlying distributions. The results indicate some unique characteristics for the different time periods. Moreover, the uncertainties associated with traffic flows and the human induced vehicle interactions, makes it difficult to have a parametric distribution model that represents headway data adequately. This result strengthens the need for site and condition specific distribution models to represent headways.

Conclusion

This study models the headway distribution of motorcycle dominated traffic. The descriptive statistics points to a non-normal distribution of the headways. Polynomial equations were also generated to ascertain the nature and all equations had high degrees (6) with high R^2 . The performance of the different non-parametric distributions was assessed using the Chi-square statistics. The test results indicate that, the kernel distribution improved the P-values and showed a much better fit which in turn gives a better description for the headways than other parametric distribution models. This study can serve as a foundation to a generalized kernel model for traffic patterns of site specific locations especially where motorcycle dominates.

References

1. Al-Ghamdi, A. S. (2001). Analysis of Time Headways on Urban Roads: Case Study from Riyadh. *Journal of Transportation Engineering*, 127(4), 289-294. [https://doi.org/10.1061/\(ASCE\)0733-947X\(2001\)127:4\(289\)](https://doi.org/10.1061/(ASCE)0733-947X(2001)127:4(289))
2. Weze, K. O. (2019). *Helmet use among motorcycle riders in Nigeria* (Doctoral dissertation, Harvard University).
3. Nwadiaro, H. C., Ekwe, K. K., Akpayak, I. C., & Shitta, H. (2011). Motorcycle injuries in north-central Nigeria. *Nigerian journal of clinical practice*, 14(2), 186-189. <https://doi.org/10.4103/1119-3077.84012>
4. Morenikeji, W., & Umaru, E. (2012). Flying without navigational aids–The case of commercial motorcyclists in Minna, Nigeria. *Transportation research part F: traffic psychology and behaviour*, 15(3), 311-318. <https://doi.org/10.1016/j.trf.2012.02.003>
5. Kudu, D., Mohammed, A. E., Garba, I. K., Suleyman, Z. A. T., & Hassan, A. B. (2012). Motor cycle (Okada) Transport as a veritable means of public transport in Bida, Niger State, Nigeria, *International Journal of Environmental Science and Technology*.
6. Thamizh Arasan, V., & Koshy, R. Z. (2003). Headway distribution of heterogeneous traffic on urban arterials. *Journal of the Institution of Engineers. India. Civil Engineering Division*, 84(nov), 210-215.
7. Bham', G. H., & Ancha, S. R. P. (2006). Statistical models for preferred time headway and time headway of drivers in steady state car-following. In *Applications of advanced technology in transportation*, 344-349.
8. Prahara, E., & Prasetya, R. A. (2018). Speed-volume relationship and headway distribution analysis of motorcycle (case study: Teuku Nyak Arief Road). In *IOP Conference Series: Earth and Environmental Science*, 106(1), 012027. <https://doi.org/10.1088/1755-1315/106/1/012027>
9. Wedagama, D. P. (2017). Time Headway Modelling of motorcycle-dominated traffic to analyse traffic safety performance and road link capacity of single carriageways. *Journal of Civil Engineering*, 24(1), 27-34.
10. Zhang, G., & Wang, Y. (2014). A Gaussian kernel-based approach for modeling vehicle headway distributions. *Transportation Science*, 48(2), 206-216. <https://doi.org/10.1287/trsc.1120.0451>



A techno-economic analysis of a single-axis tracked bifacial photovoltaic plant connected in Albanian distribution system

Andi Hida*¹, Rajmonda Bualoti ¹, Pavlina Qosja ²

¹Polytechnic University of Tirana, Electrical Power Systems Department, Albania, andi.hida@fie.edu.al; r_bualoti@yahoo.com

²AEG Partners Balkan, Energetic Department, Albania, pavlina.qosja@fie.edu.al

Cite this study: Hida, A., Bualoti, R., & Qosja, P. (2023). A techno-economic analysis of a single-axis tracked bifacial photovoltaic plant connected in Albanian distribution system. *Advanced Engineering Days*, 8, 71-74

Keywords

Techno-Economic
Bifacial module
Tracking PV
Distribution System
Power losses

Abstract

This paper presents a techno-economic analysis of a 10 MWp photovoltaic (PV) plant installed in the south-west of Albania. To increase its performance, a single-axis solar tracking system with bifacial modules has been chosen. Moreover, the optimal design and sizing of the PV plant is determined through software, considering various factors. In this context, the results show that the annual yield of the on-grid PV system will be 1,670 kWh/kWp. In the same vein, the calculations present that the internal rate of return IRR is 20.6%, which indicates that the project will have a positive return on the investment value. Meanwhile the payback period of the investment is 4.8 years, which is considered as an investment that provides high income. These values are quite attractive for investors. On the other hand, the impact of this PV system on the distribution system parameters has been studied. While an improvement is seen in the voltage levels of the nodes, some of the lines and transformers show technical losses due to their loading.

Introduction

Growing concerns about global warming, environmental pollution and security of energy supply have increased interest in the use and development of renewable energy sources (RESs). For example, according to IEA, compared to 2022, by 2027, it is expected that RESs capacity will grow by almost 2400 GW (or 75%) [1]. Several factors have influenced this increase in RES penetration, such as: market conditions, investment costs, technology diversity, resource availability, proximity to the distribution or transmission network, etc. Another very important factor are government policies such as incentive fees, support schemes, or banking policies (loans) for the support and development of these technologies.

Among RESs, solar photovoltaic (PV) can provide suitable solutions to global climate change and give its impact to the global energy crisis. Moreover, in countries like Albania (energy production in which is based almost entirely on hydropower (99.28%), always questioning its reliability), the increase in installed PV capacities would affect the diversification of sources of electricity production [2-3]. It is worth mentioning that Albania has great potential for the use of solar energy, especially in its western part where Global Horizontal Irradiation (GHI) reaches a maximum of 1750 kWh/m² per year. In this context, most of the PV plants installed in Albania (29MW) are located in the Fier area. In addition, Law 24/2023 [4] on promoting the use of energy from RESs has increased the demand for the construction of new PV power plants.

On the other hand, the performance of photovoltaic systems has always been increasing. In particular, this performance depends on the optimal design and sizing of the PV plants [5]. In the same vein, authors in [6] show that the average energy produced by a panel with single axis tracker was 1.35 times greater than that of a fixed panel system. Furthermore, authors in [7] argue that bifacial PV produce 9 % to 23 % more power than monofacial PV.

In the end, determining the most suitable point for connecting PV plants to the electrical system is a very important issue. For this purpose, their impact on network parameters should be considered, such as: voltage

levels, loading of distribution lines and transformers and active power losses [8]. In this context, this paper deals with a techno-economic analysis of a Single-Axis Tracked Bifacial Photovoltaic Plant, connected in the Fieri distribution system area.

Material and Method

The methodology used to carry out this analysis combines the previous experiences undertaken in Albania in the field of feasibility studies and potential investments in RESs, more specifically in the generation of electricity through PV plants as well as forms of good management in the provision of this service. The study is based on solar radiation data averaged and published by SolarGis, likewise based on GlobalSolarAtlas computer modelling and the calculation program PV*SOL Premium 2022 (R7) [9]. These programs are used as a model for simulating and evaluating data and performance, besides to calculate expected yield. For example, according to the simulations in SolarGis Albania, the annual average GHI for the Fieri area is about 1669.4 kWh/m².

On the other hand, the financial part has been analysed in relation to the value of the investment, the method of financing, the repayment of the loan, the return of the investment and the incomes from the sales in the energy exchange. Meanwhile, AS DAISY Off-Line Bizon software [10] was used to calculate the impact of the photovoltaic system on the parameters of the distribution system, connected to its most suitable point.

Results and Discussions

Technical analysis

The optimal design and sizing of the Single-Axis Tracked Bifacial PV Plant is shown in Figure 1. Specifically, the on-grid PV system with a total power of 10 MWp consists of: 17220 Bifacial PV modules (RECOM PANTHER 650 Wp, 20.9%), 96 inverters (SUNNY TRIPOWER CORE2 STP 110-60), 2 Smart Transformation Stations (2x6000kVA), AC and DC cables, and one bidirectional meter.

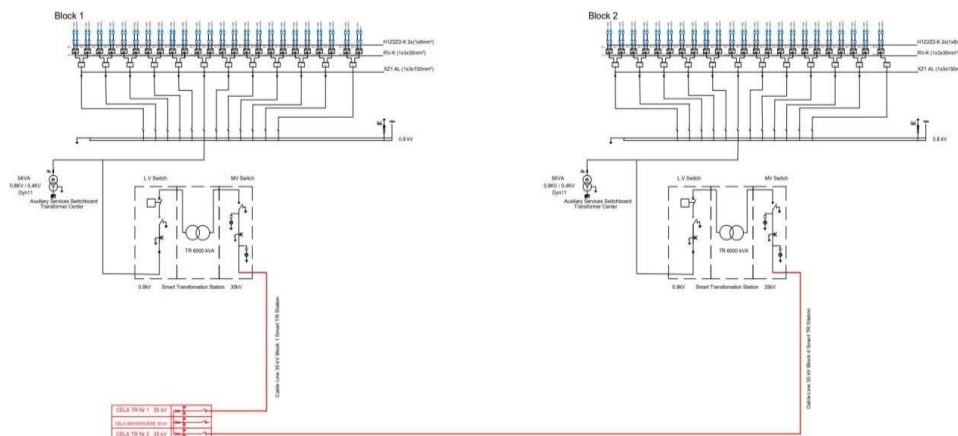


Figure 1. The principal electrical scheme of the PV plant

The on-grid PV system's, with 92% of Performance Ratio (PR), will generate 17950 MWh/Year (with annual yield 1,670 kWh/kWp). Furthermore, the other main simulation results of the technical analysis are shown in Table 1.

Table 1. Technical analysis.

Items	Value
Installed capacity	11.2 MWp (DC), 10 MW (AC)
PVs area	53492 m ²
Orientation	South (Single Axis Tracker)
CO ₂ emissions avoided	8435 ton
Assessment period	25 years
Number of working hours	1,794.94 hours/year

Financial analysis

While the total investment cost is 7.04 million €, the payback period and the Internal rate of return of the project according to the calculated flows will be respectively 4.8 years and 20.6%. Furthermore, in this calculation, it is assumed to receive a loan in the value of 80% of the total cost (with +/-3.5 % annual interest rate for 10 years). Furthermore, an average price of 113.58 €/MWh is provided for the calculation of the income from the sale of

energy (HUPX- Hungarian Power Exchange Ltd.). In addition, a more detailed presentation of the cumulative cash flow in years is given in Figure 2. These values are quite attractive for investors.

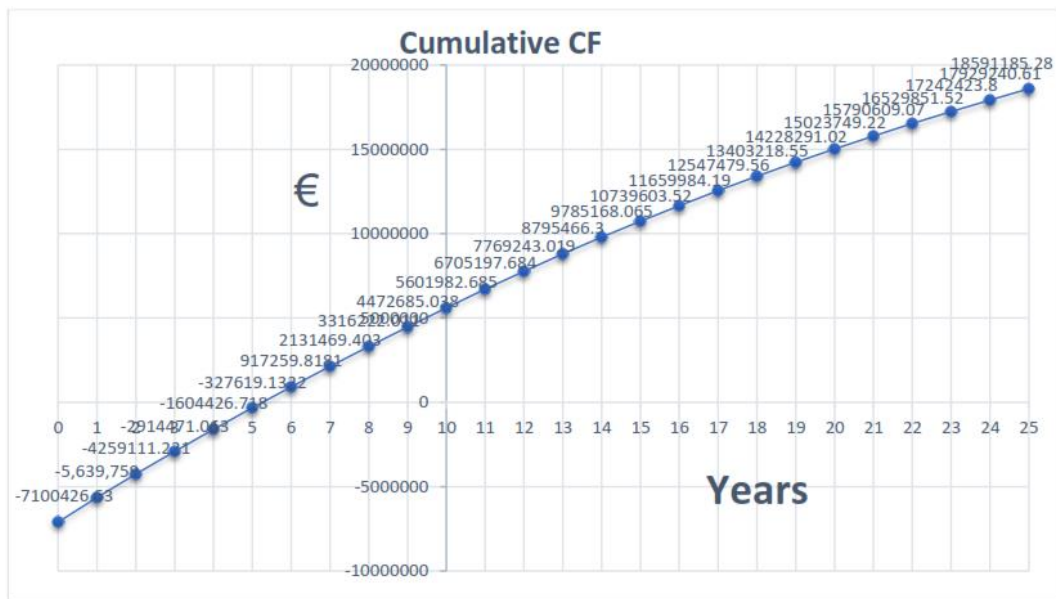


Figure 2. Cumulative Cash Flow

Connection to the distribution network

In the area where solar PV is located, the existing electrical network, at the 35 kV, 10 kV and 6 kV voltage levels, is owned by the distribution system operator. After the simulations, it turns out that the best connection point would be on the 35kV Kafaraj-Povelçe line. This is the closest line to the PV system, as well as the energy losses in this case would be lower. For this purpose, from the point of view of the stability of the static parameters of the network and its security, the connection is made through the construction of a 35 kV line with two circuits (0.7 km in total), with 120/20 mm² Aluminium Conductor steel-reinforced Cable (ACSR). In this context, Figure 3 shows the impact of the connection of the PV plant in the voltage nodes of the distribution system, as well as in the losses of lines and transformers.

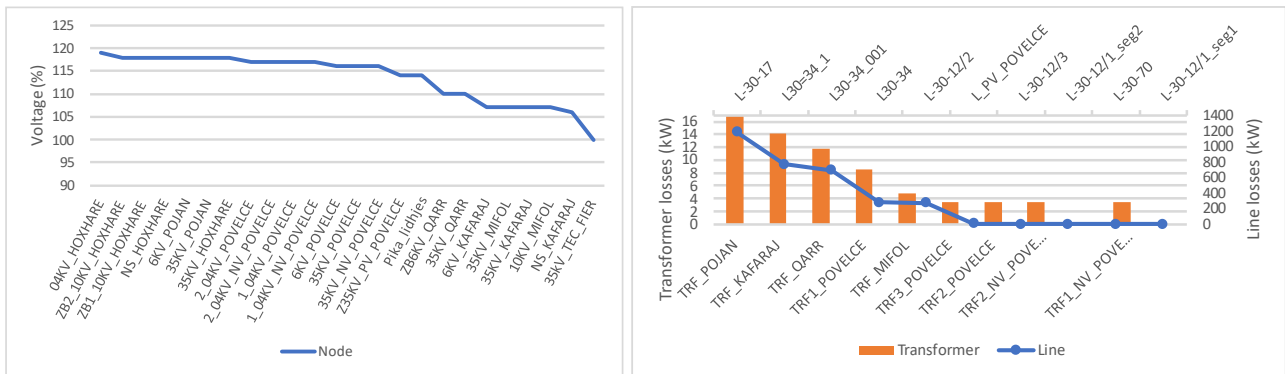


Figure 3. Voltage nodes & losses of lines and transformers of the distribution system

While an improvement is seen in the voltage levels of the nodes, some of the lines and transformers show technical losses due to their loading. However, these network parameters are expected.

Conclusion

This paper performs techno-economic feasibility analysis of a Single-Axis Tracked Bifacial PV Plant. Optimizing this 10MWp PV system, results in an annual energy production of 17950 MWh/Year. This amount of energy is expected to be sold in the energy exchange. This would bring in an internal rate of return of 20.6% IRR is, as well as a 4.8 years payback period of the investment. These values are quite attractive for investors. On the other hand, this paper analyses the impact of the photovoltaic system on the parameters of the distribution system, connected to its most suitable point. In this context, an improvement is seen in the voltage levels of the nodes. Meanwhile, some of the lines and transformers show technical losses due to their loading. The future work will perform a comparison between a Single-Axis Tracked Bifacial PV Plant and a static Monofacial PV Plant.

References

1. IEA (2022). IEA, Paris <https://www.iea.org/reports/renewables-2022>
2. Energy Regulator Authority (2022). Annual Report. The Situation of the Power Sector and ERE Activity during 2022, <https://www.ere.gov.al/en/publications/annual-reports>
3. Hida, A., Voshtina, E., Shaliu, D., Bualoti, R., & Çelo, M. (2023). Integration of PV floating with an existing hydroelectric power plant: An Albanian case study. C6-006R, 12th MAKO CIGRE Conference, Ohrid, September 17-19, 2023.
4. KPMG Albania. (2023). New Law on Promotion of the use of energy from renewable sources. Legal News.
5. Hida, A., Kërçi, T., Bualoti, R., Çelo, M., & Shaliu, D. (2022). A techno-economic analysis of a photovoltaic plant: An Albanian case study. 1st International Conference on Renewable Energies and Smart Technologies (REST), 28-29, July, 2022, Tirana, Albania.
6. Bazyari, Sh., Keypour, R., Farhangi, Sh., Ghaedi, A. & Bazyari, K. (2014). A study on the effects of solar tracking systems on the performance of photovoltaic power plants. *Journal of Power and Energy Engineering*, 2, 718-728. <https://doi.org/10.4236/jpee.2014.24096>.
7. Alam, M., Gul, M. S., & Muneer, T. (2023). Performance analysis and comparison between bifacial and monofacial solar photovoltaic at various ground albedo conditions. *Renewable Energy Focus*, 44, 295-316. <https://doi.org/10.1016/j.ref.2023.01.005>
8. Hida, A., Bualoti, R., & Çelo, M. (2023). Impact of the distributed resources on the power quality indicators of the distribution network, A Case Study in Korça, 16th International Scientific Conference on Energy and Climate Change (Promitheas), Athens, October 11-13, 2023.
9. PV*SOL. (2022). "PV*SOL, Version 2022," <https://pvsol.software/en/>
10. AS DAISY Off-Line Bizon. (2019). <http://www.daisy.cz/daisyeng/1024/index.html>



Obtaining and testing results of PF-1 brand corrosion inhibitor obtained based on the processing of chlorinated organic waste used in the oil and gas industry

Khalilov Jamshid Akmal Ugli¹, Nurkulov Fayzulla Nurmuminovich¹, Djalilov Abdulahat Turapovich¹

¹Tashkent Research Institute of Chemical Technology, Department of Technology, Uzbekistan, jamshidkhalilov885@gmail.com; fnurkulov82@gmail.com

Cite this study:

Ugli, K. J, Nurmuminovich, N. F., & Turapovich, D. A. (2023). Obtaining and testing results of PF-1 brand corrosion inhibitor obtained based on the processing of chlorinated organic waste used in the oil and gas industry. *Advanced Engineering Days*, 8, 75-78

Keywords

Corrosion inhibitors
Nitrogen
Organic compounds
Fatty acids
Gas-condensate well

Abstract

The article examines the physical and chemical properties of corrosion inhibitors obtained on the basis of the processing of organochlorine waste for the oil and gas industry. Corrosion inhibitors of metals were obtained as a result of the synthesis and their level of protection was checked. The results of IR and NMR spectra were studied.

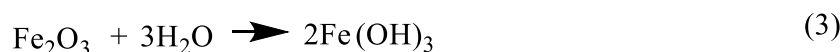
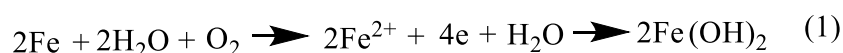
Introduction

In the global production of corrosion inhibitors composed of organic compounds, hydrocarbon-soluble inhibitors account for about 30% of the volume, the largest part of which (~70%) is used in oil refining. Corrosion of these metal-based materials has a large economic impact. According to a recent study by NACE, the total economic loss to the environment due to corrosion is USD 2.5 trillion, which is equivalent to 3.4% of world GDP. [1].

In most cases, the recommended inhibitors are organic compounds of various classes containing heteroatoms: nitrogen, sulfur, oxygen, and phosphorus. The effectiveness of the inhibitory effect of substances increases in the series of heteroatoms: O [^] N [^] S [^] P. However, since the toxicity of products also increases in this series, nitrogen-containing compounds are usually chosen for industrial use. Although it is less effective than compounds containing sulfur or phosphorus, they are a less toxic compound [2].

Corrosion inhibitors are chemicals that are injected into the well in various ways to protect the casing from internal corrosion caused by the produced fluid. It should be noted that some operators further protect parts of upstream structures after the wellhead by choosing the appropriate type and dosage of inhibitors injected into the wells.

The main metal rusting properties are:



Material and Method

Our researched PF-1 brand corrosion inhibitor was tested by gravimetric method. This method is used to determine the corrosion rate for corrosion control purposes and to evaluate the protective ability of corrosion inhibitors. The gravimetric method is based on measuring the difference in the mass of control metal samples

before and after exposure to a corrosive environment. A limitation of the use of this method is that it characterizes the average corrosion rate without taking into account the unevenness of the corrosion.

In general, when working, it is necessary to follow the current standard GOST 9.506-87 "Methods for determining the protective ability of metal corrosion inhibitors in water-oil environment".

According to it, the product based on amino compounds and fatty acids obtained from the treatment of organochlorine waste is first put into a three-necked flask equipped with a reflux condenser, a thermometer and a stirrer for interaction, and a homogeneous mass is formed. mix until Stirring was continued at a certain temperature for several hours. The obtained corrosion inhibitor was dissolved in gasoline, condensate, and motor oil media at concentrations of 1%, 3%, and 5%. Many studies have been conducted on the resulting solutions.

The physico-chemical properties and analysis results of our PF-1 brand corrosion inhibitor with this synthesized new composition were studied.

Physico-chemical characteristics of PF-1 brand corrosion inhibitor obtained on the basis of chlorinated organic waste processing:

Table 1. Physico-chemical properties of PF-1 corrosion inhibitors obtained from chlorinated organic waste processing.

Indexes	PF-1
1. Appearance	Transparent
2. Color	Pale yellow.
3. Density at 20 °C, g/cm ³	1...1,3
4. Nitrogen content, % by weight	7,0...9, 5
5. Ph environment at 20 °C	6,5-7
6. Level of protection against corrosion at a concentration of 150 mg/l	98,5
7. Solubility:	
- In gasoline	Complete
- In the condensate	Complete
- In the water	30% of weight gain
- In the case of I-20	Complete
8. Fluidity cCt at 20 °C	15

Results and Discussion

IR spectrum and analysis of PF-1 brand corrosion inhibitor. The IR-spectrum was presented to study the composition and structure of the PF-1 corrosion protection inhibitor that we synthesized and used in the test (Figure 3).

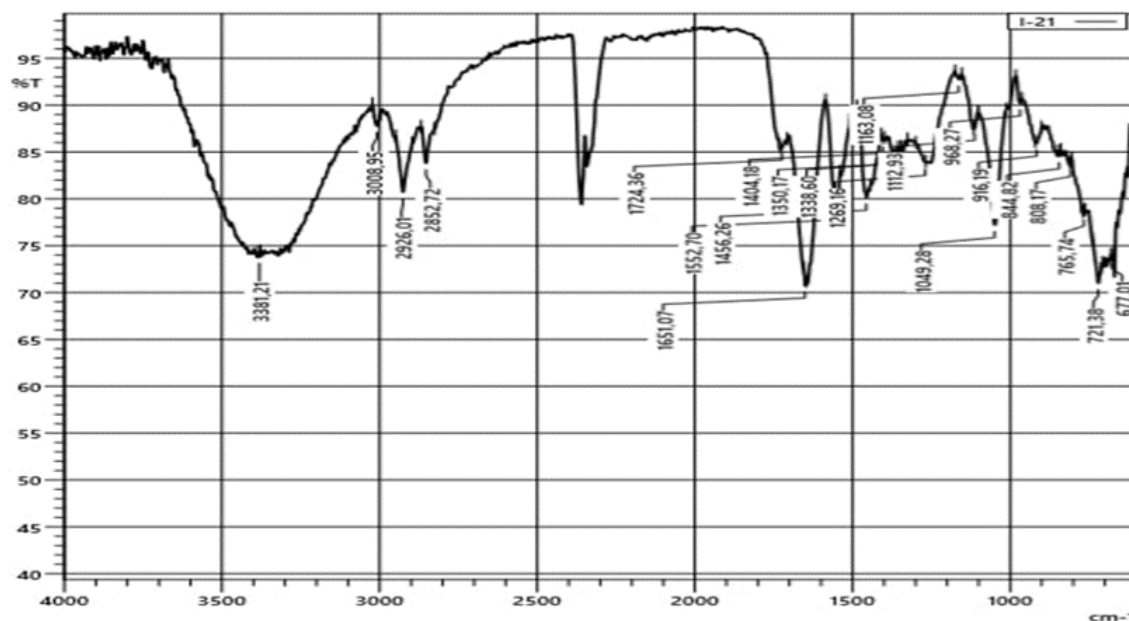


Figure 3. IR spectrum of PF-1 brand corrosion inhibitor.

The composition and structure of PF-1 corrosion inhibitor was studied using IR-spectrometer technology (IK-Fure, SHIMADZU, Japan) in the range up to 4000 cm⁻¹. The spectrum of the -N=C< groups produces valence vibrations in the region of 1651.07 cm⁻¹ and in addition 1552.7 cm⁻¹ -NH₂ in the structure. >N-CH₂ in 1350.17 cm⁻¹ and valence fields 844.82 – 808.17 cm⁻¹ contain absorption lines corresponding to -CH₂-CH₂- groups in the aromatic ring.

According to the results of this analysis, our researched corrosion inhibitor contains nitrogen, which shows that it has anti-corrosion properties.

From this table, we can see that the highest level of corrosion protection of the metal surface was applied at a concentration of 6%.

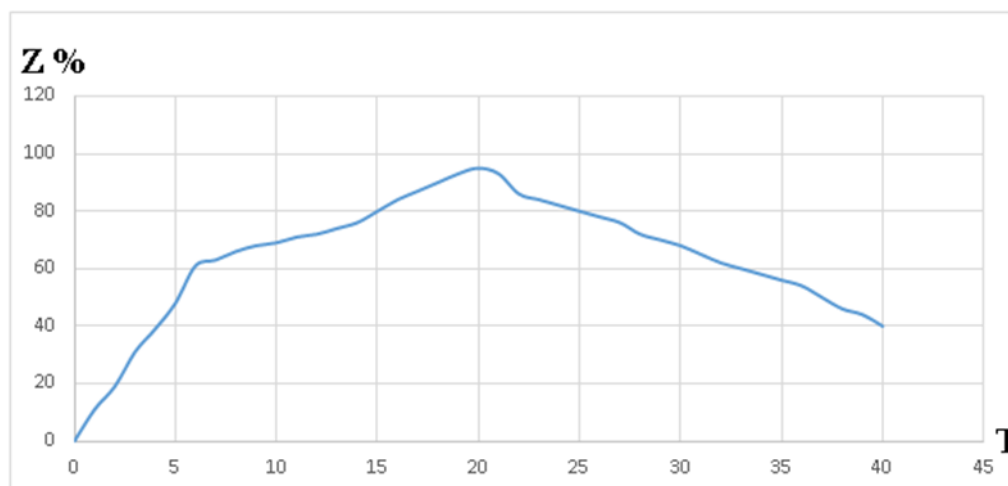


Figure 1. Protection level as a function of temperature.

Figure 1 shows the protection level of protection against corrosion at different temperatures. From this graph, we can see that the optimum temperature for our synthesized PF-1 corrosion inhibitor is 20 °C.

Table 2. Corrosion rates, protection levels and surface coverage coefficient values at different mass ratios of PF-1 brand corrosion inhibitor.

Mass ratios P:F	Corrosion rate	Protection level	θ
1:1	0,065	72,31	0,7231
1:2	0,08	89	0,89
1:3	0,071	78,98	0,7898
2:1	0,058	64,5	0,645
3:1	0,051	56,7	0,567

As a result of the test research, we can see with the help of table 1 that the best mass ratio of amine compounds and fatty acid is 1:2, and the level of protection in it is 89%.

Conclusion

The physicochemical properties of the PF-1 brand corrosion inhibitor synthesized by us and the analysis of the IR and NMR spectrum of the synthesized product were obtained. As a result of the analysis, it was found that this inhibitor contains nitrogen. These compounds have been found to be the most effective against corrosion.

Also, the obtained inhibitor was tested in different environments, at different mass ratios and temperatures. The PF-1 brand corrosion inhibitor, obtained as a result of the processing of organochlorine waste, containing nitrogen, was carried out in a condensate medium with a concentration of 1%, 3%, and 6%. As a result of the tests, the level of protection was 83.3, 90.6, 98.6 percent, respectively.

Our researched and tested PF-1 corrosion inhibitor can be used in various pipelines in the oil and gas industry in various aggressive environments.










References

1. Bowman, E., Jacobson, G., Koch, G., Varney, J., Thopson, N., Moghissi, O., ... & Payer, J. (2016). International Measures of Prevention. Application, and Economics of Corrosion Technologies Study, NACE International.

2. Perez, T. E. (2013). Corrosion in the oil and gas industry: an increasing challenge for materials. *Jom*, 65(8), 1033-1042. <https://doi.org/10.1007/s11837-013-0675-3>
3. Askari, M., Aliofkhaezrai, M., Jafari, R., Hamghalam, P., & Hajizadeh, A. (2021). Downhole corrosion inhibitors for oil and gas production—a review. *Applied Surface Science Advances*, 6, 100128. <https://doi.org/10.1016/j.apsadv.2021.100128>
4. Амиды и соли алифатических кислот - ингибиторы коррозии черных и цветных металлов в углеводородных и водных средах” Тронова Екатерина Анатольевна. Диссертация на соискание ученой степени кандидата технических наук. Санкт-Петербург-2016.
5. История развития и методы совершенствования ингибиторной защиты в ООО «Газпром добыча Оренбург» Д.А. Кузнецов. «Территории Нефтегаз» 2014.
6. Технология маслорастворимых комплексов сульфатов лантаноидов и Mg как ингибиторов коррозии и модификатор трения” Иванов Д.М. Диссертация на соискание ученой степени кандидата технических наук. Екатеринбург-2006.
7. Кашковский Р.В. “Перспективы развития метода отдельной оценки вкладов пленки ингибитора и продуктов коррозии в общий защитный эффект” Вестник



Evaluating the performance of object-based machine learning and deep learning models in classifying different maize genotypes with multispectral UAV imagery

Osman Yavuz Altuntas¹, Ismail Colkesen*¹, Umut Gunes Sefercik¹, Taskin Kavzoglu¹,
Mustafacan Saygi¹, Muhammed Yusuf Ozturk¹, Mertcan Nazar¹, Ilyas Aydin¹,
Hasan Tonbul¹

¹Gebze Technical University, Engineering Faculty, Department of Geomatics Engineering, Turkiye, icolkesen@gtu.edu.tr

Cite this study:

Altuntas, O. Y., Colkesen, I., Sefercik, U. G., Kavzoglu, T., Saygi, M., Ozturk, M. Y., Nazar, M., Aydin, I. & Tonbul, H. (2023). Evaluating the performance of object-based machine learning and deep learning models in classifying different maize genotypes with multispectral UAV imagery. *Advanced Engineering Days*, 8, 79-82

Keywords

Deep Learning
Image Classification
Machine Learning
Maize Crop
UAV Remote Sensing

Abstract

Modern remote sensing technologies play a critical role in agricultural applications, especially in recent years with the advances in unmanned aerial vehicle (UAV) technologies and artificial intelligence. Remotely sensed imagery is an invaluable data source for sustainable agricultural activities, such as precision agriculture. This study evaluates a comparative analysis of the performance of machine learning (ML) and deep learning models in classifying 12 different maize genotypes from multispectral UAV images. In this context, ortho mosaic and canopy height model obtained from UAV-mounted multispectral camera of the study area in Kirazca Agricultural Enterprise located in Arifiye district of Sakarya province were used as a main dataset. The object-based classification results show that the overall accuracy (OA) of the crop maps produced with the Rotation Forest (RotFor) and Canonical Correlation Forest algorithms was approximately 80%, while the OA value was 74.18% for Support Vector Machine algorithm. On the other hand, the popular U-Net model outperformed the ML-based models with an OA value of 97.61%. Individual class accuracy analyses revealed that the RotFor algorithm attained F-score values exceeding 90% for only 2 maize genotypes (i.e., Com. Sw. and Com. Ar.), whereas F-score values calculated with the U-Net model surpassed 95% for all 12 genotypes.

Introduction

The cereal group, providing more energy to billions than all other crops combined, is grown in large quantities across the Earth [1]. Maize is characterized by high yields and adaptability to changing conditions [2]. About 65-70% of global maize production is used for animal feed, 20% for human consumption, and 10-15% for industry [3]. The increasing global population has raised maize demand, leading to the consideration of imports for production balance [4]. Monitoring the status of cultivated maize fields is crucial for assessing crop health, optimizing agricultural practices, and ensuring timely interventions to enhance yield and sustainability. Traditional field-observation based methods in plant monitoring depends on labor-intensive and expensive methods. In contrast, modern remote sensing technologies, offering accessible, highly accurate, and cost-effective data, have been recently used effectively in crop monitoring applications. With technological advancements in recent years, unmanned aerial vehicles (UAVs) equipped with multispectral (MS) and hyperspectral sensors can provide cost-effective data at high spatial, spectral, temporal resolutions [5]. The timely acquired data is utilized in various smart agriculture applications, including crop health monitoring, weed or pesticide detection, water content estimation, crop quality assessment, and crop mapping using machine learning (ML) algorithms. In the remote sensing literature, studies on detecting crop species and genotypes are mainly based on image classification. For example, utilizing UAV MS images, Li et al. (2021) detected maize-cultivated areas. Employing an object-based image classification approach with Support Vector Machine (SVM) (achieving an accuracy of 90.27%) and Random Forest (achieving an accuracy of 92.36%). ML algorithms, the cultivated areas were determined as 96.54 and 98.77 hectares, respectively [6]. On the other hand, in another study where UAV images

were used as the primary data set, U-Net based models were used to separate maize crops. The results showed approximately 48% better classification performance than the ML algorithm [7]. Furthermore, Colkesen et al. (2023) utilized deep learning (DL) techniques for the classification of the UAV image dataset and achieved high accuracy in detecting and counting poplar tree crown structures (F-Score: 88.20%) [8].

Study Area and Dataset

Study area is located in Kirazca agricultural enterprise of Sakarya Maize Research Institute in Arifiye district of Sakarya province, Türkiye (Figure 1). In the field, 12 maize genotypes have been cultivated in parcels designed as rectangles measuring 500m² (20 m x 25 m) each. MS orthomosaic dataset obtained on July 19, 2022, from a DJI Phantom 4 UAV equipped with a five-channel multispectral camera (Red, Green, Blue, Red edge, and Near Infrared) was employed to map various maize genotypes in cultivated fields during the tassel growth stage. Aerial photographs were acquired at a flight altitude of 50m with 80% forward and 60% side overlap, and orthomosaics with a Ground Sampling Distance of 2.7cm and 16-bit resolution were produced using the structure-from-motion (SfM)-based image matching software Agisoft Metashape Professional. In addition plant heights, called Canopy Height Model (CHM), were calculated with the help of pixel differences between Digital Surface Model and Digital Terrain Model produced based on DJI Phantom 4 v2 RGB UAV [9]. CHM was added as a band to the original spectral variables to create a dataset to improve image classification accuracy.

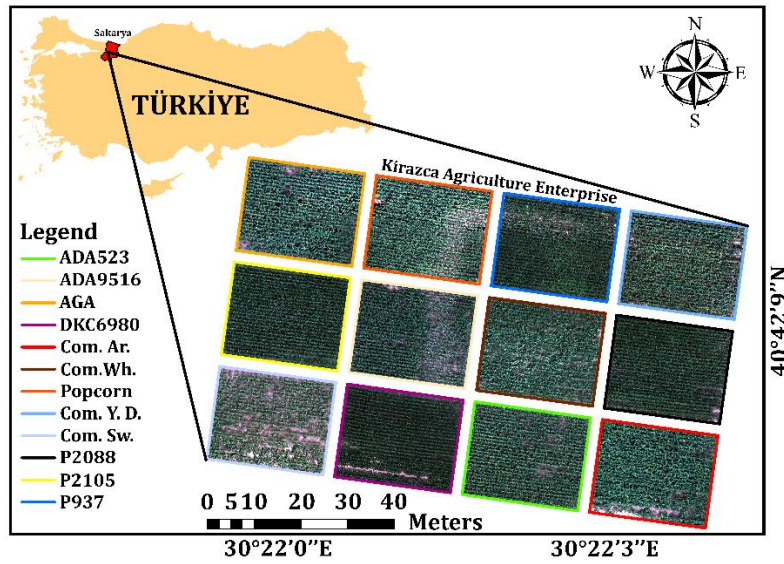


Figure 1. Study area

Methodology

In this study, state-of-the-art ML algorithms such as SVM, RotFor, and CCF, as well as a well-known DL network, U-Net, were employed to produce a crop map representing 12 maize genotypes using the MS orthomosaic dataset. Object-based classification consists of three stages: image segmentation, class labeling using ML algorithms and accuracy assessment. Image segmentation was performed using the MRS algorithm in eCognition 9 software [10], which is managed by three important parameters such as scale (S), shape (Sh) and compactness (C). Sh and C were determined by trial and error and S was determined automatically based on the ESP-2 tool developed by [11]. SVM algorithm, originally developed to separate two classes [12], later employed kernel functions to solve high-dimensional image classification problems [13]. RotFor algorithm divides the training data into subsets (K) and applies principal component analysis to ensure diversity within each subset. Individual decision trees are constructed using the all components. Unknown class labels are determined through majority votes of the individual decision trees [14]. The CCF algorithm is an ensemble learning algorithm based on constructing multiple decision trees using canonical correlation analysis that maximizes the correlation between class labels and bands [15]. The U-Net architecture is a precise, end-to-end encoder-decoder network designed for semantic segmentation with a U-shaped structure [16]. It consists of two main components: the contracting path, which employs conventional convolutional neural network design to capture contextual information, and the symmetrical expansion pathway that achieves precise localization using transposed convolutions [17]. The contracting path encodes the image into a multi-level feature representation, and the symmetrical expansion pathway combines cropped feature maps with up-sampled ones, forming the U-shaped network structure.

Results

Segmentation parameters S , Sh and C were set to 34, 0.9 and 0.9, respectively. As a result, a total of 230,223 segments were created. To generate training and test datasets, 4,200 and 1,794 segments were collected on the orthomosaic. The hyperparameters for the ML algorithms were chosen as follows: $C=500$ and kernel type=rbf for SVM, $K=8$, and $nTrees=300$ for RotFor, and $nTrees=100$ for the CCF algorithm. .

To obtain a dataset for training of DL model, maize parcels in the orthomosaic were divide into 64x64 patch sizes. Data augmentation techniques were utilized to expand the training dataset artificially, such as rotating images 90, 180, and 270 degrees clockwise. A total of 9360 patches were collected, and the dataset was subsequently partitioned randomly into three segments: 80% for training, 10% for validation, and 10% for the test dataset. All image classification processes were carried out using a high-capacity workstation equipped with an NVIDIA GeForce RTX 3090 graphics card, an Intel® Core™ i9-12900K 3.2GHz 24-Core processor running at approximately 3.2GHz, and 128GB of RAM, which is accessible within the Advanced Remote Sensing Technology Laboratory (ARTLAB) of GTU Geomatics Engineering Department. The user-defined model hyper-parameters for the training phase were chosen as follows: a patch size of 64x64, 100 epochs, a batch size of 64, a learning rate of 0.001 for the Adam optimizer, and the utilization of the Categorical Cross-Entropy loss function. As an example of the produced crop maps, two maps generated using object-based RotFor and U-net models and the calculated overall accuracy (OA) and F-score (F-S) values are given in Figure 2.

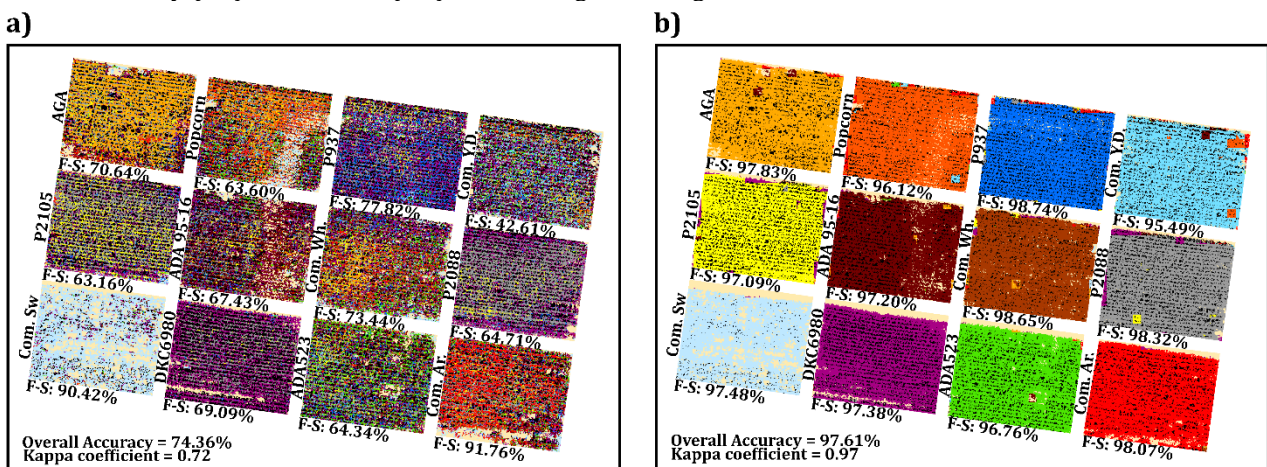


Figure 2. Crop maps produced by a) object-based RotFor and b) U-Net algorithm.

The OA values for crop maps produced through ML algorithms range from 72.30% to 74.36%. The RotFor algorithm demonstrated the highest accuracy among object-based classification methods, achieving a notable accuracy score of 74.36%. Additionally, comparable accuracy scores were noted in CCF (74.36%) and SVM (72.30%) algorithms. On the other hand, the U-Net model showed a superior performance in classifying different maize genotypes and the overall accuracy of the resulting crop map was 97.61%. When evaluating the class-based classification of maize crops, ML models achieved the highest and lowest F-score values for the Composite Arifiye (Com. Ar.) and Composite Yellow Dent (Com.Y.D) maize genotypes, respectively. In the RotFor algorithm, the F-score for Com. Ar. reached 91.76%, whereas it was 42.61% for Com.Y.D. Furthermore, the U-Net DL algorithm, which demonstrated significant superiority in overall accuracy, displayed class-based F-scores exceeding 95%. Compared to the object-based map produced by RotFor, the U-net generated crop map shows minimal confusion between classes.

Conclusion

This study aims to categorize 12 maize genotypes using ML and DL algorithms applied to MS UAV images. The quantitative assessments based on accuracy metrics reveal that the U-Net model excelled in classifying maize genotypes. While ML-based models achieved success rates above 90% for only two genotypes, the U-Net model achieved over 90% success across all genotypes. Despite the impressive performance of the U-Net model, the presence of distinctly delineated square shapes in patch-wise multi-class classification results indicates the necessity for further research on utilizing more robust DL-based models and high-resolution hyperspectral imagery.

Acknowledgment

This work was funded and supported by the Scientific and Technological Research Council of Türkiye (TUBITAK) under project no: 121Y392. Special thanks to the Ministry of Agriculture and Forestry Sakarya Maize Research Institute for their valuable contributions to the project.

References

1. Bigini, V., Camerlengo, F., Botticella, E., Sestili, F., & Savatin, D. V. (2021). Biotechnological resources to increase disease-resistance by improving plant immunity: A sustainable approach to save cereal crop production. *Plants*, 10(6), 1146. <https://doi.org/10.3390/plants10061146>
2. Slavin, J. (2004). Whole grains and human health. *Nutrition research reviews*, 17(1), 99-110. <https://doi.org/10.1079/NRR200374>
3. Bilgiç, S., Sade, B., Soyulu, S., Bilgicli, N., Cerit, I., Öz, A., Cengiz, R. & Özkan, I. (2012). Maize report. Mısır raporu. National Grain Council
4. Akkurt, E., & Demirbaş, N. (2021). Türkiye’de mısır üretiminde kendine yeterliliğin değerlendirilmesi. XV. IBANESS İktisat, İşletme ve Yönetim Bilimleri Kongreler Serisi–Plovdiv/Bulgaristan, 29-30.
5. Sefercik, U. G., Kavzoğlu, T., Colkesen, I., Nazar, M., Ozturk, M. Y., Adali, S., & Dinc, S. (2021). Land Cover Classification Performance of Multispectral RTK UAVs, ISPRS SCA’21 International Smart City Applications Conference, Karabuk, Turkey, 27-29 October 2021.
6. Lee, D. H., Kim, H. J., & Park, J. H. (2021). UAV, a farm map, and machine learning technology convergence classification method of a corn cultivation area. *Agronomy*, 11(8), 1554. <https://doi.org/10.3390/agronomy11081554>
7. Lu, T., Wan, L., Qi, S., & Gao, M. (2023). Land Cover Classification of UAV Remote Sensing Based on Transformer-CNN Hybrid Architecture. *Sensors*, 23(11), 5288. <https://doi.org/10.3390/s23115288>
8. Colkesen, I., Kavzoglu, T., Sefercik, U. G., Altuntas, O. Y., Nazar, M., Ozturk, M. Y., & Saygi, M. (2023). Deep learning based poplar tree detection and counting using multispectral UAV images. *Advanced Engineering Days (AED)*, 6, 64-67.
9. Sefercik, U. G., Kavzoğlu, T., Nazar, M., Atalay, C., & Madak, M. (2022). Creation of a Virtual Tour. Exe Utilizing Very High-Resolution RGB UAV Data. *International Journal of Environment and Geoinformatics*, 9(4), 151-160. <https://doi.org/10.30897/ijegeo.1102575>
10. Baatz, M., & Schäpe, A. (2000). Multiresolution segmentation: an optimization approach for high quality multi-scale image segmentation. *Angewandte geographische informationsverarbeitung*, 12-23.
11. Drăguț, L., Csillik, O., Eisank, C., & Tiede, D. (2014). Automated parameterisation for multi-scale image segmentation on multiple layers. *ISPRS Journal of Photogrammetry and Remote Sensing*, 88, 119–127. <https://doi.org/10.1016/j.isprsjprs.2013.11.018>
12. Cortes, C., & Vapnik, V. (1995). Support-vector networks. *Machine learning*, 20, 273-297.
13. Kavzoglu, T., & Colkesen, I. (2009). A kernel functions analysis for support vector machines for land cover classification. *International Journal of Applied Earth Observation and Geoinformation*, 11(5), 352-359.
14. Rodriguez, J. J., Kuncheva, L. I., & Alonso, C. J. (2006). Rotation forest: A new classifier ensemble method. *IEEE transactions on pattern analysis and machine intelligence*, 28(10), 1619-1630.
15. Rainforth, T., & Wood, F. (2015). Canonical correlation forests. *arXiv preprint arXiv:1507.05444*. <https://doi.org/10.48550/arXiv.1507.05444>
16. Ronneberger, O., Fischer, P., & Brox, T. (2015). U-net: Convolutional networks for biomedical image segmentation. In *Medical Image Computing and Computer-Assisted Intervention–MICCAI 2015: 18th International Conference, Munich, Germany, October 5-9, 2015, Proceedings, Part III 18* (pp. 234-241). Springer International Publishing.
17. Siddique, N., Sidike, P., Elkin, C., & Devabhaktuni, V. (2020). U-Net and its variants for medical image segmentation: theory and applications. *arXiv preprint arXiv:2011.01118*. <https://doi.org/10.48550/arXiv.2011.01118>



Advanced Engineering Days

aed.mersin.edu.tr



3D modelling of cultural heritage with point cloud generation by integrating UAV and terrestrial photogrammetry techniques

Emine Kurt*¹, İbrahim Halilullah Çetin ¹, Füsün Balık Şanlı ¹, Burak Akpınar ¹

¹Yıldız Teknik University, Department of Geomatics Engineering İstanbul, Türkiye, emine.kurt@std.yildiz.edu.tr, icetin@yildiz.edu.tr, fbalik@yildiz.edu.tr, bakpinar@yildiz.edu.tr

Cite this study: Kurt, E., Çetin, İ. H., Sanli, F. B., & Akpınar, B. (2023). 3D modelling of cultural heritage with point cloud generation by integrating UAV and terrestrial photogrammetry techniques. *Advanced Engineering Days*, 8, 83-85

Keywords

Cultural Heritage
Terrestrial Photogrammetry
Aerial Photogrammetry
3D Point Cloud
UAV

Abstract

In today's context, the preservation of cultural heritage, its transmission to future generations, and the archival in the digital environment for architectural restoration have gained momentum beyond traditional methods. In architectural restoration, surveying involves scaling and documenting the current state of structures, examining the urban design, and providing a basis for restoration projects. Photogrammetry is a commonly used method in documenting cultural heritage. In this study, UAV (Unmanned Aerial Vehicle) and terrestrial photogrammetry methods were integrated for the purpose of creating a 3D point cloud and modelling a historical building in the Yıldız Technical University Davutpaşa Campus. The building, formerly the Mızraklı Süvari Alayı Koğuşu belonging to the military, has been restored as a guesthouse. In this context, for the application of terrestrial photogrammetry in the study, 11 survey marks were established surrounding the guesthouse facades. Additionally, 205 control points were set for the facades, and a geodetic network was established in the study area for the geodetic measurements of control points. Subsequently, 554 photos were taken for the facades with an overlap ratio of 80%. For roof modelling, aerial photogrammetry was used, and 33 roof images were obtained using DJI Zenmuse P1 as the UAV. All acquired data were processed in Agisoft Metashape software to generate a 3D model. The accuracy of the results was evaluated by comparing them with ground truth values, assessing the usability of the methods in surveying studies.

Introduction

The structures that emerge as cultural heritage are treasures passed down to us from the past to the present. Our country has hosted various cultures and civilizations for centuries. These civilizations have left many legacies, and it is our duty to preserve and sustain these legacies. However, these structures are under threat due to various natural or human-made reasons. Preserving cultural heritage is not just about preserving the past; it is also crucial for future generations to access it. Therefore, the first and most important step is the documentation of these artifacts [1]. With the help of these documents, any restoration or similar work on cultural and historical structures can be supported [4]. To carry out restoration projects, it is essential to determine the current state of the structure and prepare surveys. Surveying is the collection of technical measurements that provide a reference for correcting an architectural structure if it is damaged for any reason [2]. Initially measured using classical methods, surveys have become more common over time, especially with photogrammetric methods, as different disciplines have come into play [4]. With recent developments, the integration of photogrammetry with unmanned aerial vehicles (UAVs) has made it easier to model objects in 3D quickly and economically, even in challenging and inaccessible areas, using photographs obtained with UAVs [5-6-7]. While terrestrial photogrammetry provides more detailed, precise, and close-up opportunities for indoor spaces, aerial photogrammetry offers an economical and fast modeling solution in difficult terrain conditions, large-scale archaeological areas, and areas at heights

unreachable by terrestrial photogrammetry. The choice of the appropriate technique depends on project requirements, scale, and budget.

In this study, UAV and Terrestrial Photogrammetry methods were integrated to create a 3D point cloud and model of a historical building. The accuracy of the results was evaluated by comparing them with ground truth values, assessing the usability of the applied methods in surveying studies.

Material and Method

The modeled structure is a historical building located in the Yıldız Technical University Davutpaşa campus, formerly known as Mızraklı Süvari Alayı Koğuşu belonging to the military, now restored as a guesthouse (Figure 1-a). The building consists of 12 facades and a roof. It features a concave architecture with an entrance section made of glass and other sections made of stone (Figure 1-b). Around the building, 11 survey marks were established using a Topcon HiPer SR GPS device, allowing at least two network points of control points to be observable, and a geodetic network was established. For terrestrial photogrammetry measurements, 205 control points were placed on the facades in a homogeneous distribution. The x, y, and z coordinates of the control points were acquired using a TOPCON GPT-3500 total station (Figure 1-c). Subsequently, 554 photos were taken for modeling with an overlap ratio of 80%. For aerial photogrammetry, 33 roof images were obtained by flying at an altitude of 80 m with a DJI Zenmuse P1 model drone (Figure 1-c). All acquired data were processed using Agisoft Metashape software to create a 3D point cloud and model. Agisoft Metashape is a modeling software based on the Structure from Motion (SfM) technique [5]. Initially, the captured photos were aligned, resulting in tie points, i.e., a sparse point cloud. After creating the sparse point cloud, the coordinates of the object and particular points measured in the field with a total station were transferred to the system. These transferred coordinates were individually measured in each photograph, and adjustment was performed.

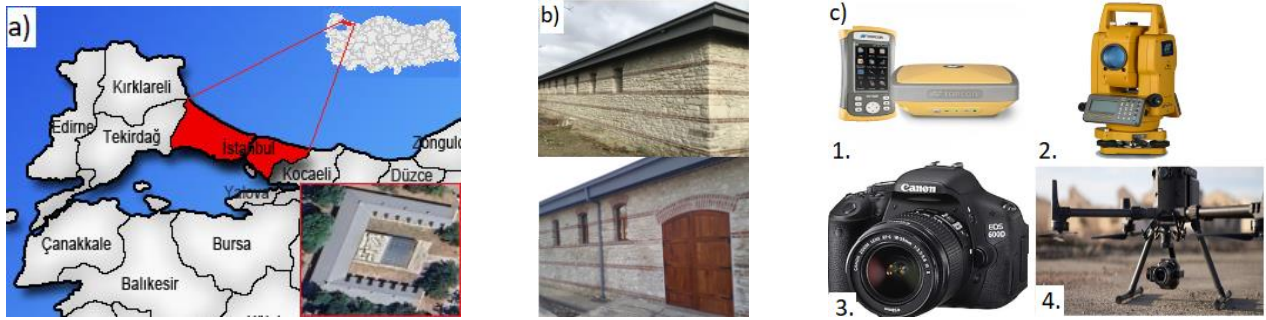


Figure 1. Location of the Historical Building (a) Guest house (b) Used Equipments (c) Topcon HiPer SR (1) TOPKON GPT-3500 (2) Canon EOS 600D Camera (3) DJI Zenmuse P1(4)

After scaling based on the measured points in this system, the metashape workflow was continued and a high-density point cloud was produced (Figure 2). Care was taken to keep the coordinate errors in the produced point cloud below 2 cm, that is, 0.5 pixels. Unnecessary points around the model were cleaned and build texture was performed.



Figure 2. The point cloud models of two different facades of the guesthouse

By integrating UAV and Terrestrial Photogrammetry techniques, the 3D point cloud and model of the cultural heritage have been generated (Figure 3). The relative accuracy of the produced model is achieved at 2 cm. When compared to ground measurements, the planimetric accuracy is calculated around 3 cm.



Figure 3. Merged terrestrial and aerial photogrammetry models

Due to tall trees surrounding the stone structure and covering its top, significant problems have been encountered in some facades and corners (Figure 4). To address this, the acquisition distance was reduced, and the number of photographs was increased. However, the decrease in acquisition distance resulted in missing point cloud data in the roofed part of the building (Figure 4a). Additionally, since the entrance facades and balcony sections of the structure are made of glass, scattering has occurred in the point clouds (Figure 4b).



Figure 4. Point cloud loss due to trees and glass-fronted facades

Conclusion

In this study, the 3D modeling of historical artifacts for survey and restoration purposes was aimed. For this purpose, facade photographs were taken with a terrestrial camera and roof photographs were taken with a UAV, resulting in the generation of a point cloud and the creation of a 3D model. The accuracy of the model is 2 cm, and the absolute accuracy obtained with terrestrial controls is around 3 cm. To achieve this accuracy, the maximum photographing distance was calculated as 20 m. However, when obstacles such as trees and generators were encountered on the facades, the photographing distance was reduced, leading to an increase in the number of photographs. Similar calculations and estimations for achieving the desired accuracy should be made during UAV acquisition, and the flight height should be estimated in advance. Point cloud losses occurred in the models due to scattering on smooth and glass surfaces. Similarly, areas where point clouds could not be generated on the facades were observed due to obstacles such as trees, generator boxes, etc.

References

1. Şaşı, A., & Yakar, M. (2018). Photogrammetric modelling of hasbey dar'ülhuffaz (masjid) using an unmanned aerial vehicle. *International Journal of Engineering and Geosciences*, 3(1), 6-11. <https://doi.org/10.26833/ijeg.328919>
2. Turan, M. H. (2004). *Mimari Fotogrametri Alanındaki Çağdaş Gelişmelerin Değerlendirilmesi*. Gazi Üniversitesi Mühendislik Mimarlık Fakültesi Dergisi, 19(1), 43-50
3. Karşlı, F., Ayhan E., Friedrich, J. (2003). *Dijital Fotogrametri Tekniklerin Mimari ve tarihi yapılarda Uygulanması*. 8. Türkiye Harita Bilimsel ve Teknik Kurultayı, Ankara
4. Duran, Z. (2003). *Tarihi Eserlerin Fotogrametrik Olarak Belgelenmesi ve Coğrafi Bilgi Sistemine Aktarılması*. Doktoral Dissertation, İstanbul Technical University, Türkiye
5. Ulvi, A., Yakar, M., Yiğit, A. Y., & Kaya, Y. (2020). İHA ve Yersel Fotogrametrik Teknikler Kullanarak Aksaray Kızıl Kilise'nin 3 Boyutlu Nokta Bulutu ve Modelinin Üretilmesi. *Geomatik*, 5(1), 19-26. <https://doi.org/10.29128/geomatik.560179>
6. Turner D, Lucieer A & Watson C (2012). An automated technique for generating georectified mosaics from ultra-high resolution unmanned aerial vehicle (UAV) imagery, based on structure from motion (SfM) point clouds. *Remote sensing*, 4(5), 1392- 1410 <https://doi.org/10.3390/rs4051392>
7. Erdoğan, A., Kabadayı, A., & Akın, E. S. (2021). Kültürel mirasın fotogrametrik yöntemle 3B modellenmesi: Karabıyık Köprüsü Örneği. *Türkiye İnsansız Hava Araçları Dergisi*, 3(1), 23-27.



LULC mapping accuracy enhancement through multispectral UAV imagery with nDSM integration

Ilyas Aydın *¹, Umut Gunes Sefercik ¹

¹ Gebze Technical University, Department of Geomatics Engineering, Kocaeli, Türkiye, ilyasaydin@gtu.edu.tr, sefercik@gtu.edu.tr

Cite this study: Aydın, İ, & Sefercik, U. G. (2023). LULC mapping accuracy enhancement through multispectral UAV imagery with nDSM integration. *Advanced Engineering Days*, 8, 86-88

Keywords

LULC
nDSM
Random Forest
UAV

Abstract

The requirement of land use and land cover (LULC) maps as a base in large variety of applications make necessary to improve low-cost and high accuracy production methods. Unmanned Aerial Vehicles (UAVs) present cost-effective alternatives for generating LULC maps when compared to traditional methods and stand out with advanced multispectral sensing technologies. This study aims to assess the multi-class LULC mapping performance of multispectral UAVs and enhance it through the integration of auxiliary data sources, in 11-classes study area. Specifically, high-accuracy normalized digital surface model (nDSM) was generated and incorporated into the classification process to enhance overall mapping accuracy. In addition, three different datasets were created with the various combinations of 68 features consisting of texture, spectral and geometric features of the segments. Object-based classification was performed with the Random Forest (RF) machine learning algorithm for all datasets, and dataset 3 (D3), consists of spectral bands + indexes + texture + geometry + nDSM, exhibited the most successful performance with an overall accuracy of 94.16%. The results clearly demonstrated that MS UAV data has high performance in LULC mapping, and NDSM increased the classification accuracy by 5%.

Introduction

Accurate land use and land cover (LULC) mapping is a pivotal first step in extracting information about many urban and environmental change-oriented studies [1-2]. Traditional space-borne and airborne sensing technologies face constraints in achieving high accuracy values for LULC map production, primarily attributed to their inherent limitations in spatial and temporal resolution. At this point, Unmanned Aerial Vehicle (UAV) is an alternative technology with providing periodic and high-resolution imagery from low flight altitudes [3-5]. In UAV-based LULC mapping approaches, two different cameras are preferable as red-green-blue (RGB) single band and multispectral (MS). RGB camera-equipped UAVs are insufficient for scientific studies such as the analyses of changes occurring in agricultural areas due to limited spectral ranges [6]. With the developments in MS UAV technologies, easier detection of spectral signatures reflected from objects has increased the performance in classification studies and encouraged research in this direction [7].

This study aims to investigate the performance of MS UAVs in LULC object-based classification using random forest machine learning algorithm, to produce and integrate auxiliary data to improve this performance. In this context, high quality nDSM, having same grid interval with classified MS orthomosaic, was generated and integrated into the classification processes. In addition, different indices, texture, and geometry were added as other auxiliary data to determine their effects on the classification accuracy. Accordingly, three datasets were created by using different combinations of the auxiliary data and their contributions were analyzed by statistical and visual approaches.

Study Area and Materials

The study area is located in the northern part of Gebze Technical University Campus in the Gebze district of Kocaeli province of Türkiye (Figure 1). The study area, which stands out with its many natural and man-made structures, has a very rich class diversity for LULC mapping. In the context of LULC mapping, the study delineates 11 different classes, encompassing red roof, concrete roof, road, bicycle path, dense vegetation, low vegetation, thorn trees, broad-leaved trees, soil, water, and shadowed areas. Aerial photos were collected by using DJI Phantom 4 MS UAV equipped with FC6360 camera includes six imaging bands as RGB composite, blue, green, red, red edge, near-infrared. This UAV is equipped with a real-time kinematic (RTK) GNSS receiver, but for the purpose of analyzing the positional accuracy of the study, eight polycarbonate ground control points (GCPs) were installed homogeneously in the study area. The 3D coordinate measurements of all GCPs were conducted using the CHC i80 GNSS receiver. In addition, the MAPIR reflectance panel V2 was used for spectral calibration with the aim of achieving maximum radiometric accuracy.

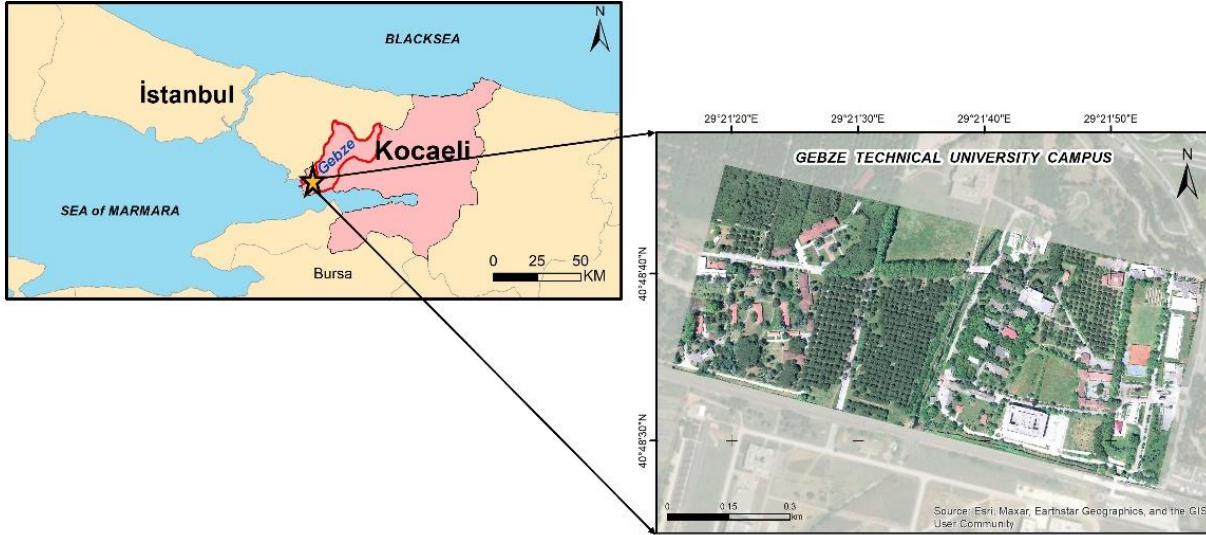


Figure 1. The northern part of Gebze Technical University campus

Methodology

This research encompasses a comprehensive methodology, starting with on-site field reconnaissance, establishing GCPs, acquiring aerial images, generating precise photogrammetric products, conducting LULC mapping, and culminating accuracy analysis of the final outputs. Considering the surface area and safe flight altitude of the study district, images were taken from a flight altitude of 110 m with a ground sampling distance (GSD) of 5.5 cm. To optimize the sensitivity of reflection detection during data collection, a 90° camera angle was chosen, and polygonal flight was performed. Furthermore, data acquisition was carried out during midday hours, leveraging ideal illumination conditions to attain the utmost radiometric accuracy in our detection processes. Subsequent to image acquisition, radiometrically calibrated high accuracy orthomosaic, digital surface model (DSM), and digital terrain model (DTM) production was generated and nDSM production was completed by taking the differential of DSM and DTM [8]. Prior to integrating for classification, the nDSM and orthomosaic data, a 10 cm co-resolution was used in the production to achieve maximum coherence, especially at the roof edges.

The multiresolution segmentation method was employed to generate the necessary segments for subsequent feature extraction. The Estimation of Scale Parameter 2 plug-in was then utilized to determine the optimal scale parameter for the segmentation process. The object-based classification approach was realized using random forest classification algorithm which is a tree-based ensemble machine learning algorithm. It is worth noting that the random forest algorithm is widely used in accurate LULC mapping purposes [9]. Optimal parameter determination (number of estimators, maximum depth, and minimum sample split) of the random forest algorithm was carried out with the GridSearchCV optimization algorithm. To train the model, representative samples were collected for each class within the study area, and subsequently, object-based classification was conducted on three distinct datasets listed in Table 1.

Table 1. Datasets used for classification

Dataset	Features
D1	Spectral bands + Indices
D2	Spectral bands + Indices + Texture + Geometry
D3	Spectral bands + Indices + Texture + Geometry + nDSM

Results and Conclusion

As a result of the classification process, accuracy assessment analysis of LULC maps produced with D1, D2 and D3 datasets yielded overall accuracy of 89.10%, 89.49% and 94.16%, respectively. In this context, it has been discerned that texture and geometric features exert minimal influence on the classification results. While the classification with D1 and D2 datasets showed very similar results, the classification with D3, involving nDSM contributions, demonstrated the highest success. It has been determined that the advantage of high-accuracy elevation data provided by nDSM facilitates the distinction between concrete roofed structures and road class, and the F1 score of road class increases by 8.3% with the D3 dataset (Table 2). The used orthomosaic image and its LULC map produced with D3 dataset are given in Figure 2.

Table 2. Class-based F1 score (%) for three different datasets

Datasets	Concrete roof	Road	Shadow	Water	Bicycle path	Dense vegetation	Soil	Low vegetation	Broad leaved	Thorn tree	Red roof
D1	82.6	88.7	90.4	95.6	93.3	90.7	83.7	78.3	93.2	91.5	98.0
D2	82.6	89.5	89.7	95.9	93.6	91.5	82.9	79.3	93.6	92.1	98.0
D3	95.3	97.8	90.7	96.3	93.1	93.0	85.3	79.5	95.6	93.3	98.1

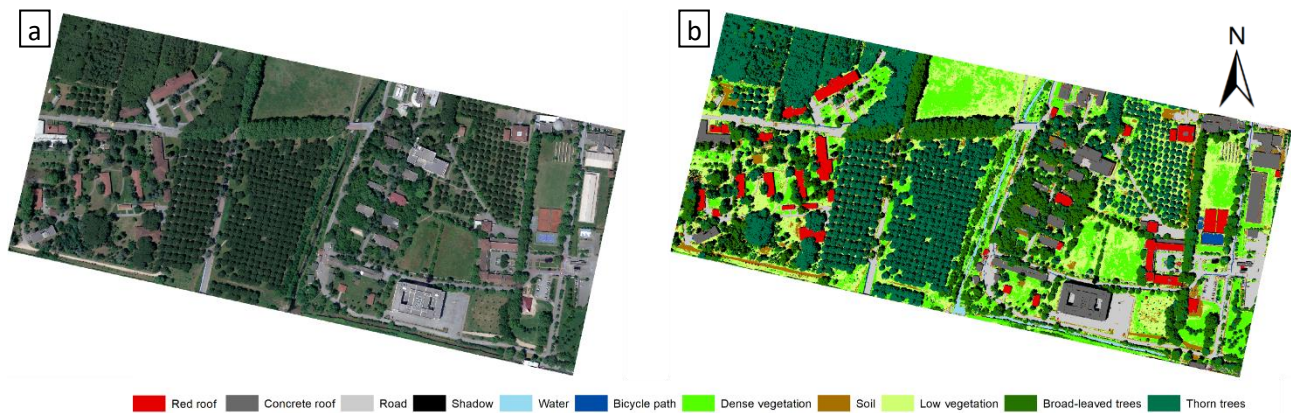


Figure 2. Radiometrically calibrated orthomosaic (a) and LULC thematic map (b)

The approach proposed in this study provided very satisfactory results and proved to be suitable for high-resolution data. Following through statistical and visual analyses, it has been conclusively established that UAVs equipped with MS sensors have yielded successful outcomes in the realm of LULC mapping.

References

1. Cuypers, S., Nascetti, A., & Vergauwen, M. (2023). Land Use and Land Cover Mapping with VHR and Multi-Temporal Sentinel-2 Imagery. *Remote Sensing*, 15(10), 2501. <https://doi.org/10.3390/rs15102501>
2. Svoboda, J., Štych, P., Laštovička, J., Paluba, D., & Kobliuk, N. (2022). Random Forest Classification of Land Use, Land-Use Change and Forestry (LULUCF) Using Sentinel-2 Data—A Case Study of Czechia. *Remote Sensing*, 14(5), 1189. <https://doi.org/10.3390/rs14051189>
3. Elamin, A., & El-Rabbany, A. (2022). UAV-based multi-sensor data fusion for urban land cover mapping using a deep convolutional neural network. *Remote Sensing*, 14(17), 4298. <https://doi.org/10.3390/rs14174298>
4. Lu, T., Wan, L., Qi, S., & Gao, M. (2023). Land Cover Classification of UAV Remote Sensing Based on Transformer–CNN Hybrid Architecture. *Sensors*, 23(11), 5288. <https://doi.org/10.3390/s23115288>
5. Cao, H., Gu, X., Sun, Y., Gao, H., Tao, Z., & Shi, S. (2021). Comparing, validating and improving the performance of reflectance obtention method for UAV-Remote sensing. *International Journal of Applied Earth Observation and Geoinformation*, 102, 102391. <https://doi.org/10.1016/j.jag.2021.102391>
6. Ju, C., & Son, H. I. (2018). Multiple UAV systems for agricultural applications: Control, implementation, and evaluation. *Electronics*, 7(9), 162. <https://doi.org/10.3390/electronics7090162>
7. Ahmed, O. S., Shemrock, A., Chabot, D., Dillon, C., Williams, G., Wasson, R., & Franklin, S. E. (2017). Hierarchical land cover and vegetation classification using multispectral data acquired from an unmanned aerial vehicle. *International Journal of Remote Sensing*, 38(8-10), 2037-2052. <https://doi.org/10.1080/01431161.2017.1294781>
8. Niederöst, M. (2000). Reliable reconstruction of buildings for digital map revision. ETH Zurich
9. Yao, H., Qin, R., & Chen, X. (2019). Unmanned aerial vehicle for remote sensing applications—A review. *Remote Sensing*, 11(12), 1443. <https://doi.org/10.3390/rs11121443>



UAV-based rockfall hazard detection via roughness analysis in Karaköprü, Şanlıurfa using photogrammetric point clouds

Nizar Polat ¹, Yunus Kaya ^{*1}

¹Harran University, Department of Geomatics Engineering, Türkiye, nizarpolat@harran.edu.tr, yunuskaya@harran.edu.tr

Cite this study: Polat, N., & Kaya, Y. (2023). UAV-based rockfall hazard detection via roughness analysis in Karaköprü, Şanlıurfa using photogrammetric point clouds. *Advanced Engineering Days*, 8, 89-92

Keywords

Photogrammetry
Rockfall
Hazard Detection
Roughness Analysis
Urban Safety

Abstract

This study focuses on rockfall hazard detection in urban terrain, particularly the Karaköprü district of Şanlıurfa, utilizing UAV-based photogrammetric dense point cloud analysis. The research introduces an innovative approach that combines advanced geospatial technology and roughness analysis to identify and assess rocks situated above ground surfaces, thereby mitigating potential risks to transportation routes and buildings. The methodology involves quantifying surface irregularity using roughness analysis, where the distance between points and their best-fitting planes is computed based on a carefully selected kernel size. The results demonstrate that this approach effectively marks rocks across the study area, albeit with considerations for potential misclassifications. The dataset is derived from a photogrammetric UAV flight, yielding over 77 million three-dimensional points, while manual examination informs the choice of a 30 cm kernel size, later applied to the entire dataset. In summary, this research showcases the potential of UAV-based photogrammetric point cloud analysis to enhance urban safety and infrastructure resilience in sloping terrains, emphasizing the significance of prior knowledge, kernel size selection, and point density for achieving accurate and reliable results. This approach holds promise for safeguarding urban populations and critical infrastructure in similar urban and geological contexts.

Introduction

Urban areas often encompass diverse landscapes, and one such terrain feature of concern is sloping ground, which may host scattered rocks of varying sizes [1]. These rocks, if not appropriately identified and managed, can pose significant risks to both the safety of city inhabitants and the integrity of surrounding infrastructure [2]. The challenge lies not only in detecting these potential hazards but also in understanding their spatial distribution, size, and degree of exposure above the ground surface [3]. In this context, the integration of advanced geospatial technologies presents a promising solution [4]. Unmanned Aerial Vehicles (UAVs), equipped with high-resolution cameras, provide an efficient means to capture detailed aerial imagery of urban slopes and their surroundings. When processed through photogrammetry, these images can generate dense point clouds, offering rich three-dimensional representations of the terrain and its features [5].

One crucial geometric attribute that becomes instrumental in assessing the danger posed by rocks on sloping urban terrain is roughness. Roughness, in this context, characterizes the irregularity and unevenness of the ground surface. When applied to a dense point cloud, roughness analysis unveils valuable insights into the topography and protrusions above the surface. It enables the differentiation of rocks from the surrounding terrain and assesses their elevation above the ground plane.

The study will take place in Karaköprü district of Şanlıurfa province, a region known for its unique geological characteristics and urban development challenges. By employing this technique, our objective is to identify and evaluate rocks that are situated above the ground surface in this specific urban landscape, thereby posing potential hazards to urban transportation routes and nearby multi-story buildings [3]. The integration of this geospatial

approach not only aids in rock hazard detection but also provides crucial information for urban planners and safety authorities to devise strategic mitigation measures [5].

The remainder of this research delves into the methodology employed for roughness analysis, the detection and assessment of above-surface rocks, and the implications for urban safety and infrastructure resilience within the Karaköprü district. By harnessing the power of modern geospatial technologies, we endeavor to enhance the proactive management of rockfall risks in this specific urban setting, contributing to the safety and well-being of city dwellers and the preservation of urban infrastructure.

Material and Method

Roughness

Roughness estimation is a fundamental aspect of three-dimensional point cloud analysis. It involves a straightforward calculation for each point in the cloud, where the 'roughness' value is determined by the distance between that point and the best-fitting plane, computed based on its nearest neighbors [6]. The 'kernel' refers to the neighborhood radius, defining the region around each point from which neighboring points are considered. Within this neighborhood, the orthogonal distance to the best-fit plane is calculated to assess roughness [7]. This calculation relies on differences in height between the central point and the average height of its neighboring points, all computed along a specified 'vertical' orientation. This approach provides a quantitative measure of surface irregularity and is invaluable in numerous applications across various domains, aiding in tasks such as hazard detection, structural analysis, and surface quality evaluation.

Point cloud generation

Obtaining a UAV-based photogrammetric dense point cloud often involves the integration of Structure-from-Motion (SfM) techniques, harnessing the capabilities of Unmanned Aerial Vehicles (UAVs) equipped with high-resolution cameras [8]. In this process, the UAV is deployed to capture a series of overlapping aerial images from various angles and altitudes over the target area. These images serve as the primary data source. Through the application of SfM algorithms, these images are meticulously analyzed and processed to reconstruct a dense point cloud. SfM techniques employ precise triangulation methods to calculate the three-dimensional coordinates of points on the Earth's surface, based on their appearances in multiple images. These computed 3D coordinates collectively form the dense point cloud, where each point corresponds to a specific location in the surveyed area [9]. This point cloud delivers an exceptionally detailed and accurate representation of the terrain or objects within the surveyed region. It serves as a foundational resource for a wide range of applications, including 3D modeling, topographic mapping, land surveying, environmental monitoring, and beyond.

Results

Within the scope of the study, a photogrammetric drone flight was carried out in the relevant region. 262 aerial photographs with 80% overlap were obtained with the flight made with Mavic 2 Pro from a height of 70m. With the processing of the data, more than 77 million three-dimensional point data were obtained (Figure 1).



Figure 1. Point cloud of the study area

The dataset underwent an initial manual examination in a part of study area, during which a meticulous search was conducted to identify and catalog rock sizes. This preliminary step is essential to facilitate subsequent roughness analysis. After careful consideration, a kernel size of 30 cm was ultimately selected as the most suitable parameter for the analysis in a part of study area. A detailed view of the obtained result is presented in Figure 2.

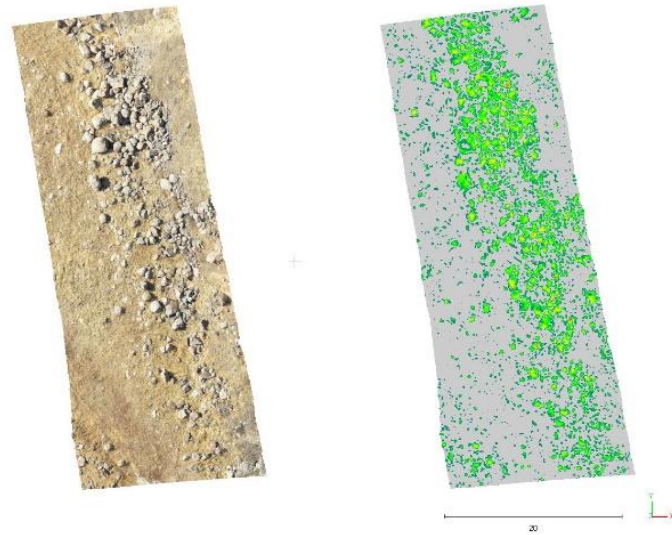


Figure 2. Close view of the results

As the kernel size provided valuable results within a limited area, these same parameters were extended to the entire dataset. The outcome marked points corresponding to rocks across the entire study area (Figure 3).

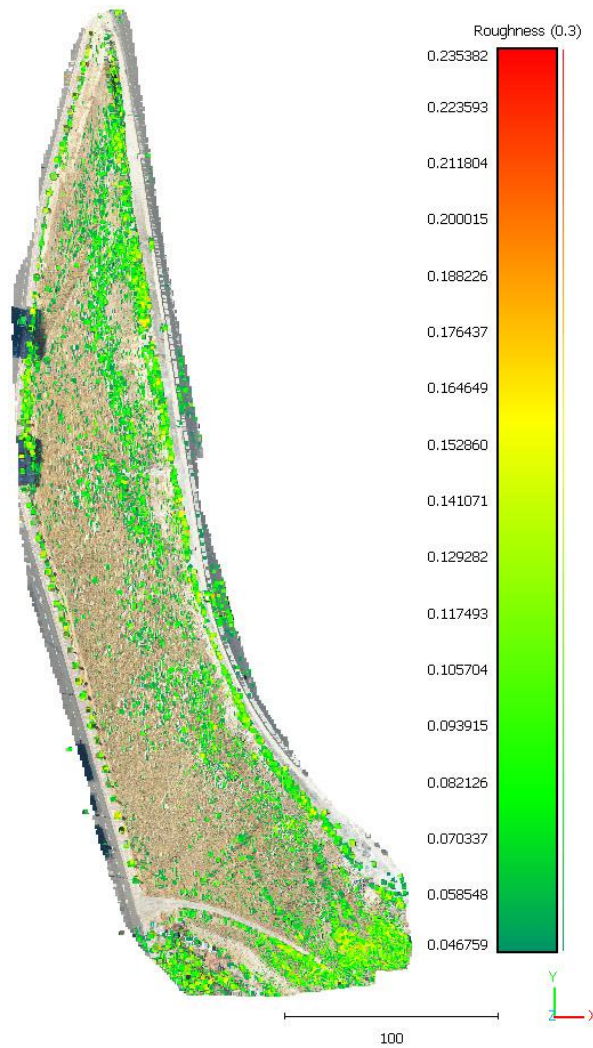


Figure 3. Roughness based rocks

However, it's worth noting that some of these points may also pertain to bushes. To mitigate the potential for such misclassifications, it may be necessary to either narrow the field of analysis or preprocess the data to remove unrelated objects.

Discussion

When conducting roughness analysis, having prior knowledge about the region can prove highly advantageous. This is particularly relevant due to the influence of kernel size selection on the potential detection of rocks, as certain rocks may be only partially or entirely overlooked based on this parameter. Therefore, having at least a general understanding of the size of rocks within the area becomes invaluable. Additionally, point density plays a critical role in this process. Ensuring that the point density within the kernel is sufficient is essential for the rocks to be effectively detected and integrated into the analysis. However, it's important to note that providing an exact point density ratio is challenging, as it can vary substantially depending on the specific dataset and workspace characteristics.

Conclusion

This study employed UAV-based photogrammetric dense point cloud analysis for rock fall hazard detection in the Karaköprü district of Şanlıurfa. The methodology centered on roughness analysis, quantifying surface irregularity through the distance between points and their best-fitting planes using a selected kernel size. The process successfully marked rocks in the study area, with attention to potential misclassifications. The dataset was obtained through a photogrammetric drone flight, producing over 77 million three-dimensional points. Manual examination informed the choice of a 30 cm kernel size, applied to the entire dataset. In summary, this research showcases the effectiveness of UAV-based photogrammetry and roughness analysis in urban rock fall hazard detection. It underscores the importance of prior knowledge, kernel size selection, and point density consideration for accurate results. This approach enhances urban safety and infrastructure resilience, with potential applications in similar urban contexts.

References

1. Giordan, D., Cignetti, M., Godone, D., Bertolo, D., & Paganone, M. (2021). Definition of an operative methodology for the management of rockfalls along with the road network. *Sustainability*, 13(14), 7669. <https://doi.org/10.3390/su13147669>
2. Vanneschi, C., Di Camillo, M., Aiello, E., Bonciani, F., & Salvini, R. (2019). SFM-MVS photogrammetry for rockfall analysis and hazard assessment along the ancient roman via Flaminia road at the Furlo gorge (Italy). *ISPRS International Journal of Geo-Information*, 8(8), 325. <https://doi.org/10.3390/ijgi8080325>
3. Yan, P., Zhang, J., Kong, X., & Fang, Q. (2020). Numerical simulation of rockfall trajectory with consideration of arbitrary shapes of falling rocks and terrain. *Computers and Geotechnics*, 122, 103511. <https://doi.org/10.1016/j.compgeo.2020.103511>
4. Albarelli, D. S. N. A., Mavrouli, O. C., & Nyktas, P. (2021). Identification of potential rockfall sources using UAV-derived point cloud. *Bulletin of engineering geology and the environment*, 80(8), 6539-6561. <https://doi.org/10.1007/s10064-021-02306-2>
5. Sarro, R., Riquelme, A., García-Davalillo, J. C., Mateos, R. M., Tomás, R., Pastor, J. L., ... & Herrera, G. (2018). Rockfall simulation based on UAV photogrammetry data obtained during an emergency declaration: Application at a cultural heritage site. *Remote Sensing*, 10(12), 1923. <https://doi.org/10.3390/rs10121923>
6. Cloud Compare. Available online: <https://www.danielgm.net/cc/> (accessed on 5 August 2023).
7. Seo, H. (2021). 3D roughness measurement of failure surface in CFA pile samples using three-dimensional laser scanning. *Applied Sciences*, 11(6), 2713. <https://doi.org/10.3390/app11062713>
8. Uysal, M., Toprak, A. S., & Polat, N. (2015). DEM generation with UAV Photogrammetry and accuracy analysis in Sahitler hill. *Measurement*, 73, 539-543. <https://doi.org/10.1016/j.measurement.2015.06.010>
9. Akca, S., & Polat, N. (2022). Semantic segmentation and quantification of trees in an orchard using UAV orthophoto. *Earth Science Informatics*, 15(4), 2265-2274. <https://doi.org/10.1007/s12145-022-00871-y>



Advanced Engineering Days

aed.mersin.edu.tr



Pixel based classification of *Lavandula sp.* using high resolution UAV orthophotos

Seyma Akca^{*1}, Nizar Polat¹

^{*1}Harran University, Department of Geomatics Engineering, Türkiye, seymakca@harran.edu.tr, nizarpolat@harran.edu.tr

Cite this study: Akca, S., & Polat, N. (2023). Pixel based classification of *Lavandula sp.* using high resolution UAV orthophotos. *Advanced Engineering Days*, 8, 93-96

Keywords

Lavander
UAV
Machine Learning
Monitoring
High Resolution

Abstract

Lavender, a member of the Lamiaceae family, is a notable plant known for its production of volatile oil. Lavender oil is prized for its antiseptic and antibiotic qualities, as well as its unique aromatic properties, making it a valuable resource in aromatherapy practices. Consequently, closely monitoring lavender plants has become a significant concern. Unmanned Aerial Vehicles (UAVs) offer a valuable solution for this task by providing high-resolution imagery through low-altitude flights and advanced digital cameras. In this study, UAVs were utilized to create orthophotos of a lavender garden. Orthophotos are meticulously corrected aerial images, ensuring consistent scale and distortion-free representation, which makes them ideal for various analytical purposes. The primary objective of the study is pixel based classification of lavender. To enhance lavender plant monitoring, machine learning techniques, specifically Support Vector Machines (SVM) and K-means clustering, were employed for binary classification. These methods were applied to analyze the orthophotos generated by the UAVs, likely to classify different sections or features within the lavender garden. In conclusion SVM provided a higher overall accuracy value for the classification results at both 1 cm and 10 cm resolutions.

Introduction

Lavender (*Lavandula sp.*), belonging to the Lamiaceae family, is a significant volatile oil-producing plant. In Turkey, various lavender species exhibit variations in the composition of their essential oil constituents, influenced by factors including species differentiation, climatic conditions, genetic attributes, harvesting and processing methodologies, among others. Furthermore, lavender oil finds application in aromatherapy practices owing to its antiseptic and antibiotic attributes, as well as its distinctive volatile oil characteristics [1].

In the province of Isparta, when calculating the Internal Rate of Return (IRR) for lavender cultivation currently underway, both fresh and dried lavender have been considered. The IRR is calculated at 22.59% for fresh lavender and 29.24% for dried lavender [2].

In the past decade, Unmanned Aerial Vehicles (UAVs) have gained widespread use in engineering projects, spanning diverse applications such as forest fire risk assessment, landslide monitoring, and cultural heritage modeling studies. One of UAV deployment's most compelling advantages is its ability to capture high spatial resolution imagery due to low-altitude flight and advanced digital cameras[3-5]. UAVs also find utility in detecting vegetation areas, assessing their condition, and monitoring reforestation efforts. The high-resolution image data obtained from UAVs is utilized to extract essential information for vegetation research using various image processing techniques [6-8]. Importantly, temporal variations in UAV-captured images, acquired at specific intervals, can be revealed through image processing, serving as valuable evidence and a basis for early detection and cost-effective interventions in Lavender cultivation areas [9].

The Lavender plant, which has commercial value and finds applications in aromatic and medical domains, has been cultivated for such purposes at Harran University's Osmanbey Campus. Within the scope of this study, UAV-based orthophotos were generated for the Lavender garden planted, and machine learning-based SVM and k-means methods were employed for binary classification with the aim of monitoring the plant's growth progress.

Material and Method

Study Area

The study area depicted with red polygon is located in the Harran University's Osmanbey Campus on a gently sloping terrain (Figure 1). This area predominantly hosts olive and pomegranate trees, covering a span of 0.0212 km². To obtain aerial imagery of this region, a photogrammetric flight plan was meticulously crafted. The flight plan involved six columns of imagery captured from a height of 30 meters, ensuring an 80% overlap between images. Using a DJI Mavic 2 Pro drone, a 20-minute flight mission was executed, resulting in a total of 418 geotagged images. After acquiring aerial imagery, we processed the data using Structure-from-Motion (SfM), a cost-efficient and user-friendly photogrammetric method that has gained popularity in recent years [9].



Figure 1. Study area depicted with red polygon in Harran University Osmanbey Campus

Support Vector Machine

Support Vector Machines (SVM) is a machine learning method developed by Vapnik in 1985. It optimizes a hyperplane for maximum class separation, using support vectors as the closest data points. When linear separation isn't possible, SVM employs the kernel trick to project data into a higher-dimensional space. For M-class problems, two approaches exist: One-Against-One generates M binary SVM classifiers, while One-Against-All applies SVM to all M choose 2 combinations. SVM finds applications in fields such as classification, prediction, and forecasting [10].

K-Means

The K-means algorithm stands out as one of the most straightforward and widely recognized clustering techniques. Its primary objective is to identify cluster centers and allocate data elements to these clusters by minimizing a squared error-based objective function. The algorithm strives to position cluster centers as far apart from each other as feasible while assigning each data point to its nearest cluster center. Typically, the Euclidean distance metric is employed to measure dissimilarity within the K-means algorithm [11].

Results

Within the scope of the study, the opportunity to produce high-resolution orthophotos from aerial photographs was realized. In this context, orthophotos were generated at two different resolutions (1 cm and 10 cm), and lavender plants were detected through classification using both K-Means and SVM methods. The obtained results are presented in Figure 2.

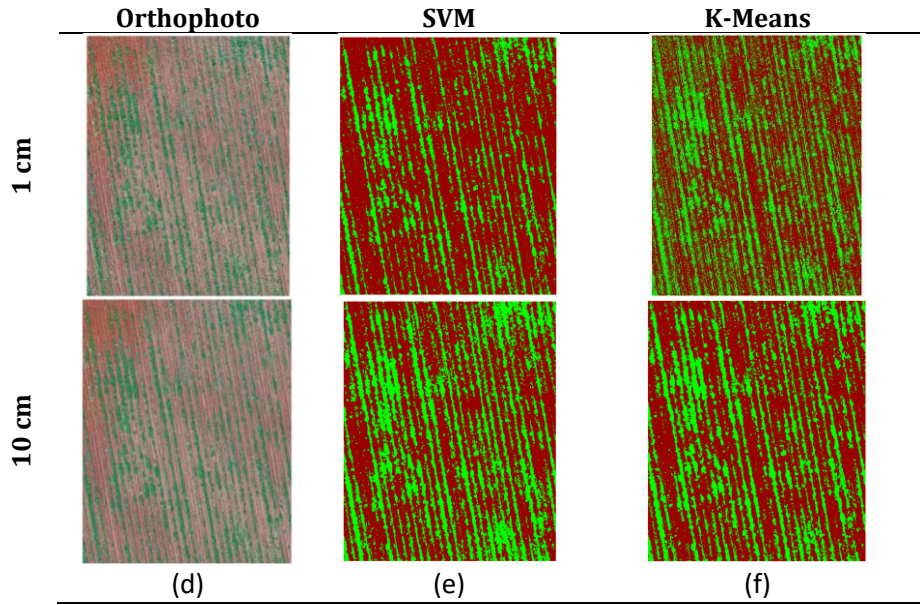


Figure 2. 1 cm and 10 cm orthophotos and classification results

As part of the study, accuracy analysis was conducted on the result images using ground truth regions of interest (ROIs) for post-classification accuracy assessment. The overall accuracy, kappa value, producer's accuracy, and user's accuracy values obtained from this analysis are presented in Table 1.

Table 1. Accuracy metrics

Methods	Global Accuracy	Producer Accuracy.	User Accuracy	Kappa
SVM 1cm	99.97	99.97	100.0	0.99
SVM 10 cm	99.68	100.00	99.39	0.99
K means 1 cm	88.82	90.35	89.25	0.77
K means 10 cm	90.71	78.05	99.96	0.80

Discussion

In visual assessment, the SVM classification result image exhibits higher resolution, appearing smoother and more comprehensible at 1 cm resolution, whereas at 10 cm resolution, it appears more complex with increased ambiguity in the delineation of planting lines. In the K-means results, the 10 cm result is smoother. According to Table 1, SVM provided a higher overall accuracy value for the classification results at both 1 cm and 10 cm resolutions. The lowest producer's accuracy was achieved in the 10 cm K-means image. The highest user's accuracy, on the other hand, was obtained with the 1 cm SVM classification.

Conclusion

In this study, machine learning methods, namely SVM and K-means, were used to classify images with high spatial resolutions of 1 and 10 cm, based on UAV data. It has been observed that the SVM-controlled classification method yielded better results compared to k-means unsupervised classification.

References

- Varli, M., Hanci, H., & Kalafat, G. (2020). Tıbbi ve aromatik bitkilerin üretim potansiyeli ve biyoyararlılığı. *Research Journal of Biomedical and Biotechnology*, 1(1), 24-32.
- Güler, K. H., & Korkmaz, M. (2018). Isparta ili orman köylerinde lavanta yetiştiriciliğinin ekonomik analizi. *Turkish Journal of Forestry*, 19(2), 156-162. <https://doi.org/10.18182/tjf.424901>
- Kabadayı, A. & Erdoğan, A. (2023). İHA Fotogrametrisi Kullanarak Yozgat Çilekçi Türbesi'nin 3 Boyutlu Nokta Bulutu ve Modelinin Üretilmesi. *Türkiye Fotogrametri Dergisi*, 5 (1), 29-35. <https://doi.org/10.53030/tufod.1313200>
- Yakar, M., Murat Yılmaz, H., Yıldız, F., Zeybek, M., Şentürk, H., & Çelik, H. (2009). Silifke-Mersin Bölgesinde Roma Dönemi Eserlerinin 3 Boyutlu Modelleme Çalışması ve Animasyonu. *Jeodezi ve Jeoinformasyon Dergisi*, 101.
- Alptekin, A., Çelik, M. Ö., Doğan, Y., & Yakar, M. (2019). Mapping of a rockfall site with an unmanned aerial vehicle. *Mersin Photogrammetry Journal*, 1(1), 12-16.

6. Alptekin, A., & Yakar, M. (2020). Determination of pond volume with using an unmanned aerial vehicle. *Mersin Photogrammetry Journal*, 2(2), 59-63.
7. Polat, N., Memduhoğlu, A., & Akça,Ş. (2022). Determining the change in burnt forest areas with UAV: The example of Osmanbey campus. *Advanced UAV*, 2(1), 11-16.
8. Khrulev, A. (2023). Analysis of pneumatic catapult launch system parameters, taking into account engine and UAV characteristics. *Advanced UAV*, 3(1), 10-24.
9. Akca, S., & Polat, N. (2022). Semantic segmentation and quantification of trees in an orchard using UAV orthophoto. *Earth Science Informatics*, 15(4), 2265-2274. <https://doi.org/10.1007/s12145-022-00871-y>
10. Akca, S., & Gungor, O. (2022). Semantic segmentation of soil salinity using in-situ EC measurements and deep learning based U-NET architecture. *Catena*, 218, 106529. <https://doi.org/10.1016/j.catena.2022.106529>
11. Orhan, U., Hekim, M., & Ozer, M. (2011). EEG signals classification using the K-means clustering and a multilayer perceptron neural network model. *Expert Systems with Applications*, 38(10), 13475-13481. <https://doi.org/10.1016/j.eswa.2011.04.149>



Influence of wheel diameter difference on their stability against derailment

Angela Shvets*¹ 

¹Ukrainian State University of Science and Technologies, Department of Engineering and Design Specialized Department «Microprocessor-Based Control Systems and Safety in the Railway Transport» (EDSD MBCSS), Ukraine, angela_shvets@ua.fm

Cite this study: Shvets, A. (2023). Influence of wheel diameter difference on their stability against derailment. *Advanced Engineering Days*, 8, 97-99

Keywords

Gondola cars
Railway
Wheel derailment factor
Mathematical modeling
Difference in wheel diameters

Abstract

In railway transport, there is a very acute problem of intensive wear of the lateral surface of the tread and wheel flanges. Traffic safety and dynamic loading of rail vehicles largely depend on the technical condition of their running gear. Therefore, this research is devoted to the study of the influence on the stability of the wheel from derailment of deviations in the running gear of cars that inevitably arise during their operation. To assess the impact on the stability of the wheel from derailment, the differences in the diameters of the wheels of one wheelset, as well as the differences in the diameters of the wheels of the wheelsets of one bogie, are considered. A freight car was chosen as the most numerous type of rail vehicle, and a four-axle gondola car was taken among the freight cars. The values of the wheel derailment factor are obtained taking into account the specified deviations of the technical condition of the wheelsets within the existing tolerances in operation.

Introduction

The increase in wear of the flanges of wheelsets of rolling stock and the side surfaces of the rail heads is one of the most serious problems of railway transport. The wear of wheels and rails depends on the physical and mechanical processes occurring in the area of their contact [1-4]. The nature and the intensity of these processes largely depend on the interaction forces of the contacting bodies and their relative displacements. Therefore, one of the possible ways to solve the problem of reducing wear is to establish conditions for reducing the dynamic loading of the contact area. The solution to the problem is reduced to minimizing the interaction forces and mutual displacements of wheels and rails in the contact area. An important aspect of this problem is also ensuring the safety of train traffic in the presence of wear of wheels and rails [5-8].

Material and Method

Traffic safety is influenced by a large number of different factors [9-12]. To assess the impact on wheel stability from derailment, this paper considers the impact of only some of them:

- the difference in diameters of wheels of one wheelset;
- the difference in diameters of the wheels of wheelsets of one bogie.

The study was carried out by the method of mathematical modeling using the model of spatial oscillations of freight cars [13-15]. Theoretical studies were carried out during the movement of a gondola car model 12-532 with standard bogies 18-100 at speeds in the range from 50 to 90 km/h in curves with radii of 350 and 600 m, with elevations of the outer rail of 130 and 120 mm, respectively. A 12-532 gondola car on 18-100 model bogies was chosen for the reason that these cars have low critical speed from the point of view of movement stability; when exceeding it, continuous oscillations of wheelsets, limited by railway lines, occur. The stationary mode of movement of the freight cars in the curve was investigated in order to establish the influence of only the factor under consideration, namely, the difference in wheel diameters. The running gear of the car, the rolling surface of the wheel, and the rail head profile were provided in normal technical condition [16, 17].

Results

Traffic safety, as you know, depends on many factors, including the design features of the track and running gear of the rolling stock, but to a greater extent, it is determined by their condition during operation. Let us consider the impact on the stability of the wheels from the derailment of the difference in the diameters of the wheels of one wheelset – in particular, the first wheel pair and the change in the diameter of the leading wheel.

Differences in the diameters of the wheels of one wheelset are considered in the range from 0 to 8 mm. Figure 1 shows graphs of changes in C_{ds} indicators during the movement of a loaded gondola car with standard bogies with an increase in the radius of the leading wheel.

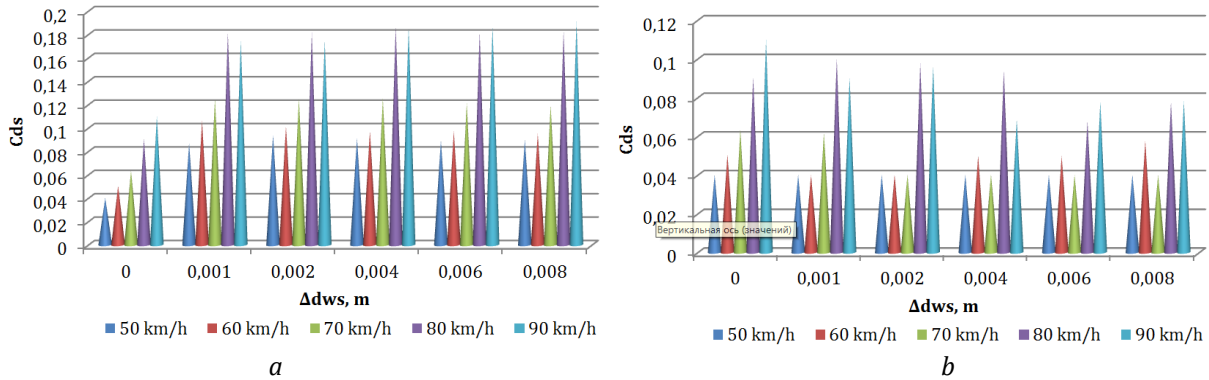


Figure 1. The influence of the difference in the diameters of the wheels of one wheelset on C_{ds} : a – $R=350$ m; b – $R=600$ m

As you know, an increase in the radius of the leading wheel directs to an increase in the longitudinal sliding of this wheel. If, at the same radii of one wheelset, its hunting had a certain negative value, then with an increase in the sliding of the leading wheel in the curves $R=600$ m, this negative value decreases (Figure 1, b). This means that the wheelset fits into the curve with a smaller striking angle.

When changing the radius of the non-running wheel, the results in the $R=350$ m curve are similar in Figure 1 (a). In the $R=600$ m curve, with a difference of 0.002 m, an increase in the wheel derailment factor C_{ds} occurs over the entire speed range.

Further, the influence on the wheel derailment factor from the convergence of the difference in the diameters of the wheels of the wheelsets of one bogie was considered (Figure 2). The results are given for the case when the radii of the wheels of the front wheelset of the bogie are greater by 0.005-0.015 m than the radii of the wheels of the rear wheelset (the radii of the wheels are the same in each wheelset).

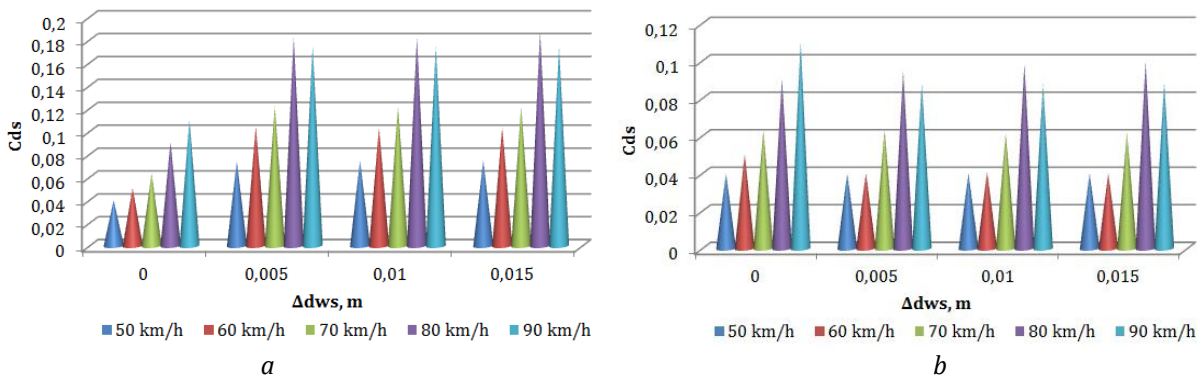


Figure 2. The influence of the difference in the diameters of the wheelsets of one bogie on C_{ds} : a – $R=350$ m; b – $R=600$ m

According to the Standards for the release of cars from depot repairs, the difference in wheel diameters in the rolling circle for one bogie should not exceed 20 mm. With an increase in the radii of the wheels of the rear wheelset, the stability indicators from derailment also increase.

The results for the case when the radii of the wheels of the front wheelset of the bogie are less by 0.005-0.015 m are similar to changes with an increase in diameters. With a decrease in the diameter of the front wheelset in the bogie, the stability indicators from derailment practically do not change in curves of both radii.

Conclusion

As a result of the theoretical studies of the spatial oscillations of a freight car, using the example of a gondola car, the values of the wheel derailment stability coefficient were obtained, which makes it possible to objectively assess the effect of the difference in the diameters of the wheel pairs of one bogie on traffic safety.

The driving performance of the car depends on the values of the set of parameters characterizing the state of the running gears of the rolling stock and the railway track. Therefore, at the next stages of research on this problem, it is necessary to solve the problems of traffic safety and minimization of wear as multi-parameter. Despite the great work done by many organizations to study the causes of intensive wear of wheels and rails, the solution to the problem cannot be considered complete due to its versatility. It is necessary to continue not only theoretical research but also specially designed experiments in natural conditions. It is advisable to develop such methods for direct assessment in real conditions of the wear of the surfaces of the rails and wheels of the rolling stock, which makes it possible to identify locomotives and cars that cause increased wear.

References

1. Blokhin, E. P., Pshinko, O. M., Danovich, V. D., & Korotenko, M. L. (1998). Effect of the state of car running gears and railway track on wheel and rail wear. *Railway Bogies and Running Gears: Proceedings of the 4th International Conference*, 313-323. Budapest, Hungary.
2. Shvets, A., Muradian, L., & Shvets, A. (2023). Investigation of wear of wheels and rails when the center of mass of cargo in gondola cars shifts. *Advanced Engineering Days*, 7, 109-112.
3. Fomin, O. V., Shvets, A. O., Bolotov, O. M., & Saparova, L. S. (2020). Definition of indicators wear in an uneven load freight rolling stock. *Bulletin of Certification of Railway Transport*, 1, 19-29.
4. Shvets, Angela O., Bolotov, O. M., Saparova, L. S., & Shvets, Angelika O. (2019). Wear wheels and rails at the uneven loading of gondola cars. *Bulletin of Certification of Railway Transport*, 1(53), 4-17.
5. Muradian, L., Pitsenko, I., Shaposhnyk, V., Shvets, A., & Shvets, A. (2022). Predictive model of risks in railroad transport when diagnosing axle boxes of freight wagons. *Proceedings of the Institution of Mechanical Engineers, Part F: Journal of Rail and Rapid Transit*, 1-5. <https://doi.org/10.1177/09544097221122043>
6. Myamlin, S., Neduzha, L., & Shvets, A. (2014). Determination of friction performance influence in the system "body-bogie" on the freight car dynamics. *Science and Transport Progress*, 2 (50), 152-163. <https://doi.org/10.15802/stp2014/23792>
7. Lazaryan, V. A., Dlugach, L. A., & Korotenko, M. L. (1972). *Stability of rail vehicle movement*. Kiev: Naukova dumka.
8. Shvets, A., Shvets, A., & Kasianchuk, V. (2020). Research of strength characteristics of element of the unit rolling stock. *Railroad car fleet*, 1 (157), 7-12.
9. Shvets, A. O. (2021). Research of stability of the freight rolling stock in noncentral interaction automatic couplers two cars. *Bulletin of Certification of Railway Transport*, 2 (66), 50-62.
10. Shvets, A. O. (2020). Stability of freight wagons under the action of compressing longitudinal forces. *Science and Transport Progress*, 1 (85), 119-137. doi: 10.15802/stp2020/199485
11. Shvets, A. O. (2023). Influence of the instability form on the traffic safety of freight rolling stock. *Advanced Engineering Days*, 6, 111-113.
12. Malysheva, A. A. (1999). Influence of difference of diameters of the wheels on their wear. *Transport. Stress loading and durability of a rolling stock*, 2, 139-143.
13. Shvets, A. O. (2019). Gondola cars dynamics from the action of longitudinal forces. *Science and Transport Progress*, 6 (84), 142-155. doi: 10.15802/stp2019/195821
14. Myamlin, S., Neduzha, L., & Shvets, A. (2013). Research of friction indices influence on the freight car dynamics. *Teka. Commission of motorization and energetics in agriculture*, 13 (4), 159-166.
15. Myamlin, S., Neduzha, L., & Shvets, A. (2013). Technical condition of sliders as one of the factors influencing the dynamics of freight cars. *Collection of scientific works DonIRT*, 35, 65-72.
16. Muradian, L., Shvets, A., & Shvets, A. (2023). Some dynamic processes at longitudinally-transverse shift of the cargo. *Scientific Journal of Silesian University of Technology. Series Transport*, 120, 187-204. <https://doi.org/10.20858/sjsutst.2023.120.12>
17. Shvets, A. (2023). Multibody model of freight railcars interaction in a train. *Transportation Energy and Dynamics*, 217-241. https://doi.org/10.1007/978-981-99-2150-8_10



The application of SVD method in image compression and digital watermarking

Ornela Gordani ¹, Aurora Simoni ¹

¹University of Tirana, Faculty of Natural Science, Department of Applied Mathematics, Tirana, Albania
ornela.gordani@fshn.edu.al, aurora.simoni@fshn.edu.al

Cite this study: Gordani, O., & Simoni, A. (2023). The application of SVD method in image compression and digital watermarking. *Advanced Engineering Days*, 8, 100-102

Keywords

Image
Algebra
Watermarking
Compression
Image Processing

Abstract

In terms of digital files, compression is the act of encoding information using fewer bits than what's found in the original file. When we say image compression, we have in mind an image that has fewer bytes than the original image but has the most important features that describe the original image. So, the aim of image compression is to reduce the image size without degrading image quality below an acceptable threshold. In MATLAB, an image is stored as a matrix. One approach is to apply the Singular Values Decomposition (SVD) to the image matrix. This method is implemented in MATLAB. In order to divide the matrix of the given image into three other matrices in MATLAB, we can use the function `svd()`. As performance metrics, we can use PSNR and Compression ratio. Digital Watermarking is defined as the process of hiding a piece of digital data in the cover data which is to be protected and extracted later for ownership verification. In an SVD-based watermarking scheme, the singular values of the cover image are modified to embed the watermark data. All tests and experiments are performed using MATLAB as the computing environment and programming language. Also, in the RStudio programming language we can see the implementation of the SVD method in image compression.

Introduction

The main objective of image compression is to reduce the redundancy of the image data to be able to store or transmit data in an efficient form. Image compression may be lossy or lossless. Lossy methods are especially suitable for natural images such as photographs in applications in which minor (sometimes imperceptible) loss of fidelity is acceptable to achieve a substantial reduction in bit rate. In other hand the Lossless compression is preferred for archival purposes.

Digital Watermarking is used for a wide range of applications, such as: copyright protection, source tracking, broadcast monitoring etc. A digital watermarking can be visible or invisible A visible watermark typically consists of a conspicuously visible message or a company logo indicating the ownership of the image. On the other hand, an invisible watermarked image appears very similar to the original. The existence of a watermark can only be determined using an appropriate watermark extraction or detection algorithm.

In MATLAB (or in RStudio), we first have to find the optimal number of singular values that we need in order to have a compressed image with the essential information. After that, we can see the error in values (numbers) or even in images. This means that we can take an image with the features that we removed from our original image during the compression process.

Also, in MATLAB we can make a digital watermarking of a given image by using the SVD and DWT (Discrete Wavelet Transform) methods.

Material and Method

Singular Values Decomposition (SVD) is a numerical technique used to diagonalize matrices in numerical analysis. SVD aims to approximate the dataset of large number of dimensions using fewer dimensions. SVD

considers a highly variable, high dimensional data points and exposes the substructure of the original data by reducing the higher dimensional data into lower dimensional data. Exposure of the substructure orders the data from most variation to the least. This helps to find the region of most variation and then later SVD can be used for reduction. The steps we need to follow to compress an image using SVD method are:

- i. Read the input image
- ii. Convert integer to double data type
- iii. Calculate the required rank
- iv. Perform SVD to obtain the three component matrices
- v. Apply approximation on the diagonal component matrix
- vi. Regenerate the matrix and remove singularity
- vii. Convert double data type to integer
- viii. Compressed image is created and displayed

We have implemented those steps on MATLAB and the result is as in the Figure 1. The compression ratio and PSNR value when we used 11 singular values are 540.5542 and 10.4012 respectively.



Figure 1. Image Compression using 11 Singular Values

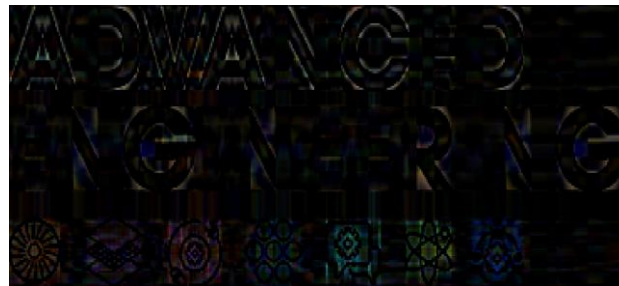


Figure 2. The error or the part of part of the image that we “removed”

Singular Value Decomposition can be used for digital watermarking. The Figure 3 show us the steps that we have to follow.



Figure 3. The flow chart of the watermarking embedding

In MATLAB, we need to use `svd()` and `dwt2()` to watermark a given image or to watermark a given image to another image.

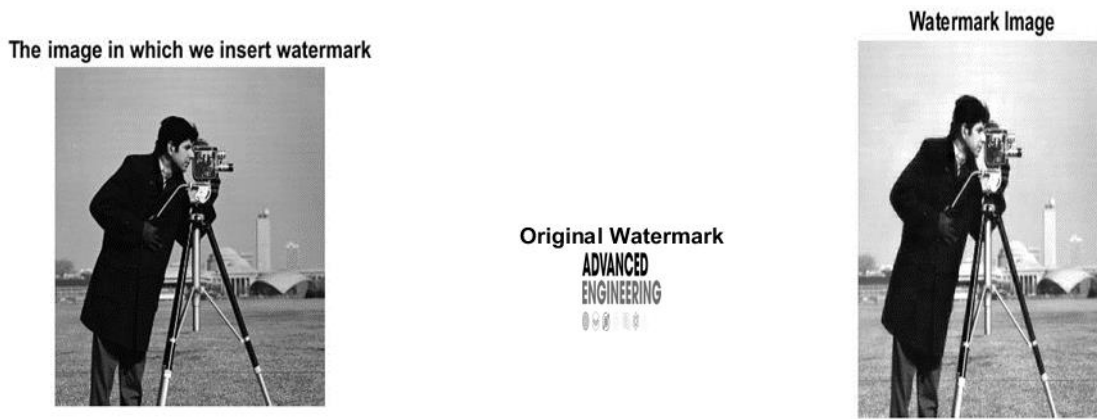


Figure 4. Watermark an image to another image

Results

In the Table 1 we can see what happened if we use different number of singular values.

Table 1. Number of singular values

Number of singular Values	PSNR	Compression Ratio
11	10.4012	37.6809
31	13.5235	13.3706
51	16.1671	8.1272
71	18.8835	5.8379
91	21.9250	4.5548

We see that if we increase the number of singular values the value of PSNR will increase and the value of compression ratio will decrease. Our duty is to see where the increase of the PSNR value is insignificant and similarly where the decrease of the Compression Ratio is insignificant.

When we watermark a given image "1" to another image "2", we have to decide what percentage of the image "1" we want to watermark to the other image "2". In the Figure 4 we have decided that 90% of the image "Advanced Engineering" will be watermark in the first given image.

Conclusion

SVD has many different applications. We decide to show you two of them: image compression and digital image watermarking. This is because we can use image compression to do digital watermarking. So, first we can do a compression of the image and then we can use this compression as a "watermark".

To do watermarking, which nowadays is heavily used in marketing, we can use other methods, for example, PSO.

References

1. Gonzalez, R. C., Woods, R. E., & Eddins, S. L. (2006). *Digital Image Processing Using Matlab*. Prentice Hall.
2. Lai, C. C. (2011). A digital watermarking scheme based on singular value decomposition and tiny genetic algorithm. *Digital Signal Processing*, 21(4), 522-527. <https://doi.org/10.1016/j.dsp.2011.01.017>
3. Singh, S. K., & Kumar, S. (2009, November). A framework to design novel SVD based color image compression. In *2009 Third UKSim European Symposium on Computer Modeling and Simulation*, 235-240. <https://doi.org/10.1109/EMS.2009.100>
4. Hernandez, J. R., Amado, M., & Perez-Gonzalez, F. (2000). DCT-domain watermarking techniques for still images: Detector performance analysis and a new structure. *IEEE transactions on image processing*, 9(1), 55-68. <https://doi.org/10.1109/83.817598>
5. Lu, W., Sun, W., & Lu, H. (2009). Robust watermarking based on DWT and nonnegative matrix factorization. *Computers & Electrical Engineering*, 35(1), 183-188. <https://doi.org/10.1016/j.compeleceng.2008.09.004>



Algorithm for determining restrictions on train control

Kostiantyn Zhelieznov ¹, Artem Akulov ¹, Oleksandr Zabolotnyi ¹, Eugene Chabaniuk ¹,
Angela Shvets*¹

¹Ukrainian State University of Science and Technologies, Department of Engineering and Design Specialized Department «Microprocessor-Based Control Systems and Safety in the Railway Transport» (EDSD MBCSS), Ukraine, ConstantinZ@i.ua, asakulov@gmail.com, zabolotnyi@i.ua, 457m@ukr.net, angela_shvets@ua.fm

Cite this study: Zhelieznov, K., Akulov, A., Zabolotnyi, O., Chabaniuk, E., & Shvets, A. (2023). Algorithm for determining restrictions on train control. *Advanced Engineering Days*, 8, 103-108

Keywords

Railway
Optimal control
Train driving modes
Driving simulators
Energy efficiency

Abstract

One of the priority areas for ensuring the stable and profitable operation of railway transport and its development and improvement is the transition to resource-saving technologies. Optimization of train control modes is one of the most important measures to address the currently pressing problem of saving fuel and energy resources for train traction. The purpose of this study is to develop an algorithm for determining restrictions on train control while complying with safety requirements and timetables. This algorithm must allow calculations to be performed quickly and without significant loss of accuracy, and the results of the calculations must meet the criteria of optimality, safety, and compliance with the train schedule. The information base for the development of the algorithm was the existing mathematical and algorithmic methods for solving isoperimetric problems of finding an optimal solution in the presence of resource restrictions. The proposed calculation method consists of using simplified calculations of the state of the train as a controlled system, without using differential equations of motion, which allows solving problems of finding optimal control almost in real-time. The results of these studies were used to create simulators for training train drivers.

Introduction

An important problem in the further development of railways is the energy efficiency of various modes of train movement. In modern conditions of a market economy, for all energy consumers, including railway transport, the most significant and determining factor in energy use is the cost of energy. The successful operation of railways in the electricity market is associated with the further development of information technologies for the management of railway transport, combining electric traction systems and the organization of the transportation process with optimal train movement modes [1-3].

It is well known that one of the ways to reduce the cost of transportation by rail is to reduce energy costs for running trains. The least expensive way to achieve this goal is to introduce training systems for training in energy-optimal and safe train control modes. There are many methods designed to calculate such modes. This paper discusses algorithms for determining restrictions on train control to construct an energy-optimal train trajectory [4-6].

Material and Method

The method of energy-optimal traction calculation, taking into account the track plan and profile, train length, characteristics of cars, traction and braking characteristics of the locomotive, and speed limits is presented in the work [7]. This technique allows for performing calculations quickly and without significant loss of accuracy, and the results of the calculations meet the criteria of optimality, safety, and compliance with the train schedule.

To implement this method, a grid is constructed in *Speed-Way* coordinates. The possibility of transition between nodes of adjacent grid sections (Figure 1) should be determined at the first stage of solving the problem of obtaining an energy-optimal train trajectory [7].

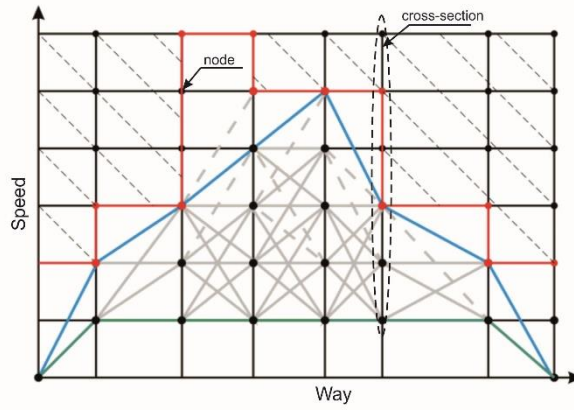


Figure 1. Possible options for the train's movement trajectory

Practically speaking, it is necessary to obtain one train trajectory that ensures minimal energy consumption for a given travel time. In the process of constructing the optimal train trajectory, it is essential to determine the possibility of transition between grid nodes of adjacent sections. Until now, this has been done by integrating the train motion equation using one of the numerical integration methods. To speed up this process, it is proposed to determine the work that a locomotive must perform in order for a train to overcome the distance between adjacent sections of the grid and change its speed from the speed at the initial node to the speed at the final transition node.

$$A_L = \Delta E_k + \Delta E_p + A_{wo} . \quad (1)$$

Here: ΔE_k – change of the kinetic energy of the train; ΔE_p – change of the potential energy of the train; A_{wo} – the work of the forces of the main resistance to the movement of the train. The first two can be accurately calculated:

$$\Delta E_k = M_t \frac{v_f^2 - v_i^2}{2} , \quad (2)$$

$$\Delta E_p = M_t \cdot g \cdot \Delta h . \quad (3)$$

Here: M_t – the mass of the train; v_f, v_i – speed in the initial and final nodes of the grid; Δh – the difference in the heights of the center of the train's mass as it moves between the sections of the grid.

To accurately determine the work of the main resistance forces on train movement, it is necessary to know the speed of the train as a function of the distance travelled between the nodes of adjacent grid sections.

$$A_{wo} = M_t \int_0^S w_o (v(x)) dx . \quad (4)$$

Here: S – distance between adjacent sections of the grid; w_o – the main specific train resistance force.

Results

The possibility of transition between grid nodes of adjacent sections means its feasibility. Each locomotive has limited train control resources, so control feasibility means the use of control that does not exceed the resources of the locomotive. First, let's look at the restrictions on train control. By controlling the movement of the train, the driver's use of traction mode and braking mode, that is, an artificial and purposeful change in the phase state of the train, is meant. The running idle mode (coasting) also changes the phase state of the train but is neither artificial nor purposeful because, in this case, a change in phase state occurs without the intervention of the driver due to natural causes. So, only two modes of train movement control are possible – traction mode and braking mode (Figure 2, a).

The main braking mode is the train's pneumatic braking mode, although some locomotives have an electric brake (rheostatic or regenerative). Thus, it is possible to construct train control restriction zones in *Force-Speed* coordinates. The traction force limitation zone shown in Figure 2 (a) is typical for AC electric locomotives and diesel locomotives. For DC locomotives, the traction force limitation zone is divided into parts in accordance with the connection schemes of the traction motors (Figure 2, b).

Admissible control in the traction mode can be limited from above, for example, by constraints on coupling and weakening of the field (Figure 3).

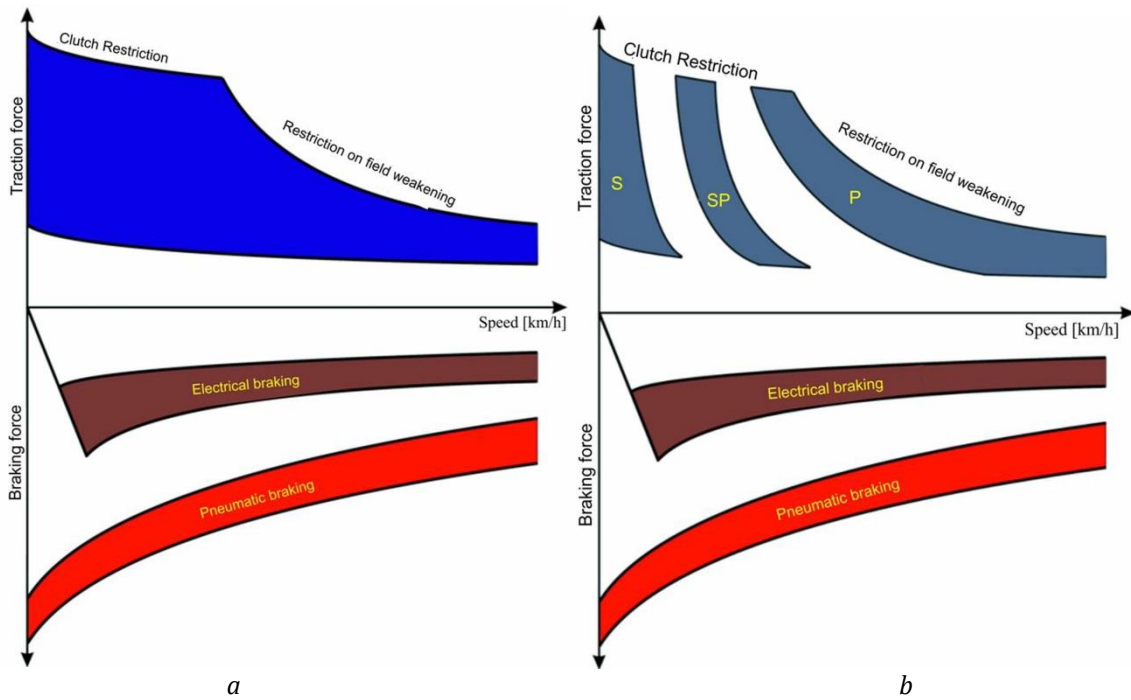


Figure 2. Train control restriction zones: a –for AC electric locomotives and diesel locomotives; b –for DC locomotives S – series, SP – series-parallel and P – parallel engines connection

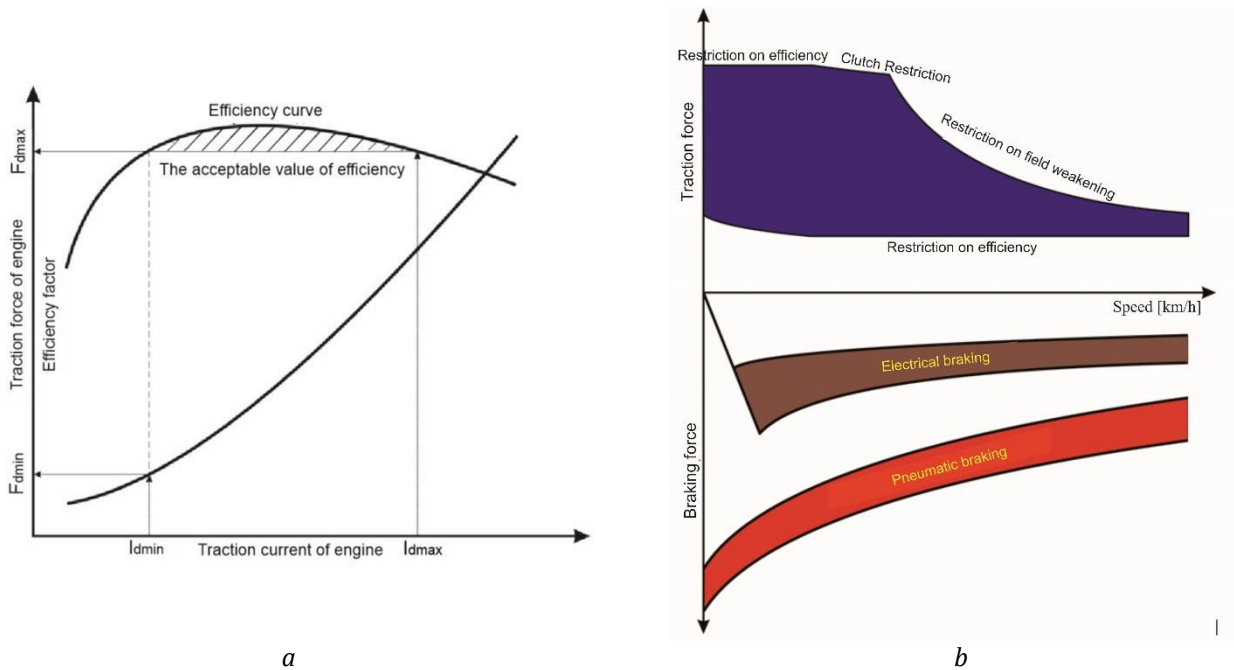


Figure 3. Acceptable train control: a – qualitative scheme of electromechanical characteristics of the locomotive engine; b – control limitation zone in traction mode

It is possible to construct a curve limiting the traction force from below based on the minimum traction current at which the efficiency has not too small value. And it is possible, using electromechanical characteristics of the locomotive engine (Figure 3, a), to allocate some acceptable level of engine efficiency and on the curve of the dependence of the efficiency on the engine traction current to determine the range of traction current ($I_{dmin} \div I_{dmax}$), and to determine, according to the dependence of the engine traction force from current, the range of the engine traction force ($F_{dmin} \div F_{dmax}$) and, then, the range of the traction force for the entire locomotive. Then, the control limit zone in the traction mode will look as shown in Figure 3 (b). In this case, the traction zone is narrowing.

It should be noted that while the control of the locomotive traction in the zone with big values of the engine efficiency reduces the losses of energy, it does not guarantee a reduction of power consumption for the traction of the train throughout the track section, because in this case, it will be necessary to use for the acceleration of the train either longer or more frequent traction modes.

When driving trains equipped with pneumatic braking means to the required extent, to regulate the speed of the train, almost always (except for stopping braking and steep descents), a braking stage is used with the discharge of the brake line in the summer for loaded trains at 0.6-0.7 ATM, and for empty trains at 0.5- 0.6 ATM. Using these ranges of brake system discharge, it is possible to calculate the curves that limit the zone of possible braking forces. In Figures 3 (b) and 4, this area is shown in red. Similar brake force zones can be constructed for other ranges of discharge of the brake system.

Electric braking is mainly used to stabilize or limit the growth of the train's speed on long descents. The use of pneumatic braking in such situations, especially for loaded freight trains, leads to a significant reduction in speed due to the fact that the processes occurring in the braking system of the train are rather slow. Consequently, the use of pneumatic braking to stabilize the speed of the train leads to a useless and excessive loss of its kinetic energy. The use of electric braking of the locomotive (especially regenerative) allows to achieve a smooth reduction or stabilization of the speed and can reduce power consumption. Therefore, it should be used in those cases where there is no need to significantly reduce the speed of the train. The zone of possible braking forces in Figures 3 (b) and 4 is shown in brown.

Next to consider is the choice of the train control mode during navigation between nodes of adjacent grid sections. Earlier, it was shown how to obtain the value A_L of the locomotive work or the brake system of the train for the transition between the grid nodes. Obviously, this work is connected with the traction and braking forces:

$$A_L = \begin{cases} \int_0^S F_t(x) dx, & \text{traction} \\ \int_0^S F_b(x) dx, & \text{braking.} \end{cases} \quad (5)$$

From this equation, it is possible to determine the traction or braking force as a function of the track:

$$F(x) = \frac{dA_L}{dx}, \quad (6)$$

or the average value of the force on the path segment $0 \div S$:

$$F_{av} = \frac{A_L}{S}. \quad (7)$$

Regarding the running mode, here, expression (1) should take the following form:

$$\Delta E_k + \Delta E_p + A_{wo} = 0. \quad (8)$$

So, the sum of the changes of the kinetic and potential energies should be compensated by the work of the forces of the main resistance on the movement of the train. Nevertheless, this condition practically always cannot be fulfilled. Therefore, in order to implement the idle running mode, it is necessary to introduce a certain threshold on force $\pm F_o$. And, if the force obtained from the expression (3) does not exceed the threshold, the idle running mode can be used. In this case, the deviation of the final speed from the speed in the final grid node should not exceed $\pm \delta v$.

When performing a transition between nodes of adjacent grid sections with equal speed, the v_i and v_f ratio between speeds is equal to:

$$v_f^2 = v_i^2 + 2aS. \quad (8)$$

If the transition is possible in the idle running mode, the acceleration is equal to:

$$a = \frac{W_i + W_o}{M_t}. \quad (9)$$

Where: W_i – resistance force to train movement from the slope of the track or downhill, W_o – the actual resistance force. Taking this into consideration:

$$v_f^2 = v_i^2 + 2S \frac{W_i + W_o}{M_t} \quad (10)$$

Now, if, supposedly, in addition to the two mentioned forces, another force acts on the train F_o , then the final speed should change:

$$v_f^{*2} = v_i^2 + 2S \frac{W_i + W_o + F_o}{M_t}, \quad v_f^* = v_f + \delta v, \quad (11)$$

After some transformations, the following result is obtained:

$$F_o = \frac{\delta v \cdot (2v_f + \delta v)}{2S} M_t \quad (12)$$

The deviation of the final speed from the speed at the endpoint can be either increasing or decreasing. Hence, the force F_o can be both positive and negative:

$$F_o^+ = \frac{\delta v \cdot (2v_f + \delta v)}{2S} M_t, \quad (13)$$

$$F_o^- = \frac{-\delta v \cdot (2v_f - \delta v)}{2S} M_t. \quad (14)$$

Thus, if, as a result of the transition between the two nodes, an average force is obtained $F_{av} \leq |F_o|$, then the deviation of the final speed (v_f^*) of the speed in the final grid node (v_f) does not exceed the value δv , i.e.:

$$|v_f^* - v_f| \leq \delta v. \quad (15)$$

Now, the control restriction zones look like this (Figure 4, a).

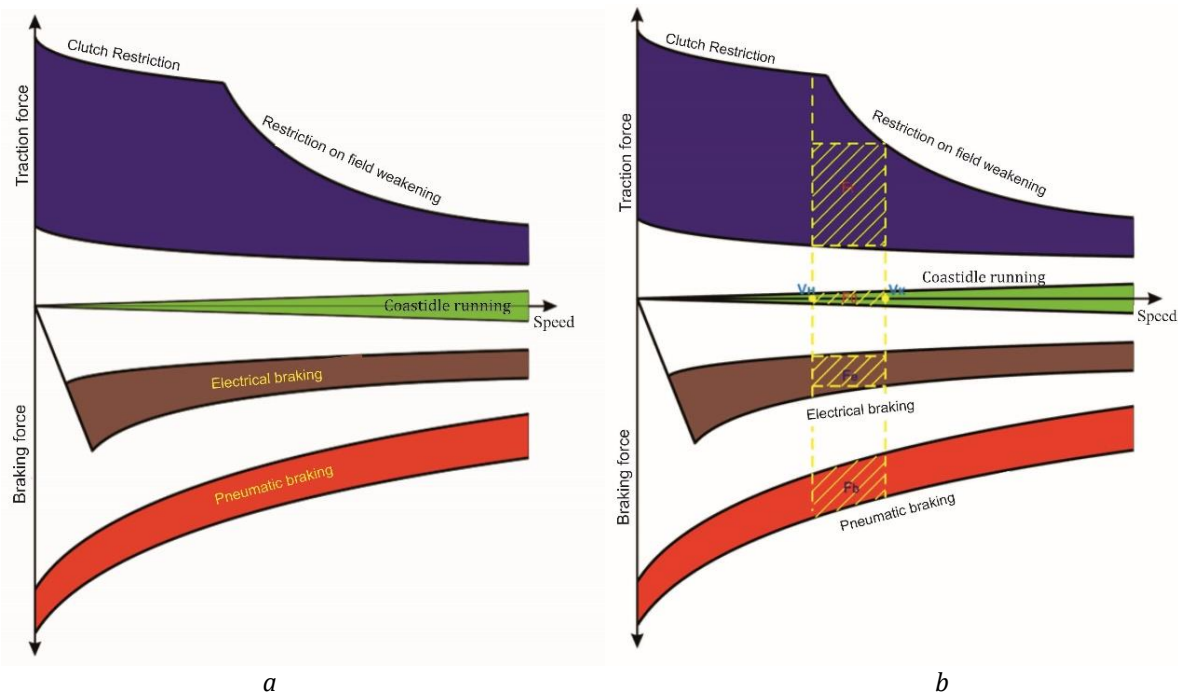


Figure 4. Train control constrains zones: a – with coasting mode; b – the entry of an average force into one of the zones of admissible controls

Having determined the average force F_{av} along a segment of the path, it is possible to check in which zone (traction, run-out, or braking), with a known change in speed ($v_i \div v_f$), it falls into (Figure 4, a) and, thus, determine the feasibility of the transition between grid nodes and the train control mode during this transition. If the average force does not fall into any of the allowable control zones, such a transition is considered impossible.

If the value of F_{av} falls within the zone of pneumatic braking, then, in this case, the control is reduced to the application of the braking stage, for which the range of pneumatic braking forces is calculated. If the value of F_{av} falls into the zone of electrically controlled braking, then it is necessary to additionally check the possibility of its implementation throughout the entire speed range ($v_i \div v_f$). If the speed falls into the run-out zone, then the idle mode of the locomotive should be applied. If the F_{av} value falls within the traction zone, the possibility of realizing the traction force in the speed range should also be checked ($v_i \div v_f$). In Figure 4 (b), zones of implemented control are crosshatched. The issue of time spent on transition between nodes of adjacent grid sections is discussed in detail in the study [7].

Conclusion

The proposed algorithm for determining restrictions on train control consists of the use of simplified methods for calculating the state of the train as a controlled system without using differential equations of motion, which makes it possible to significantly reduce the time needed for calculations. This, in turn, will make it possible to solve problems of finding optimal control almost in real-time, taking into account changing conditions while the train is moving. The practical significance of the results obtained lies in the use of a calculation method that does not require significant time to complete and can be used as a subsystem of the onboard train control system, capable of performing calculations taking into account changes in the current train situation. The results formed the basis of the software and hardware complex “Train Driver Simulator”.

References

1. Strößenreuther, H., & Halbach, J. (2005). Projekt Energie Sparen im Personenverkehr – Energiekostenmanagement für die Traktionsenergie der Deutschen Bahn, ZEVrail Glasers Annalen, 129, 356-362.
2. Akulov, A. S., Zheliezov, K. I., Zabolotnyi, O. M., Chabaniuk, E. V., & Shvets, A. O. (2022). Simulator for training mining locomotive drivers. Rudarsko-geološko-naftni zbornik (The Mining-Geology-Petroleum Engineering Bulletin), 37 (4), 27-35. <https://doi.org/10.17794/rgn.2022.4.3>
3. Nikitenko, A. & Shvets, A. (2020). Software and hardware simulators for train drivers training: overview of possibilities and effects of application. Przegląd Elektrotechniczny, 96, 11, 198-201. <https://doi.org/10.15199/48.2020.11.42P>
4. Akulov, A. S., Zheliezov, K. I., Zabolotnyi, O. M., Ursulyak, L. V., Chabaniuk, Ye. V., Chernyaev, D. V., & Shvets, A. O. (2017). Modular train simulator. Locomotive-inform, 7-8, 42-49.
5. Akulov, A., Zheliezov, K., Zabolotnyi, O., Chabaniuk, E., & Shvets, A. (2023) Training simulators for crane operators and drivers. *Engineering Today*, 2(1), 1-7. <https://doi.org/10.5937/engtoday2300003A>
6. Akulov, A., Zheliezov, K., Zabolotnyi, O., Nikitenko, A., Chabaniuk, E., & Shvets, A. (2014). Train driver trainer-simulator. Dnipro national university of railway transport named after academician V. Lazaryan. Dnipro, Ukraine, 11 p.
7. Zheliezov, K., Akulov, A., Zabolotnyi, O., Ursulyak, L., Chabanuk, Ye., Shvets, A., Kuznetsov, V., & Radkevych, A. (2019). The revised method for calculating of the optimal train control mode. Archives of Transport, 51, 3, 21-34. <https://doi.org/10.5604/01.3001.0013.6160>



Correlation of core strategic business factors in development of Albanian wood industry

Alketa Grepcka ^{*1}, Leonidha Peri ², Fatmir Basholli ³

¹Agricultural University of Tirana, Forestry Science Faculty, Department of Wood Industry, Tirana, Albania, agrepcka@ubt.edu.al

²Agricultural University of Tirana, Forestry Science Faculty, Department of Forestry Science, Tirana, Albania, leonidha.peri@ubt.edu.al

³Albanian University, Department of Engineering, Tirana, Albania, fatmir.basholli@albanianuniversity.edu.al

Cite this study: Grepcka, A., Peri, L., & Basholli, F. (2023). Correlation of core strategic business factors in development of Albanian wood industry. *Advanced Engineering Days*, 8, 109-111

Keywords

Strategic management
Wood industry
Correlation technology
Innovation
Challenges

Abstract

In Albania, a number of studies have been done for many different business categories, but there is little or no evidence for strategic management in the wood industry. Over the years, the wood industry in Albania has undergone drastic changes. Company owners say that their business is constantly changing the shape and it is important for them to change the operational model in order to: 1) improve efficiency; 2) reduce complexity; 3) reduce costs; The research was conducted in the district of Tirana and Durres. The data was collected in the wood processing companies and 30 questionnaires were processed in this regard followed by statistical analysis. The study has showed: 1) In terms of the product, companies have considered as a strong factor the development of a new product; 2) Operational management is still in its infancy, but its importance is well appreciated; 3) Most critical areas in operations management are being practiced, except for inventory and innovation. Based on the theoretical framework and the collected data, we find that although the companies aim to be leaders in the market, they are followers of the customer and innovation as a competitive advantage is missing in this field; 4) In terms of technology, 70% of companies accept the purchase of new machines as a very strong factor. 5) The development of new ideas related to the product is also accompanied by obstacles where the financial sector and developments in the region are listed in this direction; 6) The improvement of customer service and quick response in product distribution are strongly correlated; 7) Companies did not achieve the level of synchronization that would be required in an ideal supply chain management; 8) Companies should work on gathering feedback from suppliers and customers and find ways to improve their systems.

Introduction

Wood processing industries include a wide range of activities related to the processing and production of wood products. Nowadays, the wood processing industry faces several important challenges in the modern era where in our field of study it is worth mentioning: 1. Fluctuating wood prices; 2. Competition from alternative materials; 3. Lack of qualified workforce; 4. Market demand fluctuations; 5. Technology integration; 5. Supply chain disruptions; 6. Innovation and Design Trends. The wood processing industry in Albania has taken a solid progress. This industry itself contains a history of change. Until the 1990s, the forms of management were controlled and directed by a centralized state system that determined the form of technology (in large schemes), the quantity of the products on the basis of a concentrated market demand. With the breakdown of the centralized system and the opening of private enterprises, the wood processing industry underwent its changes. Therefore, from large enterprise systems concentrated in few cities of Albania, this industry began its development with a wide geographical extent but fragile and grouped in the small business category. The overpassing of transition period in Albania, the strengthening of the economy, opening of new markets in Albania and abroad and the increase in market demand have also brought a development of the industry toward expansion of the product range, the involvement of modern technology and automated lines of production and increase of specialized workforce for specific technological processes.

Over the years, the wood industry in Albania has undergone drastic changes. Company owners say that their business is constantly changing the shape. As stated above, it is important for companies engaged in this industry to have a well-defined operational management strategy. Ensuring competitive advantages by adding value from operational processes through the transformation of raw wood into final products is very important for companies in the wood processing industry. In Albania, a number of studies have been undertaken for various business categories with regard to the operational management strategy, but there is very little or no evidence for the wood industry. In this way, this study seeks to contribute by presenting the existing practices in the field of operational management and to present the need for their adoption in this direction.

Material and Methods

This is a study designed to identify the strategies that companies in the Albanian wood industry applies to operations management practices. The research was based on the development of questionnaires. The questionnaires were compiled to contain 6 sections as follows: General information, Product, processes and product variety, Strategies, Design and innovation, Operational management practices, Additional information

The questionnaires contained open and closed questions. A Likert scale five-point were used to identify the importance of product, technology and customer in development strategy of the companies. In this study, the target population was the wood processing and trading companies in Albania, registered by the National Business Center (NBC). The research was conducted in Tirana and Durres area. The questionnaires were distributed to several companies but 30 of them responded. The data were analyzed using SPSS and hypothesis testing and statistical test were carried out [1-3].

Results and Discussions

In order to maintain a competitive position in the market, every company must have its own long-term strategy.

Core competencies

As core competencies for the companies are considered products, technology and quality of their products. The companies are aiming to invest in products and machineries in order to maintain competitive advantages in market. The main direction (80%) is the production technology, followed to (70%) product development. These are considered as strong factors that also determine the development directions of the companies. A factor of 25%, is considered the market, determining that even environmental changes have an impact on the company's strategy. In practice, the idea of product improvement is the norm since operations managers are constantly looking for new ideas. A small change in products can be enough to create a substantial difference in demand. As a result, companies feel the need to make frequent adjustments to their products. Besides the market, another pressure to change the type of products comes from internal demands. Many operational activities can adapt their existing product to reduce the cost of production or can design a new product. 100% of the companies admitted that they have a special sector for design of project and admitted that during the last 10 years they have developed new ideas regarding technological products and processes the companies taken in the study [4-5].

Analyze of findings (SPSS)

From the data we are facing a low- variance. Most of answers varies between agree – strongly agree factor in Likert scale. Therefore; in our analysis we consider to use Pearson and Spearman test and to compare the results. We are aware that both of them measure the strength & direction of the relationship between variables.

Table 1. Correlation between product (P), technology (T) and client (CL)

Hypothesis	IV (X)	DV (Y)	Parametric	Non- parametric
There is a correlation between product (P), technology (T) and client (CL)	P, T and CL	P, T and CL	Pearson Correlation	Spearman correlation

Correlation is a measure of relationship between two variables. Correlation analysis is used to describe the strength and direction of the linear relationship between two variables. There are a number of different statistics available from SPSS, depending on the level of measurement and the nature of the data. Pearson product-moment correlation coefficient (r), Spearman correlation (ρ) procedures [6-8].

Table 2. Correlation between product, technology and client in development of new ideas and enhancement of the strategy of the company.

Correlations (Pearson)		1	2	3	4	5	6	7	8	9	10	11	12	13	14	15	16	17	18	
1 Product 1	4.53	0.68	1																	
2 Product 2	4.23	0.90	-0.323	1																
3 Product 3	3.93	0.87	-0.171	-0.201	1															
4 Product 4	4.40	0.67	0.345	0.325	0.047	1														
5 Product 5	4.37	0.56	-0.534	0.444	-0.09	-0.221	1													
6 Product 6	3.33	0.76	-0.156	0.439	0.035	0.27	0.027	1												
7 Product 7	3.97	0.76	-0.229	0.363	-0.107	-0.04	0.192	0.139	1											
8 Product 8	4.07	0.98	0.048	0.609	-0.197	0.271	0.143	0.247	0.141	1										
9 Production technology 1	4.57	0.73	0.065	0.16	0.007	0.225	-0.275	0.396	-0.027	0.235	1									
10 Production technology 2	4.53	0.51	-0.053	0.096	0.24	-0.04	-0.016	0.239	-0.041	0.134	-0.193	1								
11 Production technology 3	3.63	0.89	-0.006	0.111	-0.256	0.023	0.211	-0.017	0.052	0.464	-0.254	0.219	1							
12 Production technology 4	4.10	0.99	0.071	-0.259	0.247	-0.113	-0.131	0.183	-0.267	-0.007	0.062	0.369	0.199	1						
13 Production technology 5	4.27	0.64	-0.138	0.609	0.095	-0.016	0.2	0.379	0.371	0.191	0.183	-0.028	-0.186	-0.314	1					
14 Client 1	6.28	9.40	0.153	-0.058	-0.208	-0.13	0.215	-0.332	0.265	0.007	-0.389	-0.18	0.303	-0.213	-0.089	1				
15 Client 2	4.30	0.70	0.086	-0.17	0.973	-0.189	-0.291	0	0.276	-0.281	-0.074	0.213	-0.204	0.153	-0.107	-0.082	1			
16 Client 3	4.30	0.70	-0.058	0.159	0.034	0.029	-0.026	0	0.083	0.07	-0.074	0.019	0.017	0.054	0.353	0.168	-0.189	1		
17 Client 4	4.07	0.78	0.447	-0.17	-0.145	0.208	-0.137	0.077	0.061	-0.096	0.052	-0.006	-0.112	0.212	-0.174	-0.265	0.275	-0.038	1	
18 Client 5	4.30	0.84	0.073	-0.051	-0.304	-0.037	-0.096	-0.109	-0.145	0.143	-0.176	0.179	0.523	-0.203	-0.219	0.193	-0.041	-0.158	-0.032	1
19 Client 6	4.27	0.74	-0.087	0.059	0.243	-0.083	0.006	-0.102	-0.045	0.07	-0.098	0.067	0.206	0.384	0.209	0.166	-0.027	0.372	-0.091	0.033

From the matrix we notice:

1. Spearman and Pearson coefficient are quite similar with slightly differences.
2. The negative correlation are markedly low and negligible. The (r) coefficient varies between the sizes -0.10 to -0.30.
3. The low variance of variables indicates no strong relationship b/w variables. Most of the responders ranked the variables b/w 3 to 5 in Likert scale and thus provides a low variance of them. Some of the links between variables certify the sub-hypothesis.

Conclusion

The companies included in the study have a clear formulation of their mission and vision, which in itself is an important component in terms of fulfilling the company's objectives. Product technology and clients are stated in their mission. The hypothesis proved that product and technology are two important components ensuring the competitive advantages of the companies. Although the mission is clearly stated by them, the content does not distinguish their differences. Most of them are paying a lot of efforts in product, technology and customers at the same time. Fulfilling the need of market and customers made them follower and not leader. It should be considered as positive that currently the leadership of companies are moving toward compiled strategy but still need to be done in order to enforce their competitive advantages. Focusing and investing in few core competencies rather than working in all of them will ensure more their place in market [9-11].

References

1. Hunger, J. D., & Wheelen, T. L. (2013). Essentials of strategic management. Pearson.
2. Steiner, G. A. (2010). Strategic planning. Simon and Schuster.
3. Caune, J., & Dzedons, A. (2009). Strategiska vadisana. Otrais izdevums (Strategic Management. Second Edition). Riga: Lidojosa zivs, 384.
4. Hill, C. W., Schilling, M. A., & Jones, G. R. (2017). Strategic management: An integrated approach: Theory & cases. Cengage Learning.
5. Whelan, J., & Sisson, J. D. (1993). How to realize the promise of strategic planning. Journal of Business Strategy, 14(1), 31-36. <https://doi.org/10.1108/eb039535>
6. Geipele, I., & Fedotova, K. (2007). Strategic management decisions: distribution of goods in the market, marketing logistics, merchandising. RTU Publishing House
7. Hitt, M., Ireland, R. D., & Hoskisson, R. (2014). Strategic management: Concepts: Competitiveness and globalization. Nelson Education.
8. Gerry, J., & Scholes, K. (1989). Exploring corporate strategy: text and cases. Prentice Hall.
9. Davies, M., Devlin, M., & Tight, M. (Eds.). (2010). Interdisciplinary higher education: Perspectives and practicalities. Emerald Group Publishing Limited.
10. Ioan, C. C., & Carcea, M. I. (2010). The environmental dimension-An interdisciplinary research area. Environmental Engineering & Management Journal (EEMJ), 9(5), 735-741
11. Fedotova, K., & Geipele, S. (2013). Wood materials applied in civil engineering and wood industry management in Latvia: Case study. Advanced Materials Research, 804, 106-113. <https://doi.org/10.4028/www.scientific.net/AMR.804.106>



Circular economy toward a sustainable concept in the wood processing sector in Albania

Ina Vejsiu ^{*1}, Erald Kola ¹

¹ Agricultural University of Tirana, Department of wood industry, Tirana, Albania, inavejsiu@ubt.edu.al, Erald.kola@ubt.edu.al

Cite this study: Vejsiu, I., & Kola, E. (2023). Circular economy toward a sustainable concept in the wood processing sector in Albania. *Advanced Engineering Days*, 8, 112-113

Keywords

Circular economy
Wood
Sustainable
Skills
Competences

Abstract

Economic circulation is a concept that is closely aligning with sustainability. For this reason, various stakeholders strive to collaborate in defining basic concepts, analyzing key issues, and directing solutions to these problems. In this study, we have attempted to address the challenges of the wood processing sector in Albania concerning the increase in the use of wooden products and the potential export of these products. During the last years, the concept of the circular economy has taken an important role in the literature, as well as in the production sector all over the world. Saying this, in Albania we are facing the same problem. The concept of the circular economy in our country was introduced lately. The companies that operate in the wood processing sector must step forward from a linear economy to a circular one as soon as possible. This material presents some information collected based on interviews conducted with some of the wood processing companies in Albania. For this study we prepared a closed answer questionnaire in order to have a simple analysis of the results gathered. As a result of this interview, skills and competencies supporting the transformation to circular business models were presented. The companies need some innovative design idea for the reuse of their basic products.

Introduction

The concept of CE is a new concept but if we speak about applying CE and sustainability in the wood industry it is even newer. A circular economy (CE) is a model of production and consumption, which involves sharing, leasing, reusing, repairing, refurbishing and recycling existing materials and products for as long as possible (Iacovidu et al, 2021). The concept of the circular economy in Albania, was previously used in the draft of the National Integrated Waste Management Strategy (2018-2023). The main goal of the document is to introduce this concept to the interested parties with the transition needs and requirements to move from a linear economy toward a circular one [1].

Material and Methods

This research began with the need to identify strategies related to CE that could stimulate wood processing in companies. First of all, we decided to select some of the biggest companies that operates in the wood industry all over the country. Some of them are already part of the WICA (Wood Industry Cluster of Albania). It is worth mentioning the fact that we have a very good institutional relationship with WICA, which is also expressed in various collaborations and different projects with our Slovenian partners too. Saying that, for us it has been quite easy to identify major actors of the market and the also to gather the full information we need for this study [2].

After the identification and setting up meeting schedule, we had a face-to-face interview with each one of them to adapt and to identify all their efforts to go from a linear economic production into the circular economy.

The study aims to increase the recognition of opportunities in the wood processing industry as a phenomenon and watching these opportunities under the circular economy optics. The interviews were semi-structured with categorized thematic topics, which were entrepreneurship, business opportunity, CE and business idea. The topics and questions were structured and formulated all by the authors [3-5].

Results and Discussions

After the analysis of all the interviewed entrepreneurs the result obtained was that the market for production of recycled wood production was not ready and unsatisfied. These companies are not focused on this process but they are willing to go further this process if they have some inputs from the government or even the help of the WICA (which is a new entity by still is operational in supporting the wood industry sector) [6-8].

Conclusion

Looking at the development of the activity of the wood industry also in terms of climate change, we must say that we still have a lot of work to do.

Some measures, such as extending the life of products, reusing them, recycling them and using them for energy production are known in the industry practice. Other activities like waste management, needs further promotion and creating some facilities for the companies.

Most important, a systemic change of mindsets and an integrated management of all process (which is not so easy to achieve) and activities by which companies add value to their construction materials and services along value chains are needed. This implies a new perspective on processes of furniture production redefining relations among different value chains' actors, from concept through completion to demolition and recovery of materials.

They need some qualified and specialized people in their structure with ideas on reusing the wood material and for sure a big step in innovation of the machineries. Nowadays we are hearing for some successful implementations of Industry 4.0 examples in our country. Industry 4.0 can be defined as the integration of intelligent digital technologies into manufacturing and industrial processes. It encompasses a set of technologies that include industrial IoT networks, AI, Big Data, robotics, and automation. It should be emphasized that the transition to a circular economy also requires continuous staff training, which still presents some challenges for our companies [9].

References

1. Vejsiu, I. & Kola, E. (2023). Heading towards the Circular Economy in the Wood Processing sector in Albania – Perceptions of the wood processing industry actors. ICOALS IV.
2. Brydges, T. (2021). Closing the loop on take, make, waste: Investigating circular economy practices in the Swedish fashion industry. *Journal of Cleaner Production*, 293, 126245. <https://doi.org/10.1016/j.jclepro.2021.126245>
3. European Environment bureau, (2017). Circular economy opportunities in the furniture sector
4. Rebus, (2017). REBUS Furniture Sector report.
5. EFIC, (2017). The Furniture Industry and The Circular Economy - Policy paper.
6. The National Integrated Waste Management Strategy (2018-2023).
7. Kromoser, B., Reichenbach, S., Hellmayr, R., Myna, R., & Wimmer, R. (2022). Circular economy in wood construction–Additive manufacturing of fully recyclable walls made from renewables: Proof of concept and preliminary data. *Construction and Building Materials*, 344, 128219.
8. Rüter, S., & Diederichs, S. (2012). Ökobilanz-Basisdaten für Bauprodukte aus Holz (p. 303). Braunschweig, Germany: Johann Heinrich von Thünen-Institut (vTI), Bundesforschungsinstitut für Ländliche Räume, Wald und Fischerei.
9. TripleWood, 2021. https://www.triplewood.eu/de/bauen-mit-holz/kreislaufwirtschaft_de (zugriffen 15. September 2021).



Algebra and its applications in technical and engineering problems

Davron Aslonqulovich Juraev^{*1,2}, Murot Nashvandovich Bozorov¹

¹University of Economics and Pedagogy, Department of Scientific Research, Innovation and Training of Scientific and Pedagogical Staff, Uzbekistan, juraevdavron12@gmail.com

²Anand International College of Engineering, Department of Mathematics, Jaipur, India, davronzhuraev12@gmail.com

Cite this study: Juraev, D. A., Bozorov, M. N. (2023). Algebra and its applications in technical and engineering problems. *Advanced Engineering Days*, 8, 114-116

Keywords

Algebra
Algorithm
Al-Khwarizmi's work
The treatise
Principle of algebra

Abstract

This work deals with the emergence of Algebra and its applications in technical and engineering problems. History of algebra goes back to antiquity. Obviously, her appearance was caused directly connected with the first astronomical and other calculations, anyway using natural numbers and arithmetic operations. The history of algebra confirmed such original recordings, found among samples of writing of the earliest civilizations. Algebra is one of the most important disciplines in mathematics, which at first glance may seem complex and distant from everyday life. However, in fact, algebra is an integral part of our reality and has wide practical applications in a variety of situations. Algebra allows you to solve various problems: from simple arithmetic operations to solving complex equations and systems of equations. It helps us deal with unknown quantities and establish relationships between different variables. Without algebra, we would not be able to effectively solve problems related to finance, science, engineering, and even everyday problems such as budgeting or calculating travel times.

Introduction

Algebra is a part of mathematics, which, along with arithmetic and geometry, is one of the oldest branches of this science. Problems, as well as methods of algebra, which distinguish it from other branches of mathematics, were created gradually, starting from antiquity. Problems of solving and studying equations had a great influence on the development of the original arithmetic concept of number. With the introduction of negative, irrational, complex numbers into science, the general study of the properties of these various number systems also moved to algebra. At the same time, it formed its characteristic letter notations, which made it possible to write down the properties of operations on numbers in a compressed form convenient for constructing calculus over letter expressions. The literal calculus of identity transformations constitutes the apparatus of classical algebra. Thus, algebra was distinguished from arithmetic: algebra studies, using letter notations, the general properties of numerical systems and general methods for solving problems using equations; arithmetic deals with methods of calculations with specifically given numbers, and in its higher areas - with the subtle individual properties of numbers. The development of algebra, its methods and symbolism had a very great influence on the development of newer areas of mathematics, preparing, in particular, the emergence of mathematical analysis. Writing down the simplest basic concepts of analysis, such as a variable, a function, is impossible without the letter symbols of classical algebra. In its development, algebra, like any other science, has gone through a long historical path, which can be divided into several periods.

In the history of mathematics, many scientists around the world worked on the development of mathematics. It cannot be said that before Al-Khorezmi there was no algebra, in ancient times people solved the simplest algebraic problems, there were techniques for solving individual specific problems, but Al-Khorezmi was the first to introduce algebra as the science of general methods for solving numerical linear and quadratic equations, and gave a classification of these equations, which was essential for "Preliteral" algebra. Historians of science highly appreciate both the scientific and popularization activities of Al-Khorezmi.

The famous historian of science J. Sarton called him "The greatest mathematician of his time and, all things considered, one of the greatest of all time." Al-Khorezmi (full name Abu Abdullah Muhammad ibn Musa Al-

Khorezmi) father of Abdullah, Muhammad, son of Musa, native of Khorezm, mathematician, astronomer, historian and geographer of the 9th century. Even the exact dates of his birth and death have not reached us. It is only known that he was born at the end of the eighth century, and died in the second half of the ninth, more precisely after 847. Now it is conventionally accepted to consider the year of his birth to be 783, and the year of death to be 850. The scientist's homeland was Khorezm, a vast region of Central Asia, which corresponds to the modern Khorezm region of Uzbekistan. Al Khorezmi's diverse scientific interests concerned mathematics, theoretical and practical astronomy, geography and history.

Not all of the works he wrote have survived. In 975-997 he wrote *Mafatih al-'Ulum* ("Key to the Sciences"), the first Arabic encyclopedia of knowledge that was organized on scientific principles. As a scientist, Al-Khwarizmi becomes famous for his achievements in mathematics. His work on arithmetic was translated into Latin in the 12th century, and although the original is lost, the Latin translation *Algoritmi de numero Indorum* ("Al-Khwarizmi on Indian numbers") still exists. Its name gave rise to the mathematical term "Arithmetic" [1]-[3].

Works of Al-Khwarizmi

It is considered established that Al-Khwarizmi was the author of 9 works:

1. Book about Indian arithmetic (or Book about Indian counting);
2. A short book on the calculus of algebra and almukabala;
3. Astronomical tables (zij);
4. Book of pictures of the Earth;
5. Book about building an astrolabe;
6. A book about actions using an astrolabe;
7. Book about sundial;
8. Treatise on the definition of the era of the Jews and their holidays;
9. History book.

Of these books, only seven have reached us in the form of texts either by Al-Khwarizmi himself or his Arab commentators, or in translations into Latin. Al-Khwarizmi's work on arithmetic played a vital role in the history of mathematics, and although its original Arabic text is lost, its contents are known from a 12th-century Latin translation, the only manuscript of which is kept in Cambridge. This work provides the first systematic presentation of arithmetic based on the decimal positional number system. The translation begins with the words "Dixit Algorizmi" (said Algorizmi).

In Latin transcription, the name Al-Khorezmi sounded like Algorizmi or Algorizmus, and since the essay on arithmetic was very popular in Europe, the author's name became a household name - medieval European mathematicians called arithmetic based on the decimal positional number system. Later, this was the name given to any system of calculations according to a certain rule; now this term means a prescription that specifies a calculation process, starting with arbitrary initial data and aimed at obtaining a result completely determined by these initial data [4].

The algebraic book of Al-Khorezmi (*Kitab mukhtasab al-jabr and wa-l-mukabala*) consists of two parts - theoretical (theory of solving linear and quadratic equations, some questions of geometry) and practical (application of algebraic methods in solving household, trade and legal tasks - division of inheritance, drawing up wills, division of property, various transactions, measuring land, building canals). The word al-jabr (replenishment) meant transferring the negative term from one side of the equation to another, and it was from this term that the modern word "algebra" arose. Al-muqabala (contrast) - reduction of equal terms in both sides of the equation. The doctrine of linear and quadratic equations, inherited from Eastern mathematicians, became the basis for the development of algebra in Europe. The geometric part of the treatise is devoted mainly to measuring the areas and volumes of geometric figures: triangle, square, rhombus, parallelogram called rhomboid, circle, segment of a circle, quadrangle with different sides and angles, parallelepiped, circular cylinder, prism and cone [5-7].

Algebra in technical and engineering problems

One important area where algebra is applied is in electrical and electronic engineering. Algebra allows you to analyze and synthesize electrical circuits, solve equations related to current and voltage, and also model and simulate the operation of various electronic devices. In mechanics, algebra is used to solve problems involving the motion of bodies. Using algebra, you can derive equations that describe the movement of a body, determine its speed, acceleration, and predict its movement in the future. Algebra is also applicable in the fields of construction and architecture. With its help, you can solve problems related to the calculation of building structures, determination of volumes and areas, analysis of forces and loads. Due to the development of computer technology and the use of software, algebra is becoming an integral part of the work of engineers and

technicians. With its help, you can create mathematical models and solve complex problems, conduct data analysis and present research results. The basic principle of algebra is working with symbols and expressions. Knowledge of algebra allows us to analyze and solve complex problems, especially in fields related to science, economics and finance. In the business world, algebra is used to calculate the cost of goods, production planning, and analytical forecasting. Knowledge of algebra will help entrepreneurs optimize their activities and make informed decisions. In engineering, algebra is also an integral part. It is used for complex system modeling, power and electrical circuit calculations, data analysis, and hypothesis testing. Without algebra, it would not be possible to create innovative technologies and develop new products.

Conclusion

Astronomy occupied a leading place among the exact sciences in the medieval East as one of the most necessary sciences in practice; it was impossible to do without it either in irrigated agriculture or in sea and land trade. By the 9th century include the first independent works on astronomy in Arabic, a special place among them was occupied by ziji collections of astronomical and trigonometric tables (at that time trigonometry was part of astronomy), with the help of these tables the positions of the luminaries on the celestial sphere, solar and lunar eclipses were calculated, they served and for measuring time. Among the first zijis is the zij of Al-Khorezmi, which began with a section on chronology and calendar - this was very important for practical astronomy, since different peoples used different calendars at different times, and dating is important when making observations. There were lunar, solar and lunisolar calendars, and the beginning of chronology in various systems referred to an arbitrarily chosen event. This led to many different eras; different peoples dated the same event differently, in accordance with the era they adopted. Al-Khwarizmi described the Arabic lunar calendar, the Julian calendar - the calendar of the "rums" (Romans and Byzantines). Humanity owes all the greatest discoveries that have given the world geniuses to mathematics. Today everyone needs mathematics. This is the call of the times, an urgent necessity of life. Accelerating scientific and technological progress is impossible without managing the volume of mathematical knowledge at all levels, starting primarily from high school, academic lyceums, colleges and higher educational institutions.

We are faced with financial decisions every day, whether it's budgeting, calculating mortgage payments, investing, or managing debt. Algebra allows us to solve complex problems efficiently and accurately. Interestingly, the history of the emergence of algebra is not limited to Europe and having contact with her Arab civilization. Thus, the significant results achieved in the Indian science of mathematics. In particular, they introduced the concept of "zero", which later came across the Arab world to Europe and has been used by scientists. The Chinese are quite independently, since the dawn of our era, have learned to solve the equations of the first degree. They were known to the irrational and negative numbers.

References

1. Sirazhetdinov, S. Kh. & Matvievskaia G. P. (1963). Al-Khorezmi is an outstanding mathematician and astronomer of the Middle Ages. M.: Education.
2. Yushkevich, A. P. (1961). History of mathematics in the Middle Ages. M.: Fizmatgiz.
3. Bulgakov, P. G. & Rosenfeld, B. A. & Akhmedov, A. A. (1983). Muhammad al-Khorezmi. M.: Nauka.
4. Matvievskaia, G. P. (1967). The doctrine of number in the medieval Near and Middle East. Tashkent: Fan.
5. Rosenfeld, B. A. & Sergeeva, N. D. (1977). About the astronomical tracts of Al-Khorezmi. Historical and astronomical research, 13, 201-218.
6. Yushkevich, A. P. (1954). Arithmetic treatise of Muhammad bin Musa Al-Khwarizmi. Proceedings of the Institute of History of Natural Science and Technology, 1, 85-127.
7. Juraev, D. A. & Jabborov, A. J. & Juraeva, S. A. (2012). The emergence of the word "Algebra" and its role in the history of the development of mathematics. 3rd International Scientific and Practical Conference. "Current Problems and Prospects for Teaching Mathematics", November 15-16, 2012. Kursk, Russian Federation, 253-257.



Quality of irrigation water in the region of In Salah, South Algeria

Abderrahmane Ballah *¹

¹University of Amin Eloukkal Elhadj Moussa Ag Akhamouk Tamanghasset, Faculty of Science and Technology, Algeria, abderrahmane.ballah@yahoo.com

Cite this study: Ballah, A. (2023). Quality of irrigation water in the region of In Salah, South Algeria. Advanced Engineering Days, 8, 117-120

Keywords

Groundwater
Irrigation
Quality
Intercalary continental
In Salah

Abstract

Water is a vital element for the survival of all living things on a planetary scale. It is also a priority factor for any socio-economic activity. The Algerian Sahara, which covers 2/3 of the country's surface area and extends over more than 2 million km², contains significant groundwater resources stored in two major aquifers: the Intercontinental Aquifer (CI) and the Terminal Complex (CT). The intercontinental aquifer covers most of the northern Sahara. The In Salah region is part of the western hydrogeologic sub-basin of the intercontinental aquifer and forms its southeastern boundary. Groundwater deserves special attention in the global debate on the sustainable use of natural resources. The problem of groundwater salinity, caused by various human and natural factors, causes serious irrigation problems. Groundwater is the only source of water for date palms in the In Salah region. The results from physico-chemical analysis show that the groundwater presents a poor quality with very high salinity. The continental intermediate aquifer represents the main source of irrigation, in which boreholes (FS40 and FS38) are located, but this will not be possible in the future, so it is necessary to think about integrated water management to conserve resources. In this study, the salinity and sodium content of two different boreholes in the In Salah area were calculated.

Introduction

Agricultural irrigation is becoming increasingly important due to increasing food insecurity and environmental changes [1]. However, polluted water use is a major problem on a global scale [2]. The Algerian Sahara has significant groundwater resources stored in two main aquifers, the Intercalary Continental (CI) and the Terminal Complex (CT). The Intercalary Continental aquifer covers most of the northern Sahara and the boundaries of its extension were used to define the area of the northern Sahara water resources study project.

The In Salah region is part of the western hydrogeologic sub-basin of the transcontinental aquifer and forms its southeastern boundary. The agricultural areas of In Salah are located at the northwestern end, near El Barka and northeast of In Salah. The former agricultural area is about 1,262 hectares and the APFA area is 8,104 hectares. The irrigated area is 834 hectares APFA (Access to land ownership). The number of palm groves is approximately 151,000. The former agricultural area is irrigated by 15 boreholes, while that of the APFA is irrigated by 26 boreholes [4]. Unfortunately, many regions of Algeria, especially those in the Sahara, face problems with the quantity and quality of water resources for drinking water supply and irrigation. According to FAO (1998), the water requirement of a crop represents the amount of water needed to cover water losses through direct evaporation from the soil and transpiration through the plant. This represents the evapotranspiration of a crop that realizes its production potential.

Groundwater deserves special attention in the global debate on the sustainable use of natural resources. The problem of groundwater salinity is caused by a number of human and natural factors and leads to serious irrigation problems. Groundwater is the only source of water for date palms in the In Salah region. In this study, salinity and sodium ratios of two different boreholes in In Salah were calculated.

Material and Method

Study area

The commune of In-Salah is one of the oldest communes in southern Algeria and is part of the prefecture of Tamanrasset. In Salah covers an area of 43,937.50 km² and has a land use percentage of 7.88% for the prefecture of Tamanrasset. The region is located in the south of the Algerian Sahara, north of Tamanrasset Prefecture. It is located 1300 km south of Algiers and 700 km from the capital of the Tamanrasset governorate, between the Tademaït plateau in the north and the edge of the Tidikelt in the south. The oasis is located at 27°11' north latitude and 2°28' east longitude. The In-Salah region consists of three geographical features: The Tidikelt plateau, the Tademaït plain and the Oued Djarret depression (Figure 1).



Figure 1. Location of study area

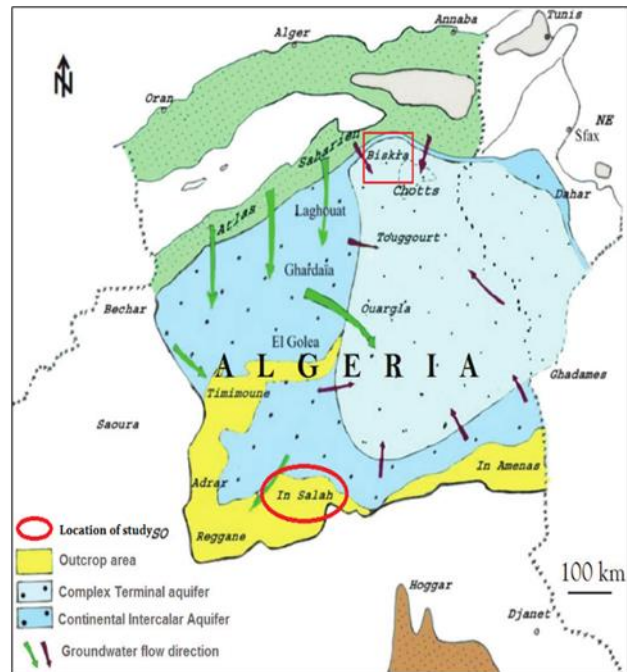


Figure 2: Map of groundwater resources (Intercontinental and Terminal Complex) [3]

Materials and methods

In order to prove and interpret the quality of water in the In Salah area, interest was shown in physico-chemical analysis of irrigation water. Sampling was carried out in two boreholes FS 38 and FS40 (Figure 3). Samples were taken by hand in plastic bottles. Analyses were carried out at ANRH in Adrar. The parameters analyzed were major cations, anions, and nitrates. The quality of the chemical analyses was checked using Diagramme software developed by the Hydrogeology Laboratory in Avignon (France).

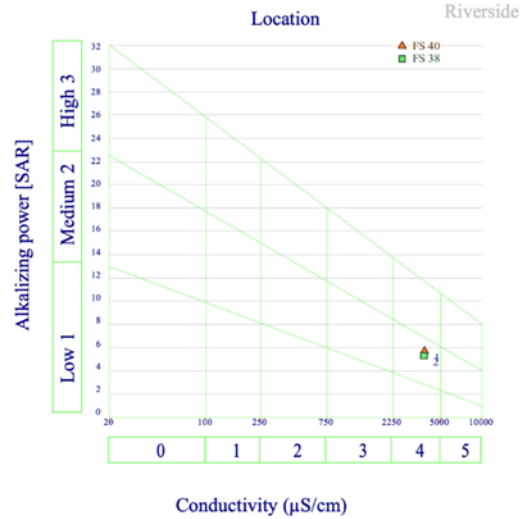
Salinity is usually measured by electrical conductivity. The values of the analyzed samples are higher than 3000 $\mu\text{S}/\text{cm}$, indicating a severe salinity of the groundwater (FAO standard). According to Madani (2008), a soil is said to be saline when its electrical conductivity is greater than 4 dS/m. However, the salinity of a soil is best assessed by the behavior of plants, so this limit can vary greatly depending on the sensitivity of plant species.

High levels of sodium in irrigation water cause the soil structure to deteriorate and become water and airtight, which has a direct impact on the health and productivity of crops through the infiltration of irrigation water into the soil. High levels of calcium and magnesium relative to sodium exacerbate this problem. This relationship is expressed by SAR (sodium absorption rate) [6] (Equation 1).

$$\text{Adjusted SAR} = \frac{\text{Na}^+}{\sqrt{\frac{\text{Ca}^{2+} + \text{Mg}^{2+}}{2}}} [1 + (8.4 - \text{pHc})] \quad (1)$$

Table 1. Geographical coordinates of boreholes

Geographic coordinates	Longitude	Latitude	Z (m)
FS 38	2° 26.913'E	27° 12.170'N	261
FS 40	2° 27.235'E	27° 12.703'N	262

**Figure 3.** Location of the two boreholes**Figure 4.** Riverside diagram

Concentrations are expressed in meq/l. The analyzed samples have SAR values ranging from 12 to 13 for FS 38 and FS 40 and are above the irrigation water quality limit.

Classification and characteristics of irrigation water

The graphical representation of the analyzed samples in the Riverside diagram [7] makes it possible to classify irrigation water (Figure 4) and therefore the various uses (crop types) (Table 2).

For the classification of irrigation water, we usually adopt the "Riverside diagram" of the US Department of Agriculture, which takes into account two main criteria: conductivity and SAR. Knowing the EC and SAR values of the water intended to irrigate our environment, we can assign a pair (C.S) that characterizes its quality. According to Servant [8], the different zones defined by the classification diagram of irrigation water are seven value levels (C1S1 - C1S2, C2S1 - C2S2, C1S3, C3S1 - C1S4, C2S3, C3S2, C4S1 - C2S4, C4S2, C3S3 - C3S4, C4S3 - C4S4).

Table 2. Classification and characteristics of irrigation water.

Pt water	SAR/ Conductivity	Ranking	Features
FS 38 FS 40	C4S2	Poor quality	Poor quality, to be used with great care only in light, well-drained soils, and for resistant plants, high risk of leaching and gypsum addition.

Conclusion

The physico-chemical study showed that the water analyzed for the two boreholes was very saline and had high mineralization. Irrigation of date palms shows that the water has a high risk of clogging, which characterizes its use for plants with good salt tolerance. Irrigation water in the In Salah area should be of great interest to those involved in the agricultural sector through a project for the drainage and reuse of wastewater, which should be used in agriculture with the knowledge that groundwater today is a non-renewable resource and needs to be conserved, which has recently been a consideration. The water required for the needs of plants must meet certain minimum quality standards. An excess of undesirable elements can be harmful:

- For crops, it results in lower yields and even the risk of poisoning consumers.
- Soil: risk of depletion, resulting in lower yields, but also risk of contamination of crops and groundwater.
- Groundwater, with risk of contamination for consumers.

References

1. Amuah, E. E. Y., Amanin-Ennin, P., & Antwi, K. (2022). Irrigation water quality in Ghana and associated implications on vegetables and public health. A systematic review. *Journal of Hydrology*, 604, 127211. <https://doi.org/10.1016/j.jhydrol.2021.127211>
2. Jongman, M., & Korsten, L. (2018). Irrigation water quality and microbial safety of leafy greens in different vegetable production systems: A review. *Food Reviews International*, 34(4), 308-328. <https://doi.org/10.1080/87559129.2017.1289385>
3. Kessasra, F., Mezerreg, N. E. H., Dehibi, D. E., Djaret, L., Bouhchicha, A., & Mesbah, M. (2023). Hydrogeological characterization of the Complex Terminal aquifer using geoelectrical investigation in the arid environment of Chetma-Biskra (South-East of Algeria). *Acque Sotteranee-Italian Journal of Groundwater*, 12(1), 39-51. <https://doi.org/10.7343/as-2023-608>
4. Remini, B., & Achour, B. (2013). The foggaras of In Salah (Algeria): The forgotten heritage. *Larhyss Journal*, 85-95.
5. Kantawanichkul, S., & Duangjaisak, W. (2011). Domestic wastewater treatment by a constructed wetland system planted with rice. *Water Science and Technology*, 64(12), 2376-2380. <https://doi.org/10.2166/wst.2011.806>
6. Bemoussat, A., Adjim, M., & Bensaoula, F. (2014). Etude des eaux souterraines de la plaine d'Henaya (bassin de la Tafna-NW Algerien). *LARHYSS Journal*, 18, 63-76
7. Richards, L. A. (1954). *Diagnosis and improvement of saline and alkali soils* (No. 60). US Government Printing Office.
8. Mermoud, A. (2006). *Cours de physique du sol: Maîtrise de la salinité des sols*. Ecole polytechnique fédérale de Lausanne, 23.



Increasing the efficiency of worn-out urban fabric areas with an emphasis on the segmentation of buildings in the 4th district of Tabriz in Iran

Shiva Sattarzadeh Salehi ^{*1}, Firouz Jafari ¹

¹ University of Tabriz, Department of Geography and Urban Planning, Iran, Sattarzadeh423@gmail.com, F-jafari@tabrizu.ac.ir

Cite this study: Salehi, S. S., & Jafari, F. (2023). Increasing the efficiency of worn-out urban fabric areas with an emphasis on the segmentation of buildings in the 4th district of Tabriz in Iran. *Advanced Engineering Days*, 8, 121-124

Keywords

Worn-out urban fabric
Tabriz
Buildings segmentation
Efficiency

Abstract

Today, residential units are the most important building blocks of cities, which occupy larger land in comparison with other uses. In the dilapidated context, the majority of the existing land use is dedicated to residential plots, but the existing dwellings in this context are not very efficient and even fail to respond to the residents' need for housing as a place of residence and peace. The purpose of the current research is to investigate the effectiveness of increasing the efficiency of the worn-out urban fabric areas with emphasis on the segmentation of buildings in the 4th area of Tabriz, which ends at Ostad Jafari Street from the north and Qods Street from the south. The research method used is a descriptive-analytical method and ArcGIS 10.8.1 software was also used to analyze the desired indicators (area, quality of buildings, orientation of residential parts, and compatibility of parts) of the range. The results of the research showed that in terms of the efficiency of building parts, they are in an unfavorable condition, and the criteria compiled for the modification of these structures will lead to an increase in the efficiency of buildings and residential parts compared to the situation before the intervention.

Introduction

The dilapidated urban fabric refers to the areas of the legal boundaries of the cities that are vulnerable due to physical wear and tear, inadequate vehicle access, facilities, services and urban infrastructures and have a low spatial, environmental and economic value (2). In general, reducing the efficiency of any phenomenon leads to its wear and tear. When life stagnates in an area of the city for any reason, the urban fabric of that area is in the process of wear and tear (5). The wear and tear of the tissue and its internal elements is either due to old age or the lack of development program and technical supervision on the formation of that tissue (4). Due to the poverty of the residents and their owners, these structures do not have the possibility of spontaneous renovation, and investors do not have an incentive to invest in them.

In the country of Iran, several factors have been effective in changing the living conditions in cities since 1961, including the increase in the number of urban dwellers, changes in the household situation, and changes in residential patterns caused by modernization. Kurdish (1). The effect of housing wear and tear on dilapidated structures is so great that, according to the approval of the Supreme Council of Architecture and Urban Planning, 3 characteristics are mentioned to identify dilapidated structures, 2 of which are smallness and building dilapidation related to the issue of housing (6). Improper housing in a dilapidated context is one of the reasons for creating or aggravating problems such as leaving the neighborhood on the part of native residents, reducing the sense of belonging and identity of new residents, reducing the willingness to repair and maintain housing, which has a significant negative impact on these areas (6). Also, it seems that the houses in the worn-out urban fabric have problems in terms of physical, infrastructure, zoning, arrangement of parts, density, occupancy level of the residential unit, proper lighting, etc., and in general, in their efficiency. They have lost their past efficiency or their efficiency has decreased.

In the city of Tabriz, due to its historical age, we are faced with many neighborhoods with old and historical contexts, about 43% of the area of the worn-out context of the city of Tabriz is located in region 4, where 44,613 people are settled. Therefore, the existing buildings in the study area are not in good physical condition, and the

rules and regulations of worn-out structures will lead to an increase in the efficiency of these units (3). Therefore, the current research aims to investigate the effectiveness of increasing the efficiency of worn-out urban fabric areas with an emphasis on the segmentation of buildings in area 4 of Tabriz city.

Material and Method

The collected data has been obtained through observation and recording of information, as well as from the data available in past research, official and unofficial statistics, organizational documents and documents that include maps of the studied area using Arc GIS 10.8.1 software.

The area studied in this research is a part of the worn-out fabric related to the 4th area of Tabriz city, which covers an area of about 2550 hectares, about 1.10% of the total area of the city. The minimum height of the area is about 1335 and the maximum is 1406 meters. In this way, the small difference of about 70 meters and the large area indicates the absence of slope and the smoothness of the land in this area. So, no slope and topography restrictions are envisaged for this area (3). 2137 hectares of the area of this area are located in flat and low slope lands, which is 83.8% of the total area of the area and 15.4% of all the flat lands in Tabriz city “Figure 1”.

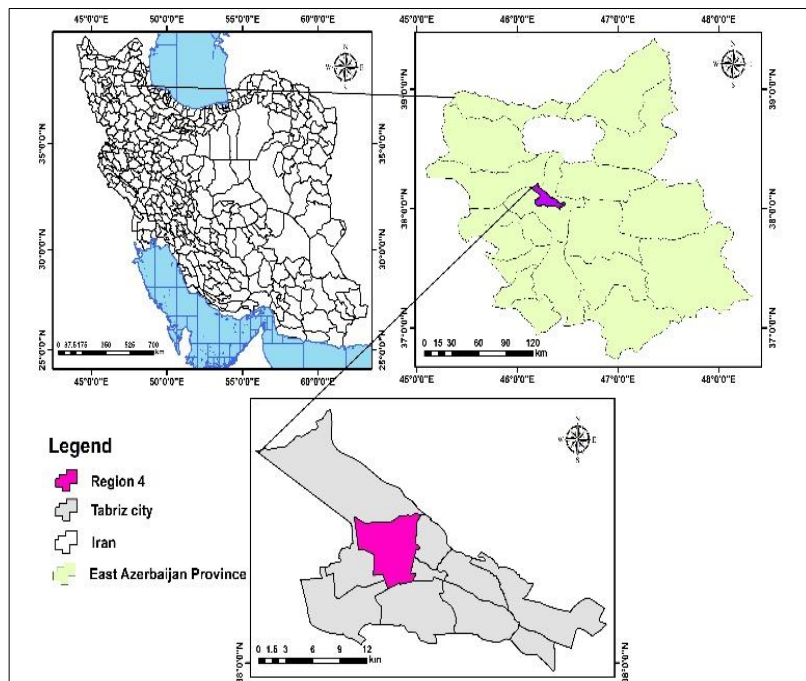


Figure 1. Map of the geographical location of the study area

Results

The area studied in this research is a part of the worn-out fabric related to area 4 of Tabriz city, which is limited between Ostad Jafari Streets from the north and Quds Street from the south, Air Force from the east and Azarbaijan Boulevard from the west. This area has been chosen as an example to measure the efficiency of housing due to its location in the worn-out context of Tabriz city. According to the calculations and estimates, the population of the studied area has decreased to 34,521 people due to the negative growth rate of region 4 in 2016. However, because the last quantitative statistics of the studied area are related to 2012, therefore, the statistics of 2012 have been used to calculate the indicators of the area. The area of the studied area is equal to 202 hectares, and the residential area of the area is 114 hectares. Among the 11,576 plots in the area, 9,801 plots or 84% of the plots have residential use. The evaluation of indicators related to residential parts are as follows:

Examining parts in terms of area

According to the information obtained about the characteristics of the area, the small size of the plots in the area is evident, so that 6726 plots, or 68.6% of the plots have an area of less than 150 square meters. The smallness of the pieces is one of the main characteristics of identifying worn fabrics in Iran. According to the studies conducted, about 46.4% of the pieces are below 100 square meters and 69.8% of the pieces are less than 150 square meters, in other words, more than half of the pieces are below the standard defined for worn texture (200 square meters). Most of the pieces are between 50 and 100 square meters. With the analysis done, it can be concluded that in terms of area, the parts are not in a very good condition “Table 1”.

Table 1. Area of residential plots

Area of parts	Number	Percent
Under 50 square meters	901	9.2
Between 50 and 100 square meters	3509	35.8
Between 100 and 150 square meters	2316	23.6
Between 150 and 175 square meters	949	9.7
Between 175 and 200 square meters	800	8.2
Between 200 and 250 square meters	830	8.5
Between 250 and 300 square meters	261	2.7
Above 300 square meters	235	2.4
Total	9801	100

Orientation of residential parts

The parts in the range are divided into 2 categories according to their location: north-south parts and east-west parts. The importance of this case is from the point of view that if the proper orientation is defined for the parts, the buildings will get the best and most benefit from natural energies such as solar radiation, wind, etc. and the use of heating systems which costs the burden on the family will decrease. In the studied area, the parts are classified into 2 categories: north-south and east-west, 74% of the parts are north-south, and have a more suitable orientation for absorbing sunlight and natural energies compared to the east-west parts. are. But the east-west parts are not suitable because of keeping and directing the heat of the midday sun "Table 2".

Table 2. Orientation of residential parts

Orientation of parts	Number	Percent
East-west piece	2552	26
North-South piece	7249	74
Total	9801	100

Compatibility of residential parts

Considering that the studied area is residential, it is necessary to measure the compatibility of other uses with residential parts. The number of uses in the area has been measured in terms of compatibility with the residential area with medium density. According to the studies, about 97.5% of the parts are suitable for residential use. Therefore, in terms of compatibility, the limited state is in favorable conditions. only 1.4% of the parts are incompatible and relatively incompatible "Table 3".

Table 3. Compatibility of parts

Compatibility of users	Number	Percent
Compatible	11286	97.5
Relatively compatible	4	0.03
incompatible	6	0.1
Relatively inconsistent	152	1.3
indifferent	128	1.1
Total	11576	100

Quality of buildings

Among the parts in the studied area, nearly 70% of the parts are in worn and damaged condition. which indicates the poor efficiency of these residential buildings. that this wear and tear is caused by the passage of time (the age of the building), the effect of the weather, or improper and undesirable maintenance. The wear and tear of a building, in addition to affecting the body of the building, also affects the materials and resistance of the building. Therefore, the safety of buildings is reduced under the influence of the mentioned factors, and as a result of any natural or human accident, there is a possibility of damage to the residents, so the house and housing, in this case, lose their efficiency as a safe place for comfort and convenience "Table 4".

Table 3. The quality of the building

Quality of building	Number	Percent
Under Construction	132	1.3
Worn out	6725	68.6
Can be kept	1688	17.2
Ruined	54	0.6
Restoration	205	2.1
Newly built	997	10.2
Total	9801	100

Discussion

Today, due to the increase in population and the development of cities in areas where the cities do not have enough land for development due to various reasons, such as natural obstacles, worn-out tissues are considered as urban potentials for development, and the ability to plan and provide land and develop the city in this There are contexts. Therefore, these contexts need to be identified, planned, and regulated, and rules and laws and implemented.

Conclusion

In dilapidated contexts, many facilities and spaces are old and dilapidated and need to be reconstructed. Many new facilities for life have not yet been created in these areas. Therefore, these contexts are facing a lack of living and welfare facilities. Due to the unfavorable economic situation, the residents of these areas often cannot solve these problems, and due to the lack of economic efficiency, the private sector is often unwilling to invest in these areas. They have lost their usefulness for their old inhabitants and gradually the inhabitants have migrated from these contexts.

The rapid growth of today's cities has turned housing into one of the acute issues facing development. What was considered in this research is the physical problems faced by worn-out urban tissues. The physical weakness in the worn-out tissue includes the weakness of the housing's physical condition, so weakness will be felt in the indicators that affect the efficiency of the housing. In the first step, the weak efficiency of housing will affect the residents in meeting their needs. Because housing as a bed for human life is in interaction with other dimensions and needs. Therefore, the need for intervention programs and criteria will be felt in worn-out tissues. However, the lack of consistency in the regulations for worn-out fabric and the lack of monitoring of the implementation of these rules has caused the problem of wear and tear in urban fabrics to remain practically unanswered.

According to the studies, the housing in the dilapidated context is in poor condition both in terms of the indicators related to the plot and the residential building, so it is necessary to pay attention to the components related to the residential plots. Also, in the renovation of old structures, the category of culture and climate should be prioritized in improvement and renovation projects.

References

1. Habibi, K. Pourahmad, A. & Meshkini, A. (2007). Improvement and renovation of old urban structures. Kurdistan University Press
2. Bromley, R. D., Tallon, A. R., & Thomas, C. J. (2005). City centre regeneration through residential development: Contributing to sustainability. *Urban Studies*, 42(13), 2407-2429. <https://doi.org/10.1080/00420980500379537>
3. Lee, S. L. (1996). Urban conservation policy and the preservation of historical and cultural heritage: The case of Singapore. *Cities*, 13(6), 399-409. [https://doi.org/10.1016/0264-2751\(96\)00027-3](https://doi.org/10.1016/0264-2751(96)00027-3)
4. Asefi, M., & Imani, E. (2016). Redefining design patterns of Islamic desirable contemporary housing through qualitative evaluation of traditional homes. *Iran University of Science & Technology*, 4(2), 56-73.
5. Zebardast, E & Norani, H (2016). Measuring the quality of life in the area of worn-out housing with historical value in the city of Isfahan. *Beautiful Arts Magazine*, 4, 29-38.
6. Jafari, F., Shalaleh, R & Asghari zamani, A (2018). Evaluation of the Segmentation of Residential land in Worn Texture with an Emphasis on Increasing Efficiency (Case Study: Region 4 of Tabriz). PHD Thesis, University of Tabriz, Iran.